

**INVESTIGATING THE ROLE OF THE
CYTOSKELETON AND SIGNALLING IN
THE SELF-INCOMPATIBILITY
RESPONSE OF *PAPAVER RHOEAS***

by

NATALIE SARAH POULTER

A thesis submitted to
The University of Birmingham
for the degree of
DOCTOR OF PHILOSOPHY

School of Biosciences
The University of Birmingham
June 2009

UNIVERSITY OF
BIRMINGHAM

University of Birmingham Research Archive

e-theses repository

This unpublished thesis/dissertation is copyright of the author and/or third parties. The intellectual property rights of the author or third parties in respect of this work are as defined by The Copyright Designs and Patents Act 1988 or as modified by any successor legislation.

Any use made of information contained in this thesis/dissertation must be in accordance with that legislation and must be properly acknowledged. Further distribution or reproduction in any format is prohibited without the permission of the copyright holder.

ABSTRACT

Many flowering plants are hermaphrodite, which poses the problem of self-fertilisation and the subsequent loss of genetic fitness in the offspring. To prevent this, plants have developed a genetically controlled mechanism called self-incompatibility (SI) which allows self (incompatible) pollen to be recognised and rejected before fertilisation can occur. The SI response of *Papaver rhoeas* (field poppy) has been extensively studied at the molecular and cellular level. Rejection of incompatible pollen occurs on the stigma surface when the pollen *S*-determinant PrpS, a transmembrane protein, interacts with the stigmatic *S*-determinant, secreted S-proteins. This triggers a calcium-mediated signalling cascade that targets the cytoskeleton and results in programmed cell death (PCD) of incompatible pollen. Work presented in this thesis investigated the localisation of PrpS and S-proteins. Other studies investigated the role of the cytoskeleton in SI. These demonstrated the involvement of the microtubule cytoskeleton for the first time. Microtubules were rapidly depolymerised and this was implicated in signalling to PCD. The actin cytoskeleton has previously been shown to exhibit biphasic alterations during SI involving depolymerisation, followed by formation of F-actin foci. Studies described here represent the first steps toward characterisation of the F-actin foci. Their potential involvement in PCD and signalling is discussed.

I dedicate this work to my wonderful family,
Sylvia, David, Mark, Stephanie & Emily.
Also to Grandma P, who would have been so proud.

ACKNOWLEDGEMENTS

First and foremost, I would like to thank my supervisor, Noni Franklin-Tong, for all her help and encouragement over the past three and a half years and for providing me with a project that I have thoroughly enjoyed. I would also like to express my thanks to all the lab members and PIs, past and present, for their support, both moral and scientific, that has helped shape my project and given me confidence in my abilities. In particular I would like to thank Candida Nibau, Maurice Bosch, Barend de Graaf, Sabina Vatovec, Ruth Perry and Natalie Hadjosif who have been fantastic colleagues, always willing to help, and more importantly, good friends. I would like to acknowledge Steve Price for his help with the embedding and sectioning of my pollinated stigmas, which was very much appreciated. I must also thank Chris Staiger for his kind donation of multiple antibodies and his transatlantic email conversations that were immensely helpful whenever I had a problem with anything actin-related! I also thank Patrick Hussey for his antibody donation. A very big thank you goes to Josh Rappoport for helping me to design the co-localisation method and for allowing me to use his Metamorph software.

I also need to thank those who work 'behind the scenes' but whose work is necessary to make my project possible. Firstly the horticultural staff, Karen, Bob, Charlie and Mike, who did such a good job setting up and looking after the poppy field. I also thank you all for spending the whole month of July in the field helping us collect pollen, doing emasculations and pollinations and listening to our made-up songs on the subject! Secondly, my thanks go to the Proteomics Department, especially Laine Wallace, Cleidi Zampronio and Helen Cooper, who helped me with my samples and took the time to discuss the results with me.

Finally, I have to say a MASSIVE thank you to my Euge, who has been a great support throughout my PhD but especially during the writing-up stage. Thank you for looking after me whilst I was writing all day, every day and you did it all without a single complaint! I promise you can have your life back now I have finished!

CHAPTER 1.....	1
INTRODUCTION	1
1.1) Pollen tube structure and function	2
1.2) The role of calcium in pollen tube growth	5
1.2) The cytoskeleton.....	6
1.2.1) The actin cytoskeleton	7
1.2.1.1) The role of the actin cytoskeleton	8
1.2.1.2) The actin cytoskeleton in pollen tubes	8
1.2.1.3) Actin binding proteins (ABPs)	11
1.2.1.3.1) Profilin	15
1.2.1.3.2) Actin-depolymerising factor (ADF)	17
1.2.1.3.3) Cyclase-associated protein (CAP)	19
1.2.1.3.4) Fimbrin.....	21
1.2.2) The MT cytoskeleton	22
1.2.2.1) The role of the MT cytoskeleton	24
1.2.2.2) The MT cytoskeleton in tip-growing cells	27
1.2.2.3) Microtubule-associated proteins (MAPs) in plants	29
1.3) Programmed Cell Death (PCD).....	31
1.3.1) Plant PCD.....	32
1.3.2) The cytoskeleton and PCD.....	34
1.4) Self-incompatibility	38
1.5) Self-incompatibility in Brassicaceae	40
1.5.1) The female <i>S</i> -determinant	40
1.5.2) The male <i>S</i> -determinant	42
1.5.3) The mechanism of SI	42
1.5.4) Downstream signalling components	44
1.6) S-RNase-type self-incompatibility	46
1.6.1) The female <i>S</i> -determinant	46
1.6.2) The male <i>S</i> -determinant	47
1.6.3) The mechanism of SI	48
1.7) Self-Incompatibility in Papaveraceae.....	51
1.7.1) The mechanism of SI	52
1.7.1.1) The role of calcium in <i>Papaver</i> SI	52
1.7.1.2) Protein phosphorylation occurs during <i>Papaver</i> SI.....	54
1.7.1.3) The role of the cytoskeleton in <i>Papaver</i> SI	55
1.7.1.4) <i>Papaver</i> SI results in PCD of the incompatible pollen.....	57
 CHAPTER 2.....	 60
MATERIALS AND METHODS.....	60
2.1) Stock Solutions	61
2.2) Plant Material.....	62
2.2.1) Plant cultivation.....	62
2.2.2) Determination of S-genotype	62
2.2.3) Production of seed	63
2.2.4) Collection of pollen.....	63
2.3) Pollen tube growth <i>in vitro</i>	64

2.4)	Pollen Treatments	64
2.4.1)	S-Proteins	64
2.4.1.1)	Production of recombinant S-proteins from E. coli.....	64
2.4.1.1.1)	Growth of E. coli and induction of protein synthesis	64
2.4.1.1.2)	Purification of inclusion bodies	65
2.4.1.1.3)	Refolding recombinant S-proteins	66
2.4.1.1.4)	In vitro induction of SI.....	66
2.4.2)	Actin Drugs	67
2.4.3)	Tubulin Drugs	67
2.5)	Pollen fixation.....	68
2.6)	Immunolocalisation.....	68
2.6.1)	Primary Antibodies	68
2.6.2)	Secondary Antibodies	69
2.6.3)	Whole-mount immunolocalisation – spinning method	69
2.6.4)	Whole-mount immunolocalisation – basket method.....	70
2.6.5)	Actin staining	71
2.6.6)	Immunolocalisation on sectioned material.....	71
2.6.6.1)	Embedding and sectioning of pollinated stigmas.....	71
2.6.6.2)	Immunolocalisation of S-proteins on pollinated stigma sections.....	72
2.7)	Fluorescence Microscopy	73
2.7.1)	Epifluorescence Imaging.....	73
2.7.2)	Confocal Laser Scanning Microscopy (CLSM).....	73
2.8)	Image analysis using MetaMorph software	74
2.8.1)	Co-localisation of F-actin with ABPs	74
2.8.2)	Measuring the apparent size of the F-actin foci	77
2.8.3)	Counting the number of F-actin foci	77
2.9)	Pollen Tube Length Measurement.....	78
2.10)	Pollen Protein Extraction	78
2.10.1)	Protein extraction for the tubulin studies	79
2.10.2)	Protein extraction for the caspase assay.....	79
2.10.3)	Protein extraction for the actin binding protein studies	80
2.10.4)	Protein extraction for F-actin isolation.....	80
2.11)	Estimation of Protein Concentration - Bradford Assay (Bradford, 1976).....	81
2.12)	Programmed cell death detection – Caspase activity assay.....	81
2.13)	SDS-Polyacrylamide Gel Electrophoresis	83
2.13.1)	Preparation of SDS-PAGE	83
2.13.2)	SDS-PAGE gel staining	84
2.14)	Western Blotting	84
2.14.1)	Protein transfer	84
2.14.2)	Antibody probing	85
2.14.3)	Alkaline phosphatase detection.....	85
2.15)	F-actin enrichment using ultracentrifugation.....	86
2.16)	F-actin pull-down assay	87
2.16.1)	Streptavidin MagneSphere Paramagnetic Particles (SA-PMPs).....	87
2.17)	Analysis of F-actin containing fractions by FT-ICR MS.....	88
2.17.1)	Sample preparation.....	88
2.17.2)	Mass spectrometry data analysis by Mascot	88
2.18)	Statistical Analysis.....	90

CHAPTER 3.....91

IMMUNOLOCALISATION OF THE MALE AND FEMALE S-DETERMINANTS IN PAPAVER POLLEN TUBES91

3.1)	Introduction	92
3.2)	Results	96
3.2.1)	The PrpS ₁ 60C antibody recognises PrpS ₁ protein	96
3.2.2)	PrpS localises to the pollen tube membrane.	99
3.2.3)	<i>In vitro</i> localisation of S-proteins	102
3.2.4)	Native S-proteins also localise to the pollen tube cortex	108
3.3)	Discussion.....	111
3.3.1)	Immunolocalisation of PrpS ₁	111
3.3.2)	PrpS could function as a membrane bound receptor	112
3.3.3)	S-proteins bind to both incompatible and compatible pollen	115

CHAPTER 4.....120

MICROTUBULES ARE AN EARLY TARGET FOR SELF-INCOMPATIBILITY SIGNALLING IN PAPAVER POLLEN.....120

4.1)	Introduction.....	121
	Part I: The published paper.....	124
4.1.1)	Preface.....	124
	Part II: Unpublished data relating to MT alterations in <i>Papaver</i> pollen tubes.....	125
4.2)	Introduction.....	125
4.3)	Results.....	125
4.3.1)	Immunoblotting of <i>P. rhoeas</i> pollen tube proteins	125
4.3.2)	Characterisation of the MT cytoskeleton in untreated pollen tubes of <i>P. rhoeas</i>	127
4.3.3)	SI triggers rapid apparent MT depolymerisation	129
4.3.4)	Compatible S-proteins have no effect on the MT cytoskeleton	131
4.3.5)	MT depolymerisation is not a consequence of growth inhibition.....	132
4.4)	Discussion	134
4.4.1)	The MT cytoskeleton in normally growing pollen tubes	134
4.4.2)	SI-mediated MT alterations do not mediate pollen tube inhibition	135
4.4.3)	MT cytoskeleton alterations in response to external stimuli.....	137
4.4.4)	The relationship between the actin and MT cytoskeletons	138
4.4.5)	Possible links between MTs, actin and signalling components	140

CHAPTER 5.....145

CHARACTERISING THE PUNCTATE F-ACTIN FOCI OF THE SI RESPONSE ...145

5.1)	Introduction	146
5.2)	Results	149
5.2.1)	Alterations to the actin cytoskeleton during SI.....	149
5.2.2)	The large punctate F-actin foci are resistant to depolymerisation	153
5.2.3)	Testing the specificity of antibodies raised against different ABPs	155

5.2.4)	ABP localisation alters during SI.....	157
5.2.5)	Co-localisation of CAP and ADF during SI	159
5.2.6)	Quantitative analysis of ABP and F-actin co-localisation	160
5.2.7)	Spatio-temporal dynamics of the SI-induced CAP, ADF and F-actin alterations.....	162
5.3)	Discussion.....	167
5.3.1)	Formation and stability of the punctate F-actin foci	167
5.3.2)	CAP co-localises with the punctate F-actin foci.....	168
5.3.3)	ADF co-localises with the punctate F-actin foci.....	171
5.3.4)	Fimbrin does not co-localise with the punctate F-actin foci.....	174
5.3.5)	Profilin does not associate with the punctate F-actin foci	175
5.3.6)	Other ABPs that could be involved in foci formation	177
CHAPTER 6.....		180
ANALYSIS OF THE SI-INDUCED F-ACTIN FOCI USING MASS-SPECTROMETRY		180
6.1)	Introduction	181
6.2)	Results	185
6.2.1)	Enrichment of F-actin using ultracentrifugation.....	185
6.2.2)	Isolation of F-actin using a pull-down assay	189
6.2.4)	Analysis of F-actin interactors using mass spectrometry.....	191
6.3)	Discussion.....	197
6.3.1)	Identification of F-actin and its interacting proteins by FT-ICR-MS	197
6.3.2)	The 14-3-3 signal proteins may interact with F-actin during SI.....	200
6.3.3)	Rab-GTPases were identified more frequently in SI samples	201
6.3.4)	Heat shock proteins may interact with F-actin during SI	203
6.3.5)	Improvements to the technique and future studies	205
CHAPTER 7.....		209
GENERAL DISCUSSION.....		209
7.1)	Investigating the interaction between PrpS and S-proteins.....	210
7.2)	Further investigations into the MT cytoskeleton during SI.....	213
7.3)	Do the punctate F-actin foci represent the point of no return?.....	216
7.4)	Linking the F-actin foci, ADF and CAP to PCD.....	219
7.5)	Concluding remarks.....	222
CHAPTER 8.....		224
LIST OF REFERENCES.....		224

APPENDIX I: PUBLISHED PAPERS

APPENDIX II: FT-ICR-MS DATA

LIST OF FIGURES AND TABLES

CHAPTER 1: INTRODUCTION

Figure 1.1. Pollen tube structure.....	4
Figure 1.2. A model of an actin microfilament.....	7
Figure 1.3. Reverse fountain cytoplasmic streaming.....	10
Figure 1.4. Microtubule organisation and assembly dynamics.....	23
Figure 1.5. Plant MT arrays during the cell cycle.....	26
Figure 1.6. The two different types of SI	39
Figure 1.7. Model of the SI response in the <i>Brassicaceae</i>	43
Figure 1.8. Two alternative models of S-RNase-type SI.....	50
Figure 1.9. Model of the SI response in <i>Papaver rhoeas</i>	53
Table 1.1. An overview of the function of several key ABPs.....	12-15
Table 1.2. An overview of the function of several key MAPs from plants.....	30

CHAPTER 2: MATERIALS AND METHODS

Figure 2.1: Micrographs of pollinated stigma squashes.....	63
Figure 2.2: Quantification of co-localisation using MetaMorph.....	76
Figure 2.3: Mascot MS/MS ions search page.....	89

CHAPTER 3: IMMUNOLOCALISATION OF BOTH THE MALE AND FEMALE S-DETERMINANT IN *PAPAVER* POLLEN TUBES

Figure 3.1. PrpS ₁ amino acid sequence and predicted topology.....	97
Figure 3.2. The PrpS ₁ 60C antibody detects PrpS ₁ protein, which is present in the membrane-enriched fraction.....	98
Figure 3.3. PrpS ₁ localises to the pollen tube membrane.....	100
Figure 3.4. Pixel intensity traces show PrpS ₁ localises to the pollen tube membrane.....	101
Figure 3.5. The S ₁ antibody recognises the recombinant S ₁ protein.....	103
Figure 3.6. S-proteins localise to the pollen tube edge in both a compatible and an incompatible reaction.....	106
Figure 3.7. Control pollen tubes do not exhibit signal along the pollen tube periphery.....	107
Figure 3.8. Sections through pollinated stigmas show S-proteins at the pollen tube cortex.....	110

CHAPTER 4: MICROTUBULES ARE A TARGET FOR SELF-INCOMPATIBILITY SIGNALLING IN *PAPAVER* POLLEN

Figure 4.1. Western blot testing specificity of monoclonal anti- α -tubulin antibody, clone B 5-1-2.....	126
Figure 4.2. Microtubule organisation in normally growing <i>Papaver</i> pollen tubes.....	128
Figure 4.3. Pollen tube cytoskeleton alterations during the SI response.....	130
Figure 4.4. Compatible S-proteins do not alter MT organisation.....	131

Figure 4.5. MT depolymerisation is not due to pollen tube growth inhibition.....	133
Figure 4.6. A possible model for pollen tube MT alterations during SI.....	144

CHAPTER 5: CHARACTERISING THE PUNCTATE F-ACTIN FOCI OF THE SI RESPONSE

Figure 5.1. F-actin alterations during SI.....	150
Figure 5.2. The punctate F-actin foci appear to increase in size but decrease in number during SI.....	152
Figure 5.3. The punctate F-actin foci are resistant to LatB-induced depolymerisation.....	154
Figure 5.4. The ABP antibodies cross-react with poppy pollen proteins.....	156
Figure 5.5. Localisation of four ABPs in untreated and 3 h SI-induced pollen tubes.....	158
Figure 5.6. ADF and CAP co-localise at 3 h post-SI induction.....	159
Figure 5.7. Quantification of co-localisation of ABPs with F-actin.....	161
Figure 5.8. Spatio-temporal analysis of CAP localisation during the SI response.....	163
Figure 5.9. Spatio-temporal analysis of ADF localization during the SI response.....	165
Figure 5.10. The percentage of F-actin co-localising with CAP & ADF increases with time after SI induction.....	166

CHAPTER 6: ANALYSIS OF THE SI-INDUCED F-ACTIN FOCI USING MASS-SPECTROMETRY

Figure 6.1. Investigating the components of the SI-induced F-actin foci.....	182
Figure 6.2. F-actin enrichment by ultracentrifugation.....	186
Figure 6.3. Visualisation of F-actin in the different fractions of the ultracentrifugation of pollen protein extracts.....	188
Figure 6.4. F-actin pull-down using SA-PMPs.....	190
Figure 6.5. Distribution of the identified proteins into functional categories.....	192
Figure 6.6. Alignment of AtCAP1 and OsCAP1 protein sequences.....	199
Table 6.1. Proteins involved in signal transduction found associating with the F-actin in 3 h SI samples	194
Table 6.2. Heat shock and chaperone proteins found associating with the F-actin in 3 h SI samples.....	194
Table 6.3. Comparison of the amino acid sequence of AtCAP1 to CAP1 proteins from different species.....	199

CHAPTER 7: GENERAL DISCUSSION

Figure 7.1. The current model of <i>Papaver rhoeas</i> SI.....	223
---	------------

ABBREVIATIONS

- ABP: Actin binding protein
- ADP: Adenosine diphosphate
- ADF: Actin depolymerising factor
- APS: Ammonium peroxodisulfate
- ATP: Adenosine triphosphate
- BCIP: 5-Bromo-4-chloro-3-indolyl phosphate
- CAP: Cyclase associated protein
- DAPI: 4'-6-Diamidino-2-phenylindole
- DMF: *N,N*-Dimethylformamide
- EDTA: Edetate disodium
- EGTA: Ethylene glycol-bis(2-aminoethylether)-*N,N,N',N'*-tetraacetic acid
- F-actin: Filamentous actin (actin MFs)
- FITC: Fluorescein isothiocyanate
- FT-ICR-MS: Fourier transform ion cyclotron resonance mass spectrometry
- G-actin: Globular actin (actin monomers)
- GC: Generative cell
- GDP: Guanosine diphosphate
- GM: Growth medium
- GTP: Guanosine triphosphate
- Jasp: Jasplakinolide
- LatB: Latrunculin B
- MAP: Microtubule associated protein
- MAPK: Mitogen-activated protein kinase
- MF: Microfilament
- MT: Microtubule
- NBT: Nitroblue tetrazolium
- PARP: poly(ADPribose) polymerase
- PCD: Programmed cell death
- PrpS: *Papaver rhoeas* pollen S
- SA-PMPs: Streptavidin MagneSphere Paramagnetic Particles
- SDS: Sodium dodecyl sulfate
- SDW: Sterile distilled water
- SI: Self-incompatibility
- sPPase: soluble pyrophosphatase
- TBS: Tris buffered saline
- TBST: TBS + 0.1 % Tween 20
- TEM: Transmission electron microscopy
- TEMED: *N,N,N',N'*-Tetramethylethylenediamine
- UT: Untreated
- VN: Vegetative nucleus

CHAPTER 1

INTRODUCTION

1.1) Pollen tube structure and function

Plant sexual reproduction is a huge area of scientific interest, with the research having the added advantage of being able to be applied to the potential improvement of crop plants (Taylor & Hepler, 1997). Not only does it have the commercial interest but one of the key components of plant sexual reproduction, the pollen tube, is now also an established model system for studying processes such as molecular mechanisms of tip growth, cell polarity control and signalling (Åström, 1997, Wang et al, 2004a). This is due to the high abundance of pollen and relatively ease with which pollen tubes can be grown *in vitro*.

In flowering plants, pollination is one of the first important steps for reproduction. This is when a pollen grain, carried by insects, animals or the wind, lands on a receptive stigma. The pollen grain then hydrates and germinates, producing a cylindrical protrusion called a pollen tube. The primary role of the pollen tube is to transport the male gametes (the sperm cells) through the transmitting tract of the pistil and deliver them into the ovary where double fertilisation occurs. The pollen tubes are guided through the female tissue to the ovary by molecular cues (reviewed in Wheeler et al, 2001) such as gamma-aminobutyric acid (GABA) in *Arabidopsis* (Palanivelu et al, 2003) or transmitting tissue-specific (TTS) protein in tobacco (Cheung et al, 1995). Pollen tubes are the fastest growing plant cells known, some growing in excess of 200nm/s (Hepler et al, 2001), and they grow exclusively by apical (tip) extension (Taylor & Hepler, 1997). There are two different types of pollen grain: binucleate and trinucleate. The majority (70%) of flowering plants, including poppy, produce binucleate pollen. This means that the pollen grain contains both a generative cell (GC) and a vegetative nucleus (VN). The GC only divides by mitosis into the two sperm cells once it is in the pollen tube. In trinucleate pollen the division of the generative cell occurs in the pollen grain

before pollen release. This type of pollen therefore contains three nuclei before pollen tube growth (Raudaskoski et al, 2001). *Arabidopsis* pollen is an example of trinucleate pollen.

Pollen tubes are highly polarised structures. They grow by tip-growth which involves the deposition of new cell wall and membrane material in a very small, defined area of the growing tip. This area is often referred to as the 'clear zone' as it is full of small vesicles carrying the cell wall/membrane material but large organelles do not enter this region. As pollen tubes have to grow over long distances they need to concentrate their cytoplasm, carrying the VN/GC complex, organelles and the cytoskeleton, in the front end of the tube, to ensure the sperm cells are delivered to achieve fertilisation. The cytoplasm is maintained at the front of the pollen tube by callose plugs that are laid down at regular intervals during pollen tube growth. The area behind the plugs then becomes vacuolated (reviewed in Franklin-Tong, 1999). A growing pollen tube therefore contains 4 distinct zones (**Fig. 1.1**):

- 1) The apical growth zone (the tip region),
- 2) The sub-apical zone,
- 3) The nuclear zone
- 4) The vacuolisation and callose plug formation zone (Åström, 1997).

Zones 3 and 4 are jointly referred to as the shank.

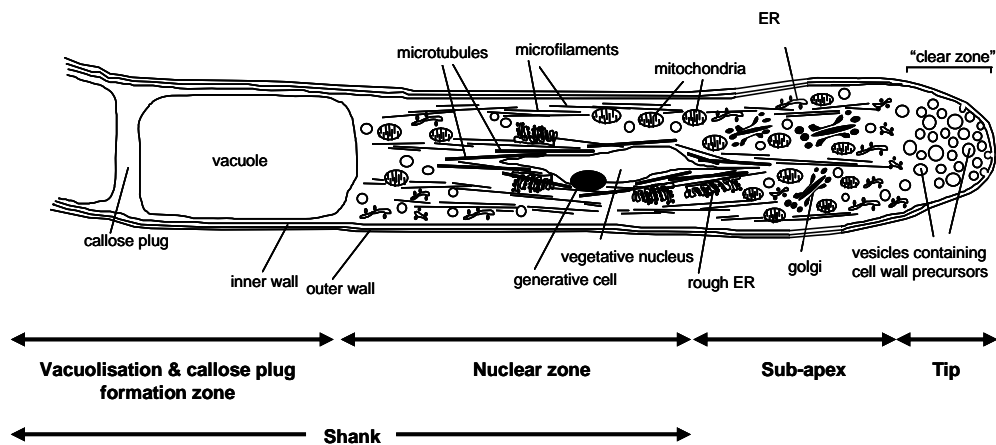


Figure 1.1. Pollen tube structure.

Diagram showing the relative positions of the 4 different zones of the pollen tube. (Figure adapted from Franklin-Tong, 1999)

The pollen tube cell wall is made up of two layers. The inner cell wall is made of callose and the outer wall is mainly pectin with some cellulose and hemicellulose (reviewed in Mascarenhas, 1993; Franklin-Tong, 1999; Krichevsky et al, 2007). The tip-region is made up of a single layer of pectin (Ferguson et al, 1998) which gives it the plasticity to allow directional growth but still maintain the integrity of the cell. The GC originates from an asymmetric division of the microspore and is surrounded by two plasma membranes with cell wall material between these membranes (Cresti et al, 1987). The GC cell wall contains arabinogalactan proteins (AGPs) but no pectins have been identified (Li et al, 1995).

As previously mentioned, pollen tubes grow by apical extension and there is no further differentiation or division of the cell. Two of the most important factors influencing pollen tube growth are a tip-focussed calcium gradient and an intact cytoskeleton. These are discussed in more detail below.

1.2) The role of calcium in pollen tube growth

Calcium is essential for pollen tube growth and plays a key role in its regulation. Ratiometric calcium studies have shown that there is a strong tip-focused calcium gradient in growing pollen tubes that is not detected in non-growing pollen (Obermeyer & Weisenseel, 1991; Rathore et al, 1991; Miller et al, 1992; Malhó et al, 1994, Franklin-Tong et al, 1997). This calcium gradient has been shown to oscillate and it has been established that this oscillatory behaviour is closely associated with pollen tube growth rate and they share the same periodicity (Holdaway-Clark et al, 1997). Work by Pierson et al (1996) showed that calcium ion entry is restricted to the extreme apex of the pollen tube where growth occurs, but later work by Franklin-Tong et al (2002) demonstrated that some calcium does enter the tube via the shank, in poppy at least. Extracellular calcium enters the pollen tube via ion channels at the tip region and, although uncharacterised, these channels are thought to be stretch activated (reviewed by Taylor & Hepler, 1997; Franklin-Tong, 1999; Hepler et al, 2001). When growth of the pollen tube ceases it is thought that these ion channels close, resulting in the dissipation of the calcium gradient required for continued growth. Any treatment, such as caffeine, that dissipates the tip-focused calcium gradient results in inhibition of tube growth. When the pollen tube is returned to normal conditions the calcium gradient is re-established and growth resumes at the point of the highest calcium concentration (reviewed by Taylor & Hepler, 1997; Hepler et al, 2001). Growth can also be inhibited by increasing calcium levels within the tube. This can be achieved by applying a weak electric field or using photo-activated caged calcium. Upon recovery the tube resumes growth in a new direction. Using these methods Malhó et al (1994) have shown that calcium is involved in reorientation of the growing pollen tube and they suggest that calcium is part of a signal transduction which

allows pollen tubes to respond to directional signals in the style that guide it towards the ovary and a successful fertilisation.

1.2) The cytoskeleton

The cytoskeleton is a network of proteinaceous filaments found in the cytoplasm of cells. It consists primarily of actin microfilaments (MFs or F-actin), tubulin microtubules (MTs) and intermediate filaments, which are filaments made of proteins such as keratin or vimentin. The cytoskeleton is a highly dynamic structure that acts as a cellular scaffold to provide structural support to maintain cell shape, as well as playing important roles in intracellular transport, cell division and cell motility. It was previously thought that the cytoskeleton was unique to eukaryotic cells, but homologues of the main groups of cytoskeletal proteins have recently been discovered in prokaryotes, where they seem to carry out similar roles to their eukaryotic counterparts (Michie & Löwe, 2006; Shih & Rothfield, 2006). The cytoskeleton of plants is made up of actin MFs and MTs. Intermediate filaments, which are thought to play a structural role, have not been identified in plant cells. There are many other proteins which interact with the cytoskeleton. For example, motor proteins used for intracellular transport along the cytoskeletal 'tracks', such as myosin (for actin) and dynein (for MTs), and also proteins involved in modulating MF or MT dynamics. Collectively these proteins are called actin-binding proteins (ABPs) and microtubule-associated proteins (MAPs). As plants do not have intermediate filaments these will not be discussed further. Instead, this work will concentrate on the actin and MT cytoskeletons, and some of their interacting proteins.

1.2.1) The actin cytoskeleton

Actin MFs are composed of actin monomers (globular (G) -actin) that have a molecular weight of 43 kDa. These monomers join end-to-end to form a double-stranded helix of between 5 and 7 nm in diameter (**Fig. 1.2**). Actin MFs have directionality, with two distinct ends; the barbed (+) end and the pointed (-) end. The barbed end has a higher affinity for actin monomers and therefore grows at a faster rate than the pointed end. This polarity allows other proteins, such as myosins, to interact with the actin MFs in a directionally specific way. Only monomers with bound ATP assemble into MFs. Shortly after assembly into MFs, the ATP bound to the G-actin is hydrolyzed to ADP, which remains bound to the MF. On the barbed (+) end of the MF a cap of ATP containing monomers is formed while the rest of the MF is composed of ADP binding monomers. The size of the ATP cap stays approximately the same in elongating MFs because, while the new ATP bound actin monomers are added to the + end of the MF, there is hydrolysis of the ATP to ADP in the oldest monomers of the cap. On the pointed (-) end of the microfilament, the ADP bound monomers disassociate from the MF. When the rate of addition and the rate of loss of monomers are balanced a process termed *treadmilling* occurs. This is when there is no net lengthening or shortening of the MF and the MF appears to ‘move’ across the cell.

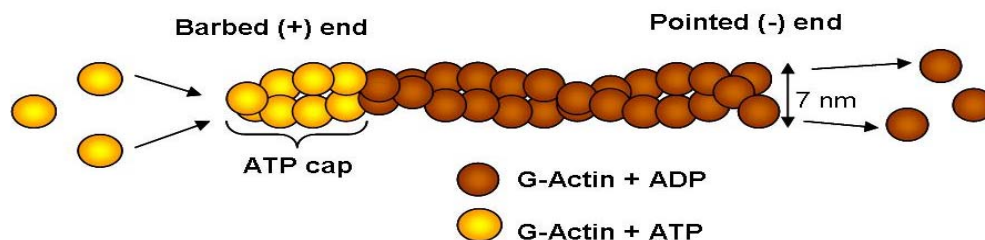


Figure 1.2. An Actin Microfilament.

A double-stranded helix composed of actin monomers (G- actin). ATP bound actin monomers are added to the barbed end of the MF & form an ATP cap. ADP bound actin monomers dissociate from the pointed end of the MF.

1.2.1.1) The role of the actin cytoskeleton

The dynamics of the actin cytoskeleton are under the strict control of signalling pathways which allow the cell to respond to external stimuli and adapt successfully to new environments. The actin cytoskeleton of mammalian cells plays a large role in cell movement, both within the cell, in the form of organelle or vesicle transport, and the motility of the cell itself. Specialised actin-rich structures called filopodia and lamellipodia (reviewed in Le Clainche & Carlier, 2008) are used by cells such as fibroblasts and keratinocytes for cell migration. Actin also has an essential role in cell division of mammalian and yeast cells where, along with myosin, it forms a contractile ring that divides the cell into two during cytokinesis. In plant cells the actin cytoskeleton also functions in diverse processes such as cytoplasmic streaming, co-ordinating endo- and exocytosis, directing the plane of cell division and cell wall synthesis and response to pathogen attack, amongst others (Meagher & Willianson, 1994; I. Kobayashi et al, 1994; Fowler & Quatrano, 1997; Y. Kobayashi et al, 1997a; 1997b; Kropf et al, 1998; Nick, 1999; McCurdy et al, 2001; Hussey et al, 2006). Recent work has also shown that the actin cytoskeleton is involved in programmed cell death pathways in plant, yeast and mammalian cells (reviewed in Franklin-Tong & Gourlay, 2008).

1.2.1.2) The actin cytoskeleton in pollen tubes

Numerous studies have shown the actin cytoskeleton to have a distinct and dynamic organisation in pollen tubes (Lovy-Wheeler et al, 2005; Geitmann et al, 2000; Kost et al, 1998). The tip region is relatively actin-free, in the sub-apex there is a fine mesh-work actin array termed an “actin collar” or “fringe”, and longitudinal actin cables are present along the shank of the pollen tube. The actin MFs are responsible for the reverse fountain cytoplasmic

streaming that occurs in pollen tubes. Cytoplasmic streaming is a directed, continuous flow of organelles and vesicles driven by the actomyosin system (Smith & Oppenheimer, 2005). It is needed to direct the flow of secretory vesicles to the pollen tube tip for growth and also to maintain the distribution of organelles in the cytoplasm. Reverse fountain streaming (**Fig. 1.3**) involves the movement of the cytoplasmic contents towards the pollen tube tip in the cortical region of the tube. In the sub-apical region, in the vicinity of the actin collar, organelles reverse the direction of their movement and go back along the actin MF in the centre of the tube. The secretory vesicles containing the cell wall/membrane material are transported to the tip region by peripheral actin MFs where they accumulate, often in the shape of an inverted cone (Cai & Cresti, 2009; Franklin-Tong, 1999; Taylor & Hepler, 1997). The extreme tip of the pollen tube is not included in the cytoplasmic streaming, instead the vesicles appear to move in a random manner in this region (Geitmann & Emons, 2000). These vesicles eventually fuse with the plasma membrane at the tip allowing tube extension. The tip-focused calcium gradient, shown to be present in all growing pollen tubes, is thought to direct the movement of vesicles in the extreme tip region by creating a sink for their fusion at the place of ion entry on the membrane (Pierson et al, 1996). More recently, fine, dynamic actin MFs, which are regulated by Rop-signalling, have been visualised in growing pollen tubes using GFP-mTalin and these are thought to direct the vesicles to the tip membrane (Fu et al, 2001). It has been demonstrated that tip growth, cytoplasmic streaming and organelle transport are all affected by cytochalasins, fungal metabolites that disrupt actin MFs, indicating that actin MFs are required for these processes (Åström, 1997; Cai et al, 1997). Several studies have shown that actin polymerisation and the stability of the MFs are essential for pollen tube growth (Gibbon et al, 1999; Vidali et al, 2001; Cardenas et al, 2008). In these studies they demonstrated that tip growth is more sensitive than cytoplasmic streaming to

inhibitors of actin polymerisation (e.g. Latrunculin B) and there is no correlation between streaming and growth rates. From this they have concluded that tip growth requires actin assembly in a process that is independent of actin based cytoplasmic streaming. Cardenas et al (2008) proposed that pollen tube growth occurs through actin polymerisation and extension of the actin filaments in the sub-apical actin fringe, which acts as a track to direct vesicles to the tip area where they fuse and growth occurs. Gossot & Geitmann (2007) have also demonstrated that actin MFs are required for pollen tubes to penetrate a stiffened medium. Actin may therefore be involved in aiding the penetration of the stigmatic and stylar tissues by the pollen tube during fertilisation. Other work in *Arabidopsis* pollen tubes has linked actin polymerisation status to calcium-permeable channels in the plasma membrane of the pollen tube (Wang et al, 2004a). This study suggests that actin, as well as being involved in growth through force generation and delivery of cell wall/membrane material to the tip, may also be able to regulate cytoplasmic calcium concentrations.

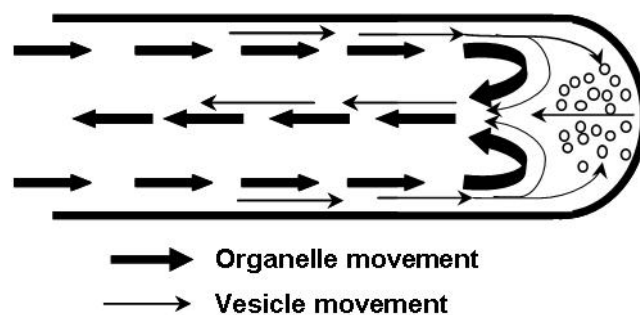


Figure 1.3. Reverse fountain cytoplasmic streaming.

The actin MFs are responsible for the reverse cytoplasmic streaming that occurs in the pollen tube. Organelles and vesicles move along the cortex of the pollen tube towards the tip. In the sub-apex the organelles reverse direction and travel in the centre of the tube. The vesicles are directed to the tip for fusion with the plasma membrane and thus tube extension. Any unfused or endocytotic vesicles are recycled back into the pollen tube. Figure adapted from Cai & Cresti (2009).

1.2.1.3) Actin binding proteins (ABPs)

The actin cytoskeleton is highly dynamic, with a pool of monomeric actin and filamentous actin both maintained simultaneously in the same cell. The dynamics of the actin cytoskeleton are controlled by various actin binding proteins (ABPs). These ABPs can be sub-divided into seven classes (Dos Remedios et al, 2003):

- Monomer-binding proteins; sequester G-actin and prevent its polymerisation.
- MF depolymerising proteins; induce conversion of F- to G-actin.
- Capping proteins; bind to the ends of MF to prevent addition and loss of monomers.
- Severing proteins; bind to the sides of MFs and cut them into two pieces.
- Cross-linking proteins; form dimers or have at least two binding sites for actin thus can form MF bundles, branched networks and 3D networks.
- Stabilising proteins; bind to the sides of MFs and prevent their depolymerisation.
- Motor proteins; use MFs as tracks to move along.

Many of the ABPs identified in mammals and yeast also have homologues in plant cells. The primary sequence of these ABPs is reasonably well conserved but biochemical analysis has shown that their specific activities vary significantly from their mammalian and yeast counterparts (Staiger & Blanchoin, 2006). There are a large number of ABPs identified to date, in 2003 Dos Remedios et al counted 162 distinct and separate ABPs. Table 1 provides an overview of the function of the main ABPs that have also been identified in plants. Only a few selected ABPs that form some of the work of this thesis will be discussed in detail here. These include: profilin, ADF, CAP and fimbrin.

Table 1.1. An overview of the function of several key ABPs

ABP	Description	Function	References
AIP1 (Actin Interacting Protein)	A WD-repeat protein	<ul style="list-style-type: none"> • Binds to and depolymerises F-actin • AIP enhances the activity of pollen ADF • Binds to the barbed ends of actin filaments to prevent elongation • AIP1 knockdown plants have severe developmental abnormalities, whereas null mutants in other organisms exhibit more minor phenotypes 	<p>Aizawa et al (1999) Allwood et al (2002) Amberg et al (1995) Ketelaar et al (2004a) Okada et al (1999) Ono (2003) Rodal et al (1999)</p>
ADF / Cofilin (Actin Depolymerising Factor)	A relatively small (15-19 kDa) actin binding protein found in virtually all eukaryotic cells.	<ul style="list-style-type: none"> • Binds both G & F-actin & enhances actin dynamics by severing actin filaments & increasing depolymerisation from the pointed end • ADF activity can be influenced by several factors: <ul style="list-style-type: none"> ➢ Phosphorylation, decreases the activity. ➢ PIP & PIP₂ binding, inhibits activity ➢ pH, high pH = severs actin filaments, low pH = binds F-actin • In tip growing cells ADF plays important role in regulating actin dynamics • Capable of nucleating actin at very high concentrations of ADF to actin. 	<p>Allwood et al (2002) Andrianantoandro & Pollard (2006) Bamburg et al (1980) Chen et al (2002) Hayden et al (1993) Hawkins et al (1993) Kusano et al (1999) Lovy-Wheeler et al (2006) Nishida et al (1984) Ressad et al (1998) Smertenko et al (1998; 2001) Yonezawa et al (1985; 1990; 1991)</p>
ARP2/3 complex (Actin Related Protein)	A stable complex of 2 actin related proteins (Arp2 and Arp3) with 5 other subunits named according to their size	<ul style="list-style-type: none"> • Caps the pointed end of actin filaments • Nucleates assembly of actin filaments in the barbed end direction as 70° branches from the mother filament • Nucleation activity is stimulated by the WASp/Scar family of proteins 	<p>Machesky & Gould (1999) Machesky & Insall (1998) Machesky et al (1994) Mullins et al (1998)</p>
CAP/Srv2p (Cyclase-associated protein)	A Subunit of adenylyl cyclase complex in yeast.	<ul style="list-style-type: none"> • Actin monomer sequestering protein • Inhibits polymerisation from both barbed and pointed ends • 1:1 binding with actin • Interaction of CAP with actin is inhibited by PIP₂ • In plants, CAP acts as a nucleotide exchange factor • Involved in species-specific signalling pathways • Linked to apoptosis via Ras signalling in yeast 	<p>Barrero et al (2002) Chaudhry et al (2007) Deeks et al (2007) Fedor-Chaikin et al (1990) Field et al (1990) Freeman et al (1995) Gieselmann & Mann (1992) Gottwald et al (1996)</p>

ABP	Description	Function	References
<p>Capping Protein (CP) (also known as: CapZ or β-actinin from vertebrate muscle and cap32/34 from <i>Dictyostelium</i>)</p>	<p>Heterodimer: α & β subunits that share extensive homology. Both required for capping activity but only β involved in actin binding</p>	<ul style="list-style-type: none"> • Binds tightly to the barbed end of actin filaments and prevents addition or loss of actin subunits • Act as a nucleator for further elongation by interacting with 2 actin subunits at once • <i>Arabidopsis</i> CP (AtCP) activity is not affected by calcium but it is sensitive to PIP₂. • AtCP is regulated by phosphatidic acid, PA inhibits the barbed end binding and nucleation activities of CP → increases in F-actin levels • Thought to be a major regulator of actin dynamics in plant cells - responsible for maintaining a large pool of free actin and small population of F-actin (together with profilin). 	<p>Amatruda et al (1990) Huang et al (2003; 2006) Schafer et al (1996)</p>
<p>Fimbrin (also known as Sac6 in yeast)</p>	<p>A member of the calponin homology (CH) domain superfamily of actin cross-linking proteins</p>	<ul style="list-style-type: none"> • Actin filament bundling protein, creates bundles with the same filament polarity • Can be regulated by pH • Some fimbrins are regulated by calcium, although <i>Arabidopsis</i> fimbrin (AtFim1) is calcium insensitive • AtFim1 protects actin filaments against profilin-induced depolymerisation 	<p>Bretscher & Weber (1980) Bretscher (1981) Glenny et al (1981) Kovar et al (2000b) Matsudairia & Burgess (1979) Pollard & Cooper (1986)</p>
<p>Formins</p>	<p>Ubiquitous, conserved proteins, defined by their formin homology domain 2 (FH2) and a proline-rich formin homology domain 1 (FH1).</p>	<ul style="list-style-type: none"> • Stimulate <i>de novo</i> actin nucleation and extension from the barbed ends • Can nucleate actin filaments from free actin monomers, or those bound to profilin • Capable of bundling actin filaments • Interact with MTs as well as with actin • Bind to barbed ends and prevent actin depolymerisation & partially protect this end from other proteins that would otherwise terminate barbed end growth • <i>Arabidopsis</i> FORMIN1 (AFH1) plays a central role in the initiation and organization of actin cables from the pool of actin monomers bound to profilin • Unlike other formins, AtFH1 is a 'non-processive' formin which moves to the sides of filaments to nucleate further filaments • Divided into 2 subgroups depending on the presence or absence of a predicted transmembrane domain • Over expression of actin nucleating domain of AtFH1 increases the number of actin cables in tobacco pollen tubes • Some formins are regulated by the Rho-family GTPases. 	<p>Bartolini et al (2008) Deeks et al (2002) Evangelista et al (2002) Lew (2002) Michelot et al (2006) Michelot et al (2005) Pruyne et al (2002) Sagot et al (2002) Wallar & Alberts (2003)</p>

ABP	Description	Function	References
Gelsolin	A protein composed of 6 conserved 125-150 amino acid gelsolin-homology domains (called G1-G6)	<ul style="list-style-type: none"> • Calcium-stimulated actin filament severing activity • Nucleates polymerisation of actin filaments • Can tightly cap barbed ends which only allows extension from the pointed end of filaments • Enhances profilin-mediated F-actin depolymerisation under high calcium concentration 	<p>Dos Remedios et al (2003) Huang et al (2004) McGough et al (2003)</p>
Myosin	A molecular motor protein composed of a head (motor/ATPase) domain, a regulatory neck domain and a tail domain which specifies function	<ul style="list-style-type: none"> • Interacts with actin and uses hydrolysis of ATP to drive the movement of myosin along the actin filament which transports organelles and vesicles within the cell • <i>Arabidopsis</i> class VIII myosins are predicted to be associated with the plasma membrane and plasmodesmata • <i>Arabidopsis</i> class XI myosins (close relatives of fungal & mammalian class V myosins) are predicted to be involved in organelle transport • Myosins have been identified in pollen tubes and are involved in the movement of organelles, vesicles and the male germ unit • Rab proteins probably regulate the association of myosins to plant organelle membranes and consequently regulate the activity of the motor proteins 	<p>Hashimoto et al (2005; 2008) Heslop-Harrison & Heslop-Harrison (1989) Liebe & Menzel (1995) Lovy-Wheeler et al (2007) Nebenfuhr et al (1999) Reisen & Hanson (2007) Reichelt et al (1999) Tang et al (1989) Van Gestel et al (2002)</p>
Profilin	An abundant, low molecular weight protein	<ul style="list-style-type: none"> • Binds specifically to monomeric actin • Highly abundant, cytoplasmic protein, typically existing in a 1:1 molar concentration with actin • When bound to profilin, G-actin cannot incorporate at the pointed end of the actin filaments or nucleate, but incorporation at the barbed end continues at the normal rate. • Sequestering action of profilin allows cells to maintain a high level of actin monomers without risking spontaneous nucleation or filament extension • Formins are designed to exploit actin monomers bound to profilin • The binding of profilin to actin is inhibited by the phospholipids PIP and PIP₂. • Acts as a nucleotide exchange factor for actin monomers (except in plants) • Over expression in plants can cause actin polymerisation or depolymerisation depending on the cell type 	<p>Carlsson et al (1977) Goldschmidt-Clermont et al (1990; 1991) Haarer & Brown (1990). Pantaloni & Carlier (1993) Perelroizen et al (1996) Pollard & Cooper (1986) Staiger & Blanchoin (2006) Staiger et al (1994) Valenta et al (1991 & 1992) Wang et al (2005)</p>

ABP	Description	Function	References
Villin	A protein with a core of 6 gelsolin subdomains and a villin headpiece at the C-terminus	<ul style="list-style-type: none"> • Bundles actin filaments in a unipolar fashion • Plant villins from lily (135-ABP & 115-ABP) bundle actin filaments in a calcium/calmodulin dependent manner • 135-ABP also severs and caps filaments in a calcium dependent manner • <i>Arabidopsis</i> villin 1 (AtVLN1) bundles filaments but is not regulated by calcium and lacks filament severing, capping and nucleating activities. • Localises to actin cables in pollen tubes & root hairs 	Huang et al (2005) Klahre et al (2000) Nakayasu et al (1998) Yokota et al (1998; 2005)

1.2.1.3.1) Profilin

Profilin is a low molecular weight (12-14 kDa) actin monomer binding protein. It was first identified in calf spleen (Carlsson et al, 1977) and later in plant cells as a pollen allergen (Valenta et al, 1991; 1992). Profilins are one of the most highly expressed of the cytoplasmic proteins (20-100 μ M, Buss et al, 1992) and are found throughout the cytoplasm. The profilins of animals and fungus have several functions but primarily they bind to monomeric actin with high affinity (Perelroizen et al, 1996) and promote nucleotide exchange (ADP to ATP) in monomers released from the MFs (Goldschmidt-Clermont et al, 1991). Profilin can also increase actin MF turnover in the presence of ADF/cofilin, by adding ATP-G-actin to the barbed end of the filament while ADF dissociates ADP-G-actin from the pointed end (Didry et al, 1998). Profilin is also involved in maintaining a pool of ATP-G-actin in the cell by preventing ATP hydrolysis (Ampe et al, 1998). This ensures that the actin is ready for polymerisation, as it has a high affinity for the growing barbed end of the MF and profilin can then enhance polymerisation by transporting G-actin to these barbed ends (Dos Remedios et al, 2003). Profilin can act to prevent spontaneous nucleation of filaments and also sequesters

actin monomers when the barbed ends of filaments are capped (Pantaloni & Carlier, 1993). The dissociation of profilin from actin is stimulated by the phospholipids phosphatidylinositol 4-phosphate (PIP) and phosphatidylinositol 4,5-bis-phosphate (PIP₂) (Goldschmidt-Clermont et al, 1990) which suggests that profilin may play a role in transmitting signals from the cell membrane to the actin cytoskeleton (Dos Remedios et al, 2003).

Plant profilins are also massively abundant, typically at a 1:1 ratio with total actin (Staiger & Blanchoin, 2006) with pollen having a profilin concentration of greater than 100 µM (Gibbon et al, 1999; Snowman et al, 2002). However, plant profilins do have slightly different properties compared to their mammalian counterparts. They still bind with high affinity to monomeric actin, which prevents spontaneous nucleation of new MFs and prevents assembly at the pointed end of existing MFs. They also shuttle G-actin to the barbed ends of filament to enhance assembly and maintain a pool of G-actin in the cytoplasm when the barbed ends are capped (Staiger & Blanchoin, 2006). The main difference is that plant profilins are unable to catalyse the ADP to ATP nucleotide exchange that occurs in other organisms (Perelroizen et al, 1996; Kovar et al, 2001a). This has led to alternative hypotheses for how ADP-actin is catalysed to ATP-actin ready for polymerisation. One idea is that the endogenous nucleotide exchange rate of plant actin is fast enough and therefore does not require an exchange factor (Kovar et al, 2001a). However, recently it has been found that another ABP, called CAP (see below), is able to stimulate the nucleotide exchange on actin monomers, which are then passed onto profilin where they can be reincorporated into growing actin filaments (Chaudhry et al, 2007).

1.2.1.3.2) Actin-depolymerising factor (ADF)

Actin depolymerising factor (ADF)/Cofilin are actin binding proteins that regulate polymerisation and depolymerisation of F-actin. ADF was first identified from embryonic chick brain extracts as a protein that depolymerised actin filaments and formed a 1:1 complex with G-actin (Bamburg et al, 1980). Cofilin was later purified from porcine brain because it had the ability to co-sediment with F-actin rather than depolymerise it (Nishida et al, 1984). It was later shown that ADF and cofilin each had the ability to both depolymerise, and bind to, F-actin and the degree of depolymerising ability was regulated by pH (Yonezawa et al, 1985; Hayden et al, 1993; Hawkins et al 1993) ADF/cofilins were subsequently identified from many eukaryotic cells (reviewed in Bamburg, 1999) and have a molecular weight of ~18 kDa. In the literature ADF/cofilin proteins are generally considered to be isoforms with similar activity and the names are often used interchangeably. For example, in plants these proteins are referred to as ADFs even though the *A. thaliana* ADF1 sequence shares 31% identity with both human ADF and mouse cofilin (Bamburg, 1999). Plant ADF was first identified in 1993 during a search for pollen specific transcripts in lily and later, from *Brassica napus* (Kim et al 1993). Plant ADF isoforms can be split into two groups: the pollen-specific isoforms and the vegetative tissue isoforms. The amino acid sequences of pollen-specific ADF from different species shows greater identity than ADF sequences taken from different tissues within the same plant (Lopez et al, 1996). ADF/Cofilins are able to bind to both G- and F-actin, with a preference for ADP-actin (Carrier et al, 1997). ADF is involved in the ‘treadmilling’ of actin MFs by increasing the off rate of monomers at the pointed end of the MF without altering the off rate at the barbed end (Dos Remedios et al, 2003). This releases G-actin into the cytoplasm where it can be incorporated into the barbed end of the filament. ADF can sever MFs and also cause depolymerisation of MFs by the same method as treadmilling if there is a

capping protein (e.g. CapZ) blocking the barbed end, preventing the reincorporation of the monomers. ADF is also capable of nucleating actin polymerisation at very high concentrations of ADF vs. actin (Andrianantoandro & Pollard, 2006). ADF can rapidly depolymerise and sever actin filaments at a high pH and bind F-actin under more acidic conditions (Yonezawa et al, 1985; Hayden et al, 1993; Hawkins et al, 1993). When bound to F-actin, ADF lies along the outside of the filament making contacts with the upper actin monomer (towards the minus end) and the bottom actin monomer. The 1:1 binding of ADF to actin subunits causes a change in the rotation of a decorated actin filament by $3\text{-}5^{\circ}$ (McGough et al, 1997). This twist in the F-actin removes the phalloidin site so that F-actin structures with ADF bound can not normally be visualised using fluorescently tagged phalloidin. The activity of ADF can be modulated via pH (as mentioned above), phosphorylation, phosphoinositides and other ABPs (reviewed in Bamburg, 1999). For example, the binding of ADF/cofilin to F-actin occurs more rapidly when the F-actin is capped by gelsolin compared to F-actin alone (Ressad et al, 1998) and the binding of tropomyosin to F-actin competitively inhibits ADF/cofilin binding and depolymerisation of the actin in vertebrates (Bernstein & Bamburg, 1982; Bamburg & Bernstein, 1991). Phosphorylated ADF has a 20-fold decrease in its affinity for actin (Ressad et al, 1998) but its activity can be restored by dephosphorylation (Agnew et al, 1995). The membrane lipids PIP and PIP₂ are able to inhibit ADF/cofilin activity by binding to the actin-binding domains of the proteins, thus preventing ADF/cofilin from binding to actin (Yonezawa et al, 1990; 1991, Kusano et al, 1999).

The general biochemical properties of ADF are also conserved in plant cells but ADF is more abundant in plants compared to other eukaryotes (Staiger & Blanchoin, 2006). The activity and localisation of ADF in pollen tubes has been investigated (Lovy-Wheeler et al, 2006;

Allwood et al, 2002; Smertenko et al, 2001; Chen et al, 2002). ADF appears to have a predominately cytoplasmic localisation, although some association with F-actin has been seen, especially around the actin collar (Chen et al, 2002). The pollen ADF from lily (LIADF1) is not regulated by phosphorylation but by co-operation/association with another protein AIP1 (Allwood et al, 2002), demonstrating not all ADFs have their activity regulated by phosphorylation. It has been proposed that the pH sensitivity of ADF regulates pollen tube growth (Lovy-Wheeler et al, 2006). The proposed model is that an increase in pH in the sub-apical region (the alkaline band) stimulates the severing activity of ADF, which in turn generates new ends for actin polymerisation and therefore pollen tube growth as described in **Section 1.2.1.2.**

1.2.1.3.3) Cyclase-associated protein (CAP)

Cyclase-associated protein (CAP), which is also known as Srv2p in yeast, is an actin-monomer binding protein of ~50 kDa (Gieselmann and Mann, 1992; Freeman et al, 1995). It was first identified in yeast as a subunit of the cAMP-generating adenylyl cyclase complex which facilitated cyclase activation by Ras (Fedor-Chaiken et al, 1990; Field et al, 1990). Mutational analysis revealed that *S. cerevisiae* cells that were deficient for CAP exhibited defects in signalling and had an altered cell shape, indicating a dual function for CAP. The CAP protein was found to have two distinct domains: an N-terminal region which binds adenylyl cyclase and a C-terminus which binds monomeric actin (Gerst et al, 1991). In complementation studies, the CAP proteins of the yeast *S. pombe* and mammalian CAP could only suppress the cytoskeleton-related morphological defects in *S. cerevisiae* associated with the loss of the C-terminal domain, and not the signalling properties associated with the N-

terminus (Kawamukai et al, 1992; Matviw et al, 1992; Vojtek & Cooper, 1993; Zelicof et al, 1993; Yu et al, 1994). These results suggest that the function of the C-terminus is highly conserved throughout evolution but the N-terminus seems to function in its own species-specific signalling pathways (Hubberstey & Mottillo, 2002). A recent study by Gourlay & Ayscough (2006) demonstrated CAP/Srv2p was the link between alterations in the actin cytoskeleton and apoptosis via Ras signalling. Plants do not have Ras and therefore cannot use the same signalling cascade as yeast. Nevertheless, Deeks et al (2007) have shown that *Arabidopsis* plants mutant for CAP1 do not have co-ordinated organ expansion, suggesting that AtCAP1 functions in plant-specific signalling pathways. CAP has been shown to localise to the leading edge of motile cells and is negatively regulated by PIP₂ (Gottwald et al, 1996).

The CAP1 protein from *Arabidopsis* is a highly abundant cytoplasmic protein with a 1:3 M ratio with total actin in suspension cells and 1:7 M ratio in leaf cells (Chaudhry et al, 2007). Like other CAPs, AtCAP1 binds to monomeric actin and can suppress the cytoskeleton related defects caused in yeast strains deficient for CAP/Srv2p (Barrero et al, 2002) but there is evidence that it is not just a simple G-actin sequestering protein. For example, AtCAP1 does not have a preference for ADP-G-actin, like yeast CAP, but binds equally well to both ADP- and ATP-G-actin. It also has a modest ability to add actin onto the barbed ends of filaments (Chaudhry et al, 2007). AtCAP1, like human CAP1 (Moriyama & Yahara, 2002), has been shown to directly enhancing nucleotide exchange on actin by more than 60 fold, even in the presence of ADF/cofilin which normally inhibits this (Chaudhry et al, 2007). Based on these results a model has been proposed whereby ADF, CAP and profilin work in concert to increase actin dynamics (Chaudhry et al, 2007): ADF depolymerises the older ADP-bound ends of actin filaments. CAP then competes with ADF for the actin monomer and

stimulates the ADP for ATP nucleotide exchange. The ATP-actin monomer is then given to profilin which is able to shuttle the actin onto the end of growing filaments. *Arabidopsis* plants that are knock-out mutants for CAP1 have disrupted F-actin in a number of cell types (Deeks et al, 2007) and over-expression results in depolymerisation of F-actin in tobacco BY2 cells (Barrero et al, 2002). These studies support the important role of CAP in maintaining the correct organisation of the actin cytoskeleton in plants. It appears that plant CAP, like the CAP proteins from other organisms, has a dual role in signalling and cytoskeleton organisation.

1.2.1.3.4) Fimbrin

Fimbrin is an actin side-binding protein of ~77 kDa that falls into the fimbrin/plastin group of actin binding proteins. It was first identified from chicken intestinal cells (Matsudaira & Burgess, 1979) and was found to localise to F-actin structures in these, and other mammalian cells (Bretscher & Weber, 1980). It was later shown to be an F-actin bundling protein (Glenny et al, 1981; Bretscher, 1981). The yeast fimbrin, Sac6p, is 46 % identical to vertebrate fimbrin (Adams et al, 1991) and has been found to localise to both actin cables and actin patches (Drubin et al, 1988). A fimbrin from *Arabidopsis* has been cloned (AtFim1; McCurdy & Kim, 1998) and has also been shown to bind to and cross-link F-actin in a calcium independent manner (Kovar et al, 2000b) and associates with F-actin *in vivo* (Kovar et al, 2001b). Fimbrins are made up of an N-terminal calcium-binding domain, containing 2 EF-hands, followed by two highly conserved, tandemly arranged, actin binding domains (ABDs). The 2 ABDs allow fimbrins to function as monomers, binding actin filaments into tight bundles. The significance of the calcium-binding domain is unclear because not all fimbrins have their actin bundling ability inhibited by calcium. For example, chicken intestinal fimbrin was not

affected by up to 5 mM calcium (Bretscher, 1981) whereas the bundling activity of human L-plastin was reduced by 1 μ M calcium (Namba et al, 1992). The plant fimbrin AtFim1 shares the general organisation of animal fimbrins except that the N-terminal domain shares limited homology with the calcium binding domains of calcium-binding proteins such as calmodulin (McCurdy & Kim, 1998) and there is also an extra 65 amino acids on the C-terminal end, but the significance of this is not known (Kovar et al, 2000b). AtFim1 has also been shown to stabilise F-actin against profilin-induced depolymerisation both *in vitro* and *in vivo* (Kovar et al, 2000b).

1.2.2) The MT cytoskeleton

Microtubules (MTs) are hollow cylinders of about 25 μ m in diameter (**Fig. 1.4**). They consist of α - and β - tubulin subunits, each with a molecular weight of \sim 50 kDa. These subunits associate to form heterodimers which polymerise to form long protofilaments. The staggered assembly of 13 protofilaments forms the wall of the cylindrical structure of the MT. Elongation of the MT is achieved by addition of tubulin heterodimers to the ends of the protofilaments. The association of heterodimers to form protofilaments requires GTP to be bound to both the α - and β -tubulin subunits. Like actin MFs, MTs are polarised structures, having both a plus and a minus end. Although both ends are capable of addition and loss of subunits, net growth of the MT occurs at the plus end while net shortening occurs at the minus end. After incorporation of the dimer into the MT, the GTP bound to the β -tubulin monomer is hydrolysed but the GTP bound to the α -tubulin, which is at the α - β dimer interface, is never hydrolysed or exchanged (Erickson & Obrien, 1992). A GTP cap forms on MTs whose rate of dimer addition exceeds the rate of GTP hydrolysis. MTs with a GTP cap are stable and, provided there is sufficient free GTP-associated tubulin, these can serve as primers for further

MT polymerisation. MTs that have a GDP-tubulin at the plus end are unstable and the MT end peels apart to release the MT heterodimers. Polymerised MTs exist in a state of *dynamic instability*, in which a MT alternates between a period of growth and a period of shrinkage. If a MT suddenly changes from net growth to rapid depolymerisation this is known as *catastrophe*. A change from shrinkage to net growth is known as *rescue*. If there is a balance between addition of subunits at one end and loss at the other, this is termed *treadmilling*.

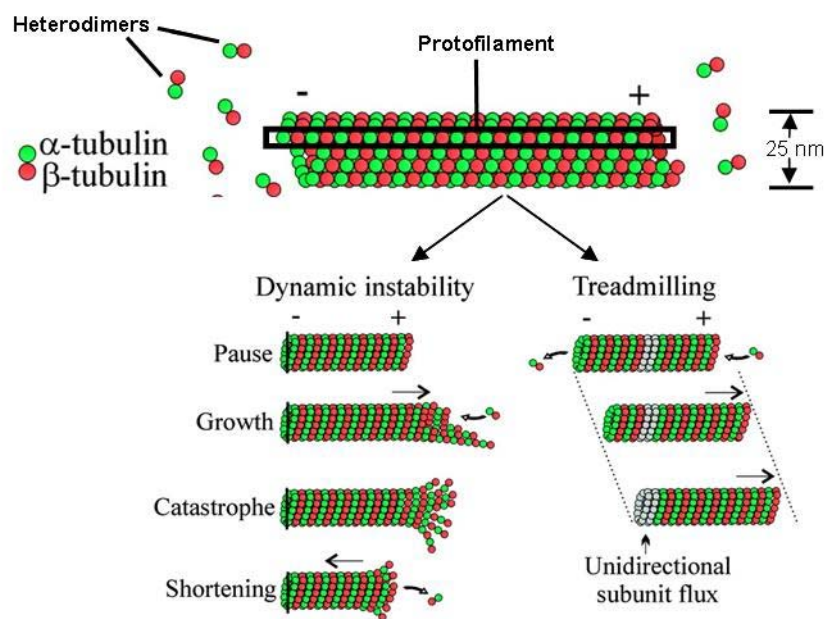


Figure 1.4. Microtubule organisation and assembly dynamics.

α - and β - tubulin heterodimers associate to form protofilaments. MTs are composed of 13 protofilaments that form a cylindrical structure of 25 nm with a plus (β -tubulin) and a minus (α -tubulin) end. Tubulin heterodimers are added preferentially at plus end and are lost at the minus end in a process called 'treadmilling'. When the MT minus end is anchored only the plus end is dynamic and this goes through phases of growth and rapid shrinkage, in a process termed 'dynamic instability'.

Figure adapted from Dixit & Cyr (2004a).

1.2.2.1) The role of the MT cytoskeleton

MTs, like actin MFs, are responsible for various cell movements and maintaining cell structure. MT motor proteins such as dynein and kinesin move vesicles and organelles along the tracks provided by the MTs in the cytosol of the cell. Specialised cellular structures like flagella are composed of MTs and these are used to propel cells through aqueous substances. MTs are also very important during mitosis and meiosis where they are involved in the separation of the chromosomes using a specialised MT array called the mitotic spindle. Although MTs are found throughout the eukaryotic kingdoms, the arrays that they form and the functions they carry out in plants differs greatly from MTs in animal or fungal cells. This difference is due to the presence of a cell wall in plant cells (Wasteneys, 2002). In many animal cells tubulin subunits are nucleated and polymerised into MTs with the aid of a specialised structure called a centrosome. The centrosome anchors the minus-ends of the MTs, which protects them from depolymerisation, and results in a radial array of MTs with the same polarity. Plant cells do not have centrosomes and the MTs are dispersed over the cortex of the cell (reviewed in Lloyd & Chan, 2004). In plants, the nuclear surface has been shown to be a MT nucleation site (Stoppin-Mellet et al, 1994; Schmit, 2002) and more recently, MTs have been seen to be nucleated at the cell cortex using GFP-tagged tubulin, where both the plus and minus ends exhibited dynamics (Shaw et al, 2003). Additionally, a proposed component of the MT organising centre (AtSpc98) has been shown to co-localise with γ -tubulin at the nuclear surface, where MTs originate, and has also been localised to the plasma membrane of *Arabidopsis* cells (Erhardt et al, 2002) providing further evidence for MT nucleation at the plant cell cortex. The resulting treadmilling MTs then self-organise when they interact or collide with one another to form structures such as parallel bundles, which can be stabilised by cross-linking proteins such as MAP65 (Chan et al, 1999), or they

can be severed by a katanin protein (McNally & Vale, 1993) to produce new MTs that can then travel in a different direction (Dixit & Cyr, 2004b; Chan et al, 2007; Wightman & Turner, 2007; Lloyd & Chan, 2008). The cortical MTs of plant cells are attached to the plasma membrane by protein bridges and one of these proteins has been identified as the 90 kDa phospholipase D (Gardiner et al, 2001; Marc et al, 1996). The cortical MTs also play an important role in determining cell shape. This is because the MTs form the tracks along which the cellulose synthase machinery moves as it deposits cellulose microfibrils into the cell wall to give the cell wall its rigidity (Paredez et al, 2006). MTs and cellulose are normally orientated perpendicular to the axis of cell growth so that directional cell growth is facilitated. The plant MT cytoskeleton forms four distinct arrays that are not present in other organisms and are involved in the development of the cell wall (reviewed in Wasteneys, 2002). These are shown in **Figure 1.5**, along with the mitotic spindle which is a conserved feature used to separate chromosomes in dividing cells. In a cell about to undergo a mitotic division a preprophase band (PPB) composed of MT bundles is formed, generally in the midplane of the cell (**Fig. 1.5a**). The position that the PPB is formed in the cell denotes the eventual site of cell plate attachment. This MT array is disassembled and the mitotic spindle is formed when the nuclear envelope disintegrates (**Fig. 1.5b**). After chromosome separation by the spindle, at the anaphase-telophase transition, the MTs reform into the bipolar phragmoplast (**Fig. 1.5c**). This MT array directs vesicles carrying new cell membrane and wall material towards the centrifugally expanding cell plate which matures into the cross-wall that separates the two daughter cells (**Fig. 1.5d**). After cell division is complete and the cells enter interphase, the MTs form a transient perinuclear array (**Fig. 1.5e**) before returning to the cortex of the cell where they are organised into bundles that are perpendicular to the axis of growth (**Fig. 1.5f**).

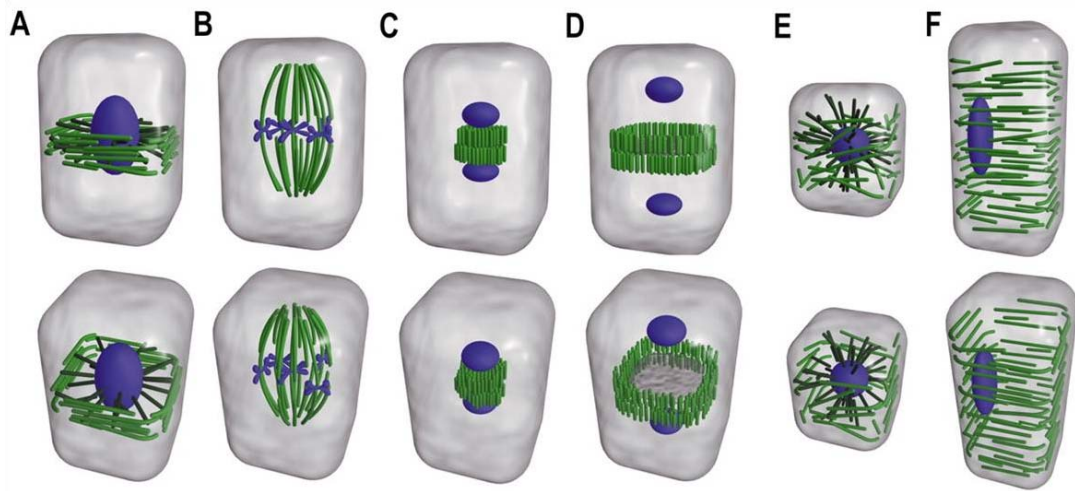


Figure. 1.5. Plant MT arrays during the cell cycle

(A) MTs form a preprophase band, which marks the future site of cell division and is linked to the nucleus by phragmosome microtubules. (B) The mitotic spindle. (C) During telophase MTs form the phragmoplast between the two daughter nuclei. (D) During cytokinesis the phragmoplast expands out towards the cell cortex allowing the cell plate to form in the position predicted by the preprophase band. (E) Following completion of cytokinesis, MTs radiate from the nucleus to the cortex and some begin to appear at the cell membrane. (F) Interphase cells have MTs arranged in parallel arrays that run perpendicular to the axis of growth.

Figure taken from Wasteneys (2002).

1.2.2.2) The MT cytoskeleton in tip-growing cells

The MT cytoskeleton of pollen tubes has been visualised in several species using immunolocalisation (Raudaskoski et al, 1987; Heslop-Harrison et al, 1988; Lovy-Wheeler et al, 2005; Gossot & Geitmann, 2007) and more recently using live-cell imaging (Cheung et al, 2008). The MTs are arranged into cortical longitudinal bundles in the shank of the pollen tube with shorter, more disorganised MTs in the sub-apex and no MTs visible in the tip. The dynamics of the MTs differ within the sub-populations: the sub-apical MTs are very dynamic, occasionally entering into the tip region, whilst the cortical MTs exhibit a relatively stable association with the cortex, although they too increase and decrease in length (Cheung et al, 2008). The MT cytoskeleton, unlike actin MFs, is not required for pollen tube growth *in vitro*. When MTs are depolymerised, using drugs such as colchicine and oryzalin, tube elongation is inhibited only when these agents are applied at very high concentrations, and even then the disruption is not as marked as treatment with cytochalasins (Pierson & Cresti, 1992; Joos et al, 1994; Laitainen et al, 2002). *In vitro* depolymerisation of the cortical MTs of *Nicotiana sylvestris* and *N. tabacum*, resulted in a disorganisation of the cytoplasm with vacuolisation occurring in the tip region and random positioning of the vegetative nucleus and generative cell within the pollen tube, suggesting movement of the GC/VN complex is dependent on MTs. MTs have also been implicated in maintaining directional growth in pollen tubes (Gossot & Geitmann, 2007). Similar experiments carried out *in vivo* on the other hand did show MTs of the vegetative cell to be necessary for pollen tube growth in the style (Joos et al, 1995) so their exact role in pollen tube growth has not yet been determined.

Root hairs are thought to elongate by a similar mechanism of tip growth as pollen tubes and share a comparable arrangement of MTs. Although, like in pollen tubes, MTs are not

absolutely required for root hair growth, root hair growth is slowed or occurs in a wavy pattern when the MT cytoskeleton is depolymerised or stabilised (Bibikova et al, 1999; Sieberer et al, 2002; Ketelaar et al, 2002). This suggests that MT dynamics are also involved in growth direction regulation in root hairs. The MTs of leguminous root hairs, although not required for growth, play an essential role in the initiation of the symbiosis between the legume and rhizobacteria by directing the curling of the root hair around the bacteria (Sieberer et al, 2005).

Although it appears MTs may not be important for angiosperm pollen tube growth, they are required for successful growth of gymnosperm pollen tubes. Gymnosperm pollen tubes have a dense mesh-work of MTs in the tip and MT-interfering drugs partially inhibit growth, resulting in swollen and sometimes branched tips and shorter tubes (Anderhag et al, 2000). MTs are also necessary for the pollen tube to achieve its main function: the delivery of the sperm cells into the ovary so fertilisation can occur. The generative cell (GC) needs to go through a mitotic division to form the two sperm cells and therefore requires MTs. The MTs of the GC are also involved in maintaining the ellipsoidal shape of the GC, which aids the gamete movement inside the pollen tube (Heslop-Harrison et al, 1988; Tiezzi, 1991; Cai et al, 2005a). Treatment of pollen tubes with MT antagonists results in a significantly slower transport of the GC in the pollen tube. This suggests that the MTs of the vegetative cell do play a role in this process, although actin alone is able to move the GC/VN complex albeit much slower than normal (Åström et al, 1995).

While MTs are not required for pollen tube growth or cytoplasmic streaming *in vitro*, it has recently been reported that mitochondria and Golgi bodies can travel along MTs in *in vitro*

motility assays (Romagnoli et al, 2003; 2007). Several kinesin-like MT motor proteins have been identified in pollen (Cai et al, 2000) which has led to the idea that MTs and F-actin may co-operate in the movement of vesicles and organelles during pollen tube growth. Cai and Cresti (2009) proposed a speculative model whereby the organelles are transported rapidly along the F-actin, using myosin motors, but are then stopped in specific sites where the kinesin motor uses MTs to finely position the organelle in the cell. As MTs depolymerisation was seen to have an adverse effect on pollen tube growth *in vivo* (Joos et al, 1995) but not *in vitro* it has been hypothesised that the organelle and vesicle transport along MTs may play an important role *in vivo* when pollen tube growth is at its most rapid (Joos et al, 1995).

1.2.2.3) Microtubule-associated proteins (MAPs) in plants

The plant MT cytoskeleton is a highly dynamic structure that requires the assembly and disassembly of distinct MT arrays throughout the cell cycle. The proteins which orchestrate the construction of these structures are called microtubule-associated proteins (MAPs). Plant MAPs have been classified into two different classes: 1) proteins that regulate MT assembly and disassembly and 2) proteins involved in MT organisation and functions based on MTs (e.g. transport) (Hamada, 2007). **Table 1.2** shows some of the key MAPs identified and studied in plant cells.

Table 1.2. An overview of the function of several key MAPs from plants

MAP	Description	Function	References
EB1	End-binding protein 1 A plus-end tracking protein	<ul style="list-style-type: none"> • Binds the plus ends of MTs • Also marked foci at the minus end of MTs • Suggested it is involved in the binding of MTs to other structures • Localises to stabilised regions of MTs • Localised to endomembranes, could be involved in movement of these structures • Increases MT rescue and decrease catastrophe in <i>Xenopus</i> 	<p>Chan et al (2003; 2005) Mathur et al (2003) Hamada (2007) Tirnauer et al (2002)</p>
Katanin	At present the only MAP involved in MT depolymerisation identified in plants.	<ul style="list-style-type: none"> • Animal katanin is composed of p60 and p80 heterodimers • The <i>Arabidopsis</i> p60 subunit has been identified and shown to have MT severing activity • Involved in the disassembly of the different MT arrays formed during the cell cycle. 	<p>McNally & Vale (1993) Burk et al (2001) Bouquin et al (2003) Burk & Ye (2002) Stoppin-Mellet et al (2002)</p>
Kinesin	MT motor proteins containing a highly conserved ~350 amino acid motor domain	<ul style="list-style-type: none"> • 61 kinesin genes identified in <i>Arabidopsis</i>, much more than in other species • Of the 14 kinesin families based on animal/yeast kinesin, 3 are missing from plants • Can be plus- or minus-end directed motors • Some kinesins can interact with MTs and F-actin e.g. GhKCH1 from cotton • May be involved in spatial control of cytokinesis 	<p>Richardson et al (2006) Muller et al (2006) Preuss et al (2004) Reddy & Day, (2001) Lee & Liu (2004)</p>
MAP65	There are 9 members of the MAP65 family of proteins in <i>Arabidopsis</i> Mass: 54-80 kDa	<ul style="list-style-type: none"> • Bind to and bundle MTs • Stabilise MTs • Overexpression causes unusually thick MT bundles • MAP65-1 co-localises with cortical MTs, the preprophase band and the midzone of the spindle and phragmoplast (where anti-parallel MTs overlap) • Other MAP65 family members localise to different MT structures • Can form dimers • MAP65-1 is regulated by phosphorylation 	<p>Jiang & Sonobe (1993) Hussey et al (2002) Van Damme et al (2004a & b) Mao et al (2005) Smertenko et al (2000; 2004; 2006) Chang et al (2005) Hamada (2007) Wicker-Planquart et al (2004)</p>
MOR1/ GEM1/ MAP200	<i>Arabidopsis</i> microtubule organisation 1 (MOR1) or gemini (GEM1) and Tobacco 200 kDa protein (MAP200) Members of the MAP215 family	<ul style="list-style-type: none"> • Involved in activating the dynamic instability of MTs • Thought to participate in MT nucleation, • Increase polymerisation and shrinkage speed • Increase catastrophe and rescue frequency • Shown to localise with MTs at all stages of the cell cycle 	<p>Whittington et al (2001) Hamada (2007) Hamada et al (2004) Kawamura & Wasteneys (2008) Twell et al (2002)</p>
PLD	Phospholipase D A 90 kDa protein	<ul style="list-style-type: none"> • There are 12 PLD genes in <i>Arabidopsis</i> • Co-localises with cortical MTs • Links MTs to the plasma membrane • Activation of PLD causes MT release from the membrane & depolymerisation 	<p>Marc et al (1996) Gardiner et al (2001) Wang (2002) Dhonukshe et al (2003)</p>

1.3) Programmed Cell Death (PCD)

Programmed cell death refers to a mechanism of cell death that is part of the normal life of a multicellular organism. It involves the removal of redundant, misplaced or damaged cells in a regulated manner (Mittler & Lam, 1996; Raff, 1998; Woltering et al, 2002; Hoerberichts & Woltering, 2003) and it is essential for development and the correct maintenance of multicellular organisms. PCD is a genetically encoded cell suicide pathway involving proteins and enzymes that kill and dismantle the cell in an organised manner (Raff, 1998; Hoerberichts & Woltering, 2003). This is in contrast to cell death via necrosis. Necrosis occurs when the cell suffers from overwhelming stress resulting in swelling, organelles destruction and bursting of the cell which, in mammals, induces the inflammatory response (Kerr et al, 1972). However, necrosis is now not thought to be the passive, accidental form of cell death as it once was, but is also thought to be regulated (Henriquez et al, 2008). Apoptosis is a specialised form of PCD that occurs in animal cells and has been extensively studied. It is characterised by cell shrinkage, nuclear condensation, DNA fragmentation, caspase activation, membrane blebbing and production of 'apoptotic bodies' which consist of cytoplasm, organelles and sometimes nuclear fragments (Elmore, 2007). These bodies are quickly phagocytosed by surrounding cells to prevent an inflammation response and secondary necrosis (Elmore, 2007). There are two basic pathways for apoptosis. The first is the mitochondrial or intrinsic pathway and the second is the death receptor or extrinsic pathway (reviewed in Green, 2000). Both pathways involve the activation of a set of proteinases called caspases. Caspases are cysteine proteases which specifically cleave after an aspartic acid residue and act to accelerate the progression of cell death (Kumar, 2007).

In the intrinsic pathway, an apoptotic stimulus causes members of the BH3-only subfamily of Bcl-2 proapoptotic proteins, such as Bid (BH3-interacting domain death agonist), to interact with the Bax (Bcl-2-associated x protein) subfamily of proapoptotic proteins. This interaction causes Bax proteins to oligomerise and insert into the mitochondrial outer membrane (Desagher et al, 1999; Eskes et al, 2000). This increases the permeability of the membrane, releasing cytochrome *c*, AIF1 (apoptosis-inducing factor 1) and Endo G (endonuclease G) into the cytoplasm. In mammalian cells, cytochrome *c* induces the formation of the Apaf-1 apoptosome which recruits and activates procaspase-9, an initiator caspase. Caspase-9 can then activate the executioner caspase-3, which goes on to cleave cellular substrates. At present there are over 400 caspase substrates identified in mammals (Luthi & Martin, 2007).

The extrinsic pathway uses death receptors such as Fas or TNFR1 (tumour necrosis factor receptor 1) situated on the plasma membrane to induce apoptosis. When the death ligand binds the receptor, adaptor proteins are recruited to the receptor and these recruit procaspase-8 or -10 which become active and can go on to activate the executioner caspase-3, allowing apoptosis to proceed (Green, 2000).

1.3.1) Plant PCD

Plants have also evolved a cell death pathway that plays an important role in many processes such as development, senescence, and embryogenesis (reviewed in Beers 1997; Lam, 2004). Both abiotic and biotic stresses can also trigger PCD in plants for example, high temperatures (Qu et al, 2009), pathogen infection (Greenberg & Yao, 2004) and SI (**see Section 1.7.1.4**). Plant PCD shares some of the same characteristics of apoptosis such as DNA fragmentation, caspase-like activity and cytochrome *c* leakage from mitochondria. However, plant cells

undergoing PCD are not engulfed by other cells like in apoptosis, they are instead eliminated by autolysis and autophagy (Beers, 1997). The cell wall is probably responsible for this difference. In addition, the cell wall can hold the ‘corpse’ of the dead cell in place within the plant (Lam, 2004). This is necessary for the formation of xylem vessels which are formed by PCD of the tracheary elements and reinforcement of their secondary cell wall to allow transport of solutes and water throughout the plant (Fukuda, 2000).

Although plant cells undergoing PCD exhibit caspase-like activities, they do not contain orthologues of mammalian caspases in their genomes (Bonneau et al, 2008). Sequence analysis revealed a group of proteases, termed metacaspases, which share some sequence and structural similarity to caspases (Uren et al, 2000) and are present in plants. It was originally thought that these proteases might be responsible for the caspase-like activities found in plants but four separate studies have shown this is not the case (Watanabe & Lam, 2005; Bozhkov et al, 2005; He et al, 2007; Vercammen et al, 2007). Metacaspases in plants do not cleave caspase substrates and are also not inhibited by caspase inhibitors (Bonneau et al, 2008). In spite of the lack of caspase activity, metacaspases have been shown to play a role in some PCD pathways. For example, the PCD of suspensor cells of an embryogenic culture of *Picea abies* is inhibited when a type II metacaspase is downregulated (Suarez et al, 2004). One protease that does have caspase-1-like (YVADase) activity is the vacuolar processing enzyme (VPE). VPE was first identified as being involved in protein maturation processes in seed and leaf (Yamada et al, 2005). Virus-induced gene silencing and T-DNA knock out mutants of VPE have subsequently demonstrated that VPE is required for TMV-induced cell death (Hatsugai et al, 2004), developmental cell death in seed integuments (Nakaune et al, 2005), and fumonisin-induced cell death (Kuroyanagi et al, 2005). Another protease, termed

saspase, has been identified in oats (*Avena sativa*) and been shown to be indirectly involved in victorin-induced cleavage of Rubisco during PCD (Coffeen & Wolpert, 2004). Saspase is a serine protease that is able to cleave many caspase substrates and its activity is inhibited by caspase inhibitors (Coffeen & Wolpert, 2004). However, experiments investigating the specific inhibition of saspase have not yet been carried out, so it is not yet known how important this enzyme is for the progression of PCD.

To date many different caspase-like activities have been identified in plants, the most common being caspase-3-like (DEVDase) and caspase-1-like (YVADase) activity (reviewed in Bonneau et al, 2008). As mentioned in **Section 1.3**, mammalian caspases are separated into initiator and execution caspases. Initiator caspase activity (caspase-8 and -9) has not been detected in plants, suggesting a different mechanism of caspase activation during PCD of animals and plants (Bosch & Franklin-Tong, 2007). Future work in this area will therefore concentrate on trying to isolate and characterise the proteases that exhibit the caspase-like activities and try and fit them into PCD pathways in plants.

1.3.2) The cytoskeleton and PCD

The MT cytoskeleton has been implicated in apoptosis in animal cells, with many anti-cancer drugs inducing apoptosis by altering MT dynamics (Gajate et al, 2000; Mollinedo & Gajate, 2003). Apoptosis generally results when the MTs of the mitotic spindle are damaged or not formed correctly so that chromosome segregation is disrupted. This activates a checkpoint pathway that delays cell cycle progression until the problem can be remedied. If the situation cannot be fixed the cell is pushed into PCD (Sorger et al, 1997). This suggests that apoptosis does not occur because of a direct effect on the MTs themselves but rather due to mitotic

arrest (Moss & Lane, 2006). There is some evidence that a protein called Bim (Bcl-2-interacting mediator of cell death) might provide a direct link between MT dynamics/integrity and apoptosis (Puthalakath & Strasser, 2002). Bim, a member of the 'BH3-only' subgroup of pro-apoptotic proteins, is able to bind to the light chain of dynein (LC8), a MT motor protein, both *in vivo* and *in vitro* and gives rise to the possibility that Bim is sequestered onto the MTs. When Bim-LC8 dissociates from the dynein complex it activates Bax, a pro-apoptotic protein, which can then induce apoptosis (Puthalakath et al, 1999). This means that Bim could act to monitor MT integrity in the cell. Although an attractive hypothesis, direct proof that Bim is sequestered to MTs is required before it can be substantiated (Moss & Lane, 2006).

Even if alterations to MTs themselves do not trigger apoptosis there is evidence that MTs do play a role in the execution phase of apoptosis (Moss & Lane, 2006). Previously it was thought that actin and myosin II were responsible for the reorganisation of the cell that occurs during the execution phase of apoptosis while the MT cytoskeleton was lost in the early stages of this phase. Now it is thought that novel apoptotic MT arrays reform during the later stages of apoptosis which contribute to the disposal of nuclear and cellular fragments (Moss & Lane, 2006).

Several studies in plant cells have noted a reorganisation of the MT cytoskeleton in cells that are undergoing PCD (Binet et al, 2001; Smertenko et al, 2003). The study by Binet et al (2001) showed that the MT cytoskeleton of tobacco cells was rapidly and severely depolymerised by addition of cryptogin, an elicitor of the hypersensitive response, which then caused calcium-dependent cell death of the infected cell. However, the authors were unable to demonstrate a causal link between the observed MT depolymerisation and cell death

because the MT stabilising drug taxol was unable to suppress the MT depolymerisation induced by cryptogein. Work by Smertenko et al (2003) on the developmental PCD in *Picea abies* embryos also described reorganisation of the MT cytoskeleton that coincided with the beginning of the PCD execution pathway. Actin rearrangements were also observed and further work in this paper showed that although the MT and actin cytoskeletons are both important for embryogenesis, it is only the actin rearrangement that is necessary for the execution of embryonic PCD.

There is a large body of evidence emerging from the animal, fungal and plant kingdoms implicating actin dynamics in the regulation of programmed cell death (Franklin-Tong & Gourlay, 2008). In the mammalian Jurkat T-cells, F-actin stabilisation using Jasp rapidly induced apoptosis and an increase in caspase-3 activation (Posey & Bierer, 1999; Odaka et al, 2000). In the same cell line, drug-induced F-actin depolymerisation in cells already undergoing Fas-mediated (extrinsic) apoptosis, led to an enhanced execution phase of apoptosis (Morley et al, 2003). In murine cell lines, actin depolymerisation via cytochalasin D caused rapid release of cytochrome *c* from the mitochondria resulting in caspase activation and apoptosis (Paul et al, 2002). In ischaemic kidney cells, apoptosis can be triggered by the actin depolymerisation drug LatB and also inhibited by actin stabilisation with Jasp (Genesca et al, 2006). The studies in mammalian cells suggest that actin alterations influence apoptosis via different mechanisms, depending on the cell type. The outcome of altering the actin dynamics by stabilisation or depolymerisation may, in part, be due to the ratio of G-actin to F-actin within the cell as this varies greatly between cell types (Franklin-Tong & Gourlay, 2008). Therefore, stabilising F-actin in a cell that normally has low levels of polymer could

cause it to enter into apoptosis. Whereas the same treatment in a cell that already has high levels of F-actin may not have a great effect.

Budding yeast cells that have mutations in actin regulatory proteins, which result in stabilised actin aggregates, or have their F-actin stabilised by Jasp, have been shown to undergo a process termed ‘actin-mediated apoptosis’ (ActMAp) (Gourlay et al, 2004). ActMAp is thought to occur when there is an interaction between the actin cytoskeleton and the ‘Ras-cAMP-PKA’ (protein kinase A) signalling cascade which is involved in cell growth and proliferation in response to the environment (Thevelein & de Winder, 1999; Rolland et al, 2002). In the mutant lines exhibiting stabilised F-actin aggregates, there was hyperactivation of the Ras-cAMP-PKA signalling pathway which resulted in mitochondrial dysfunction and ROS accumulation (a marker of apoptosis) (Gourlay & Ayscough, 2005a;b; 2006). The ABP Srv2p/CAP was required for the F-actin aggregate formation and due to the ability of its N-terminal domain to bind to adenylate cyclase and facilitate cAMP/PKA activation, it is thought to be a link between Ras signalling and actin reorganisation (Gerst et al, 1991; Mintzer & Field, 1994; Gourlay & Ayscough, 2006). Thus, actin and an ABP have been shown to be involved in apoptosis in yeast.

In plant cells, actin alterations have also been implicated in PCD. As discussed in **Section 1.7.1.3** both stabilisation and depolymerisation of F-actin can trigger PCD in pollen and depolymerisation of F-actin is involved in SI-induced PCD (Thomas et al, 2006). The actin cytoskeleton has also been shown to be involved in the PCD associated with plant-pathogen interactions. For example, the HR cell death of potato triggered by infection with the fungus *phytophthora infestans* was suppressed when the potato was pre-treated with cytochalasin B

to depolymerise the F-actin (Tomiyama et al, 1982). Actin depolymerisation has been shown to accelerate and increase the level of HR-PCD in cryptogein elicitor-induced tobacco BY-2 cells (Higaki et al, 2007). Therefore it appears that, like in yeast and mammalian systems, both stabilisation and depolymerisation of F-actin can play a role in mediating PCD in plants.

1.4) Self-incompatibility

Many flowering plants are hermaphrodite, having both male and female organs on the same flower. This leads to a high probability of self-fertilisation if the plant does not have a mechanism to prevent this. Self-fertilisation creates problems for the plant because it decreases the genetic diversity of the offspring and thus decreases the fitness of the plant. A large proportion of angiosperms have developed mechanisms to avoid self-fertilisation such as heterostyly (different flower morphs with the pistil & stamen at different heights), protogyny (the stigma matures before the anthers) or protandry (anthers mature first). One of the most important mechanisms developed by plants to prevent inbreeding is self-incompatibility (SI), which is employed by over 50% of angiosperms. SI is a genetically controlled mechanism for the recognition and rejection of self or genetically identical pollen, which promotes out-breeding and increases genetic diversity within the population. Diverse SI mechanisms have evolved at least three times independently in different lineages of flowering plants (Charlesworth et al, 2005). There are two different types of SI, illustrated in **Figure 1.6**. The first is sporophytic SI (SSI), where the SI phenotype of the pollen is determined by the diploid genome of the parent plant. In contrast, pollen from plants with gametophytic SI (GSI) has an SI phenotype determined by its own haploid genotype.

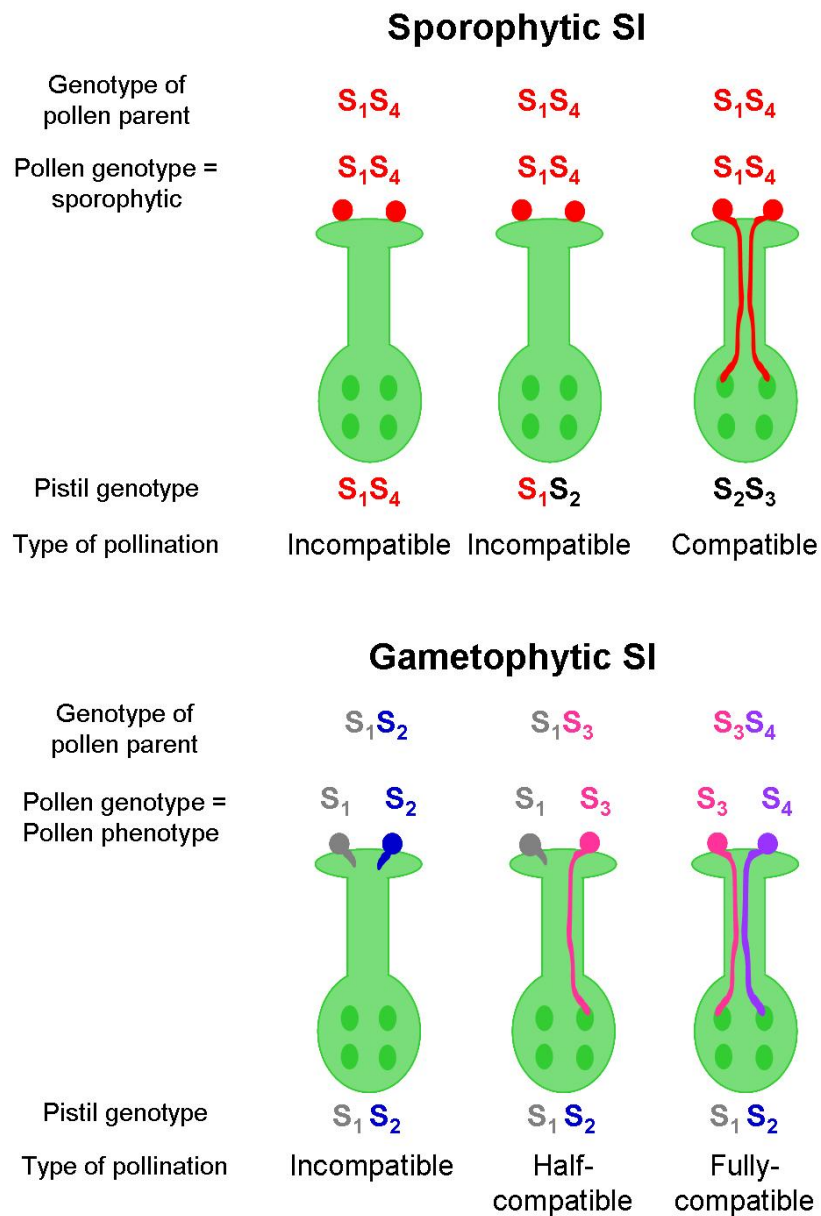


Figure 1.6. The two different types of SI

In sporophytic SI, the pollen phenotype is the same as the parent plants diploid genotype. This results in either a compatible or incompatible outcome.

In gametophytic SI, the pollen phenotype is determined by its own haploid genome, which results in three possible outcomes: fully compatible, half compatible or incompatible.

In the majority of SI systems, the recognition of self/non-self is controlled by a single, multiallelic locus termed the *S*-locus. The *S*-locus contains the two tightly linked genes that code for the pistil (female) *S*-determinant and the pollen (male) *S*-determinant which are inherited as one segregating unit (McClure, 2004; Takayama & Isogai, 2005). Pollen that lands on a stigma which carries the same *S*-allele as the pollen is recognised as ‘self’ or ‘incompatible’ pollen and growth of the pollen tube, and therefore fertilisation, is inhibited. Pollen carrying different alleles to those of the stigma is able to germinate and fertilisation is achieved. The rejection of incompatible pollen is governed by the interaction of the pollen *S*-determinant with the pistil *S*-determinant. The three main SI systems that are well characterised at the molecular level are: the *Brassicaceae*, the *Papaveraceae* and the S-RNase-type SI which includes the *Solanaceae*, *Plantaginaceae* and *Rosaceae* (Takayama & Isogai, 2005, Charlesworth et al, 2005).

1.5) Self-incompatibility in *Brassicaceae*

The *Brassicaceae* represent the only SSI system characterised at the molecular level. The SI response of this family occurs very rapidly on the stigma surface. Incompatible pollen tube growth is quickly inhibited at the stigma surface or the grains do not even hydrate properly. Numerous *S*-haplotypes have been identified in *Brassica*, for example in *B. oleracea* there are 50 different *S*-haplotypes (Ockendon, 2000).

1.5.1) The female *S*-determinant

The *S*-locus of *Brassica* is large and complex, spanning ~80-100 kb (Hiscock & McInnis, 2003). The female *S*-determinant is a serine/threonine receptor kinase called SRK (S-locus

receptor kinase) (Stein et al, 1991). SRK is composed of an extracellular domain, a single-pass transmembrane domain and a cytoplasmic serine/threonine kinase domain. The receptor domain contains the areas of hypervariability, which can diverge by up to 35% between alleles (Nasrallah, 2002) and is therefore thought to be responsible for allele specificity. SRK is expressed predominantly in the papillae of the stigma and its expression coincides with flower opening, making it readily available to act during pollination (Stein et al, 1996). In most *S*-haplotypes there is another polymorphic gene present at the *S*-locus, *SLG* (*S*-locus glycoprotein). The SLGs are 40-50 kDa, stigma-specific, secreted glycoproteins with twelve conserved cysteine residues and several N-linked oligosaccharides (Nasrallah et al, 1987; Takayama et al, 1987). The SLG and the receptor domain of SRK of a given *S*-haplotype can share up to 98% nucleotide sequence identity (Stein et al, 1991). Although both the SRK and the SLG were good candidates for the female *S*-determinant, and it was thought that they could function together to form a receptor complex during SI, gain-of-function experiments demonstrated it was SRK alone that was required for successful SI (Takasaki et al, 2000). Transgenic *B. rapa* expressing SRK₂₈ was able to reject S₂₈ pollen and therefore had acquired the S₂₈-haplotype specificity. However, plants expressing SLG₂₈ were unable to reject S₂₈ pollen, indicating SLG was not the *S*-determinant. In this experiment plants expressing both the SRK₂₈ and SLG₂₈ exhibited a stronger SI response indicating that SLG could enhance the activity of SRK (Takasaki et al, 2000). Conversely, in *B. napus* a similar gain-of-function experiment did not detect an enhancing role for SLG (Silva et al, 2001) and therefore the requirement for SLG in the SI response may be *S*-haplotype specific.

1.5.2) The male *S*-determinant

The male *S*-determinant of *Brassica* SI is a small (6 kDa), cysteine-rich pollen coat protein. It was identified independently by two different groups around the same time and hence has two different names: SCR (*S*-locus cysteine-rich; Schopfer et al, 1999) and SP11 (*S*-locus protein 11; Suzuki et al, 1999; Takayama et al, 2000). Here, the male determinant will be referred to as SCR. SCR was confirmed as the sole male *S*-determinant using gain-of-function experiments (Schopfer et al, 1999; Shiba et al, 2001) and a pollination bioassay (Takayama et al, 2001). The pollination assay involved coating the stigma with synthetic ‘self’ SCR which was then able to inhibit the hydration and growth of ‘cross’ pollen.

1.5.3) The mechanism of SI

The rapidity of the inhibition of incompatible pollen in the *Brassicaceae*-type SI had led to the hypothesis that SI was controlled by a receptor-ligand interaction. The identification of a receptor kinase (SRK) as the female component supported this view. Direct interaction between SRK and SCR was demonstrated using two different approaches by different groups. *In vitro* pull-down assays, using tagged versions of SCR and the external receptor domain of SRK, demonstrated binding of SRK₆ to SCR₆ but not to SCR₁₃, indicating *S*-specificity (Kachroo et al, 2001). Takayama et al (2001) used ¹²⁵I-labelled S₈-SCR and showed that this specifically bound to the stigmatic microsomal membranes of the S₈ homozygote. This study also demonstrated autophosphorylation of SRK₈ upon SCR₈ binding and not upon SRK₉ binding, indicating *S*-specific activation of SRK. Both these studies demonstrate the molecular basis of the recognition of self pollen. SCR is the ligand that, in an incompatible reaction, interacts with its matching *S*-haplotype receptor SRK to activate SRK via

autophosphorylation of the kinase domain. **Figure 1.7** illustrates the current model of *Brassica*-type SI which is described in detail below.

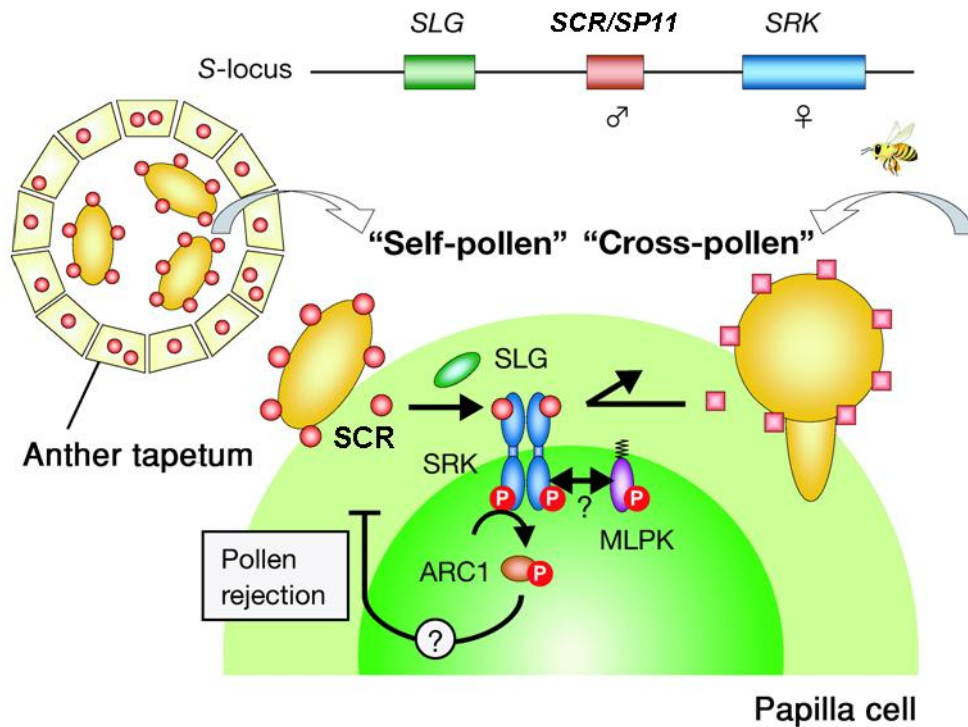


Figure 1.7. Model of the SI response in the *Brassicaceae*.

The S-locus is composed of three genes: SRK, SCR/SP11 and SLG. The female S-determinant (SRK) is a membrane-bound receptor kinase found in stigma papillae cells. The male S-determinant (SCR) is predominantly expressed in the anther tapetum and becomes incorporated into the pollen coat during maturation. SLG localises to the papillae cell wall and enhances the SI response in some S-haplotypes, although is not an essential component of SI.

Following pollination, SCR breaks through the papilla cell wall and binds to SRK in an S-haplotype-specific manner. This binding causes autophosphorylation of SRK and induces a signalling cascade that results in rejection of incompatible pollen. Some of the members of the downstream signalling cascade have been identified and include: MLPK, which may form a signalling complex with SRK, and ARC1, an E3-ubiquitin ligase that may target unknown substrates for degradation by the proteasome.

Figure taken from Takayama & Isogai (2005).

1.5.4) Downstream signalling components

Following recognition of self-pollen, by the interaction of SCR with SRK, a signal needs to be transduced throughout the papilla cell to inhibit further growth of the incompatible pollen tube. Current work is now focusing on identifying these downstream signalling components. To date, two positive mediators of *Brassica* SI have been identified: ARC1 (Armadillo-repeat-containing 1; Gu et al, 1998) and MLPK (*M* locus protein kinase; Murase et al, 2004). Several potential negative regulators have also been identified: THL1 and THL2 (thioredoxin-H proteins; Bower et al, 1996) and a homologue of a kinase-associated protein phosphatase (KAPP; Vanoosthuysse et al, 2003).

ARC1 was identified as an SRK-interacting protein through a yeast-2-hybrid approach and this interaction results in the phosphorylation of ARC1 *in vitro* (Gu et al, 1998). Down-regulation of ARC1 using antisense oligonucleotides resulted in a partial loss of the SI response, suggesting that there may be another alternate or parallel SI signalling pathway that does not rely on ARC1 (Stone et al, 1999). However, there may still be residual levels of ARC1 expression in the transgenic stigmas that could account for only a partial breakdown of SI. ARC1 has been shown to be an E3-ubiquitin ligase (Stone et al, 2003). Stone et al (2003) demonstrated that the level of ubiquitinated proteins in pistils rises in incompatible reactions but not in ARC1 antisense pistils. Proteasome inhibition also disrupts the SI response (Stone et al, 2003). Therefore, they proposed that following activation by SRK, ARC1 functions to mark proteins involved in pollen tube germination and growth for degradation via the proteasome. The second positive mediator of SI, MLPK, is a protein kinase from the subfamily of the receptor-like cytoplasmic kinases (RLCK). The kinase region of MLPK is mutated and non-functional in the self-compatible *B. rapa* var Yellow Sarson, indicating that

the kinase activity is important for function. MLPK has been localised to the plasma membrane of the stigma and it has been suggested that MLPK forms a signalling complex with SRK to mediate the SI response (Murase et al, 2004)

A yeast-2-hybrid screen of SRK interactors also identified THL1 and THL2 (Bower et al, 1996; Mazzurco et al, 2001). THL1 prevents the autophosphorylation of SRK in the absence of pollen coat proteins (Cabrillac et al, 2001) so therefore prevents constitutive activation of SRK. A *B. oleracea* homologue of the protein phosphatase KAPP was isolated and shown to dephosphorylate SRK, suggesting it too could negatively regulate SRK activation (Vanoosthuysse et al, 2003).

The actin cytoskeleton has been shown to be involved in the SI response of poppy (see **Section 1.7.1.3**; Geitmann et al, 2000; Snowman et al, 2002, Thomas et al, 2006) and recently its involvement in *Brassica* SI has been investigated (Iwano et al, 2007). This study found that in the papilla cells during a compatible reaction, bundles of actin appeared at the site of pollen attachment around the time of pollen hydration. An incompatible reaction caused actin rearrangements and probable depolymerisation of the actin in the papillae and hydration of the incompatible pollen grains was uncommon. Furthermore, Iwano et al (2007) found that the pollen coat was sufficient to cause this response. Stimulating F-actin depolymerisation with cytochalasin D prevented pollen grains from hydrating and illustrates the importance of the actin cytoskeleton in this SI system.

1.6) S-RNase-type self-incompatibility

The *Solanaceae*, *Rosaceae* and the *Plantaginaceae* families are examples of GSI and all share the same female *S*-determinant, an S-RNase. Unlike the *Brassica* SI system, rejection of incompatible pollen occurs during pollen tube growth in the style and is therefore a much slower process than in *Brassica*, indicating a different mechanism of recognition and inhibition.

1.6.1) The female *S*-determinant

The female determinant of *Solanaceae*-type SI (S-RNases) was first discovered over 20 years ago in *Nicotiana glauca* as abundant glycoproteins (~30 kDa) that co-segregated with the pistil *S*-genotype (Bredemeijer & Blaas, 1981; Anderson et al, 1986). Cloning and sequence analysis of a large number of alleles showed that these proteins were highly polymorphic, with between 39 and 98 % identity, and they were developmentally expressed (Ai et al, 1990; Clark et al, 1990; Kheyr-Pour et al, 1990). These proteins also contained a region homologous to the catalytic domain of the fungal T₂-type and Rh-type ribonucleases and were shown to have ribonuclease activity (McClure et al, 1989). S-RNases from the *Solanaceae* contain 5 conserved (C1-C5) and two hypervariable (HV_a and HV_b) domains, with the C2 and C3 domains being homologous to the fungal RNases (Takayama & Isogai, 2005). Definitive evidence that S-RNases were the sole female *S*-determinant came from plant transformation experiments (Lee et al, 1994; Murfett et al, 1994). In a gain-of-function experiment, transformation of the S_{A2}-RNase gene from *N. glauca* into an appropriate genetic background caused rejection of S_{A2} pollen (Murfett et al, 1994). Lee et al (1994) used antisense

oligonucleotides to inhibit expression of the S₂- and S₃-RNases in *Petunia* plants and showed that these plants lost the ability to reject S₂ and S₃ pollen.

1.6.2) The male S-determinant

The male determinant of was first identified in *Antirrhinum* (a member of the *Plantaginaceae*) by sequencing around the S₂-RNase gene at the S-locus (Lai et al, 2002). The male determinant is also known by two names, SLF (**S-Locus F-box**) and SFB (**S-locus F-Box**). It has now also been found in several *Prunus* species (Entani et al, 2003; Ushijima et al, 2003) and is specifically expressed in the anther and pollen grains (Lai et al, 2002). SLF contains a motif, called an F-box, which is normally involved in binding specific substrate proteins to the SCF E3-ubiquitin ligase complex which is responsible for polyubiquitylating proteins. This marks the proteins for degradation by the 26S proteasome (Craig & Tyers, 1999). Sijacic et al (2004) demonstrated that SLF was the pollen S-determinant by transformation experiments in *Petunia inflata*, where the PiSLF₂ gene was transformed into an S₂S₃ background. The resulting S₃ pollen carrying the S₂-transgene could not be rejected, whilst the S₂ pollen was rejected whether the transgene was present or not. This result is due to a phenomenon called competitive interaction, where pollen carrying two different S-specificities (in this case S₂ and S₃) causes a breakdown of SI, allowing the pollen to germinate and grow, whereas the presence of the SLF₂-transgene in S₂ pollen would have no effect as they both represent the same S-specificity.

1.6.3) The mechanism of SI

Based on the findings that the female *S*-RNase is taken up into both compatible and incompatible pollen tubes (Luu et al, 2000) and the male *S*-determinant is an F-box protein, an *S*-RNase degradation model was proposed (Entani et al, 2003; Qiao et al, 2004a; 2004b; Sijacic et al, 2004; Ushijima et al, 2003; 2004; Takayama and Isogai, 2005). In this model, when compatible pollen grows down the style the *S*-RNases are taken up into the pollen tube but the SLF interacts with them, leading to ubiquitylation and degradation by the proteasome of the non-self RNases. They are then unable to exert their cytotoxic effect and the pollen tube continues growing. In an incompatible reaction, the self interaction of SLF_x and S-RNase_x does not cause degradation of S-RNase_x, which is then able to degrade the pollen tube mRNA, leading to pollen tube growth inhibition.

Whilst there is evidence to support this degradation model, such as yeast-2-hybrid data which show an interaction of SLF with both compatible and incompatible *S*-RNases (Qiao et al, 2004b), it does not take into account other factors which have been shown to be essential for successful SI. Other genes, not linked to the *S*-locus, such as *HT-B*, *120K* and *4936-factor*, have been shown to affect SI without affecting the *S*-RNases directly (McClure et al, 1999, 2000; O'Brien et al, 2002; Hancock et al, 2005). These proteins are not involved in the uptake of *S*-RNases into the pollen tube so must play a role when *S*-RNases are inside the tube because the absence of these style-side factors allows pollen tubes to tolerate high levels of *S*-RNases without suffering any adverse effect (Goldraij et al, 2006). Studies have shown the 120k protein to label the vacuolar membrane and *S*-RNases are compartmentalised into the vacuoles (Goldraij et al, 2006). In the later stages of SI the vacuole has been seen to break down (Goldraij et al, 2006) and this has led to a second model of *Solanaceae*-type SI called

the S-RNase compartmentalisation model (McClure & Franklin-Tong, 2006). In this model the growing pollen tube takes up S-RNases, HT-B and 120K which are compartmentalised into the vacuole where the S-RNases cannot exert their cytotoxic effect. In a compatible reaction, the S-RNases remain in the vacuole where they are stable but cannot degrade RNA because they are sequestered. A hypothetical protein (PP) has been proposed to degrade HT-B, as this has been shown to be necessary for vacuolar disruption (Goldraij et al, 2006). As yet, it is not clear how S-RNases gain access to SLF, which must occur as this SLF/S-RNase interaction is what determines *S*-specificity. However, the interaction must be indirect if the S-RNases are sequestered into the vacuole. In an incompatible reaction, PP is inhibited, allowing HT-B to cause vacuolar break-down. The S-RNases are released into the cytoplasm where they can degrade RNA and thus inhibit further pollen tube growth. The two different models of *Solanaceae* SI are shown in **Figure 1.8**. Further work is required to determine which one, if either, is correct.

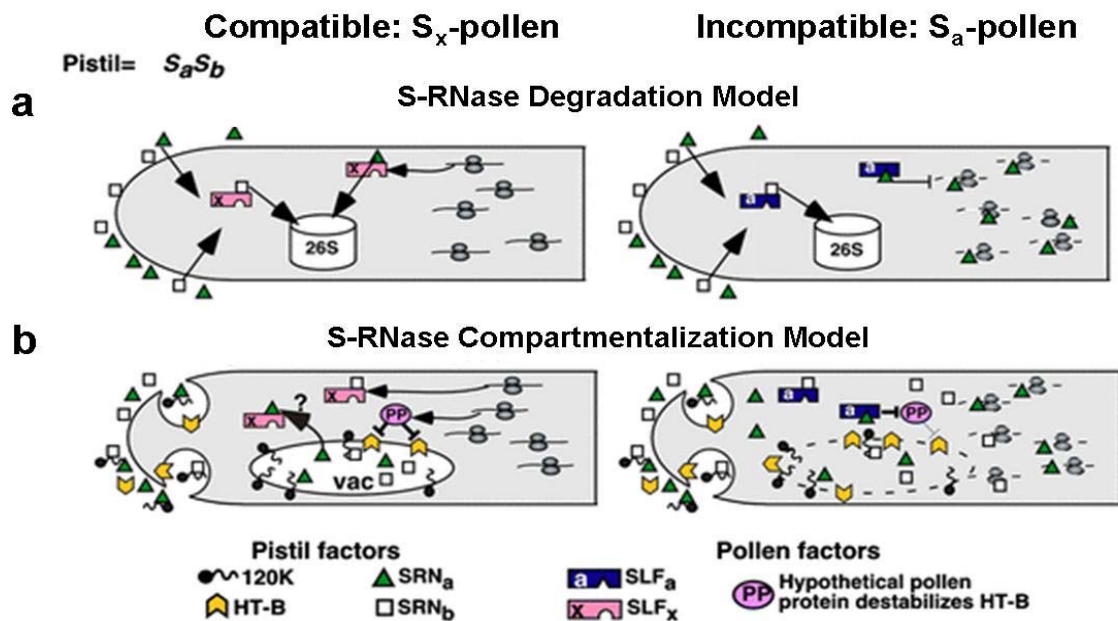


Figure 1.8. Two alternative models of S-RNase-type SI

a) The S-RNase degradation model.

In a compatible response (left), the S-RNases enter the pollen tube, interact with SLF which tags them (with ubiquitin) for degradation by the 26S proteasome. The pollen tube continues growth. In an incompatible response (right), the S-RNases interact with SLF but are not degraded by the proteasome. They degrade the RNA and inhibit further pollen tube growth.

b) The S-RNase compartmentalization model.

In a compatible response (left), the S-RNases, HT-B and 120K proteins enter the pollen tube by endocytosis and are sequestered into the vacuole, where they remain, unable to exert their cytotoxic effect on the pollen tube. A hypothetical protein (PP) acts to degrade HT-B. It is not known how SLF interacts with the S-RNases (arrow with question mark).

In an incompatible response (right) the S-RNases, HT-B and 120K proteins enter the pollen tube by endocytosis and are also sequestered into the vacuole. The action of PP is inhibited, allowing HT-B to cause vacuolar break-down, releasing the S-RNases into the cytosol where they can degrade RNA and inhibit pollen tube growth.

Figure taken from McClure & Franklin-Tong (2006).

1.7) Self-Incompatibility in *Papaveraceae*

In *Papaver rhoeas* (the field poppy), SI is under gametophytic control and is governed by a single multi-allelic *S*-locus. The number of *S*-haplotypes in *P. rhoeas* has been estimated at about 66 (Lane & Lawrence, 1993). Unlike the GSI system of the *Solanaceae*, incompatible pollen is rapidly inhibited on the poppy stigma surface and S-RNases are not involved. The rapidity of recognition and rejection is somewhat similar to the *Brassica* SI system, so it was hypothesised that *Papaver* also used a receptor-ligand interaction. A more detailed account of the male and female components can be found in **Chapter 3** which addresses recent work looking at the localisation of the two *S*-determinants. A brief description is given here. The female *S*-determinant has been identified and characterised (Foote et al, 1994). They are small proteins of around 15 kDa secreted by the stigmatic papillae cells which share ~56% - 64% identity and are proposed to act as the ligand in the SI response (Walker et al, 1996; Kurup et al, 1998). These proteins have been known as S-proteins and will be referred to as S-proteins in this thesis. However, new nomenclature has been proposed in Wheeler et al (2009) which has termed these proteins PrsS (**P**apaver **r**hoeas **s**tigma **S**) and future work will adopt this new name. Several of these S-proteins have been cloned (Foote et al, 1994; Walker et al, 1996; Kurup et al, 1998) and recombinant proteins exhibiting *S*-specific biological activity can be produced and used in *in vitro* assays. These *in vitro* assays confirm that the S-proteins act as the sole *S*-determinant, as no other stigmatic factors are necessary for the SI response to occur. The pollen *S*-determinant has only just been conclusively identified (Wheeler et al, 2009) and has been named PrpS (**P**apaver **r**hoeas **p**ollen **S**). PrpS is a membrane bound protein with no homology to previously identified proteins.

1.7.1) The mechanism of SI

As SI in *Papaver* can easily be induced in pollen growing *in vitro*, by adding the appropriate recombinant S-proteins, the downstream signalling events following self-recognition have been intensively studied in *Papaver rhoeas*. S-proteins are proposed to interact with the pollen S-determinant PrpS triggering a calcium-dependent signalling cascade in the pollen tube that affects a multitude of cellular components and ultimately leads to programmed cell death (PCD) of the pollen tube (Bosch & Franklin-Tong, 2007; Thomas et al, 2003; Thomas & Franklin-Tong, 2004). The SI response in poppy pollen has been proposed to be biphasic (Thomas & Franklin-Tong, 2004). The first step is thought to be the initial rapid inhibition of growth, followed by a later 'decision-making' phase involving PCD that makes inhibition irreversible. **Figure 1.9** is a model of the SI response in poppy pollen tubes.

1.7.1.1) The role of calcium in *Papaver* SI

One of the first events in *Papaver* SI is a large increase in the intracellular calcium concentration $[Ca^{2+}]_i$ of the pollen tube, especially in the shank region, which involves an influx of extracellular calcium (Franklin-Tong et al, 1993; 1995; 1997; 2002; Straatman et al, 2001). In the shank, resting levels of calcium are in the region of 200 nM, but upon challenge with incompatible S-proteins, $[Ca^{2+}]_i$ increases to $>1.5 \mu M$, whilst the tip focused calcium gradient, needed for pollen tube growth, is lost (Franklin-Tong et al, 1997). Release of calcium from intracellular stores is probably also involved. Calcium is a known second messenger in plant cells and this sudden increase in its concentration in the pollen tube shank is thought to be the first step in the SI signalling pathway.

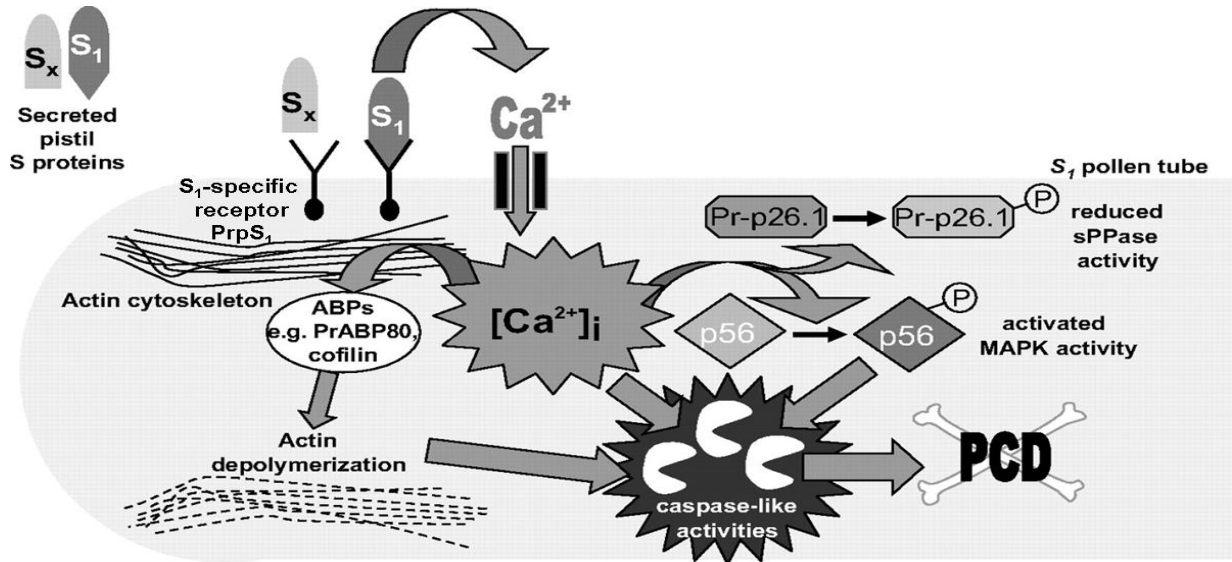


Figure 1.9. Model of the SI response in *Papaver rhoeas*

Stigmatic S-proteins interact with incompatible pollen S-receptors (PrpS₁) in an S-haplotype-specific interaction. This triggers an influx of Ca²⁺ which induces a signalling cascade in the incompatible pollen. Phosphorylation and inactivation of soluble inorganic pyrophosphatases (sPPases) Pr-p26.1a/b, results in a reduction in the biosynthetic capability of the pollen and thus inhibits growth.

The F-actin cytoskeleton is first depolymerised, which is predicted to cause rapid arrest of tip growth, and later it is organised into large F-actin foci.

The p56-MAPK is phosphorylated and activated and may signal to PCD.

The end result is PCD, involving a caspase-3-like activity, which ensures that incompatible pollen does not start to grow again.

Figure taken from Bosch & Franklin-Tong (2008).

1.7.1.2) Protein phosphorylation occurs during *Papaver* SI

Following the increase in calcium concentration in the tube there is a rapid *S*-specific phosphorylation of at least two pollen proteins called Pr-p26.1a and Pr-p26.1b (Rudd et al, 1996). These 26 kDa proteins have been identified as soluble inorganic pyrophosphatases (sPPases) (de Graaf et al, 2006). sPPases are enzymes involved in the conversion of inorganic pyrophosphate (PPi), which is formed during biosynthetic reactions that use ATP, into inorganic orthophosphate. This removal of the toxic PPi shifts the equilibrium of biosynthetic reactions towards biosynthesis (Cooperman et al, 1992). Pr-p26.1 becomes phosphorylated within 90 seconds of incompatible S-protein addition, but not after a compatible reaction, and the level of phosphorylated p26.1 increases over the next 400 sec (Rudd et al, 1996). This phosphorylation is calcium and calmodulin dependent suggesting that during the SI response Pr-p26.1 is the target of a calcium- and calmodulin-dependent protein kinase (Rudd et al, 1996). Pr-p26.1-PPase activity has been shown to be inhibited upon phosphorylation (de Graaf et al, 2006, Rudd & Franklin-Tong, 2003) and therefore, during the SI response, Pr-p26.1 would be rapidly inactivated helping to inhibit pollen tube growth.

Another target of the calcium signalling cascade in SI is the **mitogen activated protein kinase** (MAPK) p56 (Rudd et al, 2003). MAPKs are serine/threonine kinases that are activated via a MAPKKK cascade resulting in the dual phosphorylation of threonine and tyrosine residues in a TXY motif. They are known to act in plant signalling networks such as in resistance to pathogens (Zhang & Klessig, 2001; Asai et al, 2002). This 56 kDa protein is first activated 5 minutes after incompatible S-protein challenge, with peak activity around 10 minutes into the response. The activity of this MAPK remains significantly higher than normal levels for at least 30 minutes (Rudd et al, 2003). p56 activation occurs after pollen tube growth has been

inhibited, suggesting it may be involved in signalling the later, irreversible inhibition of pollen tube growth. Experiments involving the pre-treatment of pollen tubes with lanthanum, a calcium channel blocker, prevented the calcium influxes normally induced by SI (Franklin-Tong et al, 2002) and also p56 activity, thus implying calcium is essential for p56 activation (Rudd et al, 2003). Work by Li et al (2007) has demonstrated that a MAPK, probably p56-MAPK is involved in triggering the PCD signalling cascade in incompatible pollen. In this study, pre-treatment of incompatible pollen with U0126 (an inhibitor of MAPK cascades) led to a significant reduction in the levels of SI-induced DNA fragmentation and caspase-3-like activity (both key markers of PCD). Work is currently being carried out to clone and characterise p56.

1.7.1.3) The role of the cytoskeleton in *Papaver* SI

The cytoskeleton is thought to participate in mediating signal-response coupling in many cell types (Staiger, 2000). The MT cytoskeleton has not been previously studied in relation to SI in poppy. The alterations that occur in the MT cytoskeleton during SI have been investigated as part of this thesis and are described in detail in **Chapter 4**. Conversely, the actin cytoskeleton plays a pivotal role in pollen tube growth (see **Section 1.2.1.2**) and during the SI response pollen tubes have their growth inhibited, therefore the involvement of the actin cytoskeleton in SI has been studied. In normally growing poppy pollen tubes the F-actin is found in the typical arrangement of thick axial bundles in the shank region, finer bundles arranged into the actin collar in the sub-apex and little or no actin in the tip (Geitmann et al, 2000; Snowman et al, 2002). During SI, the F-actin has been found to go through a highly reproducible pattern of alterations that begin within 1-2 min of initiation of the SI response. The first phase of the alterations involves a rapid, large and sustained reduction in F-actin

levels. The percentage of F-actin reduction is more than 70%, compared to control pollen tubes (Snowman et al, 2002). The F-actin can be visualised at the cortex of the cell and in the tip region, where it is not normally present. Following this, the actin is seen as small speckles throughout the cell and later, as large punctate actin foci that persist for at least 3h post SI-induction (Geitmann et al, 2000; Snowman et al, 2002). These alterations are *S*-specific and do not occur as a result of non-specific growth inhibition (Geitmann et al, 2000). Artificial increases in cytosolic calcium levels using drugs such as mastoparan induce F-actin depolymerisation so place the calcium influx upstream of the actin alterations in the SI signalling cascade (Snowman et al, 2002). The ABPs profilin and PrABP80 (a gelsolin-like poppy protein) have been implicated in the initial depolymerisation of the F-actin (Snowman et al, 2002; Huang et al, 2004) but the large actin foci formed later in the response have not yet been studied. **Chapter 5** of this thesis begins to characterise these F-actin structures. Interestingly, the actin cytoskeleton of pear (*Pyrus pyrifolia*) pollen tubes has recently been shown to undergo a similar rearrangement into actin foci following addition of incompatible stylar S-RNases (Liu et al, 2007), although this rearrangement is much slower than that observed in poppy. Pear and poppy employ different GSI mechanisms so it is fascinating that they share this feature. Further work needs to characterise the downstream events of the actin rearrangements in pear to see if there are any more similarities between the two systems.

The level of actin depolymerisation seen during SI in poppy is far greater than is needed to inhibit pollen tube growth and it is sustained for at least 1h (Snowman et al, 2002). In some animal cells and yeast, actin depolymerisation has been shown to be a necessary component of apoptosis and alterations in actin dynamics have been shown to induce apoptotic signalling pathways (Levee et al, 1996; Kayalar et al, 1996; Rao et al, 1999; Gourlay & Ayscough,

2005a;b). This suggested that the actin alterations seen during SI could also be signalling to the PCD pathway in incompatible pollen. Further work investigated whether altering actin dynamics in pollen tubes, using both F-actin stabilising and depolymerising drugs (jasplakinolide and latrunculin B, respectively), was able to induce PCD, using DNA fragmentation as a marker (Thomas et al, 2006). This study found that both depolymerising and stabilising F-actin resulted in increased levels of DNA fragmentation, and this was dependent on a caspase-3-like activity. Moreover, counteracting the SI-induced depolymerisation using jasplakinolide enabled pollen tubes to be 'rescued' from PCD. This study demonstrated that, as well as playing a role in the initial inhibition of pollen tube growth, the depolymerisation of the actin cytoskeleton is important in triggering a PCD signalling pathway during SI.

1.7.1.4) *Papaver* SI results in PCD of the incompatible pollen

When incompatible pollen lands on a stigma, its pollen tube growth is selectively inhibited soon after germination. During development or in response to pathogen attack, unwanted cells are often removed by PCD. The SI response shares some of the features of the hypersensitive response (HR) (Dickinson, 1994; Sanabria et al, 2008), a plant defence mechanism against pathogen attack, which results in PCD of the infected cell (reviewed in Lam et al, 2001). Therefore, the involvement of PCD in the SI response was investigated. Early studies identified DNA fragmentation, a key marker of PCD, in incompatible pollen tube under going SI (Jordan et al, 2000). Leakage of cytochrome *c* from the mitochondria into the cytosol is an early marker of PCD. In mammalian cells cytochrome *c* is responsible for the activation of enzymes called caspases via the adaptor protein Apaf-1 (reviewed in Green, 2000). In poppy pollen, cytochrome *c* has been detected in the cytosol as early as 10 min after SI-induction,

with levels increasing for 120 min (Thomas & Franklin-Tong, 2004). Caspases *per se* have not been identified in plants (see **Section 1.3.1** for details) but there is evidence for caspase-like activities in plants (Lam & del Pozo, 2000; Schaller, 2004). Thus, the involvement of caspase-like activity in SI was investigated. Tetra-peptide inhibitors are useful tools for investigating the involvement of caspase-like activities. The caspase-3 inhibitor, DEVD-CHO, was used to pre-treat incompatible pollen prior to SI-induction. This pre-treatment resulted in reduced levels of DNA fragmentation, implicating caspase-3-like activities in the SI response (Thomas & Franklin-Tong, 2004). Poly (ADP-ribose) polymerase (PARP) is a classic substrate for caspase-3 and its cleavage is another marker of PCD. PARP cleavage occurs in incompatible, but not compatible, reactions and is reduced in DEVD-CHO pre-treated pollen, providing further evidence for the involvement of caspase-3-like activity in SI (Thomas & Franklin-Tong, 2004). More recent studies have used fluorescent caspase substrates, with different caspase specificities e.g. DEVD-AMC for caspase-3, VEID-AMC for caspase-6, to measure the level and timing of the caspase-like activities (Thomas et al, 2006; Bosch & Franklin-Tong, 2007; Li et al, 2007). Bosch & Franklin-Tong (2007) demonstrated that the DEVDase activity was the major caspase-like activity which reached its peak at 5 h after SI-induction. However, there was also a significant increase in caspase-6-like (VEIDase) activities detected, which followed the same temporal pattern as the DEVDase-activity. Caspase-1 (YVADase) and caspase-4 (LEVDase) activities were also detected, but these were significantly lower than the DEVDase and VEIDase activities. The localisation of the DEVDase activity was visualised in pollen tubes using CR(DEVD)₂. When this probe is cleaved by DEVDase activity it releases the fluorophore cresyl violet (CR) giving spatial, temporal and quantitative information about the DEVDase activity. In SI-treated pollen the DEVDase activity was detected in the cytosol, and high levels were detected later in the VN

and GC (Bosch & Franklin-Tong, 2007). Another recent finding is that pollen tubes undergoing SI experience a dramatic acidification of the cytosol from pH 6.9 to pH 5.5 (Bosch & Franklin-Tong, 2007). This acidification may be due to vacuolar disruption which appears to occur early in SI (Bosch et al, unpublished data). Cytosolic acidification is common in cells undergoing apoptosis (Matsuyama & Reed, 2000) so could be involved in SI-induced PCD. Treating pollen tubes with mastoparan, to artificially increase cytosolic calcium levels causes DNA fragmentation (Jordan et al, 2000) and increases caspase-3-like activities (Bosch & Franklin-Tong, 2007). This implies that the SI-induced increases in calcium levels are involved in PCD signalling. These studies provide strong evidence that PCD is employed during the SI response of poppy to ensure that self-fertilisation does not occur.

CHAPTER 2

MATERIALS AND METHODS

2.1) Stock Solutions

Growth Medium Salt Stock

2 % (w/v) H_3BO_3 ,
2 % (w/v) KNO_3 ,
2 % (w/v) $\text{Mg}(\text{NO}_3)_2 \cdot 6\text{H}_2\text{O}$,
7.2 % (w/v) $\text{CaCl}_2 \cdot \text{H}_2\text{O}$,
Sterile distilled water (SDW)

Liquid Growth Medium (GM)

13.5 % (w/v) sucrose
0.01% H_3BO_3
0.01% KNO_3
0.01% $\text{Mg}(\text{NO}_3)_2 \cdot 6\text{H}_2\text{O}$
0.036% $\text{CaCl}_2 \cdot \text{H}_2\text{O}$
SDW
Made by making a 13.5 % sucrose solution and adding 50 μl of the stock salt solution for every 10 ml of solution.

Solid GM

Liquid GM
1.2 % agarose
Heated to dissolve the agarose and then poured into Petri dishes to form a solid base for pollen tube growth.

10 x Tris Buffered Saline (TBS)

200 mM Tris-HCl, pH 7.6
730 mM NaCl
SDW

1% Enzyme Solution

(for immunolocalisation)

1% (w/v) cellulase
1% (w/v) macerozyme
5 mM MES (pH 5)
5 mM EGTA
0.4 M Mannitol
SDW

20 % Paraformaldehyde (10 ml, pH 7)

2 g paraformaldehyde
Several drops 2N NaOH
7.5 ml SDW
Heated to $>60^\circ\text{C}$ to dissolve
PIPES (pH 6.8) up to 10 ml

Aniline Blue

0.2 g aniline blue,
20 g tri-potassium orthophosphate,
SDW up to 1 L
NB. Need to leave in the light overnight to de-colourise.

5 x Loading Buffer for SDS-PAGE

12.5 % (v/v) Tris-HCl (0.5 M, pH 6.8)
2 % (w/v) SDS
10 % Glycerol
5 % B-mercaptoethanol
0.001 % Bromophenol blue

2.2) Plant Material

2.2.1) Plant cultivation

Seeds of *Papaver rhoeas* L. (Shirley) of known pedigree were potted, three per pot in John Innes No. 1 potting compost. Seeds were then covered with a thin layer of vermiculite to retain moisture and kept in a glasshouse at 15°C in 16 h light, 8 h dark cycles. Resultant plants were thinned to one per pot after growing to a height of between 5 and 10 cm. At around 8 weeks plants were allowed to harden off outside for around 4 weeks and were then transplanted to a field in rows with approximately 50 cm between plants and 90 cm between rows.

2.2.2) Determination of S-genotype

S-haplotype was determined by pollinating each plant with pollen of a known S-genotype. Once plants were in flower, two flowers, 1-2 days prior to anthesis were emasculated by removal of all anthers using forceps sterilised with 70% ethanol. Emasculated flowers were covered with a cellophane bag wired at the base to prevent entrance of insect pollinators. Emasculated flowers were pollinated the following day by application of pollen with a fine paintbrush directly onto the stigmatic rays. After pollination, cellophane bags were replaced over the flower and rewired to close the bag. Stigmas were harvested one day after pollination. The pollinated portion of the stigma was removed with a scalpel and placed in aniline blue. These were left overnight to allow the stigmas to soften. A sample of the stigma was removed, placed on a microscope slide and squashed using a coverslip. These were then viewed under a microscope using UV illumination. All families grown were two-class families and thus were pollinated with two classes of pollen, one to provide a fully

incompatible pollination and one to provide a half-compatible pollination. Those stigmas exhibiting fully incompatible pollination had easily identifiable callose in the pollen grains and few, if any, pollen tubes (**Fig. 1a**). Those exhibiting half-compatible pollinations had 50% reacting as above whilst the remainder had no callose in the grain and long pollen tubes with callose plugs at intervals along the length of the tube (**Fig. 1b**).

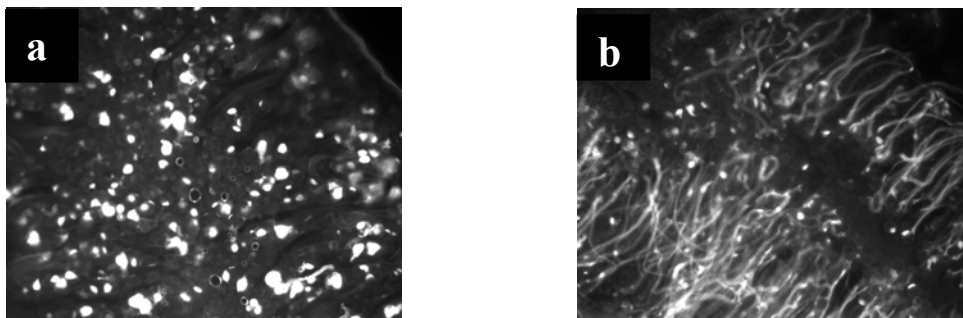


Figure 2.1: Micrographs of pollinated stigma squashes

A fully incompatible reaction (**a**) showing high amounts of callose in the pollen grains and very few pollen tubes. A half-compatible reaction (**b**) showing many long pollen tubes with callose plugs at regular intervals, as well as many callosic pollen grains.

2.2.3) Production of seed

Seed that would produce plants of a two-class family were produced following a similar method to that already described in ‘Determination of *S*-genotype’. Emasculated flowers were pollinated with pollen of known *S*-genotype and left for approximately 6 weeks. After this time the seed was collected from seed pods and stored in paper bags at 4°C.

2.2.4) Collection of pollen

Flowers at 1 day prior to anthesis were harvested approximately 15 cm below the flower. The sepals and petals were removed and the remaining stem was placed in a cellophane bag and

hung upside-down overnight in the glass house. Several stems from the same plant were placed in the same bag. The following day, pollen was released by vigorous shaking and collected by tipping into gelatine capsules. Capsules of pollen were stored in boxes containing silica gel to eliminate moisture and kept at -20°C until required.

2.3) Pollen tube growth *in vitro*

Pollen was hydrated for 30 minutes in a moist hydration chamber at 25°C. The shape of the pollen grains was used to assess the state of hydration; when desiccated, pollen grains take an elliptical form; when fully hydrated pollen grains appear spherical. The pollen was then suspended in liquid GM and transferred to a glass Petri dish containing a solid GM base (same as liquid GM but supplemented with a 1.2% (w/v) agarose (Boheringer Mannheim, UK)). The volume of liquid GM used depended on how much pollen was needed for the experiment and the size of the Petri dish. Pollen was germinated and grown in the Petri dishes for approximately 1 hour, or until pollen tubes were visible. Following growth, pollen was treated as required for the experiment.

2.4) Pollen Treatments

2.4.1) S-Proteins

2.4.1.1) Production of recombinant S-proteins from *E. coli*

2.4.1.1.1) Growth of *E. coli* and induction of protein synthesis

E. coli from glycerol stocks were plated onto plates made of LB agar (LB medium with 15 g L⁻¹ bacto-agar) plus 50 µm ml⁻¹ ampicilin and incubated at 37°C overnight. 200 ml LB

medium (10 g L⁻¹ bacto-trytone, 5 g L⁻¹ bacto-yeast extract, 10 g L⁻¹ NaCl) supplemented with ampicilin to a final concentration of 50 µm ml⁻¹ was then inoculated from a single colony and left shaking at 37°C overnight. Half (100 ml) of the overnight culture was transferred into a fresh 2 litre flask and 100ml LB broth with ampicilin (50 µm ml⁻¹) added and S-protein production was induced by adding IPTG to a final concentration of 0.5 mM. Flasks were shaken for 4 - 6 h at 37°C. The cells were collected by centrifugation at 5000 rpm at 4°C for 10 min in a Beckman ceentrifuge. The supernatant was discarded and the pellets were stored at -20°C until needed. A sample of the culture can be used to check the protein induction on SDS-PAGE.

2.4.1.1.2) Purification of inclusion bodies

To extract S-proteins from *E. coli*, the pellet was suspended in 200 ml ice-cold lysis buffer (50 mM Tris-HCl pH 8, 100 mM NaCl, 1 mM EDTA), then centrifuged for 10 min at 5000 rpm, 4°C. The supernatant was discarded and the pellet resuspended in 20 ml ice-cold lysis buffer, to which 400 µl 10 mg ml⁻¹ lysozyme and 100 µl of 50 mM PMSF were added and then incubated for 1.5 h at 4°C. Following, incubation 26 mg of sodium deoxycholate and 50 µl of 50 mM PMSF were added and the suspension incubated for a further 30 min at 37°C, during which time the solution became very viscous. The sample was sonicated on ice, using a Soniprep 150 (Sanyo), at 10 amps for 5 x 30 sec pulses with at least 30 sec on ice between pulses to allow the sample to cool. The samples were then centrifuged for 20 min at 5000 rpm at 4°C. The supernatant was discarded and the pellet was washed in 20 ml lysis buffer with 5 x 30 sec sonication on ice followed by centrifugation at 5000 rpm and removal of supernatant. This wash step was repeated 6 times. The clean inclusion bodies were stored at -20°C until needed.

2.4.1.1.3) Refolding recombinant S-proteins

The inclusion body pellet was resuspended over the course of 2 h at room temperature in 5 ml 6 M guanidine HCl and 500 mM Cysteamine (2-mercaptoethylamine) on an orbital shaker. Insoluble mass was removed by centrifugation at 5000 rpm for 15 min at 20°C and the supernatant kept. The protein concentration was determined using the Bradford assay (Section 2.11). The purity of the sample was assessed on SDS-PAGE to ensure the S-proteins were still there and most of the *E.-coli* proteins had been removed. Following concentration determination, appropriate amounts of resuspended S-proteins were added to 100 to 200 ml arginine refolding buffer (0.1 M Tris, 2 mM EDTA, 0.5 M L-arginine hydrochloride, 10 mM cystamine dihydrochloride, 5 % (v/v) glycerol, pH 8) to get a final protein concentration of 10 mg ml⁻¹. The refolding buffer needed to be pre-cooled to 15°C before addition of S-proteins. The S-proteins were added to the buffer very slowly, with the pipette immersed in the liquid and with constant stirring. The protein was left to renature at 15°C overnight before dialysis against 5 L of dialysis buffer (50 mM Tris-HCl pH 8, 100 mM NaCl, EDTA) in wide dialysis tubing with a molecular weight cut-off of 12-14,000 Daltons (Medicell International Ltd.) at 4°C. The dialysis buffer was changed at least 3 times with one occurring overnight. Once dialysis was complete the protein was reduced to 10 % of the original volume against PEG 6000, and then filtered through Miracloth (Calbiochem). The supernatant containing the S-proteins was snap-frozen in liquid nitrogen and stored at -80°C.

2.4.1.1.4) *In vitro* induction of SI

For recombinant S-proteins to be used to stimulate the SI response they first needed to be dialysed out of the dialysis buffer into liquid GM. For every 1 ml of S-protein dialysed, 1 L of GM was needed. The S-proteins were dialysed overnight at 4°C using dialysis tubing

(Medicell International Ltd.) with a cut-off of 12000-14000 Da, after which their concentration was determined using the Bradford assay (**Section 2.11**). To induce an incompatible reaction, S-proteins were added to pollen growing *in vitro* at a final concentration of 10 $\mu\text{g ml}^{-1}$, unless stated differently in the text.

2.4.2 Actin Drugs

Latrunculin B (LatB) (Calbiochem): This drug was used to depolymerise the actin cytoskeleton. A 10 mM stock solution was made up in DMSO and stored at -20°C . This was then diluted in GM to the required concentration when needed.

Jasplakinolide (Jasp) (Calbiochem): This drug was used to stabilise the actin filaments. A 1 mM stock solution was prepared in DMSO and stored at -20°C . This was then diluted in GM to the required concentration when needed.

2.4.3) Tubulin Drugs

Oryzalin (Sigma-Aldrich): This drug was used to depolymerise the MT cytoskeleton. A 10 mM stock solution was made up in DMSO and stored at -20°C . This was then diluted in GM to the required concentration when needed.

Taxol (Paclitaxel) (Sigma-Aldrich): This drug was used to stabilise the MT cytoskeleton. A 10 mM stock solution was prepared in DMSO and stored at -20°C . This was then diluted in GM to the required concentration when needed.

The appropriate concentration of these drugs/S-proteins was added to the pollen growing *in vitro* and the Petri dish gently tilted to ensure even distribution of the drug/S-proteins in the dish. The pollen was left in the drug for the time period specified in the experiment. After the specified time, the pollen was fixed in MBS then paraformaldehyde (**Section 2.5**).

2.5) Pollen fixation

Pollen was grown and treated as described above. Pollen was then fixed with 400 μ M 3-maleimodobenzoic acid N-hydroxysuccinimide ester (MBS; Pierce. 10 mM stock made up in DMSO) for 6 min at room temperature, followed by 2 % paraformaldehyde for 1 h at 4°C. Both these fixatives were slowly dripped into the growing pollen and the Petri dish gently tilted to evenly distribute the chemicals. Pollen tubes were collected using a pipette with a cut tip and placed into either falcon tubes (spinning method) or baskets (basket method; see below). The fixative was washed out with 3 changes of 1 x Tris buffered saline (TBS, pH 7.6) or actin stabilising buffer (ASB: 100 mM Pipes, pH 6.8, 1 mM MgCl₂, 1 mM CaCl₂, and 75 mM KCl) if the actin cytoskeleton was being examined.

2.6) Immunolocalisation

2.6.1) Primary Antibodies

Antibody	Titre for western blot	Titre for immunolocalisation
Mouse monoclonal anti-tubulin, clone B 5-1-2 [∞]	1:1000	1:1000
Rabbit polyclonal anti-AtCAP1. *	1:2000	1:500
Rabbit polyclonal anti-LIADF. *	1:2000	1:500
Rabbit polyclonal anti-AtFIM1.*	1:2000	1:500
Rabbit polyclonal anti-ZmPRO5.*	1:2000	1:500
Mouse polyclonal anti-LIADF1. [∪]	1:1000	1:300
Rat polyclonal anti-PrpS ₁ 60C. [§]	1:1000	1:500
Rabbit polyclonal anti-S ₁ [¶]	1:4000	1:500

[∞] Antibody from Sigma-Aldrich, UK.

* Antibodies kindly donated by Prof. Chris Staiger, Purdue University, USA.

[∪] Antibody kindly donated by Prof. Patrick Hussey, Durham University, UK

[§] Antibody made by Natalie Hadjiosif.

[¶]: Antibody already available in the laboratory.

2.6.2) Secondary Antibodies

Goat anti-mouse IgG (F_{ab}-specific) -FITC (Sigma-Aldrich, UK). Titre: 1:300

Goat anti-rabbit IgG-FITC (Sigma-Aldrich, UK). Titre: 1:200

Goat-anti-rat-FITC (Sigma-Aldrich, UK). Titre: 1:50

Goat-anti-rabbit-Cy3 (Sigma-Aldrich, UK). Titre: 1:300

2.6.3) Whole-mount immunolocalisation – spinning method

Pollen was grown, treated and fixed as described above. Following the TBS/ASB washes, which involved adding 2ml TBS/ASB, spinning the Falcon tubes at 1000 rpm in a swinging rotor centrifuge for 5 min and removing the excess liquid, the pollen was washed once in MES buffer (5 mM MES, pH 5). Cells were digested with 0.05 % cellulose and 0.05 % macerozyme in MES buffer containing 0.1 mM PMSF and 1 % BSA for 10 min. The enzyme mix was added to the pollen in the Falcon tube which was occasionally gently flicked to resuspend the pollen into the liquid. After 10 min the Falcon tubes were centrifuged at 1000 rpm for 5 min and the enzymes mix removed. The pollen tubes were then washed once in 1 ml MES and twice in 1 ml TBS, each time spinning the falcon tubes to collect the pollen at the bottom and remove the liquid. The pollen tubes were then permeabilized in 0.1% Triton X-100 in TSB for 10 min, washed three times in TBS and then block solution (TBS + 1% BSA) added. After 30 min at room temperature the block solution was removed after spinning down the pollen tubes. Samples were incubated with the primary antibody diluted in block solution for either 3 h at room temperature or, overnight at 4°C. Any unbound antibody was washed out with TBS and the pollen tubes incubated with the secondary antibodies, in the dark, for 1.5 h at room temperature. Following 3 further TBS washes, 10 µl of pollen suspended in TBS was pipetted onto a glass microscope slide using a cut tip. 5 µl of

Vectashield + DAPI mounting medium (Vector Laboratories, USA) was added, a coverslip laid gently on top and the edges sealed with clear nail polish.

2.6.4) Whole-mount immunolocalisation – basket method

Baskets were made from a 5 ml pipette tip by cutting the tip in half, placing the tip end inside the wider part of the tip and then cutting off the tip so that the end became flush with the bottom of the wider part. A 10 µm by 15 µm mesh (Merrem & La Porte, NL) was then sandwiched between the two parts of the 5 ml tip to form a basket to collect the pollen into. The mesh at the bottom has a pore size small enough to prevent the pollen from getting out but allows liquid to go through so the pollen can be washed. Pollen was grown, treated and fixed as described above. Pollen was washed by adding 1 ml of TBS/ASB to the basket, allowing it to flow through the pollen and the mesh into a glass universal and leaving it for 5 min in the wash buffer. Following the TBS/ASB washes, the pollen was washed once in MES buffer (5 mM MES pH 5). Cell walls and membranes were digested with 0.05 % cellulose, 0.05% macerozyme and 0.1 % triton x-100 in MES buffer containing 0.1 mM PMSF and 1 % BSA for 15 min. This involved adding 0.5 ml of the enzyme/detergent mix and gently moving the basket within the glass universal to ensure the pollen was in the liquid. After 15 min the enzyme/detergent solution was poured off and the pollen washed in 1 ml of MES buffer for 5 min. A further 3 x 5 min washes in TBS followed. Pollen tubes were then blocked for at least 30 min in 0.5 ml blocking solution (TBS + 1% BSA). The bottom of the baskets were then covered with Parafilm to prevent the antibody solution from going through the mesh and the samples were then incubated with 200 µl of the primary antibody diluted in block solution for either 3 h at room temperature or overnight at 4°C. Following incubation, the Parafilm was removed, any unbound antibody was washed out with 3 x 10 min TBS washes and the pollen tubes were incubated with the secondary antibodies in the dark for 1.5 h at room temperature.

Following 3 further TBS washes, 10 μ l of pollen suspended in TBS was pipetted onto a glass microscope slide using a cut tip along with 5 μ l of Vectashield + DAPI mounting medium (Vector Laboratories, USA). A coverslip was laid gently on top and the edges sealed with clear nail polish.

2.6.5) Actin staining

Actin was stained using 66 nM rhodamine-phalloidin (Invitrogen). Phalloidin only binds F-actin so no G-actin is visualised. This permits a clearer picture of the MF cytoskeleton as background signal created by monomeric actin is removed. After the final TBS washes of the immunolocalisation, rhodamine-phalloidin was diluted into TBS and incubated with the pollen tubes for at least 30 min at 4°C, but better results were achieved following incubation overnight at 4°C.

2.6.6) Immunolocalisation on sectioned material

2.6.6.1) Embedding and sectioning of pollinated stigmas

The stigmas of plants known to contain the S_1 gene were pollinated with pollen of known genotype to give either a fully compatible or a fully incompatible reaction. 1 h after pollination the top part of the stigma was cut from the plant with a razor blade and thin sections of the stigma containing the papillae cells were shaved off and placed into fixative comprising 2 % paraformaldehyde and 2 % glutaraldehyde made in 0.1 M sodium cacodylate pH 7.2. These samples were fixed overnight at room temperature. The fixative was removed and the material dehydrated through an ethanol series of 30 %, 50 %, 70 % and 90 % with the stigmas being in each solution for 15 min at room temperature. The material was transferred

to a 1:1 mix of 90 % ethanol:LR White resin (hard grade hydrophilic acrylic resin, Agar scientific) and left for 2 h at room temperature. This step was repeated once in a fresh 1:1 solution. The stigmas were then transferred to 100 % LR White (hard grade) for 5 h at room temperature. The stigmas were then transferred to size '0' gelatine capsules (Agar scientific) and filled with fresh outgassed (i.e. bubbles removed by placing in a vacuum for 15-20 min) LR White resin. The resin was then polymerised with long-ray (366 nm) UV light using a BLAK-RAY lamp, (UVP, California) for 3 days. Following polymerisation, the capsules were removed from the UV light and the gelatine capsule removed from the resin block. The block was then trimmed with a razor blade to get close to the area to be sectioned. The block was then sectioned using glass (Leica, cut via a LKB knifecutter) or diamond (Diatome) knives to a thickness of 1.5 μm using a Reichert Jung Ultracut ultramicrotome. The sections were collected in a drop of water on poly-lysine coated slides (VWR) and then the slide was placed on a warm dish warmer (Patterson) to cause the sections to expand and adhere to the slide. The dry slides were then ready for immunolocalisation.

The embedding and sectioning part of this protocol was kindly carried out by Steve Price, a technician in the laboratory.

2.6.6.2) Immunolocalisation of S-proteins on pollinated stigma sections

The pollen tube sections on the microscope slide were covered with 100 μl blocking solution (1% BSA, 0.1 % Triton-x100 in PBS) and a piece of parafilm, cut to the size of the slide, laid on top of the slide. This was incubated in a moist chamber for 1 h at room temperature. The excess liquid was tipped off the slide and 100 μl of the primary antibody/pre-immune serum, diluted 1:500 in blocking solution, was applied to the sections on the slide and covered with

parafilm. The slides were incubated with the primary antibody/pre-immune serum in a moist chamber overnight at 4°C. The slides were washed 3 x 10 min with 200 µl of blocking solution and then incubated with 100 µl of goat-anti-rabbit IgG-FITC antibody at a titre of 1:200 in the moist chamber at room temperature in the dark for 1.5 h. The slides were then washed 3 x 10 min in PBS, a small drop of VectorShield + DAPI was applied to the slide and a coverslip placed over the sections and sealed with nail varnish. The sections were then viewed under a fluorescence microscope.

2.7) Fluorescence Microscopy

2.7.1) Epifluorescence Imaging

Epifluorescence images were collected with a Nikon Eclipse Te300 microscope attached to a cooled coupled device (CCD) camera supplied by Applied Imaging, UK. Fluorescence was detected using filters for FITC and DAPI configured by Applied Imaging UK. Capture and analysis of images was achieved with a Quips PathVysion image analysis system (Applied Imaging International Ltd). Images were saved as TIF files and then manipulated in ImageJ or Microsoft PowerPoint.

2.7.2) Confocal Laser Scanning Microscopy (CLSM)

Images were collected with a BioRad Radiance 2000 laser scanning system using the 543 nm excitation line of a 1.5 mW Helium-Neon laser (Rhodamine, Cy3) and the 488 nm excitation line of a 50 mW (total) Argon laser (FITC). Full z-series stacks or single section scans of the pollen tubes were taken. The confocal microscope set up was as follows:

512 x 512 pixel box, 166 or 50 line speed scan, 3 Kalman scans

The size interval between each section of the stack ranged from 0.5 μm to 1 μm , depending on the thickness of the pollen tube. For single section scans for the localisation of PrpS₁ a line speed of 50 was used instead of 166 to give a more detailed image. Images from the confocal were saved as BioRad PIC files then viewed and manipulated using ImageJ software (Rasband, W.S., ImageJ, U. S. National Institutes of Health, Bethesda, Maryland, USA, <http://rsb.info.nih.gov/ij/>, 1997-2008). The images were then re-saved as TIF files. Further manipulation (e.g. orientation adjustments) was achieved using PaintshopPro (v 6.0) or Microsoft PowerPoint.

2.8) Image analysis using MetaMorph software

2.8.1) Co-localisation of F-actin with ABPs

A method to quantify the extent of co-localisation of F-actin with the ABPs was developed over the course of this work. This method allowed the different F-actin conformations (long filament bundles, cortical labelling and foci) to be measured for co-localisation of the ABP using the same parameters so that different SI time points could be compared. The co-localisation quantification was carried out using MetaMorph software (Molecular Devices) on single confocal slices acquired as detailed in **Section 2.7.2**. The pollen tubes in these images had been stained for both F-actin and the ABP in question. The amount of F-actin that was co-localising with the ABP was then measured. First, a threshold for co-localisation needed to be calculated. To do this the level of background fluorescence was measured. In the pollen tube image with the F-actin stained, 20 2x2 pixel boxes were placed throughout the pollen tube where there was **no** F-actin present (**Fig. 2.2a, b**). A larger, 10 x 10 pixel box was then placed around each of these 20 smaller boxes, making sure that no part of the box fell outside

of the pollen tube. These pairs of boxes placed on the actin-stained image were then transferred to the image of the ABP staining in the same pollen tube using the transfer region tool of MetaMorph (**Fig. 2.2c**). MetaMorph was used to calculate the average pixel intensity and the lowest pixel intensity of the ROIs. These were then exported into Microsoft Excel where they were used for the calculations detailed below. For the background measurement, for each pair of boxes, the average pixel intensity of the small box was divided by the lowest pixel intensity of the larger box. This resulted in 20 measurements per pollen tube. These 20 background measurements were taken for 5 pollen tubes for each of the SI time points and the average value and standard deviation of all the measurements calculated. The threshold for co-localisation was then calculated as the mean intensity plus one standard deviation. To determine whether the actin was co-localising with the ABPs the same approach was used but this time the actin image was used to place the small boxes over the areas **containing** F-actin, starting with the areas of greatest intensity (**Fig. 2.2d, f, g**). 50 different areas of actin were looked at in each pollen tube, with 5 different tubes for each SI time point. The larger boxes were then placed around the small ones making sure that some of the box was off the actin structure (i.e. including some pixels that were considered background staining) but ensuring it did not go outside the pollen tube edge. These 50 regions were then transferred onto the ABP-stained image of the same pollen tube (**Fig. 2.2e**) and measurements taken, i.e. the average intensity of the small box divided by the lowest intensity of the larger box. Those measurements that were greater than the threshold value counted as positive co-localisation and those that fell below had no co-localisation. The results were presented as the percentage of actin spots per tube that had positive co-localisation and are the mean values \pm the standard error of the means of the 5 different tubes per SI treatment time.

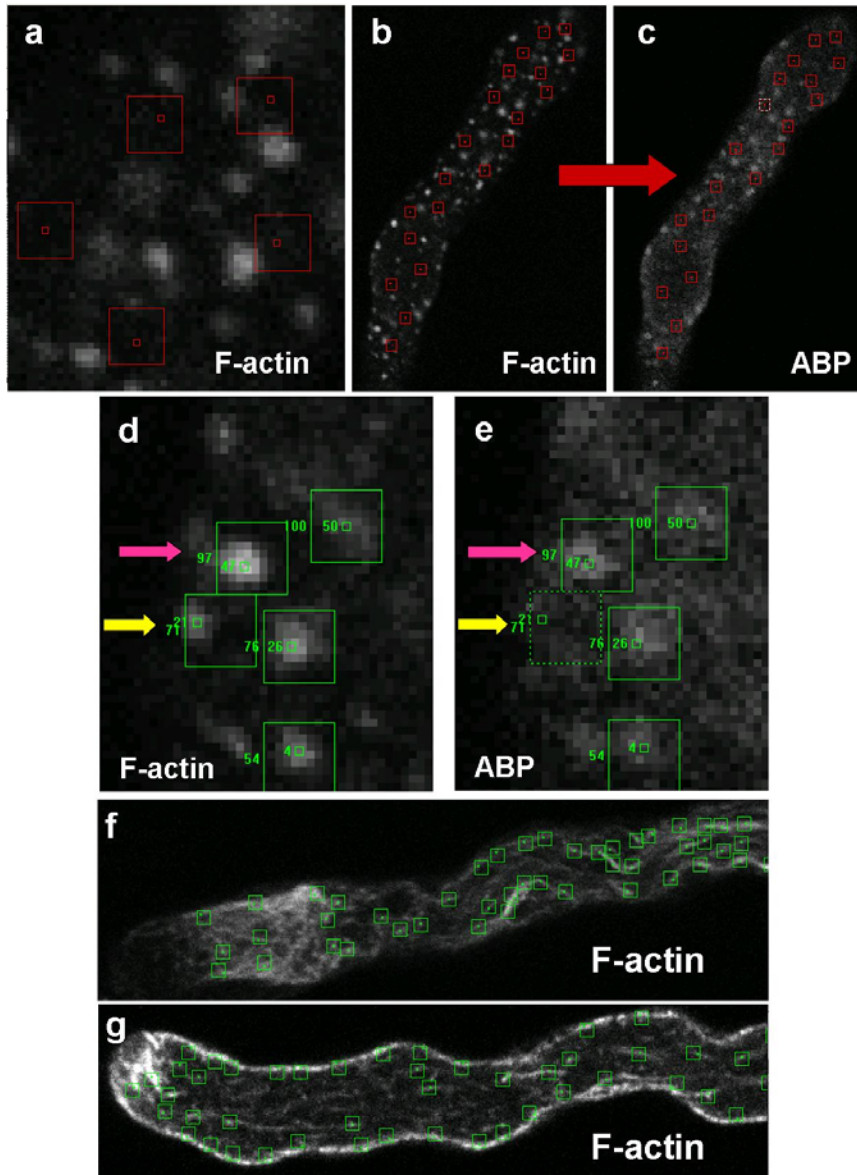


Figure 2.2. Quantification of co-localisation using MetaMorph

Single slice confocal images of pollen tubes stained for F-actin or an actin binding protein (ABP). The white pixels represent the actin or ABP, as labelled.

(a-c) Background measurements to set the threshold level for co-localisation. Regions where NO F-actin was present were selected (a). These 20 regions were spread throughout the length of the pollen tube (b). These regions were then transferred from the F-actin image onto the image of the same pollen tube stained for the ABP (c). Measurements were then taken as detailed in the text. For co-localisation measurements (d-g) areas of the tube that were labelled for actin were selected (d). These regions were then transferred to the ABP labelled image (e) and then assessed to see if the pixel intensity was above the threshold level for co-localisation. The pink arrow shows an example of positive co-localisation of the F-actin and the ABP and the yellow arrow shows an example of no co-localisation. (f) An example of regions of F-actin selected for co-localisation measurements in an untreated tube and (g) in a 10 min SI pollen tube.

2.8.2) Measuring the apparent size of the F-actin foci

Single slice images of pollen tubes labelled for F-actin were opened up in MetaMorph (Molecular Devices). Only pollen tubes which had been under-going the SI response for 30 min, 1 h, 2 h and 3 h were used as these were the time points that F-actin foci could be clearly visualised. The images were taken on the BioRad confocal (**section 2.7.2**) where 1 pixel = 0.13 μm , so this scale was set in MetaMorph. For each pollen tube section 20 actin foci were measured. These 20 foci were some of the foci which had been used previously in the co-localisation study. 10 different pollen tubes were used for each time point. The foci were measured by drawing a straight line region of interest (ROI) across the focus at its widest point. The boundaries of the foci were determined by eye, sometimes with the help of the threshold function. The length measurements of the straight line ROIs were calculated by MetaMorph and then exported into Microsoft Excel where simple statistics were carried out. Results were presented as the mean focus size \pm the standard error of the mean

2.8.3) Counting the number of F-actin foci

The same single slice images of pollen tubes with the F-actin labelled with rhodamine-phalloidin that were used for the foci size measurements were opened up in MetaMorph (Molecular Devices). Again only the 30 min, 1 h, 2 h and 3 h SI pollen tubes were used as these were the time points that F-actin foci could be clearly visualised. The edges of the pollen tube were defined using the free-line drawing tool and the inside of the draw region (the pollen tube) was coloured black using the paint tool. This prevented the F-actin foci from being visualised and influencing the areas to be investigated. Four squares, each measuring 30 x 30 pixels, were placed throughout the pollen tube area. The inside of the pollen tube region

was unpainted and the number of actin foci within the defined squares was counted. An actin focus was counted if any of it fell within the boundaries of the squares. 10 different pollen tubes, each with its 4 defined squares, were measured for each time point. The results are presented as the mean number of foci in a 30 x 30 pixel square at each time point \pm the standard error of the means, all calculated in Microsoft Excel.

2.9) Pollen Tube Length Measurement

For the measurement of pollen tube lengths, pollen was germinated, grown and treated as described in the experiment. Following treatment, pollen was fixed in 2% paraformaldehyde for 1 h at 4°C, washed 3 times in TBS and mounted on glass slides. Pollen was visualized under a Nikon Eclipse Tε300 microscope attached to a cooled coupled device (CCD) camera supplied by Applied Imaging, UK. Images were captured using a Quips PathVysion image analysis system (Applied Imaging International Ltd). Images were exported into the IPlab software (Applied Imaging International Ltd) where the final pollen tube lengths were measured (40 tubes for each of 3 independent treatments) using the measuring tool of the software. The lengths indicated are the total pollen tube lengths i.e. 1 h pretreatment time plus treatment time with the relevant drug. The measurements were exported from IPlab into a Microsoft Excel file where the *t*-test statistical analysis was performed.

2.10) Pollen Protein Extraction

Pollen was hydrated and grown in a Petri dish as described in **Section 2.3**. The size of the Petri dish and the amount of pollen used depended on the experiment. After growth and/or treatment, pollen was collected from the Petri dish using a pipette with a cut tip and put into a

1.5 ml microfuge tube. The microfuge tubes were spun at full speed for 1 min and the liquid GM removed. For long pollen tubes additional spinning may be required to allow removal of as much liquid GM as possible.

Several different extraction buffers and methods of extracting the protein were used depending on the experiment:

2.10.1) Protein extraction for the tubulin studies

For each dish of pollen grown, 150 μ L of HEPES extraction buffer (50 mM HEPES pH 7.4, 10 mM NaCl, 0.1% CHAPS, 10 mM dithiothreitol, 1 mM EDTA, 10% glycerol, protease inhibitor cocktail (Sigma)) was added to the pollen in the microfuge tube. Samples were roughly ground using plastic grinders in the microfuge tube before being snap-frozen in liquid nitrogen. The proteins were extracted as detailed below.

2.10.2) Protein extraction for the caspase assay

For each dish of pollen grown, 150 μ L of a sodium acetate based extraction buffer (50 mM sodium acetate, 10 mM L-cysteine, 0.01% CHAPS and 10% glycine, pH 6.0) was added to the pollen pellet. Again, samples were roughly ground in the microfuge tube before being snap-frozen in liquid nitrogen.

Following thawing of the samples, protein extracts were prepared by sonication: 3 x 10 sec at 10 Amps. After sonication, the samples were kept on ice for 30 min, vortexed occasionally and centrifuged for 15 min at 13,000 rpm at 4°C. The supernatant (the proteins) was then removed and stored at -20°C until required.

2.10.3) Protein extraction for the actin binding protein studies

For each dish of pollen collected, for which the majority of the liquid GM had been removed, 200 µl of 2 x Tris extraction buffer was added (100 mM Tris-HCl (pH 8), 200 mM NaCl, 2 mM EDTA, 1 M sucrose, 2 x protease inhibitor cocktail (Roche, Complete mini, EDTA-free)). The pollen was mixed with the buffer by flicking the microfuge tube and then transferred to a 3 ml glass homogeniser using a cut 1 ml tip. The pollen was ground on ice for 10 – 15 min, until the pollen appeared to be a homogenous liquid. Samples of the liquid could be checked under the microscope to confirm that the pollen grains and tubes had been ruptured to allow proteins to be released. The ground up pollen was transferred back to a microfuge tube and centrifuged at 13,000 rpm for 15 min at 4°C. The supernatant, containing the proteins, was removed and stored at -20°C until required.

2.10.4) Protein extraction for F-actin isolation

For each dish of pollen collected, from which the majority of the liquid GM had been removed, 200 µl of F-actin extraction buffer was added (10 mM HEPES (pH 6.8), 5 mM MgCl₂, 5 mM EGTA, 100 mM KCl, 1 mM DTT, 0.6 µM Biotin-Phalloidin, 0.1 % NP-40, 1x protease inhibitor cocktail (Roche, Complete mini, EDTA-free)). The pollen and extraction buffer were mixed by flicking and then transferred to a glass homogeniser using a cut 1 ml tip. Keeping the homogeniser on ice the pollen was ground up as detailed in **Section 2.10.3**. The ground pollen was transferred to a microfuge tube and centrifuged at 6000 rpm for 15 min and the supernatant collected. This centrifugation step was repeated to ensure that no debris such as pollen grains or tube walls remained in the supernatant. These protein extracts were then kept on ice ready for the next step (**Section 2.15**).

2.11) Estimation of Protein Concentration - Bradford Assay (Bradford, 1976)

Protein content was estimated by a BioRad microassay according to manufacturer's instructions (BioRad, UK). Protein assay reagent (which contains Coomassie® Brilliant Blue G-250) was added to diluted protein samples, and its absorbance measured at 595 nm with a spectrophotometer. BSA (5µg) was used as a standard. Protein concentration was derived as a function of the reading for the BSA.

2.12) Programmed cell death detection – Caspase activity assay

The presence of a caspase-like activity is one of the hallmark features of PCD. The fluorogenic caspase-3 substrate Ac-DEVD-AMC (Calbiochem) was used to establish whether caspase-like activity, and therefore PCD, was occurring in pollen tube treated with various cytoskeleton-interfering drugs. This fluorescent caspase activity assay is based on the cleavage of 7-amino-4-methylcoumarin (AMC) from the C-terminus of the fluorogenic substrate (Ac-DEVD-AMC) by a caspase-like enzyme, which is measured by an increase in the fluorescence intensity at 460 nm. This caspase substrate has the amino acid recognition sequence DEVD which is generally cleaved by caspase-3 and was derived from the caspase-3 cleavage site in PARP (Calbiochem product information). Although predominantly a caspase-3 substrate, Ac-DEVD-AMC can also be cleaved by caspases -6, -7, and -10. Pollen was hydrated and grown as described **Section 2.3**. After 1.5 h growth, the relevant treatment was added to the pollen. The pollen was left in the GM containing the treatment for 5 h at room temperature as this time period gave the highest caspase activity if PCD was occurring (Bosch & Franklin-Tong, 2007). The pollen was then collected into 1.5 ml microfuge tubes and the protein extracted as described in **Section 2.10.2**. The protein concentration was calculated using the BioRad Bradford assay as described in **Section 2.11**. The protein concentration

needed to be calculated as accurately as possible so two replicates were measured for each sample and also for the BSA standard. The protein concentration was then adjusted to $1 \mu\text{g} \mu\text{l}^{-1}$ by diluting in sodium acetate extraction buffer (50 mM sodium acetate, 10 mM L-cysteine, 0.01% CHAPS and 10% glycine, pH 6) and the protein concentration measured again. For the caspase assay $10 \mu\text{g}$ of total protein was incubated with $50 \mu\text{M}$ Ac-DEVD-AMC in sodium acetate buffer (pH 5) at 27°C to a final volume of $100 \mu\text{l}$. pH 5.0 is the optimum pH for caspase action in poppy pollen (Bosch & Franklin-Tong, 2007). If the protein concentration of the extract was less than $1 \mu\text{g} \mu\text{l}^{-1}$, the appropriate volume of protein extract was added into the well of the 96 well plate to make $10 \mu\text{g}$ of protein. The other samples in that experiment were made up to the greatest volume by adding the appropriate amount of pH 6.0 sodium acetate buffer so that all wells had the same volume of pH 6 buffer and protein before the $50 \mu\text{M}$ Ac-DEVD-AMC in pH 5.0 sodium acetate buffer was added. The fluorogenic caspase-3 substrate Ac-DEVD-AMC (Calbiochem) gives off a fluorescent signal when it is cleaved by a DEVDase (caspase 3-like) activity. Fluorescence was monitored at 460 nm using a time-resolved fluorescence plate reader (FLUOstar OPTIMA; BMG LABTECH) every 15 min over a time period of 5 h. The caspase-like activity for each sample was calculated by subtracting the fluorescence reading of the first cycle from the final (21st) cycle reading. Results are presented as percentage caspase activity relative to the untreated control or the SI-induced sample, whichever was the most appropriate for the experiment. All assays were performed on at least 4 independent samples, each measured in duplicate. *P* values were calculated using a two-way ANOVA using the statistical package MINITAB version 14.

2.13) SDS-Polyacrylamide Gel Electrophoresis

2.13.1) Preparation of SDS-PAGE

Proteins were analysed using the Biorad Mini-PROTEAN[®] 3, 1.5 mm gel kits. The percentage acrylamide gels used were 12.5 % and 15 %. The resolving gel was cast first and then the stacking gel was cast on top of the resolving gel.

12.5 % resolving gel:

4.8 ml SDW

6.3 ml Acrylamide (Protogel)

3.75 ml resolving buffer (1.5 M Tris, pH 8.8)

150 µl 10 % (w/v) SDS

75 µl 15 % (w/v) APS (Sigma-Aldrich)

15 µl TEMED (Sigma-Aldrich)

15% resolving gel:

3.6 ml SDW

7.5 ml Acrylamide

3.75 ml resolving buffer

150 µl 10% (w/v) SDS

75 µl 15% (w/v) APS

15 µl TEMED

Water-saturated butanol was poured over the top of the resolving gel (before polymerisation) to level the top of the gel and prevent evaporation. Once polymerisation had taken place, the butanol was rinsed off the gel with several changes of SDW and the stacking gel cast.

Stacking gel:

3.0 ml SDW

625 µl Acrylamide (Protogel)

1.25 ml stacking buffer (0.5 M Tris, pH6.8)

50 µl 10 % (w/v) SDS

25 µl 15 % (w/v) APS

5 µl TEMED (Sigma)

A 10 pronged comb was inserted before polymerisation of the stacking gel to form the wells. Following the polymerisation, the kit was assembled into the electrophoresis apparatus and the comb removed. The inner gel chamber was filled with 1x running buffer (25 mM Tris, 19.2 mM glycine, 0.1 % (w/v) SDS, pH 8.3) and the wells rinsed with this buffer to remove debris. Proteins to be loaded were mixed with 5 x protein loading buffer (see **Section 2.1**) to a final concentration of 1 x, boiled for 10 min and briefly centrifuged to collect the entire sample at the bottom of the tube. Gels were run at 70 Volts until protein samples had reached the bottom of the stacking gel and then increased to 150 Volts until the samples had run to the bottom of the gel.

2.13.2) SDS-PAGE gel staining

Gels were stained overnight at room temperature in Coomassie stain (0.02 % (w/v) Coomassie Blue R-250, 30 % (v/v) methanol, 10 % (v/v) glacial acetic acid) and destained in several changes of destain solution (30 % (v/v) methanol, 10 % (v/v) glacial acetic acid) on a shaker table. Following destaining, gels were dried in a gel dryer (BioRad, Model 583) for 1 h 15 min at 80°C.

2.14) Western Blotting

2.14.1) Protein transfer

Proteins were first resolved by SDS-PAGE as detailed above. The stacking gel was then removed from the resolving gel and discarded. The transfer unit was then set up as follows: a sponge, soaked in transfer buffer (20% (v/v) methanol, 25 mM Tris, 192 mM glycine, pH 8.3), was placed onto the transfer cassette, followed by 2 sheets of Whatman paper also

soaked in protein transfer buffer, the gel was then placed on top followed by a nitrocellulose membrane (Hybond-C extra (Amersham)) cut to the size of the gel. Any air bubbles were removed. A further 2 sheets of Whatman paper were placed on top of the membrane, a sponge placed on top and the cassette was closed and put into the electroblotting tank (Biorad) which was filled with protein transfer buffer. An ice pack was included in the tank to prevent overheating. BioRad power packs were used to blot the gel at 350 mA for 1.5 h. Following blotting, the nitrocellulose membrane was removed, washed briefly in TBS containing 0.1 % Tween 20 (TBST), stained with Ponceau S (Sigma; 0.1 % Ponceau S in 5 % acetic acid) to check transfer and loading, washed several more times in TBST and then placed in blocking solution (TBST, 5% (w/v) milk powder) for at least 1 h at room temperature or over night at 4°C.

2.14.2) Antibody probing

The blot was incubated with the primary antibody diluted into blocking solution for 3 h at room temperature or overnight at 4°C. The blot was then washed 3 x 10 min in blocking solution and then incubated with the secondary antibody (alkaline phosphatase-conjugated anti-mouse or anti-rabbit immunoglobulin) diluted 1:5000 in blocking solution for 1 h. The blot was then washed 3x 10 min in TBST.

2.14.3) Alkaline phosphatase detection

66 µl of Nitroblue tetrazolium (NBT: 0.5 g in 10 ml in 70 % (v/v) DMF (*N,N*-Dimethylformamide)) and 33 µl 5-Bromo-4-chloro-3-indolyl phosphate (BCIP: 0.5 g BCIP in 10 ml 100 % (v/v) DMF) was added to 9.9 ml alkaline phosphatase detection buffer (100 mM NaCl, 5 mM MgCl₂, 100 mM Tris, pH 9.5). The solution was mixed and poured over the blot and a colour change observed where the secondary antibody was present.

2.15) F-actin enrichment using ultracentrifugation

Pollen proteins were extracted (**Section 2.10.4**) in a buffer containing 0.6 μM phalloidin that promotes F-actin stabilisation (Cano et al, 1991). The extracted protein was then pipetted into 3 ml heat-sealable ultracentrifugation tubes. A volume of 50 μl was kept for each sample to serve as the 'pre-spin' control to show that F-actin was enriched after the high-speed spin. The volume in the ultracentrifuge tube was made up to the top of the tube using extraction buffer (10 mM HEPES (pH 6.8), 5 mM MgCl_2 , 5 mM EGTA, 100mM KCl , 1 mM DTT, 0.1 % NP-40, 1x protease inhibitor cocktail). The weights of the ultracentrifugation tubes were measured (to 2 decimal places) to ensure that the ultracentrifuge was correctly balanced. The tubes were heat sealed. The protein extracts were then spun at 100,000 rpm at 4°C in a Beckman TL-100 tabletop Ultracentrifuge (Beckman instruments, Inc) for 15 min to pellet the F-actin. The supernatant - the cytosolic fraction - was removed using a needle and syringe and kept. The pellet – the F-actin enriched fraction – was resuspended into extraction buffer containing biotin-phalloidin. Depending on the size of the pellet 100-200 μl of the buffer was used. The pellet was roughly re-suspended by pipetting up and down using a cut 200 μl tip then transferred to a 100 μl glass homogeniser to ensure the pellet was re-suspended as well as possible. These samples were then stored at 4°C as freezing causes F-actin depolymerisation. The fractions were tested for the presence of F-actin by staining with rhodamine-phalloidin. 5 μl of each fraction was incubated with 1 μl of rhodamine-phalloidin for 30 min at 4°C. This was then put onto a microscope slide, covered with a cover slip and sealed with nail varnish before viewing under the epifluorescence microscope (**Section 2.7.1**).

2.16) F-actin pull-down assay

The isolation of F-actin from pollen protein extract was attempted using the property of phalloidin to bind specifically to F-actin. A biotin-phalloidin conjugate (Sigma-Aldrich) was used to bind to the F-actin and the biotin acted as a tag that could be used to pull-down the F-actin and its associated components by the high-affinity binding of biotin to avidin.

2.16.1) Streptavidin MagneSphere Paramagnetic Particles (SA-PMPs)

Pollen proteins were extracted as detailed in **Section 2.10.4** and the F-actin enriched for by ultracentrifugation (**Section 2.15**). In a 1.5 ml microfuge tube, 400 µg of pollen extract was first incubated with 4 µg of biotin-phalloidin, made up to a final volume of 500 µl with extraction buffer, for 2 h at 4°C on a rotor. During this time, the SA-PMPs (Promega) were prepared for biotin binding by adding 100 µl of the fully re-suspended SA-PMPs into a 1.5 ml microfuge tube and washing in 3 x 100 µl of 2 x PBS and then once in 100 µl of extraction buffer. The washing involved adding the 100 µl solution, making sure everything was properly re-suspended and then placing the microfuge tube into the Magnetic Separation Stand (Promega) which draws the magnetic particle to the side of the tube and allows the liquid to be pipetted off easily. After incubation, the 500 µl of extract with the biotin-phalloidin was added to the SA-PMPs and left mixing on a rotor at room temperature for 1 h. The SA-PMPs were then captured using the magnetic stand and the liquid, the not bound fraction, removed and kept. The beads were then washed three times in 500 µl of extraction buffer. Each wash was kept and labelled. The streptavidin-biotin binding of this method is irreversible so to release the proteins from the SA-PMPs the SA-PMPs were re-suspended into 40 µl of 2 % SDS with 3 mM biotin made up in PBS. 10 µl of 5 x protein loading dye was then added and the mixture left to mix on the rotor for 15 min at and then boiled for 15

min before loading onto SDS-PAGE. The input, not bound and wash fractions were combined with appropriate amounts of 5 x protein loading dye, boiled and loaded onto SDS-PAGE.

2.17) Analysis of F-actin containing fractions by FT-ICR MS

2.17.1) Sample preparation

Samples containing F-actin were loaded onto SDS-PAGE. All the proteins present in the sample mix were of interest so the gel was only run for a very short while so that the proteins just entered the resolving part of the gel. The gel was then stained with Coomassie stain (**Section 2.13.2**) and then destained so that the areas of the gel containing protein were clearly visible. These areas were then cut out of the gel, and placed into a sterile microfuge tube. This was then called a gel plug. The gel plugs were then sent to the Proteomics Facility at the University of Birmingham (<http://www.genomics.bham.ac.uk/proteomics.htm>) for processing and analysis by FT-ICR-MS. The samples underwent a tryosin digest and were then analysed by a Thermo Finnigan LTQ-FT. These data from the FT-ICR-MS could then be analysed by the customer using a licensed version of the Mascot software at www.matrixscience.com (see below).

2.17.2) Mass spectrometry data analysis by Mascot

Mascot (www.matrixscience.com), is a public domain, powerful search engine that identifies proteins from primary sequence databases using mass spectrometry data. A licensed version of the software permits larger data sets to be analysed in a single search using the downloadable software Mascot Daemon. A licensed version was used here. The search that was carried out for this work was a MS/MS ion search. The search parameters were as follow:

Taxonomy: *Arabidopsis thaliana* **Database:** Swissprot **Enzyme:** Trypsin

Fixed Modifications: carbamidomethyl (C) **Variable modifications:** oxidation (M)

Report top: auto **Max. missed cleavages:** 2 **Peptide charge:** 2+ & 3+

Peptide tol. ±: 0.8 Da **MS/MS tol. ±:** 0.8 Da **Monoisotopic** selected

Data format: Mascot generic **Quantitation:** None

As the 'Report hits' in Mascot was set to 'auto' the software returns all the significant hits, i.e. proteins identified with 95 % confidence. These proteins were then investigated further to see what types of protein were interacting with actin and what their possible role in SI could be.

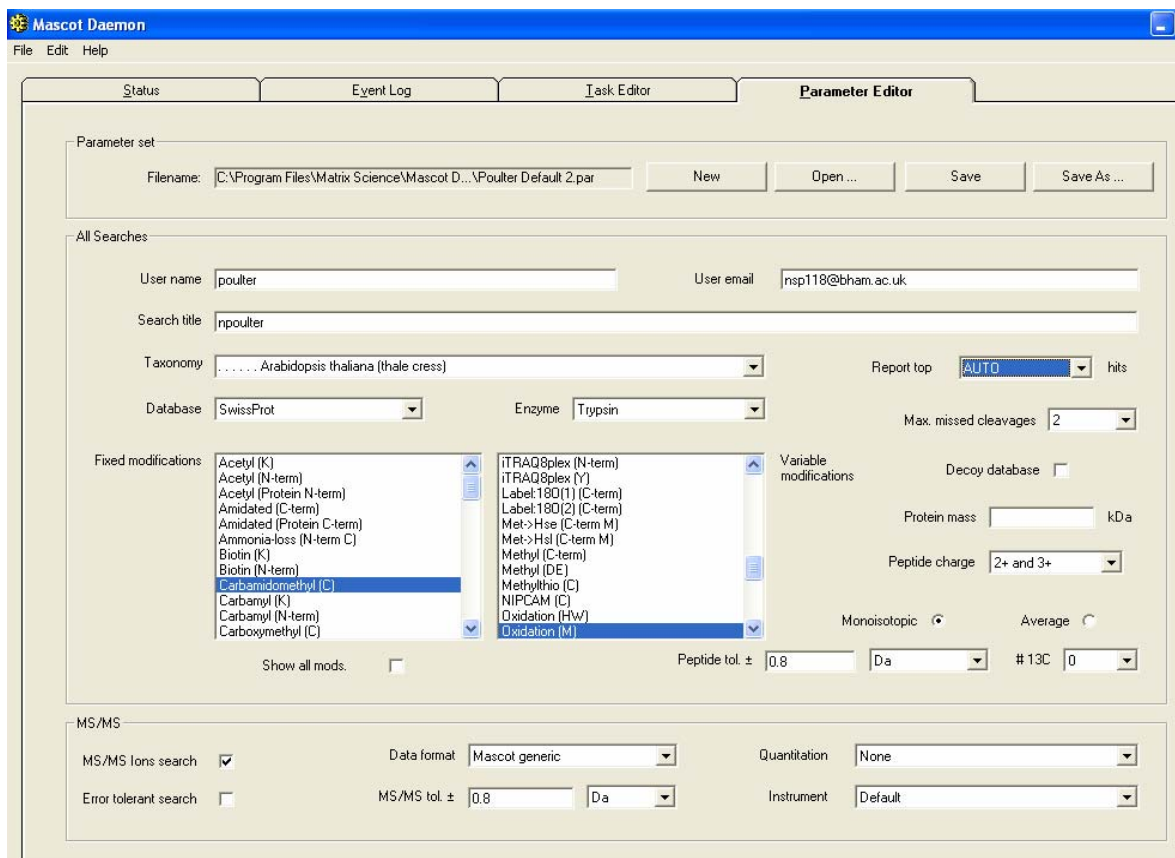


Figure 2.3. Mascot MS/MS ions search page

An example of the search parameter page of the Mascot Daemon software.

2.18) Statistical Analysis

Microsoft Excel (Microsoft Office 2003) was used to collate all numerical data, create tables and graphs and calculate simple statistics (mean and standard error) as well as calculate the *t*-tests. All other statistical analyses were carried out using the statistical package MINITAB 14. The statistical analysis used was: Two-way AVOVA, using the general linear model. *P* values <0.05 were considered significantly different.

CHAPTER 3

IMMUNOLOCALISATION OF THE MALE AND FEMALE S-DETERMINANTS IN *PAPAVER* POLLEN TUBES

3.1) Introduction

The female *S*-determinant of *Papaver* SI has been known since 1994 and is a small (~15 kDa) soluble protein secreted by the papillae cells of the stigma which has been termed S-protein (Foote et al, 1994; Walker et al, 1996; Kurup et al, 1998). The three S-protein genes that have been fully cloned to date (*S₁*, *S₃* and *S₈*) are highly polymorphic, with the predicted amino acid sequence only sharing between ~56% - 64% identity (Walker et al, 1996; Kurup et al, 1998). The amino acid variation is found throughout the S-protein (Kurup et al, 1998), in contrast to the S-proteins from the *Brassicaceae* and *Solanaceae* which have hypervariable blocks of amino acids (Nassrallah et al, 1987; Kusaba et al, 1997; Ioerger et al, 1990; 1991). Despite the low level of identity between *Papaver* S-proteins they are predicted to assume virtually identical secondary structures that consist of six β -strands with two α -helices at the C-terminal end which are all linked by seven hydrophilic surface loops (Walker et al, 1996; Kurup et al, 1998). Site-directed mutagenesis revealed that both variable and conserved residues in surface loop 6 of the *S₁*-protein and conserved residues in loop 2 are essential for recognition of incompatible pollen (Kakeda et al, 1998; Jordan et al, 1999). There are also 4 conserved cysteine residues which are thought to form disulphide bridges that are necessary to maintain the S-protein's tertiary structure and therefore functional activity (Walker et al, 1996; Kakeda et al, 1998). At the time of their identification the S-proteins from *Papaver* showed no significant homology to any previously reported gene sequence which was interesting as it suggested that *Papaver* employed a mechanism of SI that was distinct from that of the *Brassicaceae* and the *Solanaceae* (Foote et al, 1994). In 1999, a whole family of plant-specific genes was identified from the *Arabidopsis* genome which shared homology with the *Papaver* S-proteins (Ride et al, 1999). These proteins were called *S-protein homologues* (SPHs). The SPHs do not play a role in SI as they are expressed in a wide range of tissues and

Arabidopsis thaliana, a member of the *Brassicaceae*, is a self-compatible species. Self-incompatible relatives of *A. thaliana* therefore employ a different SI system to that of *Papaver* (see **Chapter 1**). The SPHs are hypothesised to act as small extracellular signalling molecules during other plant responses (Ride et al, 1999; Wheeler et al, unpublished).

Our laboratory has developed an *in vitro* SI bioassay for *Papaver*. In this bioassay, addition of incompatible recombinant S-proteins to pollen growing *in vitro* is sufficient to trigger the SI response which is a calcium-mediated signalling cascade (Franklin-Tong et al, 1993) that results in pollen tube growth inhibition and PCD (see **Chapter 1** for full details). Because of the rapidity of the SI response, it is hypothesised that SI is mediated by a receptor-ligand interaction. The female component, the S-protein, is proposed to act as the ligand which binds to the male S-receptor (reviewed in Bosch & Franklin-Tong, 2008). The male S-determinant has been somewhat more elusive than the female S-proteins and has been the subject of our laboratory's research for many years. An integral-membrane protein, SBP (S-protein binding protein), was identified from pollen which interacted with the S-proteins (Hearn et al, 1996). The SBP bound to S-proteins but in a non-S-allele-specific manner, and thus could not be the S-specific receptor. It has been proposed that SBP could be a co-receptor or accessory protein that aids the interaction of the S-proteins with the true S-receptor (Hearn et al, 1996).

Recent studies have identified the gene *PrpS* (*P. rhoeas* pollen S), which encodes a ~20 kDa protein with three to five predicted transmembrane domains, with no homology to known proteins in existing databases. Several alleles of this gene have been cloned and recent work provides convincing evidence that it is the pollen S-determinant (Wheeler et al, 2009; see Appendix I). To be a *bona fide* S-determinant *PrpS* must satisfy several criteria: (1) be linked

to the pistil component, i.e. within the *S*-locus, (2) it must be expressed solely in pollen, (3) it has to exhibit *S*-genotype specific polymorphism and (4) it has to function in *S*-specific pollen rejection. The work by Wheeler et al (2009) has established that *PrpS* fulfils these criteria. In brief; expression analysis using RT-PCR has shown *PrpS* to be pollen specific with maximum expression levels at anthesis. The 3 alleles that have been cloned (*PrpS*₁, *PrpS*₃, *PrpS*₈) are highly polymorphic (e.g. the full length *PrpS*₁ and *PrpS*₈ sequences are only 60% identical at the amino acid level) and linkage analysis reveals that the pollen *PrpS* and their corresponding pistil *S*-protein genes are tightly linked, which is a key requirement of a functional SI system.

Preliminary work on *PrpS* localisation using *PrpS*₁-GFP constructs that were transiently expressed in poppy and tobacco pollen indicated that the protein was closely associated with the pollen tube plasma membrane, although there was also some accumulation of the protein within the pollen tube which was probably caused by overexpression (de Graaf, unpublished data). These results provide evidence which support the hypothesis that *PrpS* is the membrane-bound male *S*-determinant. At the time of these studies we did not have evidence that *PrpS* was translated into a protein in pollen and had not investigated its native localisation in the pollen tube. Here we address these questions. An antibody was raised against the C-terminal portion of the recombinant *PrpS*₁ protein and this *PrpS*₁-specific antibody was used to show that *PrpS*₁ was translated into a protein and was specifically expressed in *S*₁ pollen (Hadjiosif, 2008; Wheeler et al, 2009). In this chapter we have used this antibody to confirm the predicted membrane localisation of *PrpS* using immunolocalisation. Furthermore, although the *S*-proteins have long been known to induce the SI response in incompatible pollen, their localisation in *in vivo* pollinated stigmas and in

in vitro SI-challenged pollen has never been studied. An important question was where the S-proteins were localised after SI induction and whether S-proteins interacted with both incompatible and compatible pollen tubes. Here, we have used immunolocalisation to examine the localisation of S-proteins upon SI-challenge of pollen tubes grown *in vitro* and also the localisation of S-proteins in *in vivo* pollinations of both incompatible and compatible stigmas.

The production of the anti-PrpS₁ antibody and the western blot analyses showing that PrpS₁ was only found in S₁ pollen were carried out by Natalie Hadjiosif as part of her PhD thesis (2008). These results are shown here for completeness, to demonstrate that the antibody was suitable for use in the immunolocalisation studies which formed the basis of my work.

3.2) Results

3.2.1) The PrpS₁60C antibody recognises PrpS₁ protein

The full length *PrpS₁* sequence was very hydrophobic, thus problematic to express in *E.coli*. The C-terminal domain of *PrpS₁* was therefore chosen for use in antibody production because it was the least hydrophobic domain of the protein (Hadjiosif, 2008). A His-GST-tagged recombinant protein (PrpS₁60C-HIS-GST), containing the last 71 amino acids of the PrpS₁ protein, which was predicted to span from the cytosol out into the extracellular domain (**Fig. 3.1**), was expressed in *E. coli* BL21 cells and formed inclusion bodies. These inclusion bodies, containing *PrpS₁*, were sent to Immune Systems Limited (ISL, Poole, UK) where a polyclonal antiserum was generated in rats. The affinity of the antibody for the native PrpS₁ protein was assessed using western blot analysis on total pollen tube proteins extracted from a variety of S₁- and non-S₁ containing pollen (**Fig. 3.2a**). The antibody recognised a band at ~20 kDa, the predicted molecular weight of PrpS₁, in S₁ containing pollen samples only, indicating the protein was only present in S₁ pollen tubes. The pollen proteins were also separated into soluble and membrane-enriched fractions (using Triton X-100) and assessed for the presence of PrpS₁ using western blot analysis. Figure **3.2b** shows that PrpS₁ was present in the membrane-enriched fraction, supporting the prediction of an integral membrane protein. These western blots demonstrated the specificity of the PrpS₁60C antibody for the PrpS₁ protein, therefore the antibody was suitable for use in immunolocalisation studies of PrpS₁.

a

MPRSGSVVTLFQFVGG
LCTLLGVSVAIKAIFAQDY
TLK
DLIILIVLVALSIILGGPITL
TCVK
LLGLVLHRLSFSEDQKWVVAFGTAAICDVLVLP
KNMLPMTIFSFLSPIMICV
VAVGWDCDRSGMTEGFLVGF
GKLLLVYLIKODFTFSLLCGSVLCLA
VVAKFT
EGKAEATPNPNLAGKADSPHLITQA

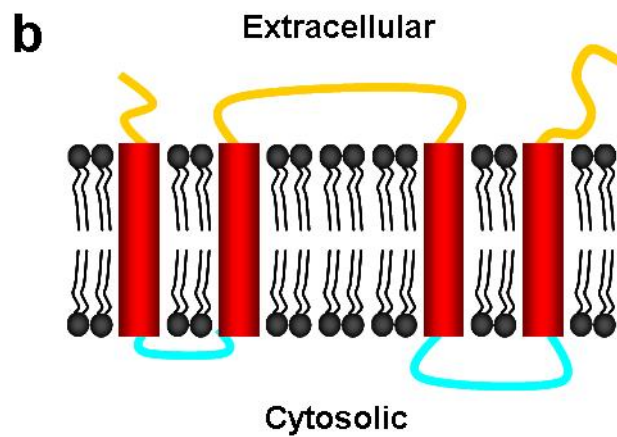


Figure 3.1. PrpS₁ amino acid sequence and predicted topology.

a) PrpS₁ amino acid sequence showing predicted domains of the protein and the C-terminal amino acids used for antibody production.

Yellow region = predicted extracellular domains.

Red region = predicted transmembrane domains.

Blue region = predicted intracellular domains.

The **underline** represents the amino acids used for the production of PrPS₁60C recombinant protein and to which the subsequent antibody was raised.

b) Cartoon illustrating the predicted topology of PrpS₁ in the membrane.

The transmembrane prediction program used here was PredictProtein (Rost et al, 2004).

Figure adapted from Hadjosif (2008)

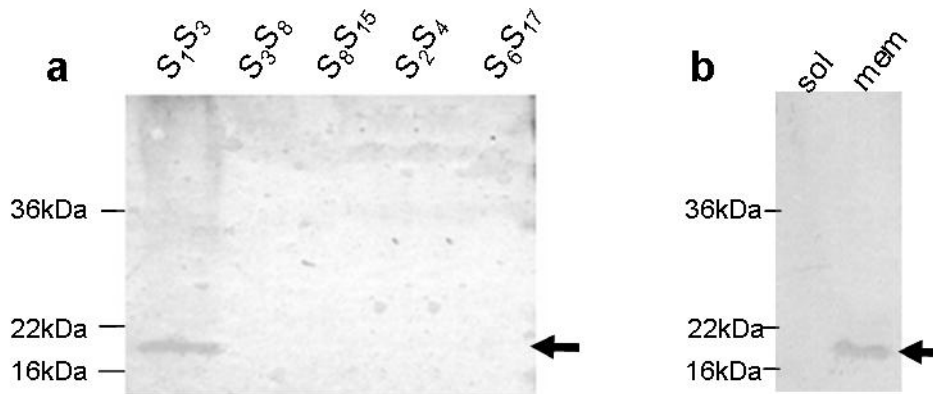


Figure 3.2. The PrpS₁60C antibody detects PrpS₁ protein, which is present in the membrane-enriched fraction.

a) Total pollen protein was extracted from different pollen haplotypes (indicated at the top of the blot) and resolved on an SDS-PAGE gel alongside a molecular weight marker (in kDa) and then blotted. The membrane was incubated with the primary antibody PrpS₁60C (1:1000) and then an alkaline phosphatase conjugated anti-rat secondary antibody (1:5000). PrpS₁ can be seen (arrow) migrating at the predicted molecular weight of ~20 kDa in S₁ containing pollen only.

b) S₁S₃ pollen proteins were separated into soluble (sol) and membrane-enriched (mem) fractions, resolved by SDS-PAGE and blotted as above. The arrow indicates PrpS₁ which is present in the membrane enriched fraction.

Figure adapted from Wheeler et al (2009).

3.2.2) PrpS localises to the pollen tube membrane.

The *Papaver* male *S*-component is a small, novel transmembrane protein (Wheeler et al, 2009). The sequence of PrpS₁ has several predicted transmembrane domains and western blot analysis demonstrated that PrpS₁ was present in the membrane-enriched fraction of pollen proteins, both of which support this idea. Immunolocalisation of PrpS₁ was required to visualise the protein in the pollen tube to confirm its localisation at the plasma membrane. Immunolocalisation of PrpS₁ was carried out on pollen from a plant carrying the S₁ allele using the PrpS₁60C antibody. The pre-immune serum was used at the same dilution as a control to ensure that any labelling that was seen with the PrpS₁60C antibody was due to the presence of PrpS₁ and not non-specific labelling. **Figure 3.3a** shows that PrpS₁ localised to the pollen tube membrane. The signal was the most intense in the extreme tip of the tube and then appeared to tail off into the shank. Some labelling could be detected inside pollen tubes labelled with the PrpS₁60C. However, this labelling was present in all pollen tubes. Furthermore, similar labelling was observed in tubes labelled with the pre-immune serum (**Fig. 3.3b**) suggesting that this was non-specific labelling by the serum. The pre-immune serum did not show any membrane labelling, indicating that the membrane localisation was specific to PrpS₁. Some labelling within the pollen tube might be expected because PrpS₁ needs to be synthesised and then transported to the tip in vesicles before it becomes incorporated into the tip membrane. There could also be membrane recycling occurring through endocytosis, especially in the tip and sub-apical area, as this is a common feature of pollen tubes (Parton et al, 2001; Camacho & Malhó, 2003; Wang et al, 2005; 2006; Samaj et al, 2005; 2006). **Figure 3.4** shows the average pixel intensity of a cross-section taken across the tip-end of the pollen tubes labelled with PrpS₁60C (**Fig. 3.4a, b**) or pre-immune serum (**Fig. 3.4d, e**). The traces of 5 other tubes for each label are also shown in **Figure 3.4c & f** to

illustrate the reproducibility of these data. These traces clearly show an increase in the pixel intensity at the edge of the pollen tubes labelled with PrpS₁60C. The average pixel intensity at the edge of the PrpS₁ labelled tube was three times as great as the average pixel intensity in the lumen of the pollen tube indicating the presence of the PrpS₁ protein which is absent from the tubes labelled with pre-immune serum.

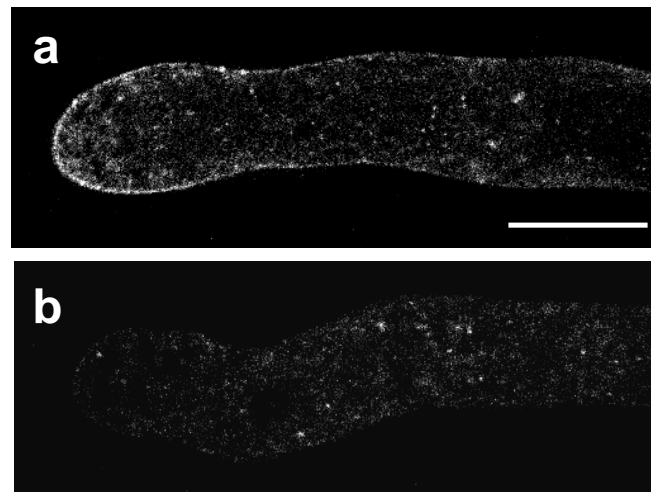


Figure 3.3. PrpS₁ localises to the pollen tube membrane.

a) An S₁ pollen tube labelled with anti-PrpS₁60C antibody (1:500) shows that the PrpS₁ signal was localised adjacent to the pollen tube plasma membrane and appeared to be more concentrated at the tip of the tube.

b) The pre-immune serum (1:500) did not show any membrane labelling, only some non-specific background labelling within the tube.

The images are single confocal sections through the centre of the pollen tube with an optical thickness of ~1 μ m. All images were gathered using identical argon laser settings to allow comparisons to be made between them. Scale bar = 10 μ m

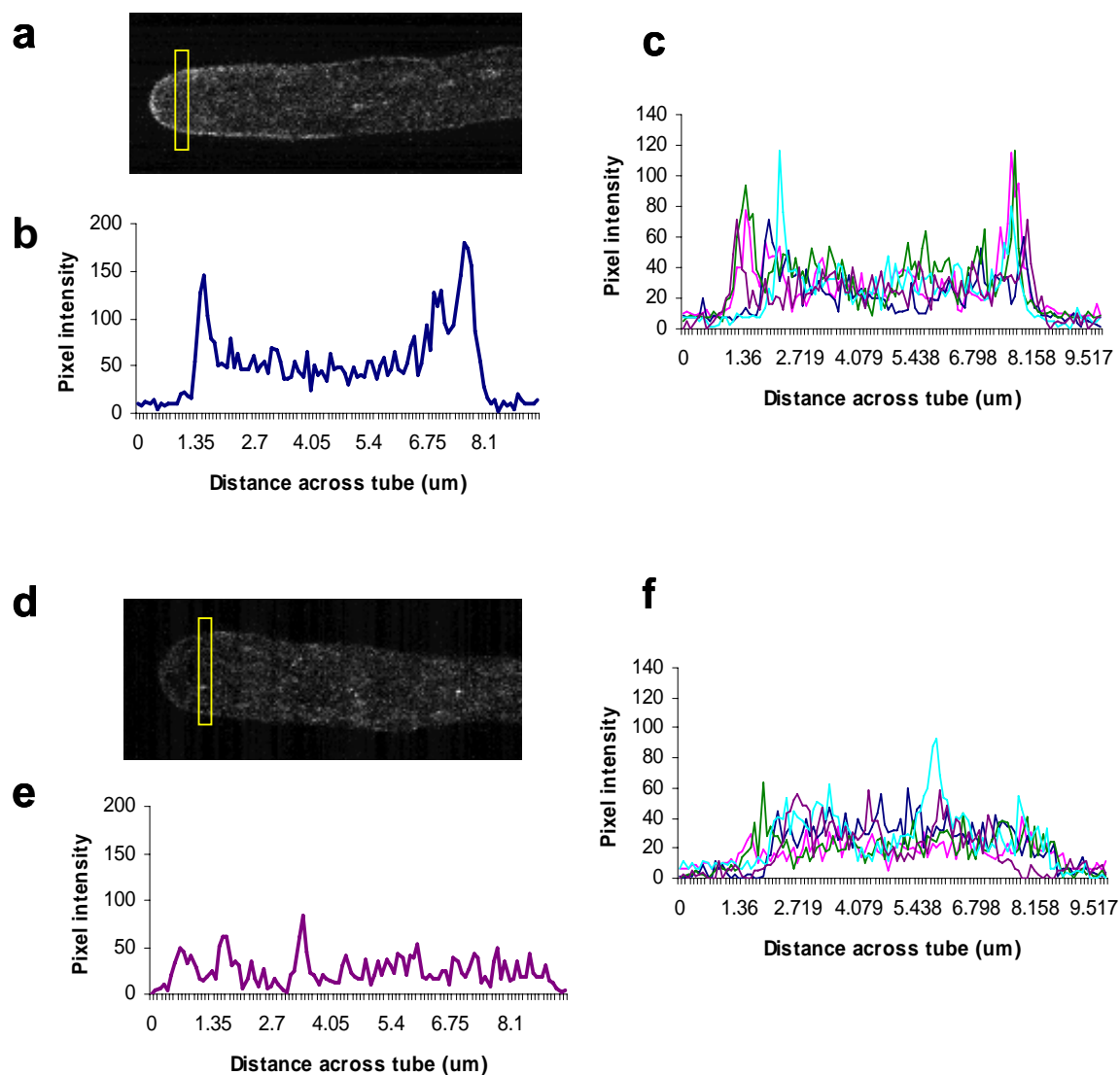


Figure 3.4. Pixel intensity traces show PrpS₁ localises to the pollen tube membrane.

A box (yellow) 5 pixel high and long enough to span the width of the pollen tube was placed $\sim 3 \mu\text{m}$ from the tip of the pollen tube labelled with anti-PrpS₁ antibody (a) or pre-immune serum (d). The pixel intensity across the tube was measured using the plot profile function in ImageJ. A typical PrpS₁ trace is seen in (b) where the edges of the pollen tube showed a definite increase in signal over the rest of the tube, indicating the presence of PrpS₁. The traces of a further 5 tubes labelled with anti-PrpS₁ antibody can be seen in (c). The pixel intensity was an average of 3 times greater at the periphery where PrpS₁ was found compared to the lumen of the tube. A typical trace of the pixel intensity across a tube labelled with the pre-immune serum where no edge-labelling was detected is shown in (e) and 5 more tubes have been analysed in (f) which all show the same pattern.

3.2.3) *In vitro* localisation of S-proteins

The female S-determinant of the SI response, the S-proteins, are secreted by the papillae cells and are assumed to come into contact and interact with the pollen when it lands on the stigma. Here, an antibody raised against the recombinant S₁ protein, already available in the laboratory, has been used to investigate the localisation of S-proteins in pollen during the SI response induced *in vitro*. The recombinant S₁ protein has few contaminating *E.coli* proteins, which can be seen in the Coomassie Blue stain of the recombinant S₁-protein solution (**Fig. 3.5, lane 1**). Also, the SI response is S-specific depending on which recombinant S-proteins are being used and all preparations contain similar profiles of *E.coli* proteins. This means we can be sure that any response seen in the pollen is due to the recombinant S-protein and not other contaminating proteins. The anti-S₁ antibody recognises the S₁ recombinant protein (**Fig. 3.5, lane 2**) and the pre-immune serum does not cross-react with any proteins present in the recombinant S₁-protein solution (**Fig. 3.5, lane 3**). These data demonstrate that the anti-S₁ antibody is suitable for immunolocalisation studies of the S₁-protein.

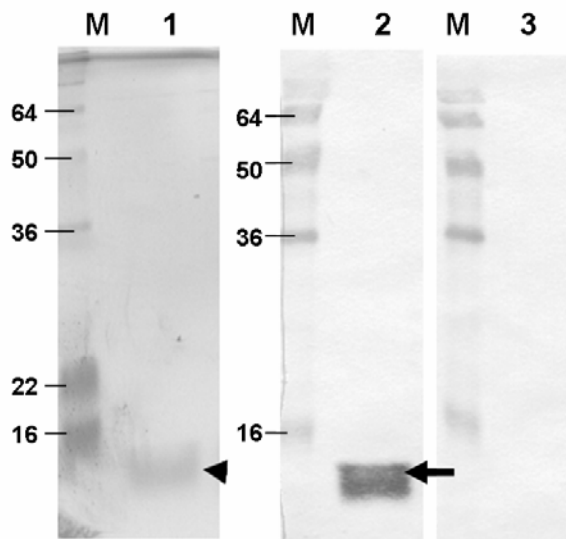


Figure 3.5. The S_1 antibody recognises the recombinant S_1 protein.

Lane 1: A Coomassie Blue stain of the recombinant S_1 protein solution shows that the preparation was clean; the *E.coli* proteins had been removed, and there was S_1 protein present (arrowhead).

Lane 2: The anti- S_1 antibody (1:4000) recognised the recombinant S_1 protein, which was ~14 kDa (arrow). The lower band could represent a degradation product of the S_1 protein.

Lane 3: The pre-immune serum did not recognise any proteins present in the recombinant S_1 protein solution.

M = marker lane (kDa). Alkaline phosphatase detection was used for the western blots.

The localisation of the S-proteins was investigated in both an incompatible and a compatible reaction (**Fig. 3.6**). Pollen containing S_1 and S_3 alleles was germinated and grown for the incompatible reaction and pollen that did not contain the S_1 haplotype (S_3S_8) was grown for the compatible reaction as a control experiment. The SI response was induced by addition of S_1 -protein for 10 min before chemical fixation and S-protein immunolocalisation. Pollen from plants of S_1S_3 haplotype in combination with S_1 recombinant protein was a half-compatible reaction as only the S_1 -protein was added to the pollen to induce the SI response. The remaining 50 % of the pollen (S_3) therefore acted as an internal compatible control which could be easily identified by staining the F-actin, as SI triggers alterations to the actin cytoskeleton in incompatible, but not compatible pollen tubes. Several control situations were

also set up to ensure that it was really the S-proteins that were being visualised, they were as follows:

- 1) Pollen grown WITHOUT addition of S₁-protein into the growth medium but during immunolocalisation it was incubated with the anti-S₁ antibody and FITC-conjugated secondary antibody (**Fig. 3.7b**)
 - To ascertain that the anti-S₁ antibody did not non-specifically bind to the pollen tube
- 2) Pollen grown WITH addition of S₁-protein into the growth medium but during immunolocalisation it was incubated with the pre-immune serum and FITC-conjugated secondary antibody (**Fig. 3.7c**)
 - To ensure the pre-immune serum and secondary antibody did not bind to the S-proteins
- 3) Pollen grown WITHOUT addition of S₁-protein into the growth medium but during immunolocalisation it was incubated with the pre-immune serum and FITC-conjugated secondary antibody (**Fig. 3.7d**)
 - To make sure that the pre-immune serum and/or the secondary antibody did not non-specifically react with the pollen tube.

If signal was detected in these situations it could be considered as non-specific background labelling. Similar labelling in the samples treated with S₁-proteins and then detected with the antibodies could then be excluded as background.

Figure 3.6 shows that the S-proteins localised to the periphery of the pollen tubes in both an incompatible (**fig 3.6a**) and a compatible (**Fig. 3.6e**) SI reaction. These data are also confirmed with the pixel intensity plots across pollen tubes immuno-labelled for S-proteins (n=10) where the intensity increases at the periphery of the tube where the S-proteins are present (**Fig 3.7**). The S-protein immuno-labelling in the incompatible reaction appeared to be

more intense than that of the compatible tubes (seen in the images and the plots). The average pixel intensity at the periphery of incompatible pollen tube was 3.7 times greater than the average pixel intensity in the lumen of the tube. In compatible tubes this increase in intensity fell to 3.2 times greater than in the lumen. A greater number of pollen tubes will need to be investigated to confirm whether this is significantly different. It was also observed that the labelling was often the most intense at the tip of the pollen tube and appeared less intense along the shank, although still visible. Although the S₁-proteins bound to the compatible pollen tubes, they did not trigger the SI response as the F-actin in these tubes remained intact (**Fig. 3.6g**), while in incompatible tubes the F-actin depolymerised and started to form the characteristic actin foci seen in SI (**Fig 3.6c**) (Geitmann et al, 2000; Snowman et al, 2002). The S-proteins were found along the periphery of compatible as well as incompatible pollen tubes so the S-proteins interacted with all pollen, regardless of *S*-haplotype. This is not entirely surprising as SBP has been shown to bind to all S-proteins non-discriminately (Hearn et al, 1996). However, SI was only triggered in the incompatible pollen tubes. The control pollen tubes did not show any labelling of the periphery (**Fig. 3.7b-d**) indicating that this signal was specific to the S-proteins. The pixel intensity traces (**Fig. 3.7e**) clearly show the difference between the labelling of the S-proteins compared to the controls, with the controls having a fairly consistent background level across the tube that is very similar to the labelling seen within the lumen of the pollen tubes treated with S-protein. The weak antibody signal seen inside the S-protein treated tubes could possibly indicate some internalisation of the S-proteins. However, a similar signal was seen in control pollen tubes that did not have S-proteins present so could not be attributable to the internalisation of S-proteins. This indicated that the signal seen inside S-protein treated pollen tubes was probably due to non-specific labelling by the antibody serum.

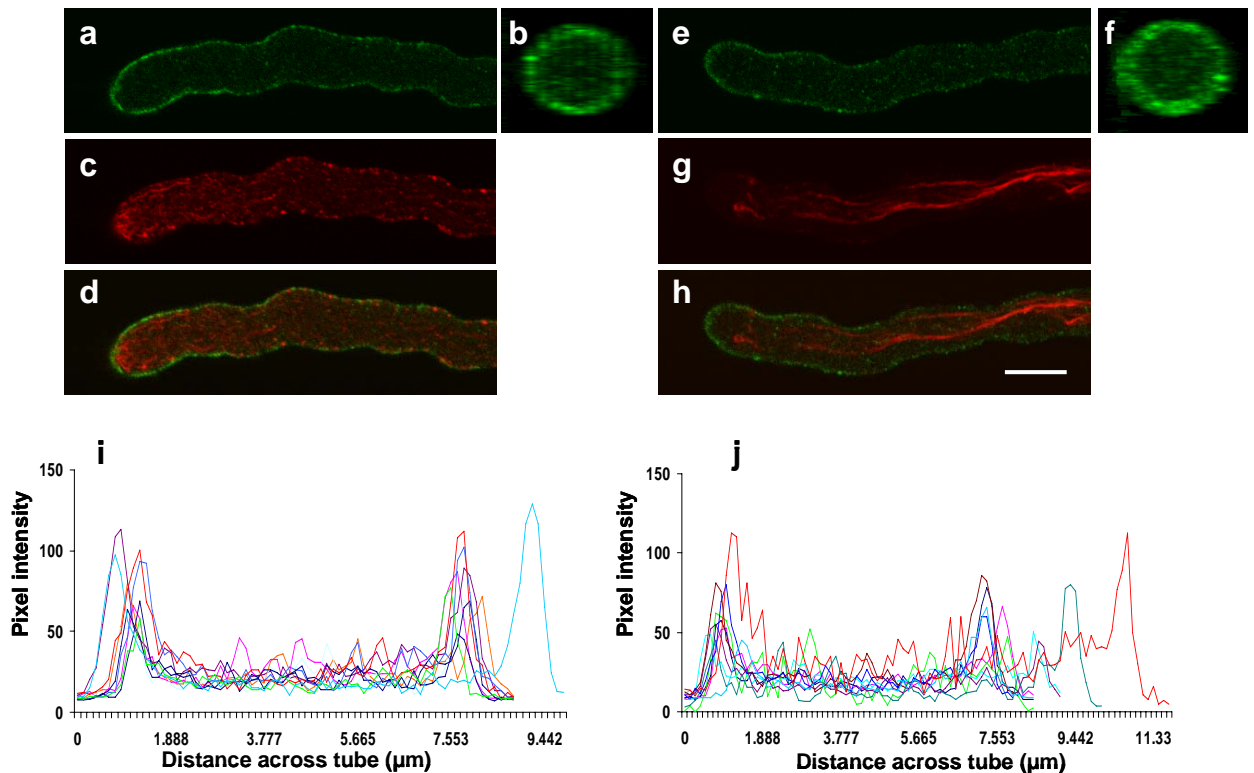


Figure 3.6. S-proteins localise to the pollen tube edge in both a compatible and an incompatible reaction.

a-d) An incompatible pollen tube showing S-proteins localised to the edge of the tube (**a,b** green) and the F-actin (red) had been depolymerised (**c**).

e-h) A compatible pollen tube also had S-proteins localised to the edge (**e,f**) while the F-actin (**g**) remained intact. Merge images of S-protein (green) and actin (red) are shown in **d** and **h**.

i,j) Pixel intensity traces across 10 incompatible (**i**) or 10 compatible (**j**) pollen tubes labelled for S-proteins show an increase in intensity at the edges of the tubes in both cases although incompatible tubes show, on average, a more marked increase compared to compatible tubes (3.7 fold increase versus 3.2 fold increase for the compatible tubes).

Images **b** & **f** are transverse sections through the pollen tube generated using ImageJ from confocal stacks. The rest are medial plane, single confocal sections. S-proteins were localised using anti-S₁ antibody (1:500) and F-actin stained with rhodamine-phalloidin. Scale bar = 10 μ m

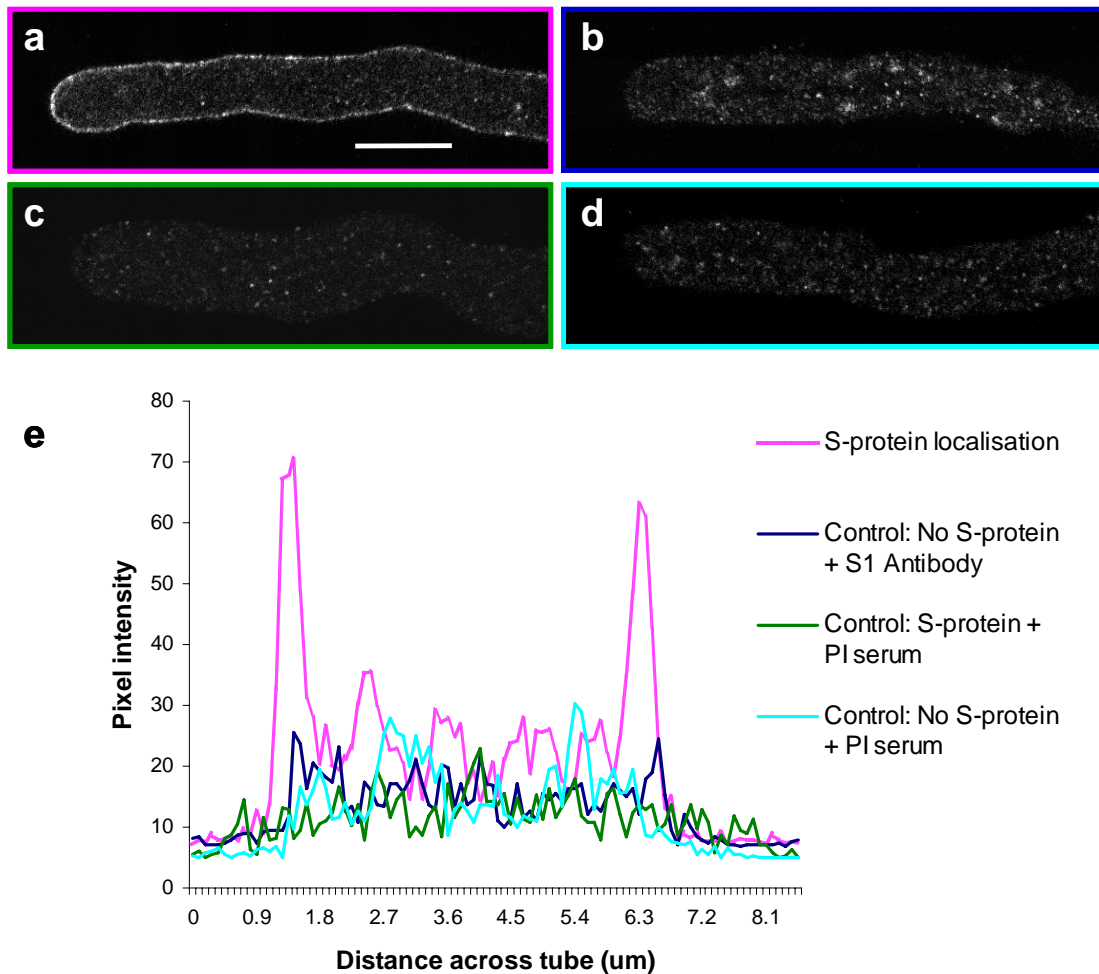


Figure 3.7. Control pollen tubes do not exhibit signal along the pollen tube periphery.

(a) An S₁ pollen tube treated with S₁-proteins and labelled with anti-S₁ antibody show distinct labelling of the pollen tube periphery, indicating the localisation of the S-proteins. The control tubes; (b) no S-proteins added but labelled with anti-S₁ antibody, (c) S-protein treatment but labelled with pre-immune (PI) serum and (d) no S-proteins and labelled with PI serum, do not have any periphery-labelling, only non-specific background labelling within the tube. This labelling is illustrated graphically by plotting the pixel intensity across the pollen tube (e).

Images are single, confocal sections through the middle of the pollen tube. Scale bar = 10 μm.

3.2.4) Native S-proteins also localise to the pollen tube cortex

One problem associated with *in vitro* S-protein localisation is that the S-proteins being used are recombinant proteins that have been denatured and then had to be refolded (Foote et al, 1994). Although we know that the S-proteins are present and the preparation is quite pure (**Fig 3.4**) we do not know what percentage is correctly folded. We know that at least some of the S-proteins are properly folded as the SI reaction is triggered in incompatible pollen when treated with an excess amount ($10 \mu\text{g ml}^{-1}$) of these recombinant S-proteins. The problem lies in the fact that the anti-S₁ antibody would recognise all recombinant S₁-proteins whether or not they are correctly folded. For that reason we cannot be sure we are looking at the specific localisation of functional S-proteins only. Therefore, we cannot be sure whether the apparent lack of specific binding is due to an excess of denatured, inactive S-proteins or whether functional S-proteins do bind pollen in a non-S-specific manner. To tackle this problem, a semi-*in vivo* approach was adopted as only native S-proteins would be available for binding.

Unpollinated stigmas from S₁S₃ poppy plants, which were producing both native S₁- and S₃-proteins, were manually pollinated with S₁S₃ pollen to give a fully incompatible reaction. Stigmas from the same S₁S₃ plant were also pollinated with S₈S_x pollen (where S_x is not S₁) to give a fully compatible reaction. **Figure 3.8 a-e** shows a fully incompatible reaction. The aniline blue staining of the pollinated papillae (**Fig. 3.8a**) shows lots of highly callosic pollen tubes just emerging from the pollen grain and no long pollen tubes. **Figure 3.8b-e** shows the S-proteins formed a continuous label around the periphery of the emerging pollen tube. The fully compatible reaction had many long pollen tubes visible in the aniline blue stained pollinated stigma (**Fig. 3.8f**) and the S-proteins also clearly labelled the edge of the pollen tubes (**Fig. 3.8g-i**). As the compatible pollen tubes were longer there was a larger area of the

pollen tube to study. The S-proteins labelled the whole length of the tube uniformly (**Fig. 3.8g**), with no particular preference for the tip which was observed in the *in vitro* experiments. Control sections that were labelled with the pre-immune serum (**Fig. 3.8j, k**) showed significantly less labelling and although there was sometimes labelling at the cortex of the pollen tube, the signal was never as bright, continuous or as consistent as the tubes labelled with anti-S₁ antibody. These *in vivo* pollination results support the findings of the *in vitro* experiments; that the S-proteins appear to bind to the periphery of both compatible and incompatible pollen tubes. The fact that the S-proteins also appeared to bind to the periphery of compatible pollen tubes indicates that there must be some kind of non-S-specific S-protein binding to the tube, perhaps involving SBP, although the SI response is clearly specific to incompatible pollen. This indicates that although the S-proteins bind to the periphery of all pollen tubes they only trigger the SI signalling pathway in incompatible pollen tubes, when the male S-component carrying the same allele is present.

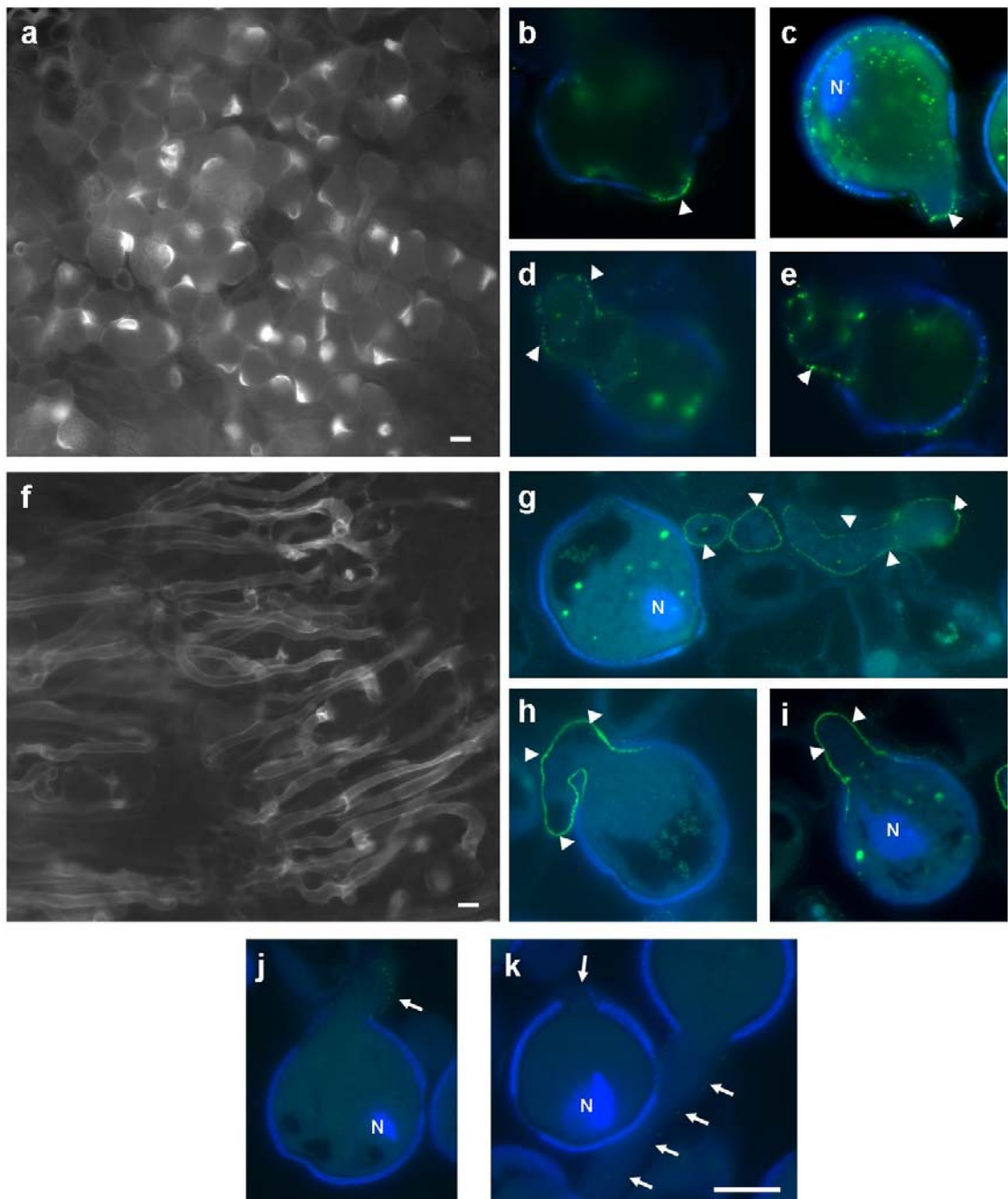


Figure 3.8. Sections through pollinated stigmas show S-proteins at the pollen tube cortex.

Stigmas were pollinated and left for 1 h before being fixed and sectioned. A fully incompatible SI response is characterised by high levels of callose in the emerging pollen tube and no long pollen tubes when stained with aniline blue (a). A fully compatible reaction has lots of long pollen tubes (f). The S-proteins (green, arrow heads) bind to the edge of both the incompatible (b-e) and compatible (g-i) pollen tubes. S-proteins can be clearly visualised running along the whole length of the pollen tube (g). Pre-immune serum (j,k) gives very little labelling along the pollen tubes (indicated with arrows). The anti-S₁ antibody was used at a titre of 1:500 and a FITC-conjugated secondary antibody was used at 1:200. N = nucleus, either vegetative or generative cell nuclei stained with DAPI (blue). Scale = 10 µm

3.3) Discussion

The localisation studies presented in this chapter demonstrate that the PrpS protein is membrane-localised, lending support to the hypothesis that the male *S*-determinant is an integral membrane protein. The *S*-proteins can be clearly seen localising to the periphery of the pollen tubes, where they would be expected to be found if they were acting as ligands as proposed. Interestingly, both our *in vivo* and *in vitro* localisation experiments of S_1 -protein show that the *S*-proteins tend to interact with all pollen, regardless of their genotype, but only trigger the SI response in incompatible (self) pollen. This means that the presence of the *S*-proteins on the pollen tube membrane is not sufficient to trigger SI, there must also be a specific interaction between the pollen- and pistil-*S*-determinants.

3.3.1) Immunolocalisation of PrpS₁

Immunolocalisation of PrpS was not as straightforward as anticipated. The PrpS signal was extremely weak, it could not be visualised using an epifluorescence microscope and on the confocal microscope the argon laser had to be set to a very high power of 70 % for the signal to be seen (compared to tubulin, which is easily visualised with a power of 2-5 %). Immunolocalisation is never 100 % effective, as each of the pollen tubes is not exposed evenly to the enzyme treatment or antibodies, so some of the tubes that should be labelled are not. This is a limitation of the technique and is unavoidable. The problem was further compounded by the fact that only a maximum of 50 % of the pollen tubes would be expected to be labelled. This was because the antibody was specific for PrpS₁ and the pollen was from an S_1S_3 diploid plant and would, therefore, contain approximately equal amounts of each of the S_1 and S_3 haplotypes. When the PrpS signal was detected it was extremely weak and this

could be because of two main reasons: (1) the quality of the antibody and (2) the level of protein expression. The western blots shows that the PrpS₁60C antibody detects PrpS₁ in pollen protein extracts but this is when the protein is completely denatured so all epitopes are available for binding. In its native conformation the C-terminal domain used to generate the antibody may not be in an easily accessible position, hindering PrpS detection by immunolocalisation in pollen tubes. The C-terminal domain of PrpS₁ is predicted to pass through the membrane (see **Fig. 3.1**) so this could influence detection. In terms of protein expression levels, it is possible that the amount of PrpS protein present in some pollen tubes falls below the threshold level of detection by fluorescence microscopy. If PrpS is acting as a receptor, as our model of *Papaver* SI predicts, it may not need to be abundant within the cell as only relatively few protein molecules may be necessary to transduce the signal generated by the receptor-ligand interaction to the rest of the cell. For example, the SRK protein of *Brassica* SI is a receptor kinase and its RNA and protein levels have been found to be 140-180 times lower than the secreted SLG protein, which in some species enhances the SI response (Stein et al, 1991; 1996; Takasaki et al, 2000). Another point to consider is that for a PrpS₁ signal to be seen on a western blot a large amount of protein (40-100 µg) needed to be loaded and the blot developed for a long period of time (Hadjiosif, 2008). This indicates that PrpS is a low abundance protein in the pollen tube, so may not be detected by immunolocalisation in all tubes.

3.3.2) PrpS could function as a membrane bound receptor

Although the PrpS signal is weak there is clearly labelling along the periphery of the pollen tube that is absent in the pre-immune serum control. Thus the PrpS localisation studies support the hypothesis that PrpS is a transmembrane protein. The PrpS images show that this

protein is most abundant in the pollen tube tip and sub-apex and less so in the shank. PrpS labelling was never seen running the whole length of the pollen tube, as was the case for the S-protein localisation. This does not necessarily mean that it is not present in the shank. Pollen tubes are tip-growing cells, so elongate by addition of new cell wall and membrane material into the tip of the pollen tube only (reviewed in Taylor & Hepler, 1997). This means that PrpS would be added into the membrane in the tip region and as the tube elongates the area that was previously in the tip would become part of the shank region. PrpS could be being recycled by endocytosis, a process that is highly active in pollen tubes (Parton et al, 2001; Moscatelli et al, 2007). In pollen tubes there is an excess of membrane material delivered to the tip that needs to be actively recovered by endocytosis and redirected back into the secretory pathway to regulate the membrane economy of the cell. Once PrpS reached the sub-apical zone it could be recycled by endocytosis and then reincorporated into the tip. This would maintain a higher concentration of the receptor protein in the tip, the first region of the pollen tube to come into contact with the stigmatic tissue. Concentrating a receptor into an area of the membrane that comes into contact with the ligand (the incompatible S-proteins) would substantially boost signalling. There may still be some PrpS in the shank but it would be less abundant and therefore more difficult to detect using antibodies. Similarly, the mammalian epidermal growth factor receptor (EGFR), which is the most studied of the receptor tyrosine kinases (RTKs), is estimated to be recycled 3-5 times, through internalisation into endosomes and then returned to the plasma membrane, before it is selected for degradation (Clague & Urbe, 2001). If PrpS is being recycled, it could also explain why there is some PrpS signal detected inside the pollen tube.

As PrpS is proposed to be the pollen *S*-determinant we need to tie it in to events that are already known about the SI response. One of the earliest events in poppy SI is a large influx of calcium, with the largest influx measured 100 μm behind the growing tip (Franklin-Tong et al, 1997). This influx is accompanied by the loss of the tip-focused calcium gradient (Franklin-Tong et al, 1997; 2002). As this calcium influx occurs almost instantaneously it has been proposed that the pollen *S*-determinant could itself be a calcium-permeable channel, or a component of a calcium-permeable channel, that opens upon interaction with incompatible *S*-proteins (Franklin-Tong et al, 1997). If this were the case we would expect to see PrpS in the shank and not in the tip area but the results are the opposite (although it could be present in the shank but is undetectable by immunolocalisation). As mentioned earlier, PrpS is incorporated into the membrane at the tip of the tube due to the tip-growing nature of pollen tubes, so it could be that it is in an inactive form at this point and needs further modification, which occurs in the shank, to become functional. As pollen are tip growing cells, having the “*S*-receptor” concentrated in the tip region would be advantageous. This is because *in planta* the tip would be the first part of the germinating pollen tube to come into contact with the stigma and thus the “receptor” would be in the best position to send signals to the rest of the tube/grain to stop tube growth in an incompatible reaction. Importantly, *in vivo* most incompatible pollen do not show long pollen tubes but instead are inhibited shortly after pollen tube emergence so do not have a ‘shank’ region *per se*. However, preliminary data support the hypothesis that PrpS is involved in calcium influx (Wu & Franklin-Tong, unpublished data).

Most of the (few) plant transmembrane receptor and ligand partners identified to date are receptor-like kinases (RLKs; Wang et al, 2001; Nam & Li, 2002; Gomez-Gomez et al, 2001)

including the SRK-SCR receptor-ligand pair from the *Brassica* SI system (Takayama et al, 2001; Kachroo et al, 2001). There has also been a GPCR (G-protein-coupled receptor) identified recently which interacts with the phytohormone abscisic acid (Liu et al, 2007). Some transmembrane receptors, including one from plants, have been shown to be endocytosed upon interaction with their ligand and it has been proposed that these activated receptors can continue to signal from the intracellular compartments (Haugh, 2002; Robatzek et al, 2006). Because PrpS does not share any homology with the RLKs, GPCRs, or any other receptor identified to date, these proteins represent a novel class of transmembrane receptors that could function in a unique, as yet unidentified, manner. It may be possible that PrpS is endocytosed after interaction with the S-proteins and signals to the cell from the intracellular compartments. Future work could investigate PrpS localisation after SI-induction, to see if the signal observed in these studies might implicate endocytosis of PrpS during SI. If so, this could hint at an internal signalling pathway and direct further studies to find out which other components are involved.

3.3.3) S-proteins bind to both incompatible and compatible pollen

The S-proteins have been shown to bind to both incompatible and compatible pollen tubes, although the SI response is clearly only triggered in the incompatible pollen. This result is perhaps not surprising, especially in the *in vivo* pollinations, as the S-proteins are secreted by the papillae of the stigma. Upon pollination the pollen touches these papillae and their secreted S-proteins and as the pollen tube tries to grow towards the ovary it could easily become coated in the S-proteins. The *in vitro* experiments also show the same result, indicating that S-proteins do bind to the pollen tubes even if the tubes are not touching cells secreting S-proteins, although the compatible pollen tubes appear to have a less intense S-

protein signal compared to the incompatible tubes. Hearn et al (1996) identified a poppy pollen glycoprotein called SBP (**S**-protein **b**inding **p**rotein) which was originally thought to be the pollen S-component as it fulfilled many of the criteria; it was specific to mature pollen, expressed just prior to anthesis and was plasma membrane associated, but it was found to bind to all S-proteins alleles in a non-S-specific manner. This meant that SBP could not be the pollen S-component. It is now thought to be an accessory protein, or co-receptor, for the SI response. As the evidence suggested that SBP is integrated into the plasma membrane, this puts it in a good position to interact with the S-proteins so could aid the binding of the S-proteins to the real S-receptor and could also participate in the signalling events that follow (Hearn et al, 1996). Research has shown that if SBP-S-protein binding was reduced by point mutation of some S-protein residues, the ability of the S-proteins to inhibit incompatible pollen tube growth was also reduced. This demonstrates that SBP is also required for the SI response (Jordan et al, 1999). As SBP is present in all pollen tubes and can interact with all the S-proteins alleles it could be the protein that is binding to the S-proteins, causing them to localise along the pollen tube in both the compatible and incompatible situations. This non-S-specific interaction may not be as strong as the interaction between the S-proteins and PrpS so that may explain why the compatible tubes have less intense S-protein labelling than the incompatible tubes in the *in vitro* experiments.

The tip area also appears to have more S-protein signal than the rest of the tube. This could be because the tip has a more concentrated distribution of PrpS, so if S-proteins and PrpS were interacting there would be more S-proteins binding to this area and they would also be more likely to stay bound during the immunolocalisation procedure if the interaction is stronger than the binding with the SBP. The fact that S-proteins can be clearly seen localising along

the shank of the pollen tube lends support to the idea that PrpS, and probably SBP, are present there, but PrpS is at an undetectable level. Although the labelling of the pollen tube periphery with S-proteins is very clear, there also appears to be some signal within the tube. This could be due to endocytosis of S-proteins. However, control pollen tubes that do not have S-proteins present and those labelled with PI serum also show similar labelling within the pollen tube lumen, suggesting that this signal is probably background labelling.

Pollen tubes are known to have very active endocytosis, especially in the sub-apical region (Parton et al, 2001; Camacho & Malhó, 2003; Samaj et al, 2005; 2006; Moscatelli et al, 2007). Interestingly the female S-component of the gametophytic SI system of the *Solanaceae* (the S-RNases) is taken up by endocytosis into both compatible and incompatible pollen tubes (Luu et al, 2000). Other factors which are required for SI in this system in addition to the S-RNases, such as HT-B and 120 K, are also taken up into the pollen tubes from the extra cellular matrix of the pistil (Lind et al, 1996; McClure et al, 1999; Hancock et al, 2005; Goldraij et al, 2006). The two possible models of the RNase SI system suggest that compatible S-RNases are either degraded by the proteasome or compartmentalised into the vacuole to prevent cytotoxicity. In an incompatible reaction, S-RNases are either left in the cytoplasm or are released from the vacuole, which requires the action of the other SI factors, where they degrade RNA and inhibit pollen tube growth (reviewed in McClure & Franklin-Tong, 2006). The pistil S-proteins of poppy could also be internalised, but the fluorescence microscopy carried out here may not have the resolution to confirm whether this is happening or not. Based on the current model of poppy SI, where the S-proteins are acting as ligands that interact with a receptor to trigger SI (reviewed in Bosch & Franklin-Tong, 2008), there is no need for the S-proteins to be taken into the tube. On the other hand S-RNases need to be

endocytosed to exert their action on pollen RNA to stop pollen tube growth and prevent self-fertilisation. To ascertain whether endocytosis of S-proteins is occurring a technique with higher resolution than the microscopy used here, such as EM immunogold labelling of the S-proteins, needs to be used. Even if S-proteins are endocytosed, this is unlikely to play an active role in *Papaver* SI based on the current model. This is due to the rapidity of the response, where many downstream events such as the calcium influx and cytoskeleton alterations have already occurred within a few minutes of incompatible challenge (Franklin-Tong et al, 1997; 2002; Geitmann et al, 2000; Poulter et al, 2008). This is not to say that S-proteins are not taken into the pollen tubes. They may still be endocytosed but it may just be a consequence of the membrane recycling that is constantly occurring in pollen tube as they grow, as demonstrated by many experiments using membrane staining dyes such as FM4-64 or nanogold particles (Parton et al, 2001; Camacho & Malhó, 2003; Wang et al, 2005; 2006; Samaj et al 2005; 2006; Moscatelli et al, 2007).

Although the results in this chapter do not demonstrate that the male *S*-determinant (PrpS) and the female *S*-determinant (S-proteins) directly interact, they provide evidence that PrpS is membrane localised and is therefore likely to be a transmembrane protein as predicted. Based on the similar localisation of both the *S*-determinants, there is the possibility that interaction between the two could take place to trigger the SI response. Further work needs to be carried out to investigate the interaction between the two components. Double-labelling immunolocalisation experiments using fluorescence to show co-localisation of the two components are unlikely to work as the S-protein signal would mask the much weaker PrpS signal. If this route were to be investigated, further EM immunogold would need to be undertaken. Studies using *PrpS₁* antisense oligonucleotides to down-regulate PrpS₁ expression

have shown an alleviation of the SI response which was not present when sense oligonucleotides were used (Wheeler et al, 2009). Also, a 15 amino acid peptide corresponding to the predicted extracellular domain of PrpS₁ was able to specifically block the interaction of PrpS₁ with the S₁-proteins resulting in rescue from SI-induced pollen tube growth inhibition (Wheeler et al, 2009). Both of these results provide support for PrpS playing a crucial role in poppy SI by interacting with the S-proteins. Techniques such as slot blotting, co-immunoprecipitation and yeast-2-hybrid are now needed to demonstrate a direct S-specific interaction between PrpS and S-proteins and these experiments will form the basis for future work in this area.

CHAPTER 4

MICROTUBULES ARE AN EARLY TARGET FOR SELF- INCOMPATIBILITY SIGNALLING IN *PAPAVER* POLLEN

4.1) Introduction

As mentioned in **Chapter 1**, the plant cytoskeleton is made up of two major components: the actin microfilaments, which are also known as F-actin, and microtubules (MTs), as well as many cytoskeleton binding proteins which modulate the dynamics of the cytoskeleton. The pollen tube actin cytoskeleton has previously been shown to undergo a series of well characterised alterations during the SI response of poppy (Geitmann et al, 2000; Snowman et al, 2002). Further work has shown that actin depolymerisation or stabilisation can push the pollen tube into PCD, demonstrating the actin alterations observed during SI are involved in the PCD of incompatible pollen (Thomas et al, 2006; Thomas & Franklin-Tong, 2004). The MT cytoskeleton has not previously been studied in SI.

The organisation of the MT cytoskeleton in pollen tubes has been studied in several species (Raudaskoski et al, 1987; Heslop-Harrison et al, 1988; Lovy-Wheeler et al, 2005; Gossot & Geitmann, 2007; Cheung et al, 2008), all of which exhibit a similar arrangement. The role of the MT cytoskeleton in pollen tubes remains unclear as it is not required for angiosperm pollen tube growth *in vitro*, but is necessary for gymnosperm pollen tubes to maintain normal growth (see **Chapter 1** for full details).

Due to their cortical localisation in plant cells, MTs are in a good position to respond to external stimuli and participate in signalling cascades. There are a number of examples where MT reorganisation and/or apparent depolymerisation occur in response to specific stimuli. Abiotic stimuli, such as freezing and dehydration have been shown to stimulate apparent MT depolymerisation in spinach mesophyll cells (Bartolo & Carter, 1991). Gravity also can stimulate MT reorientation (Himmelspach et al, 1999) and salt stress affects cortical MT

organisation and growth in *Arabidopsis* (Shoji et al, 2006). Toxic metals can also trigger alterations to the MT cytoskeleton; lead disturbs the MT organisation in the root meristem of *Z. mays* in a concentration-dependent manner (Eun et al, 2000) and aluminium causes depolymerisation of *Arabidopsis* root cortical MTs (Sivaguru et al, 2003). There are also examples of the MT cytoskeleton altering its organisation in response to biotic stimuli during plant-microbial interactions, such as in response to infection by pathogenic fungi or symbiotic interactions with *mycorrhiza* or *rhizobia*. These interactions involve predominantly cytoskeleton reorganisation, reorientation and/or focusing of the MT cytoskeleton around the infecting body. However, rapid apparent depolymerisation of MTs has also been reported, for example, in elicitor-treated tobacco cells and in parsley- and soybean-*Phytophthora* interactions (Gross et al, 1993; Binet et al, 2001; Cahill et al, 2002). Nod factor signalling also stimulates alterations to MT organisation in root hairs, with rapid localized apparent MT depolymerisation and later increases in MT arrays reported (Timmers et al, 1999; Weerasinghe et al, 2003). However, a recent report showed that while changes in MT dynamic instability were observed, there was no evidence for MT depolymerisation (Vassileva et al, 2005). Nevertheless, there is good evidence that plant-pathogen and plant root-Nod factor interactions involve relatively rapid and specific alterations to the MT cytoskeleton (see Takemoto & Hardham, 2004 for a recent review).

As MTs appear to respond to many different stimuli it is plausible that they may be responding to SI specific signals. As the actin cytoskeleton plays such an important role in *Papaver* SI, and the actin and MT cytoskeletons have been shown to have a close association in pollen tubes (Lancelle & Hepler, 1991), the involvement of the MT cytoskeleton in the SI response of poppy was investigated.

Much of this work has already been published, so this chapter has been split into two sections:

Part I: This section is a published paper:

N. S. Poulter, S. Vatovec and V. E. Franklin-Tong (2008). Microtubules are a target for self-incompatibility signalling in *Papaver* pollen. *Plant Physiology*, **146**, 1358-1367.

Part II: This section contains some of the extra experiments carried out by myself that were not included in the published paper. I have also included some of the many images I collected of the pollen tube MT cytoskeleton, as these illustrate MT features or different SI time points but could not be shown in the paper due to space restrictions. This section includes an extended discussion taking into account the extra results presented here, as well as the results published in Poulter et al (2008).

Part I: The published paper

N. S. Poulter, S. Vatovec and V. E. Franklin-Tong (2008). Microtubules are a target for self-incompatibility signalling in *Papaver* pollen. *Plant Physiology*, **146**, 1358-1367.

4.1.1) Preface

I carried out the majority of the practical work. Sabina Vatovec worked in the Franklin-Tong lab as an undergraduate project student under my supervision. She worked with me to learn all the techniques used here and independently contributed some of the caspase activity and tube length data. Noni Franklin-Tong is my supervisor so had overall control of the project. All three of us contributed to the writing of the manuscript.

Part II: Unpublished data relating to MT alterations in *Papaver* pollen tubes

4.2) Introduction

Some of the experiments investigating the involvement of the pollen tube MT cytoskeleton in the SI response of poppy could not be included in Poulter et al (2008) due to space constraints. Here, I have taken the opportunity to include some more images of MTs in normal pollen tubes, as well as an extended SI time series to show the MT alterations in more detail, over a longer period of time. I have also included the results of some control experiments that were not considered to be necessary for the paper, which are shown here for completeness.

4.3) Results

4.3.1) Immunoblotting of *P. rhoeas* pollen tube proteins

This project relied on the technique of immunolocalisation to study the cytoskeleton of pollen tubes from *P. rhoeas*. The antibody that was used was a monoclonal anti- α -tubulin antibody, clone B5-1-2 (Sigma-Aldrich, UK). This antibody was raised against the sarkosyl-resistant filaments from *Strongylocentrotus purpuratus* (sea urchin) sperm axonemes. The antibody was said to recognise an epitope located at the C-terminal end of the α -tubulin isoform in a variety of organisms, although its specificity for plant tubulin had not been tested. A western blot analysis of total pollen protein extracts was carried out to test the cross-reactivity of this antibody with poppy tubulin. A strong, single band of approximately 50 kDa, the size of α -tubulin, was detected using the antibody at a titre of 1:1000 (**Fig. 4.1**). This result indicated

that the monoclonal anti- α -tubulin antibody, clone B5-1-2 does recognise poppy α -tubulin and is specific for this protein. Therefore, it could be used with confidence in tubulin immunolocalisation studies.

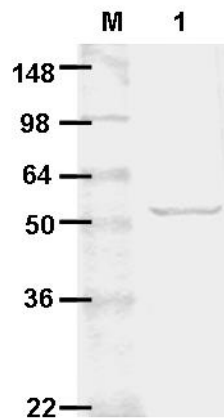


Figure 4.1. Western blot testing specificity of monoclonal anti- α -tubulin antibody, clone B 5-1-2.

M = marker (kDa), lane **1**: crude pollen protein extract.

Total pollen protein extracts were separated by SDS-PAGE, blotted onto nitrocellulose and probed with the anti- α -tubulin antibody, clone B5-1-2 (1 in 1000 dilution). Detection was with alkaline phosphatase. The antibody recognised a single band of approx 50 kDa, representing α -tubulin.

4.3.2) Characterisation of the MT cytoskeleton in untreated pollen tubes of *P. rhoeas*

In order to establish whether the MT cytoskeleton is altered during the SI response it was first necessary to characterise the cytoskeleton in poppy pollen tubes that were growing under normal conditions. Poulter et al (2008) described the organisation of the MTs in poppy pollen tubes, but here several other features are described in more detail. *Papaver* pollen tubes have a very similar MT arrangement to that found in other species (Raudaskoski et al, 1987; Åström et al, 1995; Gossot & Geitmann, 2007). In the tip region there was a relatively MT-free zone, instead it had a diffuse fluorescence which probably represented tubulin dimers. In the sub-apical region there was an array of short MT bundles which appeared throughout the lumen of the tube, they were not all cortical in this area (**Fig. 4.2a**). The beginning of these short MT bundles often corresponded with the actin “basket” or “collar” region. Behind this short MT region, in the shank of the pollen tube, there were longer, more regularly organised longitudinal MT bundles (**Fig. 4.2b**). These were mainly axial and cortical, as shown by the transverse section taken through the pollen tube (**Fig. 4.2d**) and the confocal top and mid-plane sections (**Fig. 4.2e, f**). Pollen tubes have a vegetative nucleus (VN) and also a generative cell (GC), which will eventually form the two sperm cells that will participate in double fertilisation (**Fig. 4.2c**). In addition to the cortical MTs of the pollen tube, the GC has its own set of MTs. These MTs form a clearly visible cage-like structure inside the GC which is thought to give it its characteristic spindle shape (**Fig. 4.2b, c**). A hook-like MT projection from the GC was frequently seen (arrow), which appeared to link the GC to the VN inside the pollen tube.

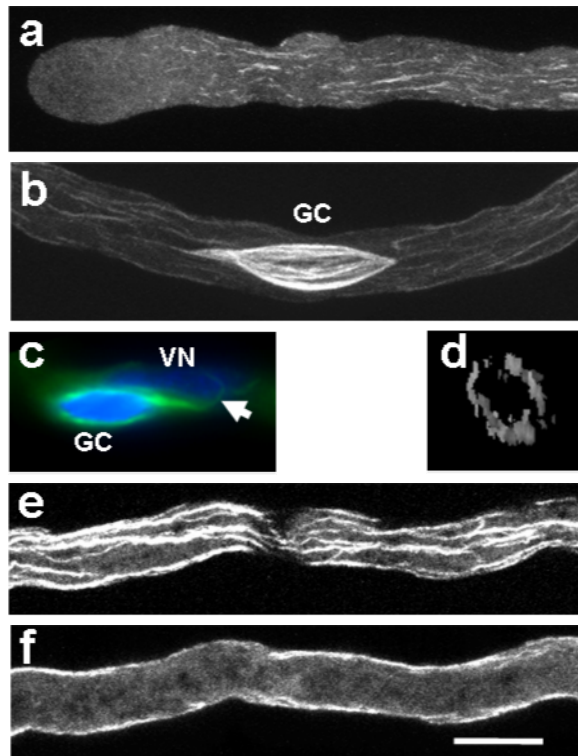


Figure 4.2. Microtubule organisation in normally growing *Papaver* pollen tubes

a) Relatively few MT bundles were detected in the tip region. Behind this region were shorter MT bundles and behind this, in the mid-region, longer cortical MTs were visualised. **b)** In the shank region cortical MTs were longitudinally-arranged; a separate population of generative cell (GC) MTs are thought to give the GC its spindle shape.

c) The MTs of the GC (green) often formed a hook-like structure (arrow) that appeared to link the GC with the vegetative nucleus (VN). The DNA was stained with DAPI (blue).

d) A transverse section through the pollen tube and longitudinal single optical sections (1 μm) at the top (**e**) and through the middle (**f**) of the pollen tube show MTs were primarily cortical.

MTs were detected using immunolocalisation with anti- α -tubulin antibody clone B5-1-2 (1:1000). Images in **a** and **b** are full projections of confocal images. Scale bar = 10 μm

4.3.3) SI triggers rapid apparent MT depolymerisation

Poulter et al (2008) showed that SI caused rapid apparent MT depolymerisation, with alterations occurring as early as 1 min after SI induction. Here, a more detailed dissection of the time scale of the response, ranging from 2 min to 3 h after SI-induction, is shown (**Fig. 4.3**). SI stimulated MT depolymerisation very early in the SI response. At 2 min after SI the MTs were virtually undetectable (**Fig. 4.3e**); the pollen tubes exhibited a diffuse staining which probably represented tubulin subunits. This diffuse staining was maintained for up to 3 h after SI induction, with no secondary MT structures forming in the later stages of the SI response (**Fig. 4.3u**). The MTs of the GC appeared to take longer to respond to the SI signals than the cortical MTs. At 2 min after SI the GC MTs appeared not to be greatly affected (**Fig 4.3f**). By 15 min SI they looked as if they were disintegrating within the GC (**Fig 4.3j**) and this continued throughout the SI response. After 1 h SI large ‘blobs’ of tubulin were seen in the lumen of the pollen tube in the vicinity of the GC (**Fig 4.3r, arrows**). It appeared as if some of the tubulin had come out of the GC into the pollen tube lumen, possibly indicating disruption of the GC membrane and wall. After 3 h SI this phenomenon was still occurring but MTs were still visible inside the GC (**Fig 4.3v**). These pollen tubes were also stained with rhodamine-phalloidin to co-localise the F-actin and check the well-documented phases of actin alterations during the SI response (**Fig. 4.3c, g, k, o, s, w**). This allowed us to correlate the MT events with the actin alterations already described (Geitmann et al, 2000; Snowman et al, 2002). The majority of the MTs had depolymerised when the F-actin labelled the pollen tube cortex (**Fig. 4.3e & g**) and remained depolymerised whilst the F-actin assembled into large punctate foci (**Fig. 4.3u & w**).

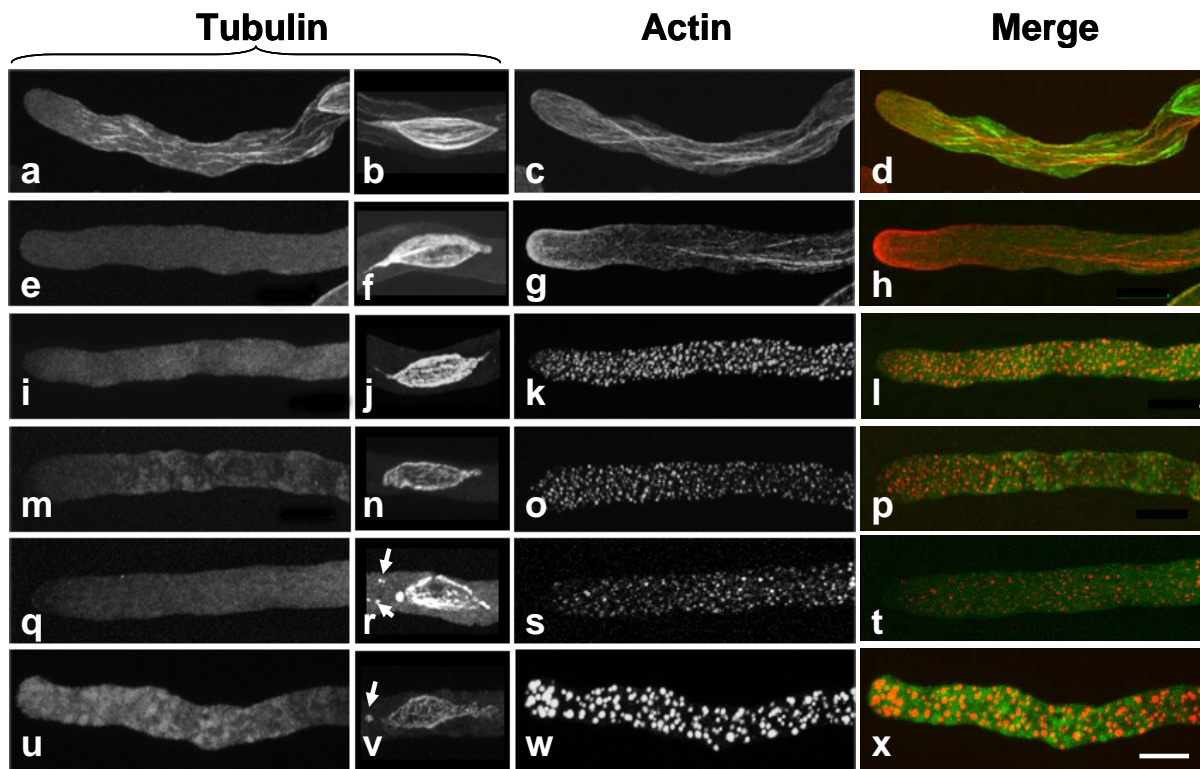


Figure 4.3. Pollen tube cytoskeleton alterations during the SI response.

a-d) An untreated pollen tube showing MT organisation in the tube (**a**) and the GC (**b**) and actin in the same tube (**c**), (**d**) is a merge of tubulin (green) with actin (red). At 2 min post-SI induction (**e-h**) the cortical MTs were virtually completely depolymerised (**e**) but the GC MTs were less affected (**f**). F-actin could be seen in the tip and many of the bundles had depolymerised (**g**). After 15 min SI (**i-l**) the F-actin had formed small foci (**k**) while the cortical MTs remained depolymerised (**i**) and the GC MTs appeared to have started to degrade (**j**). At 30 min after SI (**m-p**) the MTs remained depolymerised (**m**) and the GC MTs continued to degrade (**n**) whilst the F-actin was still seen as foci (**o**). After 1 h SI (**q-t**) little had changed and after 3 h SI (**u-x**) the F-actin had formed very large punctate foci (**w**) whilst the MTs remained depolymerised (**u**) and the GC MTs appeared disintegrated (**v**). Arrows indicate tubulin that appeared to have come out of the GC.

MTs were detected using immunolocalisation with anti- α -tubulin B5-1-2 (1:1000); F-actin was co-localised using rhodamine-phalloidin. Images are full projections of confocal sections. Scale bar = 10 μ m.

4.3.4) Compatible S-proteins have no effect on the MT cytoskeleton

Induction of SI by addition of incompatible recombinant S-proteins (S_1 and S_3 proteins to S_1 and S_3 pollen; see materials and methods for full details) resulted in alterations to the MT cytoskeleton. To ensure that the response seen was S-allele specific, and not just the result of the addition of recombinant S-proteins, a compatible challenge was carried out. Pollen from plants with a compatible S-haplotype (S_4S_6) was grown and recombinant S_1 - and S_3 -proteins were added and left for 3 h before fixation and tubulin imaging. **Figure 4.4 a-c** shows the MT organisation in the tip and sub-apex, the GC and the shank of a control pollen tube. **Figure 4.4 d-f** is a pollen tube that had been treated with compatible S-proteins for 3 h and shows that the MT organisation remained unaltered throughout the tube. This demonstrated that the depolymerisation observed in SI (see **Fig. 4.3**) was S-allele specific and was only caused when incompatible S-proteins interacted with the pollen tube.

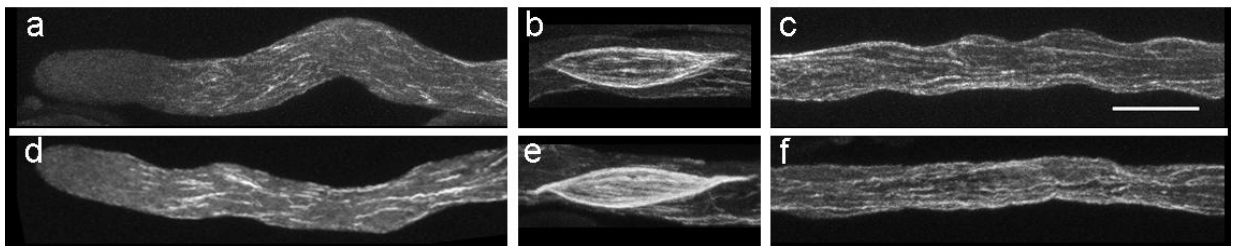


Figure 4.4. Compatible S-proteins do not alter MT organisation

(**a-c**) An untreated pollen tube exhibited the normal MT organisation in the tip and sub-apical region (**a**), the GC MTs (**b**) and the shank region (**c**).

(**d-f**) A pollen tube treated with compatible S-proteins for 3 h. The MT organisation throughout the pollen tube remained unchanged.

MTs were detected by immunolocalisation of anti- α -tubulin. Scale bar = 10 μ m

4.3.5) MT depolymerisation is not a consequence of growth inhibition

During the SI response, growth of the pollen tube is rapidly arrested. In order to ensure that the MT depolymerisation we observed during SI was due to SI specific signals, and not a consequence of pollen tube growth inhibition, pollen was treated with either caffeine or EGTA. Caffeine has been reported to cause dissipation of the tip-focused calcium gradient and the calcium influx in pollen tubes, which inhibits tube growth (Pierson et al, 1996). EGTA is a calcium chelator. Thus, addition of EGTA into the GM interferes with the ion homeostasis of the pollen tube and results in arrested pollen tube growth (Pierson et al, 1994). The concentrations used were 10 mM caffeine and 200 μ M EGTA, both for 10 min, as these are reported to be sufficient to stop pollen tube growth in *P. rhoeas* (Geitmann et al, 2000). Tubulin was visualised using immunolocalisation and images were gathered by CLSM (**Fig. 4.5**). The control pollen tube (**Fig. 4.5a**), grown on GM, exhibited the normal MT distribution as described above. Neither a 200 μ M EGTA (**Fig. 4.5b**) nor a 10 mM caffeine (**Fig. 4.5c**) treatment appeared to have had any effect on the organisation of the MT cytoskeleton. This demonstrated that inhibiting pollen tube growth alone does not cause MT depolymerisation. The MT cytoskeleton must, therefore, be responding to SI specific signals when it depolymerises during the SI response. Geitmann et al (2000) demonstrated a similar result for actin organisation in pollen tubes, which was also not greatly altered after non-specific growth inhibition.

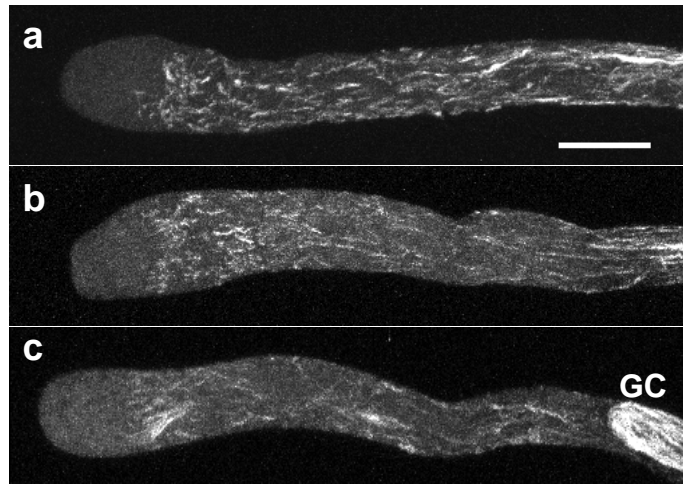


Figure 4.5. MT depolymerisation is not due to pollen tube growth inhibition

- a) A control pollen tube grown in GM had the normal MT cytoskeleton organisation.
- b) A pollen tube treated with 200 μ M EGTA for 10 min. The MT cytoskeleton showed no major alterations.
- c) A pollen tube treated with 10 mM caffeine for 10 min. The MT cytoskeleton showed no major alterations. Generative cell (GC) MTs were also unaffected.

MTs were detected using immunolocalisation with anti- α -tubulin antibody clone B5-1-2. All images are full confocal projections. Scale bar = 10 μ m.

4.4) Discussion

4.4.1) The MT cytoskeleton in normally growing pollen tubes

In the present study immunolocalisation has been used to investigate the organisation of the MT cytoskeleton in poppy pollen tubes before and during the SI response. This has revealed that within normally growing poppy pollen tubes there are three distinct zones with different MT organisations. The apical region of the pollen tube appears to be virtually devoid of MT bundles. The sub-apical region contains short MT bundles which have a net axial orientation and appear throughout the lumen of the tube. The shank of the pollen tube has many longitudinally orientated, cortical MTs. The MTs behind the GC/VN complex tend to be longer and more organised than those towards the tip-end of the pollen tube.

This MT organisation concurs with the study by Gossot and Geitmann (2007) that also looked at poppy pollen tubes. The poppy MT organisation is also very similar to that of tobacco pollen tubes, with the exception that the MTs in the shank of tobacco pollen tubes are sometimes helicoidally arranged, whereas in poppy they are not (Raudaskoski et al, 1987). It is known that growing pollen tubes have a tip-focused calcium gradient (Obermeyer & Weisenseel, 1991; Rathore et al, 1991; Miller et al, 1992; Malhó et al, 1994, Franklin-Tong et al, 1997) and that MT stability is also dependent on calcium concentration in a calmodulin-dependent manner (Keith et al, 1983; Bartolo & Carter, 1992; Fisher et al, 1996; Raudaskoski et al, 2001). Therefore, the high concentration of calcium in the tip of the pollen tube could explain the absence of MTs in this region. The shank region of the pollen tube exhibits low calcium concentrations so MTs in this region should be more stable. Two proteins (161 kDa and 90 kDa) have been identified in tobacco pollen tubes which are associated with the

membrane and can bind to MTs (Cai et al, 2005b). These proteins are proposed to link the cortical MTs with the pollen tube membrane, thus making them more stable than the MTs in the sub-apex.

There are some similarities between the organisation of the actin cytoskeleton and that of the MT cytoskeleton. F-actin is also absent from the tip of the pollen tube and an actin collar forms in the sub-apical region with longitudinal F-actin extending back along the shank of the pollen tube. Unlike the longitudinal MTs in the shank, the F-actin of the shank is not only at the cortex, but also throughout the lumen of the tube. The short MT bundles that are present in the sub-apical region tend to be behind the actin collar, suggesting that this actin structure may be preventing MTs from entering the tip region, as it has been proposed to do with large organelles such as lipid globuli and amyloplasts (Heslop-Harrison & Heslop-Harrison, 1990). There does not appear to be any clear co-localisation of the F-actin with the MTs in any region of the pollen tube. This is contradictory to reports that the majority of cortical MTs show a close association with F-actin in pollen tubes of *Nicotiana* (Lancelle and Hepler, 1991). However, this may be a limitation of the fluorescence imaging technique we used, as the association shown by Lancelle & Hepler (1991) was with high resolution electron microscopy imaging.

4.4.2) SI-mediated MT alterations do not mediate pollen tube inhibition

SI induces very rapid alterations to the cortical MT cytoskeleton, which are apparently depolymerised within 1 minute of SI induction, whereas compatible S-proteins do not induce any alterations in the pollen tube MT organisation even after 3 h of exposure. Notably, the GC MTs were not as dramatically or rapidly affected by SI as the cortical MTs of the pollen tube.

This could be because they are contained within the GC and are therefore physically 'protected' from the signals for longer by the GC wall and membrane which surrounds them. The MTs of the GC have also been shown to be more resistant than the cortical MTs of the pollen tube to cold-induced MT depolymerisation (Åström et al, 1991). This resistance to depolymerisation may be due the acetylation of the α -tubulin in the GC MTs which is thought to stabilise them (Åström, 1992).

The SI time series data demonstrate that the cortical MT cytoskeleton is a very early target for SI signals. However, since altering tubulin dynamics in pollen tubes using oryzalin and taxol did not cause inhibition of pollen tube growth, MT depolymerisation clearly does not contribute to the inhibition of incompatible pollen tube growth, but must play some other role. The MT depolymerisation induced by SI is also not a consequence of growth inhibition, demonstrated by the normal MT cytoskeleton in EGTA- and caffeine-treated pollen tubes. Although both the MT and actin cytoskeletons respond very rapidly to SI signals, they exhibit very different responses. In contrast to F-actin, which also depolymerises rapidly, the MT cytoskeleton remains depolymerised, whilst the F-actin reorganises into punctate actin foci later in the response. While the actin cytoskeleton is well established as being essential for tip-growth in plant cells (Åström, 1997; Cai et al, 1997; Gibbon et al, 1999; Vidali et al, 2001), the role of the MT cytoskeleton in plant cells is more variable and controversial, depending to some extent on the cell type (Wasteneys, 2002; 2004). In some tip-growing plant cells, MT-disrupting drugs do have a distinct effect on tip growth. For example, in root hairs of *Medicago truncatula* depolymerising the MT cytoskeleton leads to a loss of directionality of growth (Sieberer et al, 2005) and in *A. thaliana* depolymerising or stabilising MTs in root hairs also leads to a loss of growth direction as well as the formation of multiple,

independent growth points in a single root hair (Bibikova et al, 1999). In Poulter et al (2008) we have shown that in *Papaver*, like other angiosperm pollen tubes (Raudaskoski et al, 1987; Pierson & Cresti, 1992; Joos et al, 1994; Hepler et al, 2001; Raudaskoski et al, 2001), MTs do not play any obvious role in regulating the rate of tip growth as neither depolymerising nor stabilising the MTs had any effect on final pollen tube length. However, the MTs are clearly responding to SI-specific signals. A possible reason for such a rapid response is that the MTs are involved in division of the GC into the two sperm cells that are required for the double fertilisation event in plant reproduction. They are also involved in movement of the GC/VN complex within the pollen tube (Åström et al, 1995; Laitainen et al, 2002). Therefore, a rapid disruption of the MTs would ensure that the sperm cells never reached the ovary, preventing fertilisation even if the pollen tube continued growing.

4.4.3) MT cytoskeleton alterations in response to external stimuli

Poulter et al (2008) and the introduction to this chapter discussed how emerging data suggest that, because of their localisation in the cell, the cortical MTs may act as both targets and mediators of signalling cascades. The data presented here and in the paper show that our results contribute to the suggestion that MTs may function in signalling networks. We demonstrated that the pollen tube MT cytoskeleton is rapidly and specifically targeted by incompatible S-proteins and the MT depolymerisation that occurs appears to be necessary, but not sufficient, for SI-induced PCD.

Although many studies point towards a role for MTs in signalling to cellular responses (Bartolo & Carter, 1991; Gross et al, 1993; Himmelspach et al, 1999; Timmers et al, 1999;

Eun et al, 2000; Binet et al, 2001; Cahill et al, 2002; Sivaguru et al, 2003; Weerasinghe et al, 2003; Shoji et al, 2006), there is a paucity of firm evidence to date indicating a functional role for MTs in mediating these interactions, or playing a role in the outcome. Evidence for a functional role for both MT and F-actin dynamics was established as being involved in mediating non-host resistance to *Erisiphe pisi* in barley (Kobayashi et al, 1997a) and, more recently, it has been shown that wheat cultivars may use transient MT disassembly as a means of cold acclimation. Cold-resistant plants undergo a rapid, but transient, partial depolymerisation of root cortical MTs, followed by formation of cold-stable MTs, while in cold-sensitive cultivars MTs remained intact (Abdrakhamanova et al, 2003). This study also demonstrated that transient artificial depolymerisation of the MTs, with pulse drug treatments, was sufficient to induce freezing tolerance, indicating that MT depolymerisation plays a functional role. Our results also indicate that MT depolymerisation plays a functional role in SI-mediated PCD, as preventing MT depolymerisation during SI significantly decreased the levels of caspase-3-like activity (discussed in detail in Poulter et al, 2008). Although our data and the studies described above implicate a role for MTs in signalling, their exact function remains unclear.

4.4.4) The relationship between the actin and MT cytoskeletons

We have provided evidence that SI triggers both actin depolymerisation (Snowman et al, 2002) and apparent MT depolymerisation. Furthermore, we demonstrated that artificially depolymerising actin using LatB can trigger MT depolymerisation in pollen tubes. Short LatB treatments caused disorganisation of the MTs in the tip and sub-apical region of the pollen tube. Treatment of pollen tubes with F-actin depolymerising agents inhibits pollen tube growth (Åström, 1997; Cai et al, 1997; Gibbon et al, 1999; Vidali et al, 2001). If the pollen

tube is not growing, the calcium channels in the tip of the tube, that are thought to be stretch activated (reviewed by Taylor & Hepler, 1997; Franklin-Tong, 1999; Hepler et al, 2001), would not be open, leading to loss of the tip-focused calcium gradient. If it is the high calcium gradient that prevents MT bundles from forming in the tip in normally growing pollen tubes, loss of this high calcium concentration could account for the presence of MTs in the tip in LatB treated, non-growing, pollen tubes. The observation that the MTs in the shank of the pollen tube remained unaffected could be due to the stabilising effects of the proposed membrane-MT proteins discussed earlier, or it could be attributed to the unchanged calcium levels in the shank region. Prolonged LatB treatments caused depolymerisation of the MTs throughout the length of the pollen tube (this study; Gossot & Geitmann, 2007). Thus, MTs appear to require an intact actin cytoskeleton to maintain their organisation. Since disruption of the MT cytoskeleton did not stimulate F-actin depolymerisation, this suggests the actin cytoskeleton does not require MT stability to retain its integrity. Together, these data provide evidence for one-way signalling between the F-actin and MTs in pollen tubes.

In plant cells there are various studies demonstrating some kind of interaction between the actin and MT cytoskeletons, but the direction of the signalling varies between species and cell type. For example, there is evidence that MTs and F-actin can interact when making protoplast ghosts (Collings et al, 1998) and stabilising MTs with taxol in rye root tips increases F-actin stability during freezing (Chu et al, 1993), suggesting some kind of physical interaction between the two cytoskeletons. In some cases, MT dynamics can influence actin dynamics. For example, drug-induced MT disassembly in root hairs of *Hydrocharis* and *Arabidopsis* (Tominaga et al, 1997; Collings et al, 2006) and in characean internodal cells (Foissner & Wasteneys, 2000) intensified the effects of actin-targeted drugs. In contrast,

cortical MTs in fern cells were affected by the actin-depolymerising drug, cytochalasin B, suggesting the dependence of MTs on intact actin MFs (Kadota & Wada, 1992), as is the case in pollen tubes (Gossot & Geitmann, 2007; Poulter et al, 2008). There are also examples where F-actin and MT rearrangements appear to be completely independent of each other (Kobayashi et al, 1997a). In *Papaver* pollen tubes it appears that there is one-way crosstalk from actin to MTs, although this may not be a direct interaction (Poulter et al, 2008). However, the SI response of poppy requires both actin depolymerisation (Thomas et al, 2006) and MT depolymerisation for PCD to progress normally (Poulter et al, 2008), providing evidence for an integrated signalling network between the two cytoskeletons.

4.4.5) Possible links between MTs, actin and signalling components

Exactly how interactions between the actin and MT cytoskeletons are achieved is not yet clear, although emerging data are beginning to provide some clues. Identification of proteins that bridge these interactions has confirmed functional interactions between MTs and actin microfilaments in animals and fungi (reviewed by Goode et al, 2000). In plants, a 190-kD polypeptide from tobacco BY-2 cells, two actin-binding kinesins, GhKCH1 and GhKCH2, from cotton fibres and a pollen specific protein SB401 have been shown to interact with both MTs and actin microfilaments (Igarashi et al, 2000; Preuss et al, 2004; Huang et al, 2007; Xu et al, 2009). These may represent the first firm evidence of links between these two dynamic cytoskeletal components in plant cells.

How these interactions are regulated is still unclear. However, there are hints about potential links between MTs and signalling components. For example, MT depolymerisation can be triggered by elevated cytosolic free Ca^{2+} ($[\text{Ca}^{2+}]_i$) (Cyr, 1991), suggesting that $[\text{Ca}^{2+}]_i$ acts as a

second messenger to signal to mediate MT depolymerisation. It is well established that SI involves large increases in $[Ca^{2+}]_i$ and that this signals to mediate actin depolymerisation (Franklin-Tong et al, 1993; 1997; Snowman et al, 2002). As actin appears to signal to MT depolymerisation in pollen tubes, this strongly implicates $[Ca^{2+}]_i$ as an upstream signalling component.

Rop GTPases have recently been shown to be involved in signal-mediated regulation of organisation of both cortical actin microfilaments and MTs in *Arabidopsis* leaf pavement cells (Fu et al, 2005). The study by Fu et al (2005) showed that RIC1 co-localises with cortical MTs and plays a role in organising them into bundles while ROP2 interacts with RIC1 to oppose this action, by sequestering RIC1 away from the cortical MTs. The data suggest that ROP2 regulates cortical MT activity through the action of RIC1. Furthermore, ROP2 also interacts with RIC4, which is involved in microfilament organisation. RIC1 can inhibit ROP2-RIC4 interactions, which regulates microfilament organisation (Fu et al, 2005). These data not only provides the first evidence of a signalling network regulating MT organisation, but they also provide the first firm mechanistic evidence for cross-talk between MTs and actin microfilaments.

Thus, there is good evidence emerging that MTs may interact with several key signalling components to play an integral role in mediating signalling events. Our data clearly implicates MTs as an early target for the SI signalling network in pollen tubes. As SI is mediated by a receptor-ligand interaction at the plasma membrane, it is perhaps not surprising that the cortical MTs are involved. However, as rather little is known about signalling to MTs in any plant system, with the exception of the cell cycle, there is clearly much still to be explored.

From what little is known, there are clearly hints to other signalling components that may potentially be involved in mediating SI. **Figure 4.6** is a model that attempts to combine the available data on MT-F-actin interactions and the SI response, to present possible scenarios of what might be happening to the MTs during SI. **Figure 4.6a** shows a typical, untreated pollen tube and **Figure 4.6b** shows one undergoing SI. One of the first events in SI is the influx of calcium into the shank of the pollen tube (Franklin-Tong et al, 1993; 1997). As MTs are known to be sensitive to high concentrations of calcium (Weisenburg, 1972; Cyr, 1991), in a calmodulin-dependent manner (Keith et al, 1983; Fisher et al, 1996), this initial influx of calcium could have a direct effect on the MTs, causing them to rapidly depolymerise (**Step 1**). A 90 kDa protein, subsequently identified as phospholipase D (PLD), was identified in tobacco BY-2 cells (Gardiner et al, 2001). PLD has been shown to bind to cortical microtubules and is involved in their association with the plasma membrane (Gardiner et al, 2001). Moreover, stimulating PLD activation with *n*-butanol had a dramatic effect on cortical microtubule organisation, causing them to detach from the membrane and partially depolymerise (Dhonukshe et al, 2003). Calcium can also activate PLD (reviewed in Wang, 1999). During SI the calcium influx could activate PLD (**Step 2**), causing the MTs to be released from the membrane and subsequently depolymerised by a MAP. To date, only two MAPs from plants, katanin and MAP18, have been shown to sever and depolymerise MTs (Burk et al, 2001; Stoppin-Mellet et al, 2002; Burk & Ye, 2002; Bouquin et al, 2003; Wang et al, 2007) so these proteins may play a role in the SI response (**Step 3**). Alternatively, the MT depolymerisation could be due to the SI-induced F-actin depolymerisation as Poulter et al (2008) demonstrated that MTs require an intact F-actin cytoskeleton to retain their integrity. In this case, the calcium influx causes the F-actin to depolymerise (Snowman et al, 2002) (**Step 4**). The MTs are probably interacting with the F-actin through proteins such as SB401,

a protein isolated from *Solanum berthaultii* pollen that binds to and bundles MTs and F-actin and is regulated by phosphorylation (Huang et al, 2007; Liu et al, 2009). The MTs could register the F-actin depolymerisation through these protein interactions and subsequently depolymerise themselves (**Step 5**). Another signalling component that could be involved is Rop GTPase. As mentioned earlier, ROP2 has been shown to regulate both the cortical MT and F-actin cytoskeletons in *Arabidopsis* pavement cells through their interaction with RIC1 and RIC4 (Fu et al, 2005). ROP2 is not expressed in pollen tubes but many other ROPs are (Zheng & Yang, 2000; Gu et al, 2003). Currently the roles of ROP8, -9, -10 and -11, which are expressed in pollen, are not known so these proteins could be playing the role that ROP2 does in pavement cells, i.e. activated ROP inactivates the MT bundling RIC4. If this was occurring then the MTs would probably be more susceptible to depolymerisation (**Step 6**). Although this model is highly speculative it provides ideas for future avenues of study to try and elucidate how the MT cytoskeleton is responding to the SI-specific signals.

In summary, we have demonstrated that the MT cytoskeleton is a very early target for SI signals. It is rapidly depolymerised, but changes are quite distinct from those of the actin cytoskeleton. We found that F-actin depolymerisation can result in MT depolymerisation, but not *vice versa*, implicating one-way cross-talk between these components. Notably, cortical MT depolymerisation itself, unlike actin depolymerisation, is not sufficient to trigger PCD. However, stabilisation of MTs significantly reduced SI-induced caspase-like activity, suggesting that MT depolymerisation, although on its own is insufficient to trigger PCD, is required for SI-induced PCD to progress. Thus, SI targets the MT cytoskeleton and its depolymerisation appears to play a functional role. The next challenges will be to identify

which MT associated proteins (MAPs) and signalling components are involved and to establish the function of this striking response.

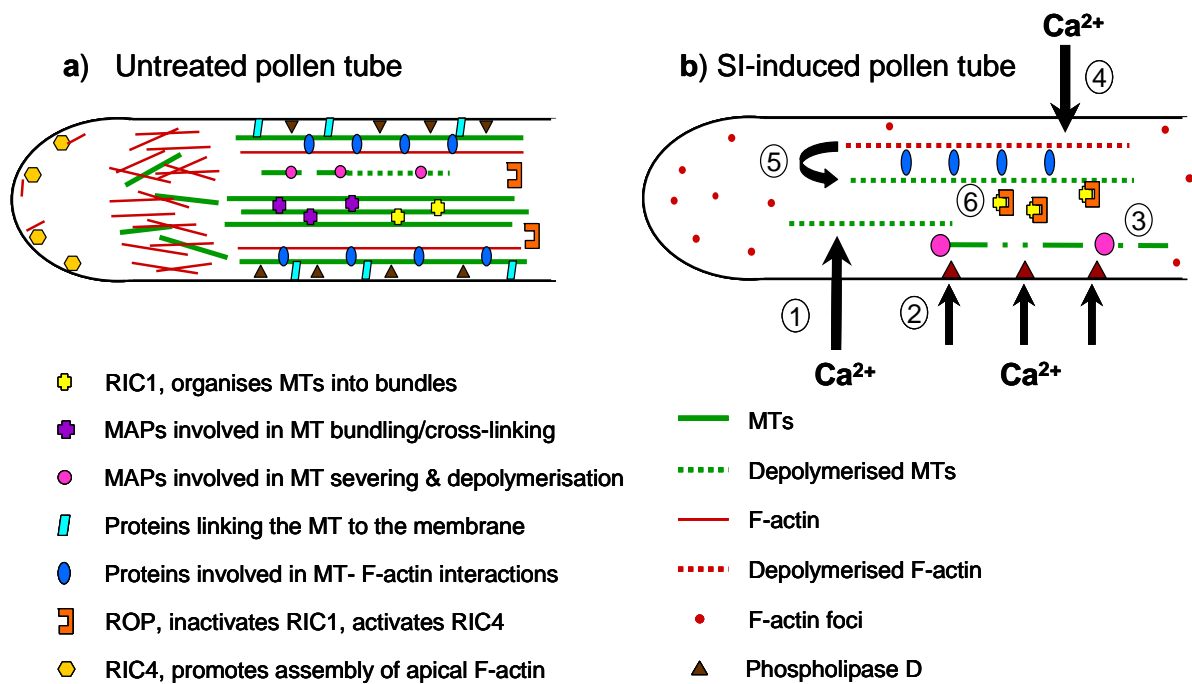


Figure 4.6. A possible model for factors involved in pollen tube MT alterations during SI

During the SI response the MTs are rapidly depolymerised. How this could be achieved is illustrated here.

- a) In an untreated pollen tube the MTs form longitudinal bundles at the cortex of the cell. These MTs are attached to the membrane by proteins such as phospholipase D. MAPs such as MAP65 cross-link MTs into bundles and katanin is responsible for MT severing and depolymerisation. F-actin and MTs may be associated via proteins that interact with both cytoskeleton components, for example the protein SB401 from pollen.
- b) The SI response involves an influx of calcium into the shank of the pollen tube. The influx of calcium (**step 1**) could have a direct depolymerising effect on the MTs as MTs are known to be sensitive to high calcium concentrations. Alternatively, (**2**) the calcium influx could activate phospholipase D which would cause the MTs to detach from the membrane and start to depolymerise. This depolymerisation could be aided by a MT depolymeriser such as katanin or MAP18. (**3**). Another possibility is that the depolymerisation of the F-actin that occurs during the early stages of SI (**4**) could be responsible for the subsequent MT depolymerisation as Poulter et al (2008) demonstrated the MTs rely on the F-actin to maintain their integrity. (**5**) The depolymerisation could be transmitted through the proteins that bind to both cytoskeleton components. Rop GTPases could also be involved (**6**) by inactivating proteins involved in MT bundling such as RIC1.

CHAPTER 5

CHARACTERISING THE PUNCTATE F-ACTIN FOCI OF THE SI RESPONSE

5.1) Introduction

The actin cytoskeleton is a major target for signalling cascades in both plants and animals. In plants, a wide range of abiotic and biotic stimuli, such as light, pathogen attack and SI, can trigger actin alterations (Nick, 1999; Staiger, 2000). It is generally accepted that it is the actin binding proteins (ABPs) that are responsible for transducing the extracellular signals into changes in cytoarchitecture and actin function. Many of the ABPs identified in plants to date have their activity regulated by phospholipids, calcium and post-translational modification (see **Section 1.2.1.3**) suggesting that they are responding to external signals. Recently, in plants it has been shown that three abundant ABPs, profilin, cyclase-associated protein (CAP), and actin-depolymerising factor (ADF) co-operate to stimulate actin turnover *in vitro* (Chaudhry et al, 2007). Profilin is an actin-monomer binding protein involved in preventing spontaneous nucleation and maintaining a pool of ATP-actin ready for polymerisation (Dos Remedios et al, 2003; **Section 1.2.1.3.1**). Unlike mammalian profilin, plant profilin is unable to stimulate nucleotide exchange on actin (Kovar et al, 2001a; Perelroizen et al, 1996)

CAP/Srv2p is a bifunctional protein, the C-terminal binds actin monomers and the N-terminal binds the adenylyl cyclase complex in yeast and is involved in signalling (Fedor-Chaikin et al, 1990; Field et al, 1990; Gerst et al, 1991; Gieselmann & Mann, 1992; Freeman et al, 1995; **Section 1.2.1.3.3**). The N-terminal of yeast Srv2p and human CAP1 has also been shown to bind to ADF/cofilin when it is bound to G-actin, which acts to promote actin turnover (Moriyama & Yahara, 2002; Quintero-Monzon et al, 2009). *Arabidopsis* CAP1 (AtCAP1) is thought to be involved in plant-specific signalling pathways as *Atcap1* mutants exhibit developmental defects (Deeks et al, 2007), as well as altered actin organisations (Deeks et al, 2007; Barrero et al, 2002).

ADF is also a key regulator of actin dynamics (see **Section 1.2.1.3.2**). It is able to bind to both G- and F-actin and depolymerises F-actin by severing (Andrianantoandro & Pollard, 2006) and by increasing the off-rate of G-actin from the minus end (Carlier et al, 1997). At high concentrations of ADF to actin, ADF can nucleate actin polymerisation (Andrianantoandro & Pollard, 2006) and can also speed up actin polymerisation by contributing to barbed-end formation; the increased ATP-F-actin supports higher levels of nucleation by the Arp2/3 complex (Ichetovkin et al, 2002). ADF is regulated by pH, phosphorylation and phospholipids (reviewed in Bamberg, 1999).

The actin cytoskeleton is essential for the tip growth of pollen tubes (Gibbon et al, 1999; Vidali et al, 2001) and has been shown to be an early target of the SI signalling cascade in poppy (Geitmann et al, 2000; Snowman et al, 2002). The alterations that occur to the actin cytoskeleton during SI follow a distinct and reproducible pattern that starts with a large and sustained depolymerisation of 56 – 74 % of the F-actin in the pollen tube (Snowman et al, 2002) followed by the formation of small actin foci and later, larger punctate F-actin foci. The initial depolymerisation of F-actin during SI contributes to the inhibition of pollen tube growth, to ensure that fertilisation is unable to occur. The SI response of poppy also triggers PCD of incompatible pollen (Thomas & Franklin-Tong, 2004) and recent work has shown that F-actin depolymerisation is necessary and sufficient for PCD initiation (Thomas et al, 2006).

The formation of the F-actin foci occurs later in the response, after the cessation of pollen tube growth, so are unlikely to play a role in pollen tube growth inhibition. The actin

alterations that occur after the initial depolymerisation are dramatic and unusual changes. The small F-actin foci give way to larger, punctate foci that persist for at least 3h post SI-induction (Geitmann et al, 2000; Snowman et al, 2002). These actin aggregates contain at least some F-actin, as they are able to be visualised using rhodamin-phalloidin. These F-actin aggregates are unusual structures. They appear to be superficially similar to two different structures found in yeast. The first is actin patches, which are involved in endocytosis and are very dynamic structures (reviewed in Ayscough, 2005). The second is F-actin structures termed ‘actin bodies’ that form in quiescent yeast cells (Sagot et al, 2006). Actin bodies are stable structures containing the ABPs capping protein and fimbrin, amongst others (Sagot et al, 2006). Apart from in SI, F-actin aggregates have not been described in pollen tubes. Although large F-actin focal adhesions have been observed in pollen tubes growing *in vivo* (Pierson et al. 1986; Jauh & Lord, 1995) their star-shape and localisation differ considerably from the SI-induced foci.

To date, studies on the SI-mediated actin responses have focused on the initial phase of depolymerisation and no analysis of the large punctate actin foci, or what is involved in their formation, has taken place. This chapter aimed to characterise these curious F-actin structures.

5.2) Results

5.2.1) Alterations to the actin cytoskeleton during SI

The dramatic actin cytoskeleton alterations that occur during the SI response have been described previously (Geitmann et al, 2000; Snowman et al, 2002) and are shown in **Figure 1**. In a normally growing pollen tube (**Fig. 5.1a**) the F-actin is organised into a typical pollen tube arrangement with a relatively F-actin-free tip, an actin collar in the sub-apical region and longitudinal F-actin bundles along the shank. Upon induction of the SI response, the F-actin in the shank rapidly depolymerised, F-actin was detected in the tip and there was prominent F-actin labelling at the cortex of the pollen tube (**Fig. 5.1b**). This cortical labelling was replaced by small actin foci that were seen throughout the tube (**Fig. 5.1c, d**). The foci at the cortex of the tube appeared to increase in size and gradually the number of small foci in the middle of the tube appeared to decrease (**Fig. 5.1e**). In the later stages of SI, the majority of the large punctate F-actin foci localised to the cortex and were found throughout the pollen tube (**Fig. 5.1f, g**). These SI-induced alterations appeared to be an active, organised process, involving F-actin shifting from a primarily plasma membrane localisation at around 10 min post-SI (**Fig. 1b, c**) to a distribution of small F-actin foci in the lumen of the tube at around 30 min after SI-induction (**Fig. 5.1d, e**) and then into large F-actin aggregates, with a primarily plasma membrane localisation from 1h and onwards after SI (**Fig. 5.1f, g**).

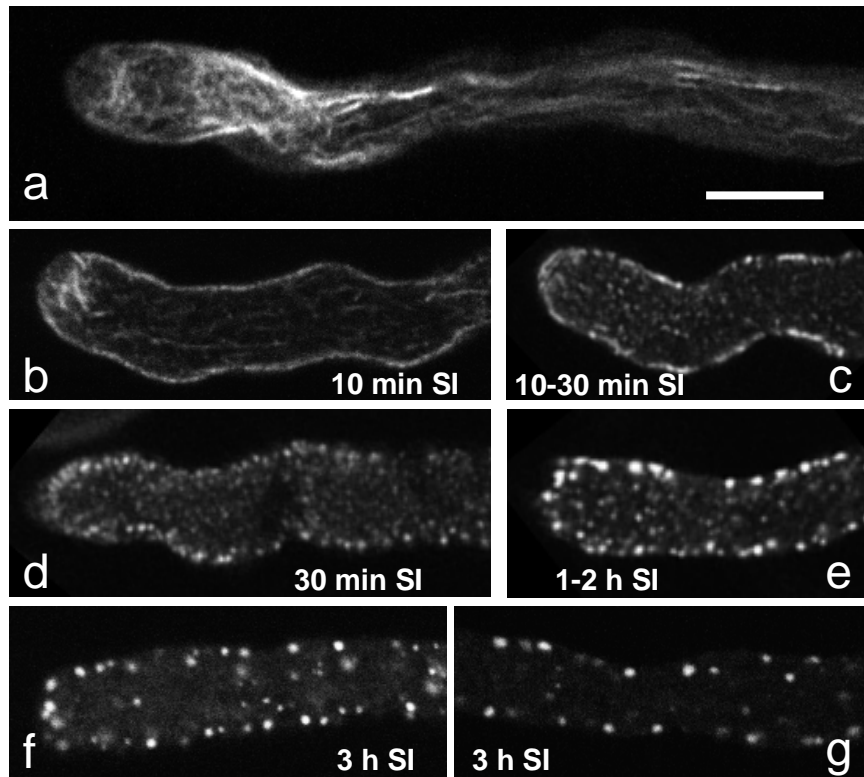


Figure 5.1. F-actin alterations during SI

- (a) F-actin organisation in an untreated pollen tube.
 (b) Early in the SI response depolymerisation of much of the F-actin occurred throughout the pollen tube but there was clear F-actin labelling at the cortex and in the tip.
 (c, d) The continuous F-actin cortical labelling was subsequently lost and small actin foci formed throughout the tube.
 (e) These F-actin foci appeared to increase in size at the cortex of the tube
 (f, g) The number of small foci in the middle of the tube decreased, leaving the majority of the large punctate actin spots at the cortex along the whole length of the pollen tube.

Images are single confocal sections. F-actin is stained with rhodamine-phalloidin.
 Scale bar = 10 μ m.

As the number of F-actin foci appeared to decrease as the size of the remaining foci appeared to increase, this suggested that aggregation of the foci was occurring as a result of SI stimulation. This observation was therefore tested quantitatively. The diameter of twenty F-actin foci per pollen tube ($n = 10$) was measured at various time points after SI induction. There was a gradual increase in the apparent focus size over time (**Fig. 5.2a**). At 30 min post-SI, when F-actin foci first became visible, the mean diameter of the foci was $0.69 \pm 0.01 \mu\text{m}$. By 1 h after SI-induction the F-actin foci had significantly increased in size to $0.82 \pm 0.02 \mu\text{m}$ (t -test, $p < 0.001$, ***) and there was a further significant increase in size by 3 h SI when the F-actin foci had a mean diameter of $0.96 \pm 0.02 \mu\text{m}$ (t -test, $p < 0.001$, ***). The observed increase in apparent size occurred concomitantly with a decrease in the mean number of foci present in a 30×30 pixel area of the pollen tube (**Fig. 5.2b**). The foci number more than halved, decreasing from 5.3 ± 0.4 foci per area/pollen tube at 30 min after SI to 2.5 ± 0.2 foci at 3 h post-SI. It has previously been shown that F-actin levels do not increase again after the maximal F-actin depolymerisation is achieved at 30 min post-SI (Snowman et al, 2002). This suggests that the observed increase in F-actin foci size is unlikely to be due to F-actin assembly. Since the number of foci also decreases, these observations support the hypothesis that the F-actin remaining after the initial depolymerisation phase act as “seeds” for the aggregation of the large punctate foci seen later in the response.

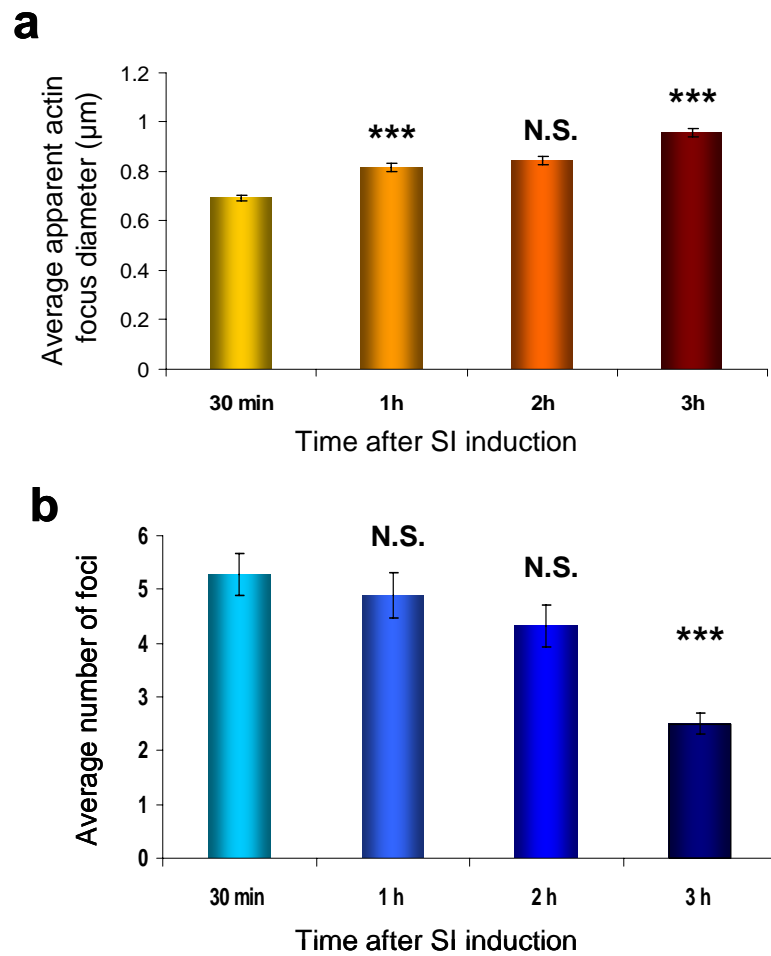


Figure 5.2. The punctate F-actin foci appear to increase in size but decrease in number during SI.

(a) The width of 20 F-actin foci per tube ($n = 10$) was measured (in μm) using Metamorph software. The apparent size of the foci increased during the SI response.

(b) The mean number of F-actin foci in a defined area (a 30×30 pixel box) in the pollen tube decreased over the course of the SI reaction (4 boxes per tube, $n = 10$).

The significance values relate to t -tests carried out between that time point and the previous time point, *** = $p < 0.001$, NS = no significant difference.

5.2.2) The large punctate F-actin foci are resistant to depolymerisation

The F-actin bodies of quiescent yeast cell, which are superficially similar to the SI-induced F-actin foci, have been shown to be very stable structures (Sagot et al, 2006). They were highly resistant to concentrations of Latrunculin A that normally depolymerise all the F-actin structures within the cell. These F-actin bodies only form in yeast when the cells are starved, i.e. under stress, so they could share some features with the F-actin foci seen in pollen during SI. Thus, the stability of the large SI-induced F-actin foci was tested using the F-actin depolymerising drug latrunculin B (LatB).

In control pollen tubes, the F-actin cytoskeleton (**Fig. 5.3a**) was dramatically affected by treatment with 1 μ M LatB for 10 min (**Fig 5.3b**). Virtually all visible F-actin had been depolymerised, which is in agreement with a previous study where the same treatment resulted in a reduction in F-actin level of 46.9 ± 3.8 % (Thomas et al, 2006). Pollen tubes that had undergone 3 h of SI had the characteristic large F-actin foci (**Fig 5.3c**). Treatment of these SI-induced tubes with 1 μ M LatB for either 10 min (**Fig 5.3d**) or 30 min (**Fig 5.3e**) had no visible effect, with the F-actin aggregates remaining prevalent in the pollen tube. These data demonstrate that the SI-induced actin foci are very stable, much more so than any other F-actin structure in the cell. LatB acts by forming a 1:1 complex with G-actin to prevent further polymerisation of filaments, which results in depolymerisation of existing F-actin (Coué et al, 1987; Spector et al, 1989; Morton et al, 2000). With this in mind, we can postulate that there is little or no turnover of actin filaments in these structures, or the turn-over that is present is very slow.

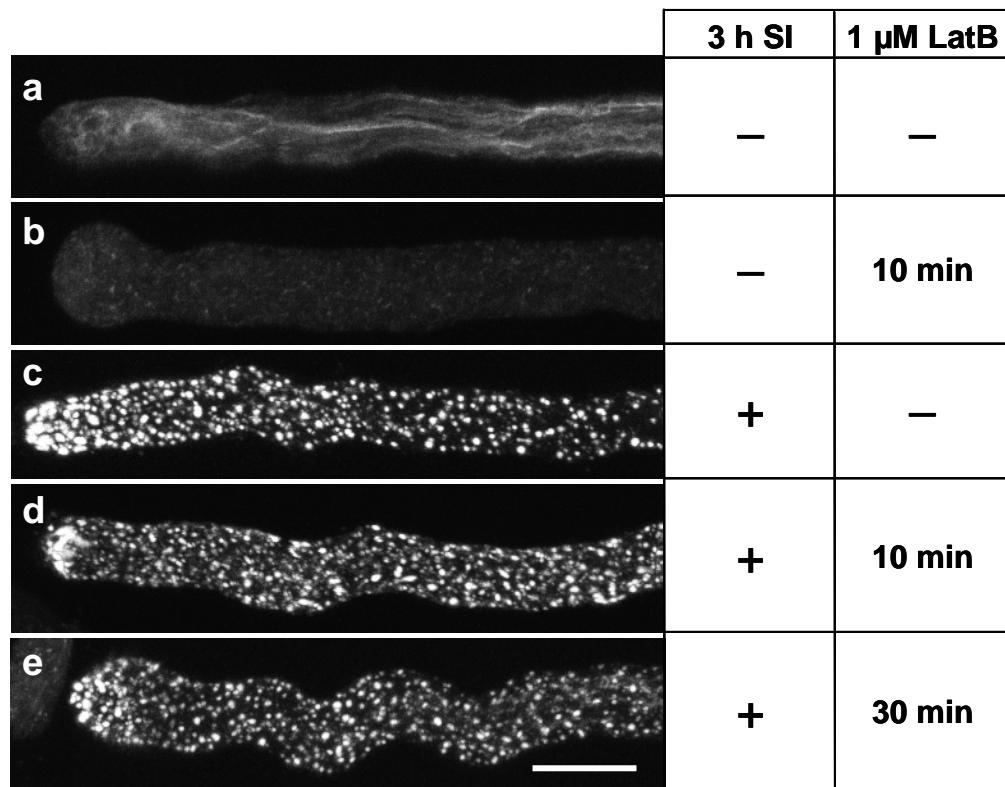


Figure 5.3. The punctate F-actin foci are resistant to LatB induced depolymerisation

- (a) F-actin in an untreated pollen tube.
- (b) 10 min 1 μ M LatB resulted in depolymerisation of the majority of visible F-actin.
- (c) 3 h SI resulted in numerous large punctate F-actin foci.
- (d) 3 h SI followed by 10 min 1 μ M LatB treatment, punctate F-actin foci were still visible.
- (e) 3 h SI followed by 30 min 1 μ M LatB treatment, punctate F-actin foci were still visible.

All images are full projections of confocal sections. Actin was visualised using rhodamine-phalloidin. Scale bar = 10 μ m

5.2.3) Testing the specificity of antibodies raised against different ABPs

The formation and maintenance of the F-actin foci must involve the concerted effort of several ABPs. The formation of the punctate actin foci appears to be an active process, however, we do not know whether these foci are formed by *de novo* F-actin assembly or whether existing F-actin is moved around the tube. Nevertheless, ABPs must be the driving force behind their formation. Work by Snowman et al (2002) showed that the initial F-actin depolymerisation step probably involved the actin monomer binding protein profilin, but this ABP on its own was insufficient to explain the huge levels of actin depolymerisation seen during SI. Later work suggested that PrABP80, a poppy gelsolin, could also contribute to this initial depolymerisation event (Huang et al, 2004). Here, we wanted to examine which ABPs might be involved in the formation or maintenance of the punctate F-actin foci. Immunolocalisation of four major ABPs was carried out to examine their presence and possible co-localisation with the SI-induced F-actin foci. The ABPs that were investigated here were chosen as representatives of the different classes of ABPs and comprised: profilin (monomer binding), CAP (monomer binding with possible signalling capabilities), fimbrin (cross-linking) and ADF (severing and dynamizing). Antibodies raised against these proteins from different plant species were kindly donated by Prof. Chris Staiger of Purdue University, Indiana, USA and Prof. Patrick Hussey of Durham University, UK.

To ensure that the antibodies cross-reacted with the corresponding poppy ABPs, western blot analysis on total protein extracts from pollen were carried out (**Fig. 5.4**). The antibodies to the ABPs all showed cross-reactivity with the poppy proteins, indicated by a strong band which ran at the expected molecular weight. The anti-AtCAP1 (Chaudhry et al, 2007) identified poppy CAP at ~55 kDa (**Fig. 5.4a**), the fimbrin antibody, anti-AtFIM1, recognised poppy

fimbrin at ~75 kDa (**Fig. 5.4b**), the rabbit anti-LIADF and the mouse anti-LIADF1 (Allwood et al, 2002) both cross-reacted with poppy ADF at ~18 kDa (**Fig. 5.4c, d**) and the anti-ZmPro5 (Kovar et al, 2000a) recognised poppy pollen profilin (~14 kDa; **Fig. 5.4d**). This confirmed that these antibodies were specific for the ABPs and were thus suitable for use in immunolocalisation.

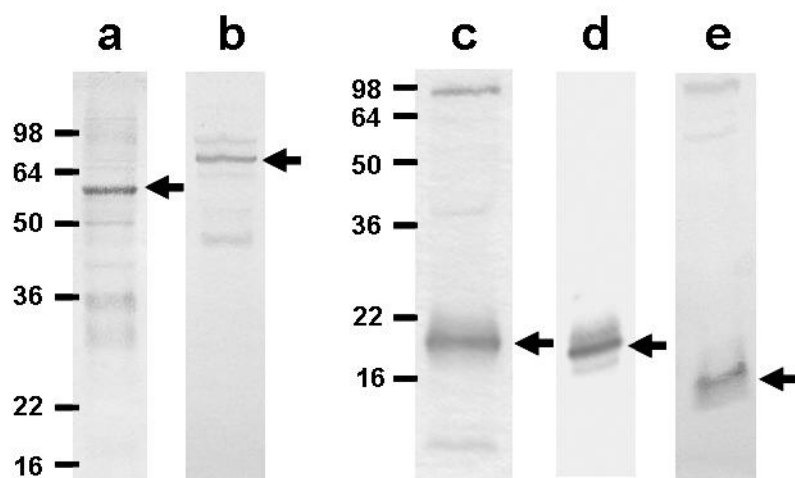


Figure 5.4. The ABP antibodies cross-react with poppy pollen proteins

- a) The anti-AtCAP1 (1:2000) recognises a prominent band ~55 kDa representing poppy CAP (arrow).
- b) The anti-AtFim1 (1:2000) recognises a prominent band ~75 kDa representing poppy fimbrin (arrow).
- c) The rabbit anti-LIADF (1:2000) identifies a prominent band ~18 kDa representing poppy ADF (arrow).
- d) The mouse anti-LIADF1 (1:1000) identifies the same ~18 kDa band representing poppy ADF (arrow).
- e) The anti-ZmPro5 (1:2000) identifies a strong band ~14 kDa representing poppy profilin (arrow).

Marker, in kDa.

5.2.4) ABP localisation alters during SI

In order to perform co-localisation of the ABPs with F-actin, rhodamine-phalloidin staining of the F-actin was used in conjunction with the anti-sera. The localisation of the ABPs was examined in normally growing, untreated pollen tubes and compared to the organisation observed in pollen tubes that had been undergoing SI for 3 h, which corresponded to when the large F-actin foci had formed. SI induced alterations in the localisation of all the ABPs examined (**Fig. 5.5**). In untreated pollen tubes (**Fig. 5.5a**), CAP (green) was visualised as small speckles throughout the pollen tube with no detectable localisation to the F-actin (red). After 3 h SI, a significant amount of CAP co-localised with the large F-actin foci (**Fig. 5.5b**, seen as yellow). However, although reduced compared to the UT pollen tube, there was still a substantial cytosolic CAP signal, indicating that not all the CAP co-localised with the F-actin. In an untreated pollen tube, ADF (green) appeared as a diffuse signal throughout the cytoplasm, with a tendency to exhibit stronger signal towards the cortex of the pollen tube. There was also no visible co-localisation with the F-actin (**Fig. 5.5c**). At 3 h post-SI, ADF had rearranged into foci that co-localised with the F-actin. Like CAP, there was still some cytosolic ADF signal, indicating not all the ADF associated with the F-actin (**Fig. 5.5d**).

Fimbrin (green), exhibited some co-localisation with the F-actin (seen as yellow), as well as being visualised as fine speckles throughout the normally growing pollen tube (**Fig. 5.5e**). After 3 h SI, fimbrin no longer co-localised to the F-actin and was visualised as a patchy signal throughout the pollen tube (**Fig. 5.5f**). Profilin (green; **Fig. 5.5d1**) was visualised as a cytosolic protein with no apparent co-localisation with the F-actin in normal pollen tubes (**Fig. 5.5g**). After SI-induction the localisation of profilin altered and it formed small foci but these did not co-localise with the F-actin (**Fig. 5.5h**). The profilin signal was also

substantially weaker in SI compared to untreated pollen tubes. Thus, the localisation of all the ABPs altered during SI, but only CAP and ADF appeared to co-localise to the large F-actin foci.

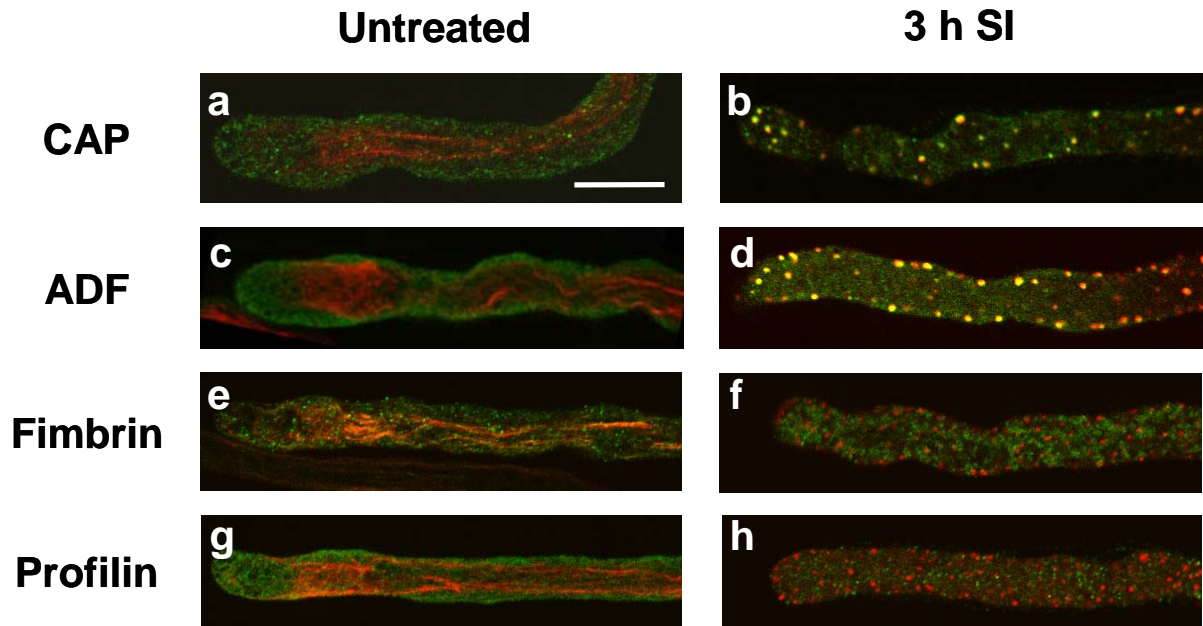


Figure 5.5. Localisation of four ABPs in untreated and 3 h SI-induced pollen tubes

Representative typical images of F-actin (red; rhodamine-phalloidin) and ABPs (green; FITC-conjugated antibody). Co-localisation is shown by overlap of the probes (yellow signal). Left panel shows untreated pollen tubes; right panel shows pollen tubes after 3 h SI induction.

- (a) CAP immunolocalisation in an untreated pollen tube
- (b) CAP immunolocalisation after 3h SI
- (c) ADF immunolocalisation in an untreated pollen tube
- (d) ADF immunolocalisation after 3h SI
- (e) Fimbrin immunolocalisation in an untreated pollen tube
- (f) Fimbrin immunolocalisation after 3h SI
- (g) Profilin immunolocalisation in an untreated pollen tube
- (h) Profilin immunolocalisation after 3h SI

Images are single confocal sections. Scale bar = 10 μm

5.2.5) Co-localisation of CAP and ADF during SI

To test whether CAP and ADF were present in the same structures, dual immunolocalisation with the CAP rabbit antiserum and an ADF mouse antibody was performed. Confocal imaging confirmed that the two proteins co-localised after SI induction (**Fig. 5.6**). Together these data suggest that both CAP and ADF are potentially implicated in playing a role in the formation/maintenance of the large punctate F-actin foci, at least at this late time point.

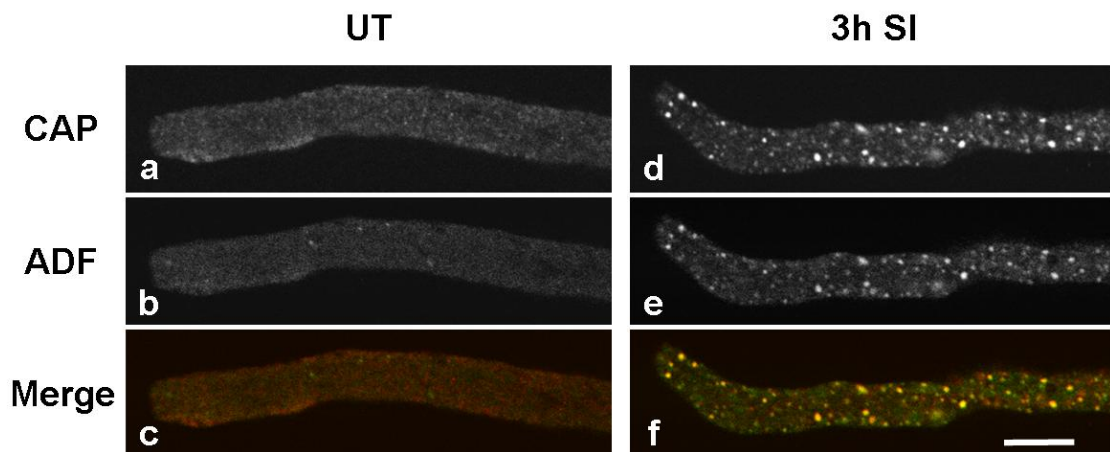


Figure 5.6. ADF and CAP co-localise at 3 h post-SI induction

In an untreated pollen tube both CAP (**a**) and ADF (**b**) were visualised throughout the cytosol. After 3 h SI, both CAP (**d**) and ADF (**e**) had formed foci which co-localised (**f**).

Images are single confocal section. In the merge image, CAP is seen as red and ADF is green. Co-localisation is seen as yellow. Scale bar = 10 μm .

5.2.6) Quantitative analysis of ABP and F-actin co-localisation

Although the imaging data indicated that ADF and CAP co-localised to the F-actin foci it was thought necessary and useful to attempt to quantify the extent of co-localisation. This would provide a measure of the alterations and would also allow the temporal dynamics to be analysed in more detail. The levels of fimbrin and profilin co-localisation to actin were also quantified, to ensure that the quantification method was able to distinguish between positive and negative co-localisation. A method to quantify the co-localisation was developed using Metamorph software (Molecular Devices). It was deemed necessary to develop a new methodology as standard co-localisation software/algorithms examine the level of co-localisation across a whole image, whereas we are interested in specific structures. Moreover, the structures we wished to analyse alter their shape from long filamentous structures to rounded foci during the course of the SI response. Briefly, the method involved selecting 50 regions of interest (ROIs) in a single confocal section of each pollen tube ($n = 5$) where F-actin was labelled with rhodamine-phalloidin. The ROIs were transferred to the image labelled for the corresponding ABP and the fluorescence signal of the ABP was measured. ROIs with ABP intensities above the threshold level were considered as positive co-localisation (see **Section 2.8** for details).

The data (**Fig. 5.7**) show that co-localisation of CAP, ADF and profilin with F-actin was very low in untreated pollen tubes ($16.8 \% \pm 4.0$, $20\% \pm 3.3$ and $31.2\% \pm 3.0$, respectively), whereas fimbrin showed higher levels of co-localisation ($46.6 \% \pm 8.1$). Following 3 h SI, the percentage co-localisation of CAP and ADF with F-actin rose by 77.9% and 74.7% respectively, representing a significant increase compared to untreated pollen tubes (t -test, $p < 0.001$, ***). In contrast, the levels of profilin and fimbrin co-localisation with F-actin

decreased significantly (t -test, $p < 0.05$, *) by 3 h post SI-induction. This confirms the imaging data and indicates that the method for quantifying co-localisation was valid. The quantification provides a good idea of the extent of the alterations in ABP localisation during SI and firmly establishes that CAP and ADF co-localise with the punctate F-actin foci.

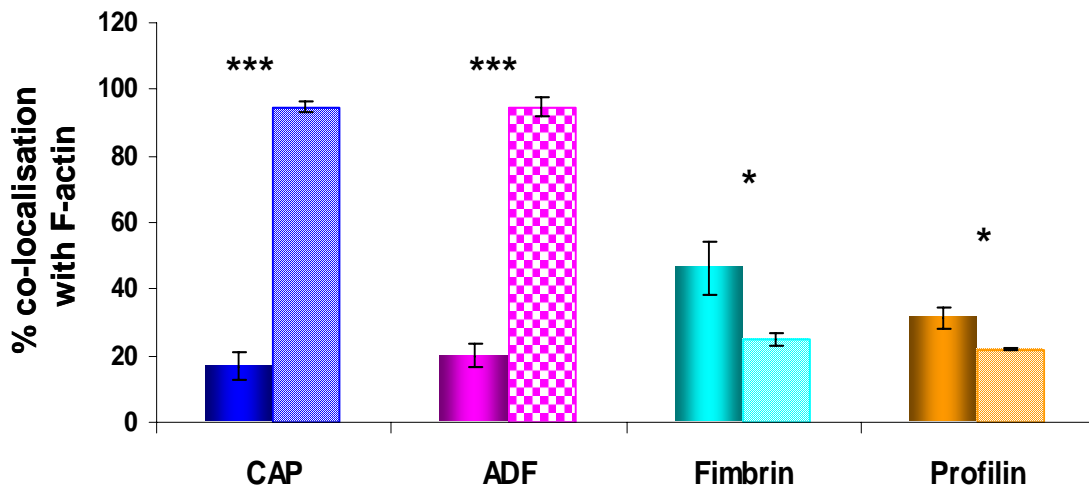


Figure 5.7. Quantification of co-localisation of ABPs with F-actin

50 F-actin areas per tube ($n=5$ tubes per treatment, per ABP) were assessed for co-localization with each of the 4 different ABPs in untreated pollen tubes (solid colour bars) and pollen tubes that had been under-going SI for 3 h (patterned bars). The ABPs CAP (blue) and ADF (pink) both showed highly significant increases in co-localization with F-actin in the 3 h SI treatment compared to the untreated tubes (*** = $p < 0.001$). Fimbrin (aqua) and Profilin (orange) both showed a significant reduction in co-localization with F-actin in the 3 h SI compared to the untreated pollen tubes (* = $p < 0.05$).

5.2.7) Spatio-temporal dynamics of the SI-induced CAP, ADF and F-actin alterations

As both CAP and ADF co-localised with the F-actin foci at 3 h SI we wished to assess the spatio-temporal dynamics of the alterations in the localisation of the two ABPs. Immunolocalisation was therefore carried out on pollen tubes that had been undergoing SI for various time periods. Single confocal sections were analysed to determine the extent of the either CAP and F-actin (**Fig. 5.8**) or ADF and F-actin (**Fig. 5.9**) co-localisation.

In untreated pollen tubes CAP was visualised as small speckles throughout the tube (**Fig. 5.8a**). By 10 min SI, when the F-actin was found adjacent to the pollen tube membrane (**Fig 5.8e**), CAP localisation had not visibly changed (**Fig. 5.8d**) and no co-localisation was detected (**Fig. 5.8f**). After 30 min of SI, the CAP had started to form small foci (**Fig. 5.8g**), some of which co-localised with the small actin foci (**Fig 5.8i, arrows**). During the later stages of SI the level of co-localisation appeared to increase. At 3 h SI, CAP had formed foci throughout the tube (**Fig 5.8j, m**), which co-localised with the large F-actin foci (**Fig 5.k, n**). A full confocal projection of a pollen tube shows the extent of the CAP-actin co-localisation (**Fig. 5.8m-o**). Although there was considerable association of CAP with the large F-actin foci, there was still some diffuse labelling throughout the tube. This indicates that a proportion of the CAP was still present in the cytoplasm and not all of it was associated with F-actin.

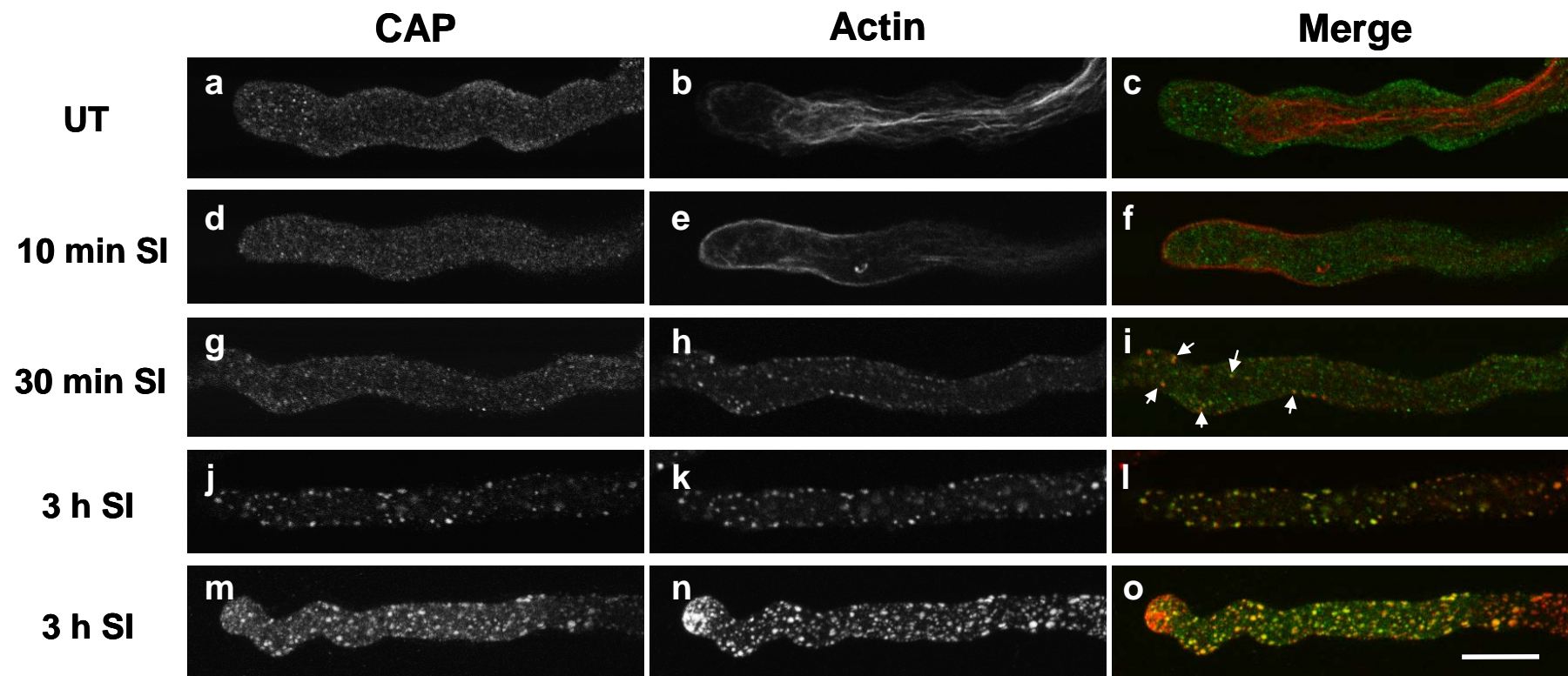


Figure 5.8. Spatio-temporal analysis of CAP localisation during the SI response.

(a-c) In an untreated tube, CAP appeared as small foci throughout the cytoplasm which did not co-localise with the F-actin.

(d-f) At 10 min after SI induction the actin labelled the cortex of the pollen tube but the CAP localisation had not changed.

(g-i) At 30 min post SI the actin had formed small foci, some of which co-localised with the small CAP foci (arrows).

(j-l) At 3 h after SI the CAP had formed foci which co-localised with the large actin foci.

(m-o) Full confocal projections, demonstrating the extent of CAP-F-actin co-localisation at 3 h SI.

Images **a-l** are single confocal sections. CAP was detected with anti-AtCAP1 (1:500), actin was co-localised with rhodamine-phalloidin. Scale bar = 10 μ m.

ADF was visualised in the cytoplasm of untreated pollen tubes, with slightly more intense labelling towards the cell cortex (**Fig. 5.9a**). After 10 min SI ADF appeared to localise more tightly to the cortex of the pollen tube (**Fig. 5.9d**) where it co-localised with the F-actin (**Fig. 5.f, yellow**). At 30 min SI, ADF had started to form small, fuzzy foci (**Fig. 5.9g**) which co-localised with the F-actin foci (**Fig. 5.9i, arrows**), although not all the F-actin spots had associated ADF. As the F-actin foci became larger, there was more co-localisation of ADF and at 3 h SI ADF had formed large punctate foci (**Fig. 5.9j**) which co-localised with the F-actin (**Fig. 5.9l, o**). Again, like CAP, a large proportion of the ADF appeared to be associated with the F-actin, there was still a diffuse ADF labelling throughout the pollen tube, indicating that some ADF was still present in the cytoplasm.

Quantitative analysis of CAP and ADF association with F-actin (**Fig. 5.10**) revealed that the trend for co-localisation was similar for the two ABPs. There were significant increases in the level of co-localisation of ADF with F-actin occurring at 10 min and 30 min post-SI induction (*t*-test, $p < 0.001$ and $p < 0.01$, respectively) and CAP-F-actin co-localisation increased significantly at each time interval up until 1 h after SI-induction (*t*-test, $p < 0.05$ for each time point). In the early stages of the SI response ADF showed a more pronounced co-localisation with the F-actin compared to CAP. However, the greatest difference in the extent of ADF and CAP co-localisation with F-actin, which occurred at 10 min post-SI, was not statistically significant (*t*-test, $p = 0.055$). Post 1 h SI-induction, the extent of CAP and ADF co-localisation with F-actin was virtually identical, with nearly 100 % of the F-actin foci co-localising with both ABPs. This co-localisation was maintained for at least 3 h post SI-induction. No further significant changes in alteration were observed after 1 h SI, suggesting that the early shifts were the most dramatic.

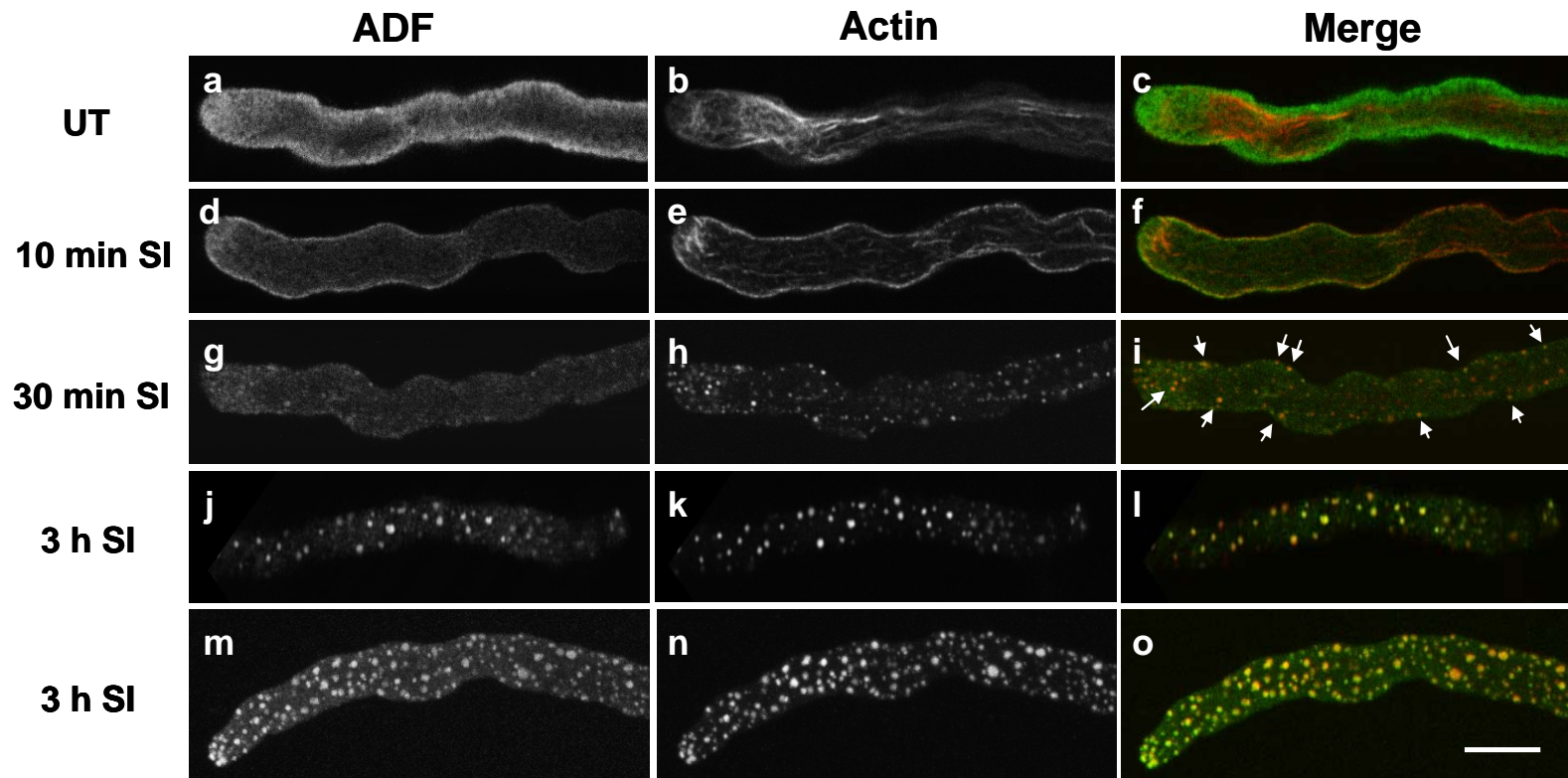


Figure 5.9. Spatio-temporal analysis of ADF localization during the SI response

(a-c) In an untreated pollen tube ADF appeared diffuse throughout the cytoplasm and did not co-localise with the F-actin.

(d-f) At 10 min after SI induction there was some co-localisation of ADF and F-actin at the cell cortex.

(g-i) At 30 min post SI the F-actin had formed small foci, some of which co-localised with the small ADF foci (arrows).

(j-l) At 3 h after SI the ADF had formed foci which co-localised with the large F-actin foci.

(m-o) Full confocal projections, demonstrating the extent of ADF-F-actin co-localisation at 3 h SI.

Images **a-l** are single confocal sections. ADF was detected with anti-LIADF1 (1:500), actin was co-localised with rhodamine-phalloidin. Scale bar = 10 μ m.

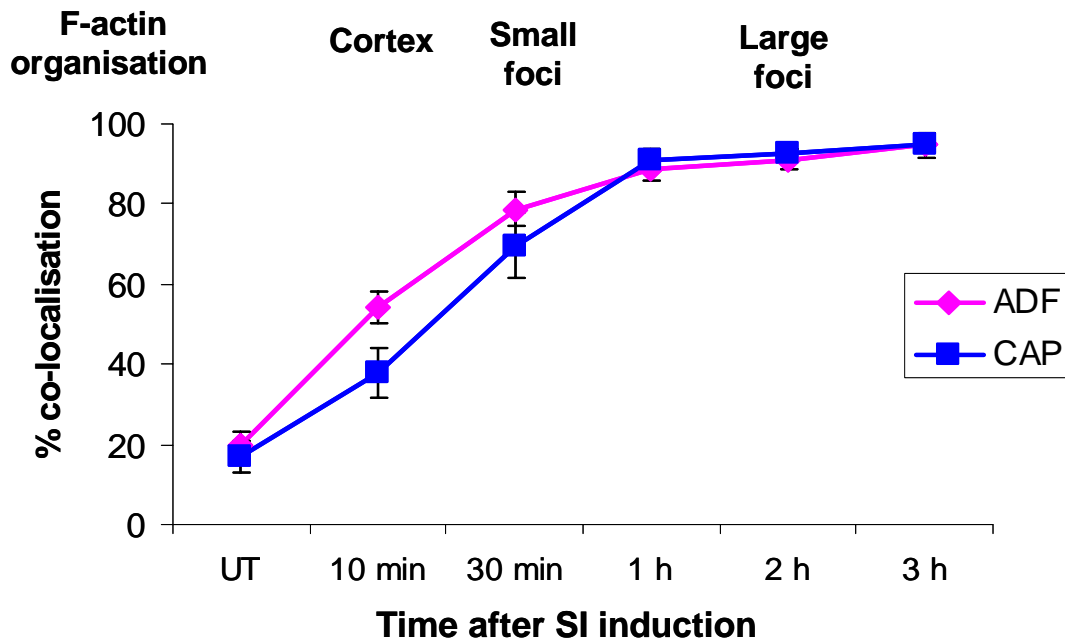


Figure 5.10. The percentage of F-actin co-localising with CAP & ADF increases with time after SI induction.

50 F-actin areas per tube (n=5) were assessed for co-localisation with CAP or ADF at the given time points after SI induction and in untreated pollen tubes using Metamorph software as described. Both CAP & ADF co-localisation with F-actin increased significantly with time after SI induction (*t*-test, UT vs. 3 h SI; $p < 0.001$ for both). At 10 min SI the level of co-localisation of ADF with F-actin appeared much greater than the level of CAP-F-actin co-localisation, but these values were not significantly different (*t*-test, $p = 0.055$).

5.3) Discussion

This chapter represents the first steps in characterising the composition, formation and dynamics of the punctate F-actin foci that are characteristic of the later stages of the poppy SI response. The earlier phase in the actin alterations, the massive F-actin depolymerisation (Geitmann et al, 2000; Snowman et al, 2002), has been demonstrated to be involved in inhibition of pollen tube growth and has also been shown to be necessary and sufficient for triggering PCD in the pollen (Thomas et al, 2006). Here, we have established the temporal dynamics of the formation of the punctate F-actin foci and have demonstrated that a subset of the known regulators of actin dynamics, CAP and ADF, associate with these structures. These studies therefore provide the first insights into the mechanisms involved in the formation of these intriguing structures, which appear to be actively formed during the SI response.

5.3.1) Formation and stability of the punctate F-actin foci

This study has shown that the F-actin foci decrease in number, but increase in apparent size over the course of the 3 h SI that was examined here. During this time period the F-actin foci also increased their association with the ABPs CAP and ADF. Although we have documented an increase in the size of the F-actin foci during SI, we have not used a live-cell approach and therefore cannot address whether this involves addition of actin to existing foci or whether the foci themselves aggregate. However, the finding that LatB had very little effect on the stability of the foci, suggests that they are formed through aggregation and not further polymerisation. Moreover, the F-actin foci were found to be much more stable than any other F-actin array found in pollen tubes. This unusual stability was also observed in the actin bodies of quiescent yeast cells (Sagot et al, 2006). These actin bodies were highly resistant to

LatA depolymerisation, were immobile and showed no F-actin turnover. It was proposed that the actin bodies acted as stores of F-actin that immediately became available for actin patch and cable formation when the cells re-entered the proliferation cycle (Sagot et al, 2006). However, in SI the large F-actin foci are formed in pollen tubes that have been undergoing SI for 1 h and are beyond the 'point of no return' which occurs between 15 and 45 min after SI-induction (Thomas & Franklin-Tong, 2004). This critical point involves the activation of the caspase-like activities that commit the cell to PCD and allow the inhibition of tube growth to be permanent (Thomas & Franklin-Tong, 2004). The SI-induced F-actin foci are therefore not likely to be acting as a reserve of F-actin for when the cell 'recovers' from SI, as this will not occur. In mammalian cells undergoing apoptosis, actin is highly resistant to cleavage by interleukin-1 β -converting enzyme (ICE)-like proteases (Song et al, 1997), though the explanations for this property are unknown. One possibility is that specific ABPs bind to or are associated with the F-actin structures, which acts to stabilise the actin against depolymerisation or cleavage.

5.3.2) CAP co-localises with the punctate F-actin foci

This study has demonstrated that CAP localises to the F-actin foci formed during the SI response and the extent of their co-localisation increased up until 3h post SI-induction. This was surprising as CAP is an actin monomer binding protein (Gieselmann & Mann, 1992; Freeman et al, 1995; Chaudhry et al, 2007) and thus we might expect it to have a cytoplasmic localisation, like that seen in the untreated pollen tubes. In mammalian cells, CAP is found throughout the cytoplasm, concentrated at lamellipodia and associated with the F-actin stress fibers, where it plays a positive role in F-actin assembly (Freeman & Field, 2000). Also, in the budding yeast *S. cerevisiae*, Srv2p/CAP has been shown to localise to actin patches via an

interaction with the F-actin binding protein Abp1 (Lila & Drubin, 1997; Balcer et al, 2003). Other studies in yeast cells have shown that formation of F-actin aggregates is dependent on Srv2p/CAP activity and requires the C-terminal, actin binding region of Srv2p/CAP (Gourlay et al, 2004). Furthermore, the actin bodies in quiescent yeast also contain Srv2p/CAP (Sagot et al, 2006). So it appears that CAP can associate with F-actin, either directly or indirectly, under certain conditions. In *Arabidopsis*, CAP has been shown to act as a nucleotide exchange factor for plant actin (Chaudhry et al, 2007). A new model for plant actin dynamics was proposed where CAP is centrally positioned between ADF and profilin. The model predicts that ADF binds to the older, ADP-actin part of the actin filament and depolymerises/severs it. The G-actin remains ADP-bound until CAP competes with the ADF for binding to the G-actin and stimulates the nucleotide exchange. The ATP-actin is then passed over to profilin which is able to incorporate the actin monomer onto the barbed end of a growing filament (Chaudhry et al, 2007). As the SI-induced F-actin foci have both CAP and ADF, but no detectable profilin, associated with them, coupled with the finding that they are resistant to LatB depolymerisation, indicates that this actin cycling process is unlikely to be occurring in these structures.

The finding that CAP co-localises with the SI-induced F-actin foci is of considerable interest as it potentially provides some insights into the mechanisms involved in the later SI events. One of the processes implicated is interaction with signalling networks. For example, in the yeast *S. cerevisiae*, CAP/Srv2p has been shown to interact with adenylyl cyclase which facilitates Ras activation of adenylyl cyclase to initiate the cAMP-PKA signalling cascade (Fedor-Chaiken et al, 1990; Field et al, 1990; Gerst et al, 1991; Mintzner & Field, 1994). CAP has also been associated with signalling in plants during co-ordinated organ expansion (Deeks

et al, 2007). So, although plants do not have Ras, it has been hypothesised that AtCAP1 has developed its own plant-specific signalling pathway (Deeks et al, 2007). Thus, CAP represents an attractive candidate for linking F-actin reorganisation into foci to signalling cascades. Although the signalling cascades that might be involved are not known, this implicates the formation of the punctate F-actin foci, and association of CAP to these structures, as an active process that most likely signals to later events involved in the SI response.

It is known that SI triggers PCD (Thomas & Franklin-Tong, 2004; Bosch & Franklin-Tong, 2007) and it has been demonstrated that F-actin depolymerisation is linked to PCD in pollen (Thomas et al, 2006). The finding that CAP associates with the F-actin foci suggests that this later process may also be involved in the PCD signalling network, although this requires further investigation. An interesting link between stabilised actin, CAP and apoptosis has recently been established in yeast (Gourlay & Ayscough, 2006). Accumulation of aberrant aggregations of stabilised F-actin in yeast cells, formed by treatment with jasplakinolide (Jasp) or through mutations of specific ABPs, leads to 'actin-mediated apoptosis' (ActMAp). ActMAp involves hyperactivation of the RAS-cAMP-PKA signalling pathway, which results in mitochondrial dysfunction, accumulation of ROS and subsequent cell death (Gourlay et al, 2004; Gourlay & Ayscough 2005a;b; 2006). Gourlay and Ayscough (2006) showed that CAP/Srv2p co-localised with the stabilised actin aggregates in these cells and importantly, apoptosis was dependent on the C-terminal, actin monomer binding domain of CAP/Srv2p. Interestingly, stabilisation of F-actin using Jasp in pollen tubes also triggered PCD (Thomas et al, 2006). In the light of this current study, it seems that later in SI there is also an actin stabilisation phase comprising the formation of the F-actin foci. As these structures are

associated with CAP it suggests that their formation may be involved in signalling to PCD. Although Ras is absent in plants, so the signalling pathway cannot be the same, it is tempting to speculate that CAP has developed a plant-specific signalling pathway that can also lead to PCD when stable actin aggregates are detected in the cell. It would be interesting to see if Jasp-stabilised actin filaments also have CAP localising to them, which would lend further support to a role for CAP in PCD signalling. This will be explored in future studies.

5.3.3) ADF co-localises with the punctate F-actin foci

Immunolocalisation of ADF in untreated poppy pollen tubes showed that ADF does not co-localise with the F-actin array, but instead appears as diffuse staining throughout the cytoplasm, with a slightly increased concentration at the cortex. ADF has previously been localised to the cytoplasm of *Narcissus* pollen tubes using both an anti-LIADF antibody (Allwood et al, 2002) and an anti-ZmADF1 antibody (Smertenko et al, 2001). In contrast, a further study using immunolocalisation of ADF in lily pollen tubes that have undergone rapid freeze-fixation, showed ADF localising to the actin collar as well as the cytoplasm of the shank of the pollen tube (Lovy-Wheeler et al, 2006). Live-cell imaging of tobacco pollen tubes using GFP-NtADF1 (Chen et al, 2002) showed ADF associating with the long actin cables in the shank of the pollen tube, as well as with the actin collar in the sub-apical region. Pollen expressing only low levels of the fusion protein only had ADF localising to the actin collar, which the authors interpreted as meaning ADF associates preferentially with this actin mesh under normal conditions. The ability to visualise ADF localising to the actin collar may therefore be dependent on the fixation procedure applied, as the actin collar is known to be extremely sensitive to fixation (Lovy-Wheeler et al, 2005). One other point to consider is that

these studies have all been carried out in pollen tubes from different plant species so a differential inter-species ADF localisation, although unlikely, cannot be excluded.

Whilst we did not visualise ADF binding to the F-actin in the untreated pollen tubes in this study, we can be fairly confident that it does interact with the F-actin in pollen as it is found in the pellet of co-sedimentation assays (Allwood et al, 2002; Chen et al, 2002; Smertenko et al, 2001; Chapter 6, this thesis). It also needs to interact with F-actin to increase the actin dynamics vital for pollen tube growth: by severing F-actin in the sub-apical region, ADF creates fragmented filaments with more free barbed ends for further polymerisation, which is needed to drive pollen tube growth (Chen et al, 2002; Lovy-Wheeler et al, 2006). After SI induction in *P. rhoeas* pollen tubes, ADF co-localised with the F-actin foci, with increasing levels of association as aggregation progressed. An interesting feature of the SI-induced F-actin foci is that even though ADF is binding to the foci, phalloidin is also able to bind. In normal F-actin structures ADF and phalloidin binding are mutually exclusive because the binding of ADF causes a twist in the actin filament that removes the phalloidin binding site (McGough et al, 1997). The only other F-actin structure which can be labelled by both ADF and phalloidin is a Hirano body (Maciver & Harrington, 1995). Hirano bodies are intracellular aggregates of F-actin and other proteins that are often found in neurons of people with neurodegenerative disorders (e.g. Alzheimers) (Hirano, 1994). Unlike the SI actin foci, the Hirano bodies are not linked to a stage in cell death because they can be formed in mouse fibroblasts or *Dictyostelium* where they are not toxic (Maselli et al, 2002).

ADF activity has been shown to be regulated by pH, polyphosphoinositides and phosphorylation (reviewed in Bamburg, 1999). Both phosphorylation and binding to

polyphosphoinositides disrupt the ability of ADF to bind to actin, whereas changes in pH alter the effect of ADF on actin dynamics. Phosphorylation of the Ser-6 residue of ADF decreases the activity of this protein in plants (Smertenko et al, 1998) and phosphorylation of Ser-3 does the same in many other species (reviewed in Bamburg, 1999). In plants, this phosphorylation is carried out by a calmodulin-like domain protein kinase that is activated by calcium (Smertenko et al, 1998; Allwood et al, 2001), making ADF indirectly controlled by calcium. However, regulation of ADF by phosphorylation may be species-specific as pollen-specific LlADF1 is not regulated by phosphorylation, instead it is regulated by the ABP AIP1 (Allwood et al, 2002), whereas the tobacco pollen-specific NtADF1 is regulated by phosphorylation (Chen et al, 2002). Although SI involves a calcium-dependent signalling cascade, which might allow ADF to be phosphorylated by a CDPK, we do not believe that it is responsible for the actin rearrangements observed. This is because ADF clearly associates with the F-actin during SI, indicating it is not inactivated by phosphorylation. The same is true for control by polyphosphoinositides. ADF binds to the F-actin foci so therefore is unlikely to be bound to either PIP or PIP₂.

It is well established that pH affects the ability of ADF to regulate actin dynamics. Most ADFs, including those from plants, show a greater ability to depolymerise F-actin at alkaline pH (Hayden et al, 1993; Moon & Drubin 1995; Carlier et al, 1997; Gungabissoon et al, 1998; Ressad et al, 1998; Allwood et al, 2002). At lower pH, around pH 6, ADF binds to and stabilises F-actin. This pH regulation is highly relevant to the events triggered in the later SI phase because recent work has demonstrated that there is a dramatic acidification of the cytosol where the pH of the pollen tube drops from around pH 6.9 in an untreated tube to about pH 5.5 in an SI-induced tube (Bosch & Franklin-Tong, 2007). This drop in pH could

trigger the relocation of ADF from the cytosol to the F-actin, where it could act to generate or stabilise F-actin foci. Andrianantoandro & Pollard (2006) found that when the F-actin is highly decorated or saturated with ADF, as the SI-induced F-actin foci appear to be, severing of the filaments is not observed. They also found that if there is a very high concentration of active ADF in an area of a cell this can stimulate nucleation of actin filaments to promote further assembly. As there is a significant increase in the level of ADF-actin co-localisation by 10 min SI, the ADF could actually be playing a role in the nucleation of the F-actin foci that we start to see by 30 min SI. Thus, these data implicate ADF as playing a key role in modulating these later SI events, comprising formation of the F-actin foci.

5.3.4) Fimbrin does not co-localise with the punctate F-actin foci

Fimbrin is an actin side-binding protein and in plants it has been shown to cross-link and stabilise actin filaments in a calcium-independent manner (Kovar et al, 2000b). *Arabidopsis* fimbrin 1 (AtFim1) has been shown to decorate dynamic actin filaments in *Tradescantia* stamen hairs (Kovar et al, 2001b). In quiescent yeast cells, fimbrin/Sac6p associated with the stable actin bodies and was necessary for their formation or maintenance (Sagot et al, 2006). In this study, fimbrin was seen to co-localise with F-actin bundles in untreated pollen tubes to a much greater extent than any of the other ABPs examined. This is consistent with a role in filament cross-linking or bundling. At 3 h SI fimbrin no longer co-localised to the F-actin which was a little surprising as these actin foci are higher-order actin structures that clearly require proteins to cross-link the filaments. As calcium has been shown not to influence the bundling activity of AtFim1 it seems unlikely that the SI-induced calcium influx would alter the activity of fimbrin in an SI-induced pollen tube. The SI-triggered acidification of the cytosol described above may play a role however, as there has been a report that F-actin

binding by mammalian fimbrin is reduced at pH 6.5 compared to pH 6.9 or 7.4 (Glenny et al, 1981). Thus at pH 5.5, the pH of the cytosol during SI, fimbrin may no longer be able to bind to the F-actin and therefore would not be able to bundle it.

5.3.5) Profilin does not associate with the punctate F-actin foci

Profilin localisation has previously been studied in lily and tobacco pollen tubes using immunolocalisation (Mitterman et al, 1995; Vidali & Hepler, 1997) where it was found to be cytoplasmic. Profilin was also found in the cytoplasm of roots and root nodules of bean (Vidali et al, 1995). Here, profilin also appears to localise throughout the cytoplasm of untreated pollen tubes, although there is a slight increase in signal intensity towards the membrane of the cell compared to the lumen. The increased profilin signal at the periphery of the pollen tube was also seen in chemically fixed lily pollen, but it was thought to be an artefact of the fixation procedure because cryofixation and sectioning of pollen tubes revealed uniform profilin labelling (Vidali & Hepler, 1997). In this current study, chemical fixation did not inhibit labelling of other ABPs within the lumen of the pollen tube (for example, fimbrin), but it is an issue worth bearing in mind. However, this study is interested in the co-localisation of the ABPs with the F-actin. As much of the F-actin is towards the periphery of the cell during SI, the problems associated with the fixation procedure should have little bearing on our results.

During SI, profilin has been proposed to play a role in the depolymerisation of F-actin that occurs almost immediately after SI-induction (Snowman et al, 2002). The sequestering ability of profilin is increased in the presence of Ca^{2+} (Kovar et al, 2000a) and SI triggers a Ca^{2+} influx that precedes the F-actin depolymerisation (Franklin-Tong et al, 1993; 1997). However,

profilin did not appear to have sufficient calcium-stimulated sequestering ability to account for the high level of F-actin depolymerisation observed in SI (Snowman et al, 2002). A poppy pollen gelsolin-like protein, PrABP80, was subsequently identified and together with profilin could account for up to 50 % F-actin depolymerisation (Huang et al, 2004).

It was thought unlikely that profilin would play a role in the formation of the punctate actin foci because the foci are primarily made up of F-actin as they can be visualised with rhodamine-phalloidin. Profilin was therefore used as a negative control to show that not all ABPs localised to the F-actin foci. At 3 h SI, profilin was still apparent throughout the cytoplasm of the pollen tube but the labelling was much weaker. There were some bright spots visible but it was thought that they were, at least in part, due to antibody precipitation. The image analysis and co-localisation quantification both show that profilin and F-actin hardly have any overlap in localisation in normal or SI treated pollen tubes. This finding is in line with profilin's role as an actin monomer binding protein. In mammalian and yeast cells profilin acts as a nucleotide exchange factor which sequesters G-actin in its ADP form and catalyses the exchange of ADP for ATP (Nishida, 1985; Goldschmidt-Clermont et al, 1992). ATP-actin polymerises more readily than ADP-actin so profilin can then shuttle these ATP-actin monomers onto the barbed ends of actin filaments, increasing polymerisation. In plant cells, profilin lacks the nucleotide exchange ability (Perelroizen et al, 1996; Kovar et al, 2000a), which is instead carried out by the protein CAP (Chaudhry et al, 2007). A model has been proposed whereby profilin acts as a sequestering protein when the barbed ends of filaments are capped but when these ends are not capped, profilin shuttles ATP-actin onto the ends of growing filaments with the same critical concentration as G-actin alone (Perelroizen et al, 1994;1996; Kang et al, 1999). The fact that very little profilin is found co-localising

with the actin foci supports the hypothesis that the foci are predominantly F-actin and there is little polymerisation occurring at 3 h SI.

5.3.6) Other ABPs that could be involved in foci formation

In this study only four ABPs were investigated, two of which did not associate with the F-actin foci. It is highly likely that other proteins are involved in the formation of the foci. The punctate foci are very large F-actin structures (up to ~1 μm diameter) so some kind of actin cross-linking or bundling proteins must be involved in their formation. There is relatively little information known about ABPs in plants that are capable of producing supramolecular arrays from existing filaments (Kovar et al, 2000b). Fimbrin, the villin-like 135-ABP and 115-ABP from lily, the formin AtFim1 and the LIM protein NtWLIM have all been shown to have filament bundling capabilities in plants (reviewed in Higaki et al, 2007). We have seen that fimbrin does not seem to be involved in the punctate F-actin foci of SI so other proteins must be performing the role of cross-linking/bundling the F-actin. The villin-like proteins from lily pollen (*Lilium longiflorum*), 135-ABP and 115-ABP, have been identified and are able to bundle actin in a calcium/calmodulin-dependent manner (Yokota et al, 1998; Nakayasu et al, 1998). *A. thaliana* VILLIN1 (AtVLN1) also bundles actin filaments and has been shown to protect filaments against ADF-mediated depolymerisation (Huang et al, 2005). Therefore the localisation of villins should be investigated to ascertain if they are playing a role in the formation of the SI-induced F-actin foci. Actin nucleating proteins such as the Arp2/3 complex could be involved in the initiation of foci formation. Homologues of all of the Arp2/3 complex components have been identified in the *Arabidopsis* genome but, as yet, no information on cellular localisation of Arp2/3 is available in plants (Ren & Xiang, 2007).

Formins can also nucleate new actin filaments and in plants have been shown to move to the sides of the nucleated filaments where they nucleate another new filament (Michelot et al, 2006). In addition, formins are also capable of bundling actin filaments (Michelot et al, 2006) and have been shown to do so in pollen tubes (Cheung & Wu, 2004). As many formins have been found to be membrane-localised (Favory et al, 2004; Deeks et al, 2005) they may be good candidates for involvement in the SI foci formation as these seem to occur frequently at the cell membrane. Thus, formins deserve further investigation. Capping proteins are also likely to be involved as the dynamics of the actin foci during SI appear to be much reduced compared to other F-actin structures. Therefore, further characterisation of the ABPs involved in the SI-induced actin foci is required in the future.

In summary, we have shown that the punctate F-actin foci formed during SI have both ADF and CAP proteins heavily co-localising with them. This association of actin with the ABPs probably contributes to the increased stability of the foci. We have speculated on the role that these ABPs may be playing in the formation of the foci and how they could be linked to PCD. The involvement of other ABPs, such as villins and capping proteins, will also need to be investigated. Future work will need to concentrate on elucidating the function of the punctate F-actin foci and their associated ABPs, and also investigating whether mitochondria are contained within the foci as both ADF and CAP have been associated with mitochondria during apoptosis in mammalian cells (Chua et al, 2003; Wang et al, 2008). Currently, we have been unable to depolymerise the F-actin structures using LatB to analyse the effect of their loss on PCD. Further experiments will look at trying to prevent their formation to see if PCD is abolished. This might be achieved by using antisense oligonucleotides designed against the ABPs proposed to be involved in the formation of the foci. Antisense oligonucleotides could

also be used to determine whether CAP and ADF are involved in PCD signalling. This could be investigated by comparing the level of PCD occurring in pollen tubes down-regulated for these proteins against normal pollen tubes undergoing SI, using a caspase assay or a DNA fragmentation assay (TUNEL). Live-cell imaging would also be useful to assess the dynamics of the F-actin alterations that occur during SI.

CHAPTER 6

ANALYSIS OF THE SI-INDUCED F-ACTIN FOCI USING MASS- SPECTROMETRY

6.1) Introduction

The previous chapter attempted to characterise the large F-actin foci which are formed during the later stages of SI. The approach involved investigating the co-localisation, and hence probable involvement, of various ABPs with the F-actin foci. Although useful, this approach is somewhat limited as we are only able to test for ABPs and other proteins that we have antibodies or probes for and it is a time-consuming process. The method also relies on our ability to choose proteins that are potentially implicated in the process, so novel proteins or proteins not previously known to interact with F-actin would not be identified.

The work presented in this chapter comprises preliminary data using an alternative approach aimed at identifying proteins associated with the F-actin foci. The identification of these proteins could provide an insight into what components might be involved in the F-actin foci formation and what role they might play in SI signalling. **Figure 6.1** shows what is currently known about the F-actin foci and their associated proteins and indicates the factors that still need to be investigated.

We took the approach of isolating the F-actin foci from SI-induced pollen tubes and using mass spectrometry to identify components associated with the F-actin foci. F-actin from untreated pollen tubes was also examined so that we could make comparisons with components that were associated with the F-actin under normal conditions and those that were induced by SI-specific conditions.

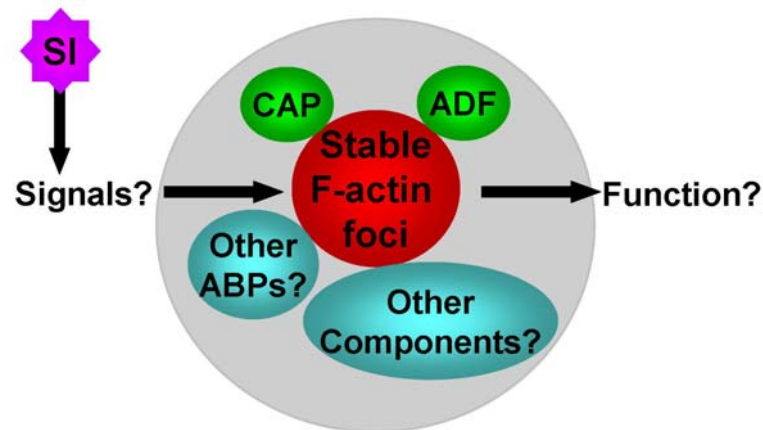


Figure 6.1. Investigating the components of the SI-induced F-actin foci.

We know that the SI-induced F-actin foci are stable structures and co-localise with ADF and CAP. Future work will concentrate on identifying other components associated with these structures, the signals involved in their formation and their possible function. An F-actin pull-down coupled with analysis of the associated proteins by mass spectrometry is one approach that has been used to study this.

Co-sedimentation assays are commonly used to identify proteins that interact with F-actin (for examples see: Maekawa & Sakai, 1987; Blobel et al, 1996; Srivastava & Barber, 2008; Dixon et al, 2008). Indeed, co-sedimentation assays have been employed to verify the interaction of various ABPs with F-actin in pollen (Allwood et al, 2002; Chen et al, 2002; Smertenko et al, 2001; Kovar et al, 2001b). However, this approach normally uses a recombinant protein of interest and investigates whether it binds to a pure sample of F-actin. In our case, during SI, we are interested in analysing F-actin structures that only form during a particular stage of the SI response and therefore we need to analyse cell extracts and enrich for these specific structures in order to identify interacting protein complexes.

Recently there has been an increase in the use of affinity purification of protein complexes directly from cell lysates. The components of these multi-protein complexes are then identified through mass spectrometry (reviewed in Gingras et al, 2007). This two step approach offers advantages over traditional protein-interaction methods such as yeast-2-hybrid because it can be performed in near physiological conditions in the relevant cell, allowing post translational modifications, that can influence complex formation, to be carried out. This affinity purification-mass spectrometry approach has been used in the budding yeast *Saccharomyces cerevisiae* to connect an estimated 60 % of the proteome (Krogan et al, 2006; Gavin et al, 2006; Gingras et al, 2007). The combination of affinity purification followed by analysis by mass spectrometry has also been employed several times in plant cells to identify proteins of interest. For example, Manzano et al (2008) used affinity purification of ubiquitinated proteins followed by mass spectrometry to identify a total of 200 putative ubiquitinated proteins in *Arabidopsis*. Davis et al (2007) also used this method to demonstrate that the *Arabidopsis* phosphatidylinositol phosphate kinase 1 (AtPIP1K1) binds to F-actin. An F-actin pull-down assay, using biotin-tagged phalloidin, has been used successfully by Yeung et al (1998) to identify tyrosine phosphorylated proteins that interacted with F-actin in macrophages. The use of phalloidin, which only binds to F-actin, should ensure that F-actin-containing structures are enriched for in pull-downs and analysed.

The data presented in this chapter represents preliminary attempts at analysing the SI-induced F-actin foci by a combination of an F-actin pull-down and mass spectrometry. There were unexpected problems associated with the detection of certain proteins by mass spectrometry, which are discussed later. There were also issues relating to the cost of the approach and the time limitation, both of which resulted in the absence of replication. Despite these limitations,

there was a noticeable difference between the proteins associated with the SI F-actin and those associated with the untreated sample. This has provided us with some interesting candidates for future study and demonstrates that this approach can be used to analyse events involving the F-actin during SI.

6.2) Results

6.2.1) Enrichment of F-actin using ultracentrifugation

In order to isolate the F-actin foci that form later in the SI response a purification protocol to enrich for F-actin needed to be developed. It was thought necessary to do a two-step enrichment of F-actin from pollen tube protein extracts. The first step involved an enrichment of F-actin using ultracentrifugation. Pollen tube proteins from both untreated and 3 h SI treatments were extracted in the presence of phalloidin to stabilise the F-actin during the extraction procedure. After the removal of pollen grains and cell wall material, the extracts were subjected to ultracentrifugation. Cano et al (1991) found that centrifuging polymorphonuclear leukocyte lysate samples at 80,000 rpm for 1 h did not significantly increase the amount of F-actin in the pellet compared to a 15 min spin. Therefore, the pollen extracts were spun at the maximum speed of 100,000 rpm for 15 min to pellet the majority of the F-actin present in the extract. The total protein (pre-spin), supernatant and pellet fractions were loaded onto SDS-PAGE and then blotted for the presence of actin and the ABPs that were investigated in **Chapter 5** (CAP, ADF, fimbrin and profilin).

Figure 6.2a shows that the ultracentrifugation enriched for F-actin. The amount of actin in the pellet fraction was considerably greater than in the total protein extract in both the untreated and SI samples. As the pellet fraction represented an enrichment of F-actin, the blots for the ABPs investigated which ABPs co-sedimented with the F-actin in the pellet. Co-sedimentation suggests interaction between the two proteins. The data presented in **Chapter 5** demonstrated that CAP, ADF and profilin mainly localised to the cytoplasm in untreated pollen tubes and fimbrin showed some co-localisation with the F-actin. During SI, CAP and

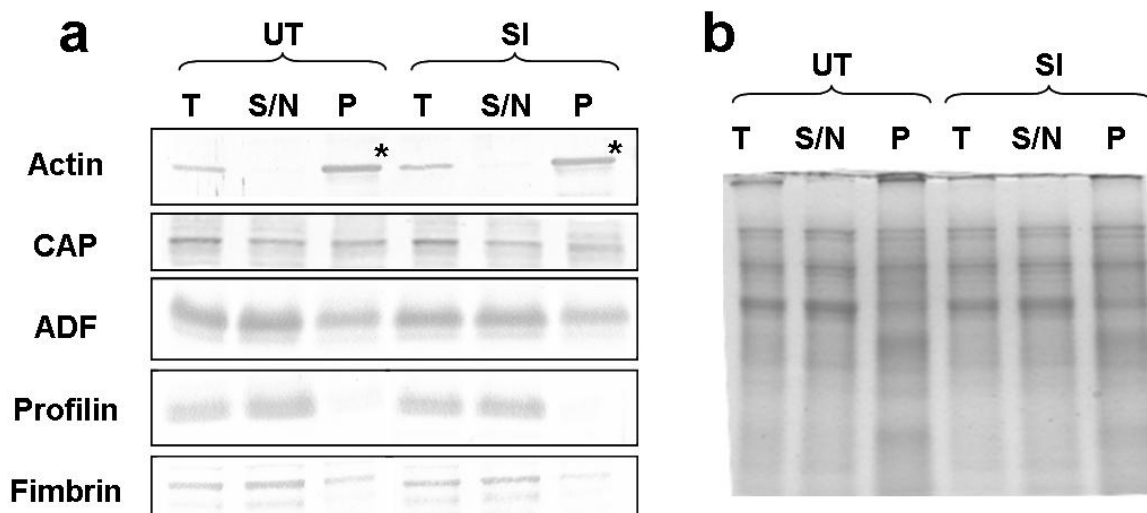


Figure 6.2. F-actin enrichment by ultracentrifugation.

UT = untreated extracts, SI = Self-incompatible extracts,
 T = total protein, S/N = supernatant, P = pellet, * = actin in pellet

(a) Western blot analysis of actin and ABPs. Proteins from each of the three fractions were separated by SDS-PAGE and blotted onto nitrocellulose membrane. The membranes were then probed with the antibodies detailed below. Detection was carried out with alkaline phosphatase.

Actin was enriched in the pellet of both UT and SI (anti-ZmAct, 1:2000).

CAP was present in both the supernatant and the pellet of UT and SI (anti-AtCAP1, 1:2000).

ADF was also present in the supernatant and pellet of UT and SI (anti-LIADF1, 1:2000).

Profilin was present in the supernatant but not in the pellet of both UT & SI (anti-ZmPRO5, 1:2000).

Fimbrin, most of the fimbrin was in the supernatant fraction but some was present in the pellet. There appeared to be a greater amount in the UT pellet compared to the SI pellet (anti-AtFim1, 1:2000).

(b) Coomassie blue stain shows there was equal loading of proteins.

ADF both co-localised with the F-actin foci, whereas profilin and fimbrin did not. Western blot analysis (**Fig. 6.2a**) revealed CAP and ADF to be present in both the supernatant and pellet fractions, indicating they were present in the cytoplasm as well as associated with the F-actin. Although the immunolocalisation of ADF and CAP in **Chapter 5** did not show any substantial co-localisation of the proteins with the F-actin, ADF at least has been localised to the F-actin in lily and tobacco pollen tubes. Thus, ADF, and probably CAP, are likely to interact with F-actin to some extent in poppy under normal growing conditions which accounts for their presence in the F-actin-enriched pellet in untreated samples. Profilin was only found in the supernatant, confirming its role as an actin monomer binding protein. Fimbrin was found predominantly in the supernatant, with higher levels detected in the pellet fraction of the untreated compared to the SI-induced sample, again confirming F-actin co-localisation data from **Chapter 5**.

F-actin can be visualised using phalloidin conjugated to rhodamine. To confirm the western blot analysis above, F-actin was visualised in samples of the total protein, supernatant and pellet fractions by labelling with rhodamine-phalloidin and examination by epifluorescence microscopy. **Figure 6.3** shows how F-actin enrichment was visualised in the pellet fraction compared to the supernatant and total protein fractions in both SI and untreated protein extracts.

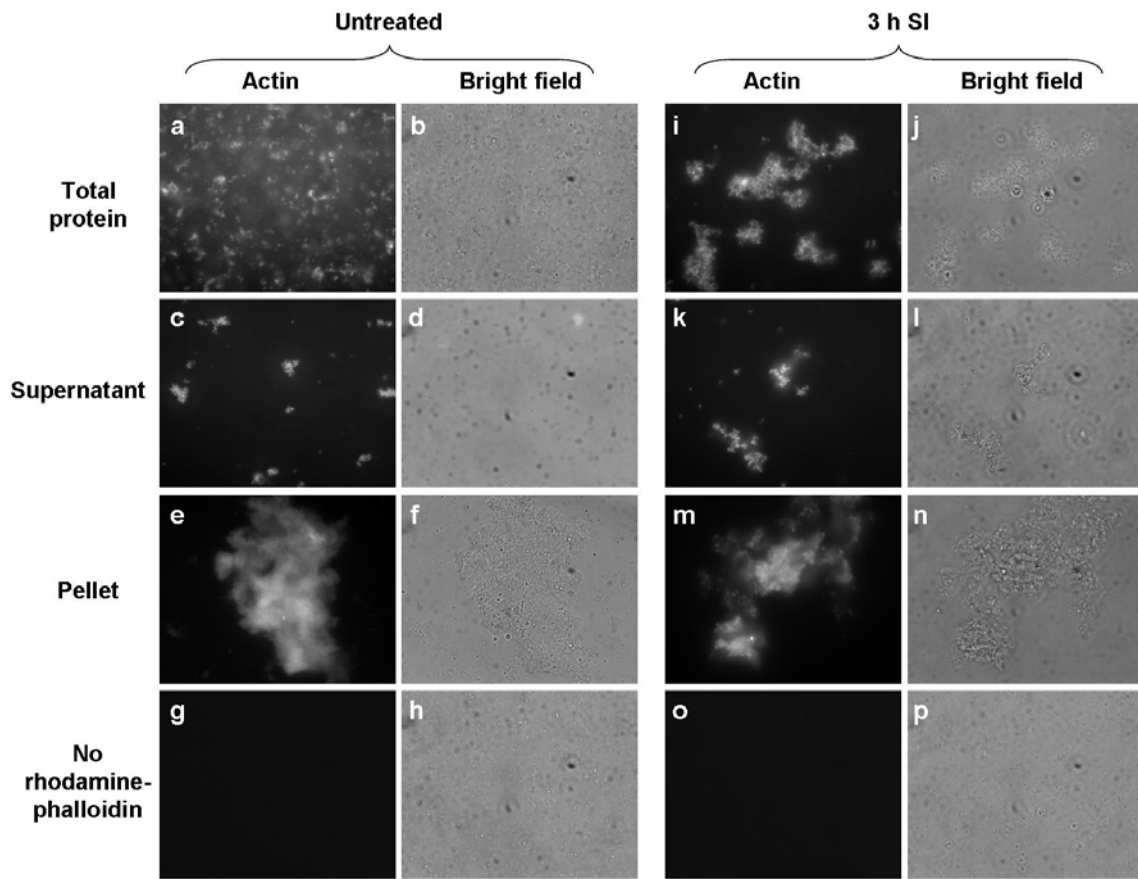


Figure 6.3. Visualisation of F-actin in the different fractions of the ultracentrifugation of pollen protein extracts.

Proteins were extracted from SI-induced or untreated pollen and subjected to F-actin enrichment by ultracentrifugation. The pellet fraction was re-suspended and a sample of each fraction was incubated with rhodamine-phalloidin and the F-actin visualised using epifluorescence microscopy. Bright field images of the same area were also taken.

(a, b) Substantial amounts of F-actin were visualised throughout the total protein extract of untreated pollen.

(c, d) After ultracentrifugation the amount of F-actin in the untreated supernatant was greatly reduced

(e, f) The untreated pellet fraction contained large aggregates of cellular material that contained F-actin.

(i, j) The amount of F-actin in the total protein extract of SI-induced pollen appeared less than in the untreated sample but more aggregated.

(k, l) The SI supernatant had reduced levels of F-actin compared to the total protein

(m, n) The SI pellet had large aggregates of cellular material that contained F-actin.

(g, h, o, p) The controls, which did not contain rhodamine-phalloidin, demonstrated that the cellular material did not auto-fluoresce.

The fluorescence images were all taken with a fixed exposure time of 400 ms.

6.2.2) Isolation of F-actin using a pull-down assay

The second step in the isolation of F-actin from pollen protein extracts was an F-actin pull-down from the pellet fraction of the ultracentrifugation. Phalloidin conjugated to biotin was added to the re-suspended pellet fraction. Following incubation, which allowed the phalloidin to bind the F-actin, the biotin-phalloidin was pulled out of the extract using Streptavidin MagneSphere Paramagnetic Particle (SA-PMPs; magnetite beads coated in streptavidin). Any unbound proteins were washed from the SA-PMPs and the resulting SA-PMPs, which were binding F-actin and its associated proteins, were boiled in sample buffer and subjected to SDS-PAGE. **Figure 6.4a** shows that although some of the actin in the pellet fraction did not bind to the SA-PMPs, there was still a substantial amount of actin that was pulled-out of the extract (arrow). The Coomassie blue staining of the gel (**Fig. 6.4b**) shows that in the bound fraction there were many different proteins, indicating that these proteins were potentially interacting with the F-actin.

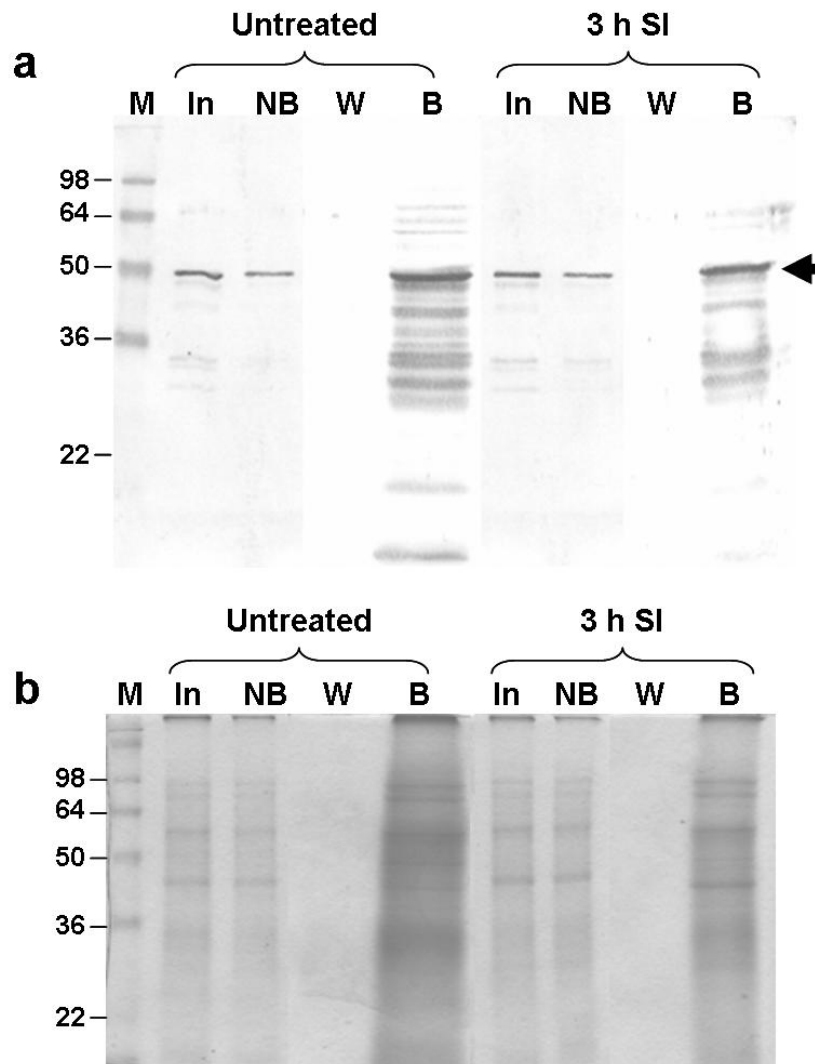


Figure 6.4. F-actin pull-down using SA-PMPs.

Proteins were extracted from SI-induced or untreated pollen and subjected to F-actin enrichment by ultracentrifugation. The pellet containing the F-actin was re-suspended, incubated with biotin-phalloidin and used in an F-actin pull-down assay using SA-PMPs.

(a) A western blot for actin (arrow). Both the untreated and SI samples had actin in the input (**In**). Some of the actin came off in the not-bound fraction (**NB**) but the washes (**W**) were actin-free. The SA-PMPs containing the bound F-actin (**B**) were boiled to release the F-actin and its associated proteins.

(b) Coomassie blue showing loading of the different fractions of the pull-down assay.

M = marker (kDa), the blot was probed with anti-ZmAct (1:2000) and detected using alkaline-phosphatase.

6.2.4) Analysis of F-actin interactors using mass spectrometry

Once the F-actin and its associated proteins had been isolated from the pollen tube protein extracts they were analysed by mass spectrometry. The Fourier Transform Ion Cyclotron Resonance Mass Spectrometry (FT-ICR-MS) is the highest performance mass spectrometry technique available. It is ideal for identifying species from a complex mixture because it has a high resolution that is able to distinguish between ions of a very similar mass (Pinto et al, 2002). As the F-actin appeared to be interacting with a wide range of proteins (**Fig. 6.4b**), this technique seemed to be the most appropriate. The University of Birmingham provides a service through the Proteomics Unit that analyses samples digested by trypsin by FT-ICR-MS. The resulting peptides were searched against an *Arabidopsis* protein database using a licensed version of the Mascot software (Matrix Science). The full list of protein hits for both the untreated and 3 h SI samples can be found in the **Appendix II**.

To get an overall idea of the types of proteins being identified by the mass spectrometer, the protein 'hits' for both the SI and untreated samples were categorised according to the general functions shown in **Figure 6.5**. The proportion of proteins involved in metabolism and energy production were comparable between SI and untreated samples. The untreated sample had three times as many of its proteins involved in protein synthesis compared to SI samples. Compared to the untreated control, the SI sample showed increased levels of heat shock and chaperone proteins (10 % versus 5 %), cytoskeleton proteins (13 % versus 7 %) and signal transduction proteins (12 % versus 8 %). Actin was identified in both samples (7 different peptides for untreated and 16 peptides for SI), indicating enough of the F-actin was isolated to be detected by FT-ICR-MS. However, surprisingly none of the ABPs, identified by western blot analysis as interacting with F-actin, were detected by mass spectrometry.

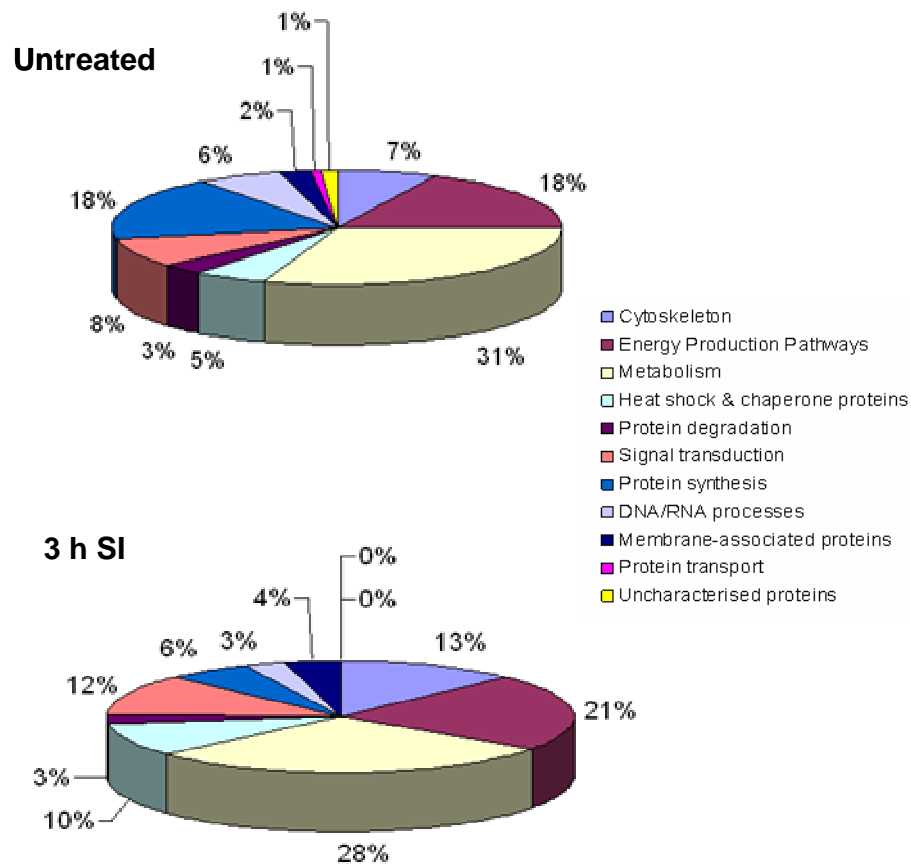


Figure 6.5. Distribution of the identified proteins into functional categories.

A graphical representation, for both the untreated and 3 h SI samples, of the percentage of the proteins identified by FT-ICR-MS that fall into each of the different functional categories. SI samples had a greater proportion of proteins in the cytoskeleton, signal transduction and heat shock and chaperone protein classes. Untreated samples had a much larger proportion of proteins associated with protein synthesis.

Of the proteins identified in the SI sample, 53 % were specific to SI, i.e. the protein identification number was not found in the untreated sample. However 56 % of these proteins had proteins of similar function in the GM sample, such as different sub-units of the same complex or different isoforms. Bearing in mind *P. rhoeas* genomic data is not currently available and this analysis has been carried out against *Arabidopsis* sequences we cannot be certain that these 'specific' hits are really unique to SI. For example, the most significant hit in the SI sample is an 'ATPase synthase subunit beta-2, mitochondrial' which is not found in the untreated sample. Nevertheless, the 'ATPase synthase subunit beta-1, mitochondrial' is found in the untreated sample and 5 peptides out of the 6 assigned to this protein are also found in the beta-2 subunit in the SI sample. Thus, we can be fairly confident that ATPases, for example, are present in both samples but we cannot really place much significance on the type of ATPase identified.

As the formation of the F-actin foci during SI appears to be an active process and the data presented in **Chapter 5** pointed towards a possible role for the foci in SI signalling cascades, the proteins identified that were involved in signalling were investigated more thoroughly. The SI sample exhibited an increase in proteins involved in signal transduction (shown in **Table 6.1**) and heat shock and chaperone proteins (shown in **Table 6.2**). The proteins that were specific to the SI sample are shown in red lettering. Notably, 14-3-3 proteins, Ras-like proteins, heat shock proteins and chaperonins appeared to be more abundant in the SI-induced samples.

Table 6.1. Proteins involved in signal transduction found associating with the F-actin in 3 h SI samples.

Protein ID	Protein Name	Score	No. of Peptides	Cellular localisation
14332_ARATH	14-3-3-like protein GF14 omega	146	6	
14333_ARATH	14-3-3-like protein GF14 psi	145	5	
14312_ARATH	14-3-3-like protein GF14 iota	99	4	
14311_ARATH	14-3-3-like protein GF14 omicron	99	6	
14310_ARATH	14-3-3-like protein GF14 epsilon	83	4	
RAA1C_ARATH	Ras-related protein RABA1c	68	5	TGN-PGV
RAA2A_ARATH	Ras-related protein RABA2a	68	4	TGN-PGV
ARA3_ARATH	Ras-related protein ARA-3	55	3	Polarised secretion
RABD1_ARATH	Ras-related protein RABD1	52	4	ER-Golgi
RBH1B_ARATH	Ras-related protein RBH1B	52	2	Golgi –ER retrograde transport
ARA4_ARATH	Ras-related protein ARA-4	50	2	TGN-PGV
RAA1A_ARATH	Ras-related protein RABA1a	50	3	TGN-PGV

Protein ID: the protein identification number in the UniProt database.

Score: the score retrieved by the MASCOT programme, the higher the score the more confidence we have in the protein hit. As the number of protein hits reported was set to ‘AUTO’ only significant hits were reported. Thus, all protein hits in this analysis were significant ($p < 0.05$).

No. of peptides: the number of different peptides identified by the MS analysis.

Proteins written in red were only found in the SI sample. Proteins written in black were found in both the untreated and SI samples.

The cellular localisation of the Rab-proteins is according to Vernoud et al (2003).

TGN-PGV = trans Golgi network – post Golgi vesicles

Table 6.2. Heat shock and chaperone proteins found associating with the F-actin in 3 h SI samples.

Protein ID	Protein Name	Score	No. of Peptides
HSP73_ARATH	Heat shock cognate 70 kDa protein 3	354	9
HSP71_ARATH	Heat shock cognate 70 kDa protein 1	284	12
HSP72_ARATH	Heat shock cognate 70 kDa protein 2	212	9
HSP83_ARATH	Heat shock protein 81-3	74	6
CH60B_ARATH	Chaperonin CPN60-like 1, mitochondrial	67	4
CH60A_ARATH	Chaperonin CPN60, mitochondrial	67	3
BIP1_ARATH	Luminal-binding protein 1	66	4
BIP2_ARATH	Luminal-binding protein 2	66	4
ENPL_ARATH	Endoplasmic homolog	52	12
TCPE_ARATH	T-complex protein 1 subunit epsilon	28	3

Annotations are the same as in **Table 6.1**. Proteins written in red were only found in the SI sample. Proteins written in black were found in both the untreated and SI samples.

The 14-3-3 family of proteins are highly conserved throughout the eukaryotic kingdom and act as signalling regulators. They have been shown to be involved in many cellular processes such as signal transduction, apoptosis and cell-cycle control (DeLille et al, 2001; van Hemert et al, 2001; Ferl et al, 2002). The SI sample contained 5 different 14-3-3 protein hits with a total of 16 different peptides. Although the untreated also contained some 14-3-3s, the number of protein hits and different peptides identified was much reduced (3 proteins and 9 different peptides), suggesting that these proteins were less abundant in the untreated sample. This is supported by the emPAI (exponentially modified protein abundance index) in the Mascot search. The emPAI gives an estimate of the relative quantitation of the proteins in a mixture (Ishihama et al, 2005). The emPAI scores for the SI 14-3-3s were higher than the untreated, indicating these proteins were relatively more abundant in the SI sample. This could indicate that 14-3-3s are involved in the SI-induced signalling cascades.

The Ras-like proteins identified all belong to the Rab family of small GTPases found in plants. Small GTPases act as molecular switches in cells, cycling between an active, GTP-bound state and an inactive, GDP-bound state. Rab-GTPases function in endocytosis and intracellular membrane trafficking (reviewed in Zerial & McBride, 2001). The mass spectrometry analysis identified Rab-proteins in both the SI and untreated samples and the proteins found in both are shown in black in **Table 6.1**. In the SI sample, 7 different Rab-proteins were identified, with 19 different peptides, compared to only three proteins and 6 different peptides in the untreated sample. This could indicate that although the Rab-proteins are associated with F-actin in the untreated sample, they are more prevalent in the SI. The emPAI numbers for the Rab-proteins in the SI sample were either equal to, or double those of

the untreated sample, indicating higher abundance in SI-induced pollen. Endocytosis and membrane trafficking is constantly occurring in growing pollen tubes so it is a little surprising that the SI sample exhibited increased numbers of Rab-GTPases compared to the untreated sample.

The second class of proteins that exhibited a higher frequency in the SI compared to untreated sample was the heat shock and chaperone proteins. Heat shock proteins are a family of proteins that are up regulated in response to stress and act as intra-cellular chaperones for other proteins. SI can be considered as a form of stress as it results in PCD of the incompatible pollen, so heat-shock proteins could play a role in SI. The heat shock protein that was unique to the SI sample was heat shock protein 81-3 (HSP81-3). This protein is a member of HSP90 family of heat shock proteins (Milioni & Hatzopoulos, 1997). The other proteins that were unique to the SI sample were Chaperonin CPN60 (mitochondrial) and T-complex protein 1 (TCP-1) subunit epsilon. CPN60 is a member of the type I chaperonin proteins. Typically these proteins function as a pair of stacked rings, made up of 7 subunits (Hemmingsen et al, 1988; Saibil, 2000). Unfolded proteins enter into the central cavity of the complex, which provides an isolated environment for protein folding. The TCP-1 is part of the group II chaperonin complex called CCT (chaperonin containing TCP-1) or TRiC (Hill & Hemmingsen, 2001) and shares significant homology with the chaperonin CNP60 (Hemmingsen, 1992).

6.3) Discussion

Here, we have developed a method to analyse the composition of the F-actin foci formed during the later stages of the SI response of poppy. These preliminary results indicate that ultracentrifugation enriches for F-actin and samples can be further purified through an F-actin pull-down. Mass spectrometry can be used to identify proteins that are associated with the F-actin foci. Moreover, this approach identified differences between the SI and untreated samples.

6.3.1) Identification of F-actin and its interacting proteins by FT-ICR-MS

Although actin itself was identified by mass spectrometry from our F-actin pull-down samples, not one ABP was identified as a significant hit. This is somewhat surprising as at least two ABPs (CAP and ADF) have been identified in this current work as interacting with F-actin and were shown to be present in the pellet fraction that was used for the pull-down assay. Also, many other studies have demonstrated that ABPs associate with F-actin under normal physiological conditions (reviewed in Dos Remedios et al, 2003), so we would expect at least some of these proteins to be identified by mass spectrometry.

The reason why such proteins are not being identified could be due to several factors: (1) the protein levels in the sample were not high enough for detection; (2) there was too much protein in the sample for the trypsin digestion and separation of peptides to be fully successful; or (3) the proteins are not adequately conserved between *P. rhoeas* and *Arabidopsis* so the peptides produced by the trypsin digestion are not assigned to the correct proteins. As both ADF and CAP could be clearly visualised using western blot analysis, there

should be sufficient protein in the sample to be detected by FT-ICR-MS. From the Coomassie blue staining of the bound fraction of the pull-down assay we could see that there were many different proteins present. As the trypsin digestion was carried out in the gel, it is thought that there may not have been sufficient cleavage of the proteins to produce the peptides necessary for protein identification. This problem is probably not helped by the fact that we are searching against an *Arabidopsis* database and, although many proteins are highly conserved between *P. rhoeas* and *Arabidopsis*, any amino acid sequence difference would mean that the peptides are not assigned to the correct protein. **Table 6.3** illustrates an example of the amino acid sequence similarity and identity of an ABP (CAP1) from different species. *Oryza sativa* and *Arabidopsis* share the highest homology. **Figure 6.6** shows the amino acid sequence alignment of the *Oryza sativa* and *Arabidopsis* CAP1 proteins with the trypsin cleavage sites highlighted in yellow (arginine) and green (lysine). Only one of the peptides produced from a trypsin digest is conserved between the two plant species (boxed in red). This illustrates how, even though the two protein sequences show high levels of identity, any amino acid change can affect the resulting trypsin digestion peptide, altering the mass and resulting in the peptide not being recognised as part of its mother protein when compared against the *Arabidopsis* sequence database. Therefore, poppy ABPs may not be conserved well enough with the *Arabidopsis* ABPs to be recognised as the same protein after the trypsin digestion. Because we are unable to identify ABPs, which we are fairly certain are associated with the F-actin, other F-actin interacting proteins that we are not aware of are also likely to be missed from our investigation. Nevertheless, this approach has still revealed differences between the SI and untreated samples, and has provided some interesting candidates for further investigation.

Table 6.3. Comparison of the amino acid sequence of AtCAP1 to CAP1 proteins from different species

Organism	% Identity	% Similarity
<i>Dictyostelium discoideum</i>	38.2%	57.4%
<i>Saccharomyces cerevisiae</i>	28.7%	47.7%
<i>Xenopus laevis</i>	35.7%	52.9%
<i>Oryza sativa</i> (japonica cultivar-group)	59.5%	75.7%
<i>Homo sapiens</i>	36.5%	54.5%
<i>Mus musculus</i>	36.7%	54.2%

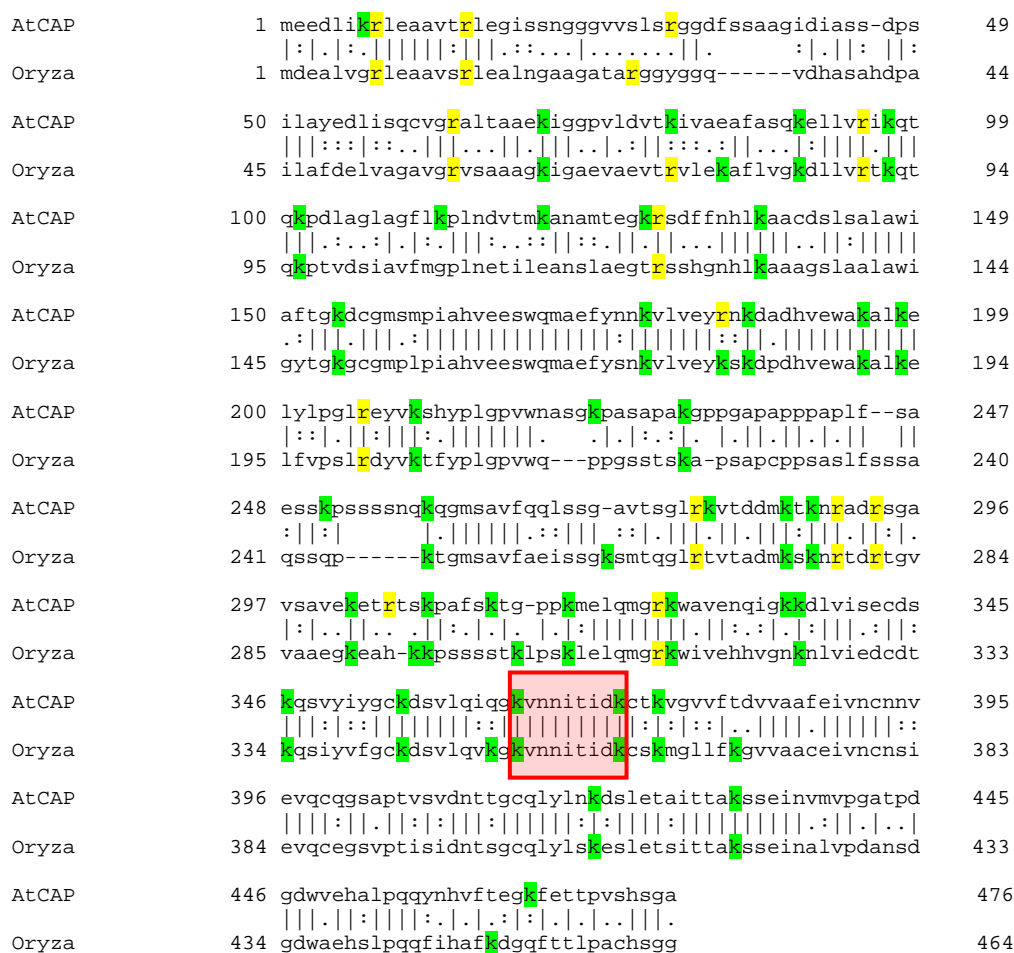


Figure 6.6. Alignment of AtCAP1 and OsCAP1 protein sequences

An alignment of the amino acid sequences of CAP1 from *Arabidopsis* and *Oryza sativa*. Trypsin cleaves peptides on the C-terminal side of lysine (green highlight) and arginine (yellow) residues expect when a proline is present at the C-terminal side. There is only one conserved tryptic digest peptide between the two proteins (red box).

6.3.2) The 14-3-3 signal proteins may interact with F-actin during SI

The FT-ICR-MS identified a number of 14-3-3 isoforms in both the SI and untreated samples. The 14-3-3s are small (25-35 kDa) proteins that are present in all eukaryotes. These proteins form homo- or hetero-dimers and act in signalling pathways by binding to a phosphorylated target protein resulting in a change to the target proteins structure that regulates its activity (Delille et al, 2001). Although the exact function of 14-3-3s is unknown, they have been shown to play a role in various cellular processes such as cytoskeleton reorganisation, stress response and apoptosis (van Hemert et al, 2001; Ferl et al, 2002). The SI response of poppy is a stress response that involves cytoskeletal rearrangements and results in PCD (Bosch et al, 2008), so the 14-3-3 proteins could be good candidates, not previously identified, that could be involved in SI signalling.

Plant 14-3-3s have been shown to require the binding of a divalent cation to an EF hand-like motif in the C-terminal for them to become active (Lu et al, 1994). In SI there is a rapid increase in the cytosolic concentration of calcium (Franklin-Tong et al, 1993; 1995; 1997) which could activate the 14-3-3s during SI. It has been suggested that 14-3-3s may play a role in receptor localisation and/or regulation of signalling (van Hemert et al, 2001). For example, in humans, stimulation of platelets leads to the translocation of 14-3-3 zeta, PI3-kinase and the platelet receptor GPIb-IX to the actin cytoskeleton. It has been suggested that 14-3-3 zeta may be involved in translocating the receptor and PI3-kinase signalling proteins to the cytoskeleton, thereby regulating the formation of a signalling complex in a specific location (Munday et al, 2000). As the 14-3-3s identified here were isolated from an F-actin pull-down it is possible that the 14-3-3s are interacting with the F-actin and could be mediating protein-

protein interactions or subcellular localisation of other signalling proteins (not yet identified) onto the F-actin.

Although 14-3-3s have been linked to the regulation of apoptosis in animal cells, they normally act in an inhibitory manner (Xing et al, 2000) so may not be involved in the PCD that is observed in SI. For example, it has been demonstrated that 14-3-3 proteins can bind to BAD, a pro-apoptotic member of the Bcl₂ family of proteins. This 14-3-3 binding inhibits BAD activity, resulting in inhibition of apoptosis (Zha et al, 1996). However, it is known that there is no Bcl₂ gene in plants.

Further work will need to investigate whether 14-3-3s are consistently identified as interacting with F-actin during the SI response. If so, further studies will need to explore the proteins that are being regulated by the 14-3-3s in order to try and elucidate what role they may be playing in SI.

6.3.3) Rab-GTPases were identified more frequently in SI samples

The SI-induced sample had seven different Rab-proteins identified as potential F-actin interactors, compared to only three in the untreated sample. This large increase in the number of Rab-proteins in the SI-induced sample suggests that they may be playing a role in the SI response. Rab-GTPases have emerged as central regulators of intracellular trafficking. They are the largest family of the GTP-binding protein superfamily, with 57 being identified in *Arabidopsis* (Vernoud et al, 2003). In their inactive GDP-bound state Rab-proteins are located in the cytoplasm of the cell and active GTP-bound Rab-proteins are membrane associated. Most Rab-GTPases are involved in the targeting, docking and fusion of vesicles to the

acceptor membrane but some regulate the budding process involved in vesicle formation (Ma, 2007). The Rab-GTPases are known to be important for pollen tube growth with over-expression experiments in tobacco resulting in inhibition of pollen tube growth and loss of directionality (de Graaf et al, 2005; Cheung et al, 2002). In *Arabidopsis*, loss of the pollen-expressed RABA4D led to a disruption of polar growth and altered cell wall patterning (Szumlanski & Nielsen, 2009). Rab-GTPases also play a role in intracellular signalling with membrane trafficking as many receptor-ligand pairs continue to emit signals throughout the endocytic pathway (Miaczynska et al, 2004).

The identification of a large number of Rab proteins from an F-actin pull-down is a little surprising as the class of small GTPases that are known to act as regulators of the actin cytoskeleton are the Rop (**R**ho **o**f **p**lants) proteins (Xu & Scheres, 2005; Nibau et al, 2006). Rops have been shown to be active in pollen tubes where they regulate the dynamic F-actin in the tip of the pollen tube (Fu et al, 2001; Cheung et al, 2003; Kost, 2008). However, no Rops were identified by the FT-ICR-MS in either the SI or untreated sample. In SI, the F-actin foci are evenly distributed throughout the length of pollen tube, with many of the larger foci showing a preference for the cell cortex. It is possible that the F-actin foci are engulfed by, or associated with, the endo-membrane system which acts to distribute the F-actin throughout the pollen tube. This could explain why Rab-proteins are so prevalent in the SI sample. Rab-proteins have also been implicated in vesicle transport along cytoskeletal filaments (Zerial & McBride, 2001). As most of the intracellular transport in pollen tubes occurs along the F-actin (Cai & Cresti, 2009), this could explain why some Rabs are identified as potential F-actin interactors in untreated pollen tubes. Also, as there is active endocytosis occurring during normal pollen tube growth (Parton et al, 2001, Moscatelli et al, 2007), it might be expected

that there would be more Rabs identified in the untreated sample compared to the SI sample. As activated Rabs are associated with membranes it is possible that membranous material was pelleted with the F-actin in the ultracentrifugation step, then co-purified with the F-actin and subsequently identified by FT-ICR-MS, when they were not really interacting with the F-actin foci. Further work needs to clarify the association of Rab-proteins with the F-actin in SI-induced pollen tubes. A co-localisation approach, similar to that described in **Chapter 5**, could be carried out using antibodies raised against Rab-proteins to see if these proteins localised to the F-actin foci during SI. So, as it stands, it is not clear what the relationship, if any, Rabs have with the SI response.

6.3.4) Heat shock proteins may interact with F-actin during SI

In the SI sample six heat shock and chaperone proteins were identified that were not present in the untreated sample, indicating that these may play a role in the SI response. Many heat shock proteins are up-regulated in response to stress; some act as molecular chaperones to prevent denaturation of proteins and others dissociate protein aggregates, refolding monomer from these aggregates or targeting them for proteolytic degradation (Liang & MacRae, 1997). SI is a form of stress, so it is perhaps not surprising that heat shock proteins are more prevalent in the SI sample. Many of the heat shock proteins identified here in pollen have previously been linked to actin in other cell types. For example, the TCP-1 complex is involved in correctly folding both actin and tubulin under normal cellular conditions (Liang & MacRae, 1997). It may not, therefore, be playing a role in the SI response, despite being identified in the SI sample. Other, potentially more interesting hits were HSP83.1 and HSP70, which will be discussed further.

HSP83.1 falls into the HSP90 group of heat shock proteins. In *Arabidopsis*, the expression of *hsp90* genes was very low at control temperatures but was strongly induced by heat shock and arsenite stress (Miloni & Hatzopoulos, 1997) so could potentially be up-regulated in response to SI. The mammalian HSP90 and HSP100 have been shown to be actin binding proteins that act by cross-linking branched actin filaments (Koyasu et al, 1986; Park et al, 2007). This property of HSP90 is interesting for our SI context, as the F-actin foci formed during SI appear to be high-order structures that would require proteins to cross-link the filaments to maintain their structure. As fimbrin, an F-actin cross-linker, has been shown to be absent from the F-actin foci in SI (see **Chapter 5**), HSP90 (HSP83.1) could potentially be involved in the formation of the foci by cross-linking the filaments. However, mammalian HSP90 has been shown to be regulated by calmodulin in a calcium-dependent manner - when HSP90 is complexed with calcium-calmodulin it loses its ability to bind to F-actin (Nishida et al, 1986). Although SI involves a transient increase in cytosolic calcium levels at the beginning of the response (Franklin-Tong et al, 1993; 1997), the F-actin foci isolated here were from pollen that had been undergoing SI for 3 h. Therefore, the initial increase in calcium concentration may not have any bearing on the F-actin binding activity of HSP90 at 3 h SI.

HSP70 is also upregulated in response to stress and has been shown to be induced early after adenovirus infection. A study by Macejak & Luftig (1991) on human cell lines (HEp-2) demonstrated that infection of these cells with adenovirus resulted in stabilisation of the actin filaments, making them resistant to depolymerisation by latrunculin. The authors proposed that HSP70 was responsible for this stabilisation of the F-actin. Their study also showed that heat shock of the HEp-2 and HeLa cells resulted in rearrangement of F-actin around the nucleus, which was also resistant to latrunculin-induced depolymerisation, and *in vitro* HSP70

could stimulate actin polymerisation from monomers. Our studies have shown that the SI-induced F-actin foci are resistant to concentrations of latrunculin that would normally depolymerise most of the F-actin in the cell (see **Chapter 5**). HSP70 could therefore be implicated in playing a role in the formation of the F-actin foci and could also be responsible for their increased stability.

Although not identified here, small heat shock proteins (sHSPs), such as HSP27, have been shown to interact with F-actin. Hsp27 acts as an F-actin capping protein, preventing polymerisation (Miron et al, 1988; 1991) when it is not phosphorylated. However, when phosphorylated (in response to stress), HSP27 it has been proposed to bind to the sides of F-actin to protect it from actin severing proteins (Mounier & Arrigo, 2002). This type of reaction could possibly be occurring in SI. Further work needs to be carried out into the involvement of the HSPs in the SI response. It will be interesting to see if HSPs, and which ones, are consistently identified as interacting with the F-actin in SI by replication of the experiment. If they are consistently detected then future work will need to concentrate on deciphering their role in the SI response.

Thus, these studies have opened up possible new avenues of research. Future work can investigate the possible involvement of the 14-3-3s in the SI signalling network and the contribution of the HSPs to the stability of F-actin foci.

6.3.5) Improvements to the technique and future studies

Although the resolution of the FT-ICR-MS is said to be high enough to analyse complex mixtures, and therefore negates the need for 2-dimensional gel electrophoresis (Pinto et al,

2002), in our case this has not been very successful as many proteins that were known/expected to be in the sample were not identified. Thus, a 2D-gel approach of the purified F-actin foci may be necessary to provide further purification of the components of the complexes we are interested in. A simple improvement to the procedure tested here is to send less protein to be analysed by the mass spectrometer to try and improve the trypsin digest step and provide better resolution of the proteins in the mixture. Other approaches for isolating F-actin containing complexes also need to be investigated. The use of non-denaturing, native protein gels could be employed after the ultracentrifugation step to try and isolate complexes containing actin which could then be analysed by FT-ICR-MS. This technique was attempted once, but due to time constraints could not be fully investigated, and therefore forms the basis for future work in this area.

The preliminary results presented here show that many of the proteins identified through the mass spectrometry analysis were present in both the untreated and 3 h SI samples. Whilst this is perhaps not surprising, as many of the components would interact with F-actin in the pollen tube under normal growing conditions, it makes it difficult to distinguish between components that are important during SI and those that are not. However, it is likely that it is the relative concentrations of the proteins binding to the F-actin during SI that is important. The post-translational modifications may also play a role, such as the phosphorylation state of the protein. The FT-ICR-MS should preserve post-translational modification and this should be investigated in further studies. A new technique of quantitative proteomics called iTRAQ (isobaric tag for relative and absolute quantitation), which chemically labels the N-terminus of the peptides with tags of different masses for each sample (Zieske, 2006), could also be employed to investigate the relative amounts of the proteins in the untreated versus 3h SI

sample. Using this method, up to 4 different samples can be measured in one single experiment, making it suitable for analysing F-actin interactors at different time points throughout the SI response. Such quantitative proteomic approaches might prove useful for future studies.

This chapter has identified several classes of proteins that are potentially interacting with the F-actin foci during SI. The pull-down, coupled with mass spectrometry, has identified significantly different subsets of proteins in the SI compared to the untreated control. Furthermore, these proteins are different to those identified by mass spectrometry in previous subcellular fractionation experiments on SI-induced pollen, such as proteins with DEVDase activity (Bosch & Franklin-Tong, unpublished data) or phosphorylated proteins (de Graaf & Franklin-Tong, unpublished data). This suggests that the proteins identified by mass spectrometry do really interact with F-actin and we are not just pulling out random proteins. One point to consider is that a lot of the protein hits identified by FT-ICR-MS were associated with mitochondria (15 in SI and 10 in untreated). This could indicate that the mitochondria are interacting with the F-actin. This is likely to be occurring in untreated pollen, as mitochondria are transported along the actin filaments. In animal cells, there have been reports that actin and ABPs interact with the mitochondria during apoptosis (Chua et al, 2003; Wang et al, 2008). Therefore, an increase in mitochondrial-associated proteins in the SI sample could hint at an actin-mitochondria interaction during SI, but this still needs to be tested. It could also mean that these mitochondrial proteins are only present in the sample because they are associated with the mitochondria and not because they themselves are interacting with the F-actin or playing a role in SI. The mitochondria are also likely to have

been pelleted along with the F-actin in the ultracentrifugation step, which could explain why such a large proportion of the protein hits are associated with the mitochondria.

In conclusion, although the technique needs some improvement and the results need to be verified by further replication, F-actin pull-down coupled with mass spectrometry appears to be a promising avenue for future studies into the F-actin foci.

CHAPTER 7

GENERAL DISCUSSION

The results presented in this thesis cover a broad range of factors involved in the SI response of *Papaver rhoeas*, from the components involved in the initial recognition of ‘self’ through to several cytoskeleton-related downstream events that are triggered by this recognition.

7.1) Investigating the interaction between PrpS and S-proteins

Chapter 3 investigated the localisation of the male and female *S*-determinants, whose interaction in an incompatible reaction triggers many downstream events. I have shown that PrpS (the male *S*-determinant) localises to the pollen tube membrane, as predicted by its transmembrane domains and hypothesised role as a novel receptor. The *S*-proteins (female *S*-determinant) bind to both compatible and incompatible pollen tubes but clearly only trigger SI in the incompatible pollen tubes. Wheeler et al (2009) demonstrated that the predicted 35 amino acid extracellular loop of PrpS is functionally involved in mediating the SI response using *PrpS* antisense oligonucleotides. More recent work, using slot blot analysis, has further demonstrated *S*-specificity: *S*₁-proteins only bind to peptides designed against the 35 aa extracellular domain of PrpS₁ and not the extracellular domain of PrpS₈ (Vatovec, unpublished data). In the future, other techniques will need to be employed to further investigate the interaction between PrpS and *S*-proteins to answer questions such as:

- Can PrpS be visualised at the cell membrane in living cells?
- Do PrpS and *S*-proteins interact directly and if so, which domains are important for this interaction?
- Does PrpS form a multimeric structure?
- Are the PrpS and the *S*-proteins endocytosed into the pollen tube?

Techniques such as fluorescence resonance energy transfer (FRET) and bimolecular fluorescence complementation (BiFC) are gaining popularity in plant sciences where they can be used to visualise protein-protein interactions in living cells and thus also give information on the cellular localisation of the interaction (reviewed in Bhat et al, 2006 and references therein). These approaches require the proteins of interest (PrpS and S-proteins) to be tagged with fluorophores. The poppy pollen tube would need to be transformed with the tagged PrpS protein using particle bombardment. Alternatively, *Arabidopsis* could be stably transformed with the construct and pollen from the transformant grown *in vitro*. The fluorophore-tagged S-proteins could then be added as normal to pollen tubes in the *in vitro* bioassay. Protein-protein interaction would result in a fluorescent signal (usually YFP) becoming visible at the site of interaction. Site-directed mutagenesis of PrpS and S-proteins could then be used to determine which amino acids are important for the interaction and S-specificity.

The current SI model predicts a receptor-ligand interaction between the male and female S-determinants, with the S-proteins acting as the ligand. PrpS is a small protein, only 20 kDa, so it seems likely that it could multimerise into a larger complex or form a pore in the membrane (Tierney & Stowell, 1998; Vig et al, 2006) that could act as an ion channel involved in the SI-induced calcium influx. Indeed, Hadjiosif (2008) found two splice variants of PrpS, known as PrpSa and PrpSb, which differ at the C-terminus and are both expressed at the protein level. FRET has been used to analyse acetylcholine receptor assembly and subunit stoichiometry (Drenan et al, 2008). This could be applied to PrpS by labelling the two splice variants with different fluorophores (CFP and YFP) and seeing if there is interaction between them using FRET. If there was FRET, this would suggest dimerisation at the very least.

Another microscopy technique that could potentially be applied to visualise PrpS in live cells is **Total Internal Reflection Fluorescence Microscopy (TIR-FM)**. TIRF illumination selectively excites fluorescently tagged proteins/receptors at, or very close to, the cell membrane, typically within a region <100 nm thick. TIR-FM therefore generates a much higher signal-to-noise ratio compared to other epifluorescence techniques, allowing single molecules to be visualised (Beaumont, 2003; Schneckenburger, 2005). This technique could be applied to study the localisation and distribution of PrpS along the pollen tube membrane.

TIR-FM, in conjunction with fluorescence correlation spectroscopy (TIR-FCS) has been used to investigate receptor-ligand kinetics in animal cells (Lieto et al, 2003) so could be applied to studying the kinetics of PrpS-S-protein interaction. TIR-FM can also be used to study endo- and exocytosis of proteins (Beaumont, 2003; Schneckenburger, 2005). This could be useful for studying PrpS and S-proteins because work by Robatzek et al (2006) on the pattern recognition receptor FLS2 in *Arabidopsis* has shown that this receptor is internalised by endocytosis upon interaction with its ligand partner flg22. They propose it is possible that the activated receptor can signal from intracellular compartments through interaction with MAPK cascades. There is also considerable evidence that the mammalian receptor EGFR can continue to participate in signalling pathways whilst it is in endosome compartments (reviewed by Haugh, 2002). It is possible that PrpS is also endocytosed after interaction with the S-proteins. TIR-FM has been used successfully in pollen tubes to study secretory vesicles (Wang et al, 2006) so future work could investigate PrpS dynamics using TIR-FM.

7.2) Further investigations into the MT cytoskeleton during SI

In **Chapter 4** I described studies that showed for the first time that the MT cytoskeleton is a target for SI signals, as it rapidly depolymerises. I demonstrated one-way cross-talk from the actin cytoskeleton to the MT cytoskeleton, with the MT cytoskeleton requiring an intact F-actin network to maintain its integrity. I also showed that the SI-induced MT depolymerisation somehow feeds into the PCD signalling pathway (Poulter et al, 2008). An extensive discussion in **Chapter 4** examined the possible role of the MT cytoskeleton in SI, how MTs respond to external stimuli in other systems and the relationship between the MT and actin cytoskeletons, so this aspect will not be further discussed here. Instead, I will concentrate on potential future studies to examine the role of the MT cytoskeletal changes in the SI response.

One important question is what is the exact timing of the SI-induced cytoskeletal alterations? The data in Poulter et al (2008) demonstrated that MTs require intact F-actin to maintain their organisation, suggesting that the MT depolymerisation seen in SI is due to the F-actin depolymerisation. However, both these cytoskeletal alterations occur so rapidly that it is very difficult to ascertain the actual sequence of events using fixation and immunolocalisation. It also makes the investigation of MAPs potentially involved in the SI-induced MT depolymerisation, such as katanin, very difficult as the MT cytoskeleton is depolymerised one min after SI. Therefore, co-immunolocalisation studies of MAPs with MTs during SI, similar to those carried out for the ABPs with the F-actin foci, would not be very useful as it would be difficult to obtain fixed samples within one minute of SI induction. Thus, live-cell imaging using green fluorescent protein (GFP) fusions of cytoskeleton-associated proteins would provide useful tools to analyse the alterations that occur in the cytoskeleton during SI.

In plant cells, GFP-fusions to the actin binding domains (ABD) of the mouse-talin (GFP-mTn) and *Arabidopsis thaliana* fimbrin1 (GFP-ABD2) are the most widely used probes to study F-actin dynamics (Kost et al, 1998; Ketelaar et al, 2004b; Sheahan et al, 2004; Wang et al, 2004b; Sano et al, 2005). The MT cytoskeleton has also been studied using GFP fusions to proteins such as *Arabidopsis* microtubule end-binding protein 1a (AtEB1a-GFP) or *Arabidopsis* alpha-tubulin 6 (GFP-TUA6) (Hasezawa et al, 2000; Chan et al, 2003; 2007; Timmers et al, 2007; Brandner et al, 2008; Cheung et al, 2008). Such GFP- and GFP-derivative fusions could be employed in the future to study the timing, dynamics and nature of the relationship between the two cytoskeletons during SI and could be especially important to identify the very early SI events.

The only MAPs identified in plants with MT depolymerising ability are katanin (Stoppin-Mellet et al, 2002) and MAP18 (Wang et al, 2007). Therefore they represent good candidates to be potentially involved in the SI-induced MT depolymerisation. As mentioned above, immunolocalisation of katanin/MAP18 during SI would probably be futile as the MTs are depolymerised so quickly. Therefore, another approach to investigate their involvement needs to be considered. Antisense oligonucleotides have previously been used successfully in poppy to demonstrate the important roles of PrpS (Wheeler et al, 2009) and Pr-p26 (de Graaf et al, 2006) in the SI response. A similar approach could be used to 'knock-down' katanin and/or the MAP18 protein levels during SI to see if MT depolymerisation was prevented, thus implicating them in that process.

A prominent component of the SI response that was not studied in relation to the SI-induced MT cytoskeleton alterations was calcium. MTs are known to be sensitive to high levels of

calcium (Weisenburg, 1972). There has also been a report that there are calcium-permeable channels in *Arabidopsis* pollen tubes that are regulated by actin, such that F-actin depolymerisation causes an increase in cytoplasmic calcium concentrations (Wang et al, 2004a). If this is the case in poppy pollen tubes, then the MT depolymerisation seen as a consequence of F-actin depolymerisation are likely to involve calcium. One way of checking whether this is the case, is to pre-treat the pollen tubes with a calcium channel blocker (e.g. lanthanum) and then depolymerise the F-actin with LatB. If the MTs still depolymerise this suggests that calcium is not involved in this process; if they do not depolymerise, it suggests that calcium is required. However, during SI there is a large increase in cytoplasmic free calcium levels (Franklin-Tong et al, 1993; 2002) and the MT depolymerisation seen during SI is much more rapid than that seen with LatB-induced F-actin depolymerisation, suggesting that calcium plays a role in the SI-induced MT depolymerisation.

Thomas et al (2006) demonstrated that stabilising F-actin with jasplakinolide during SI resulted in significantly lower levels of PCD compared to SI alone. However, the level of PCD in these jasplakinolide treated tubes was still significantly higher than untreated controls. Equally, counteracting the SI-induced MT depolymerisation with taxol resulted in significantly lower levels of PCD, although this treatment also did not reduce caspase-like activities to basal level. In pollen tubes treated with taxol, the F-actin cytoskeleton was still able to depolymerise, indicating that actin depolymerisation was sufficient for PCD to occur. An interesting experiment would be to use jasplakinolide in conjunction with taxol prior to SI induction to see if preventing both the MT and F-actin depolymerisation lowered the incidence of PCD to basal levels. This would indicate that MT and actin depolymerisation are both necessary for maximal SI-induced PCD to occur. One point to remember with these

types of experiments is that we are using cytoskeleton targeted drugs. Although the drugs we have used here are widely used and are accepted as being specific to their target, we cannot completely rule out side-effects. We also cannot be sure that they are 100 % effective, for example in the case of taxol, we do not know if every pollen tube treated with it has all of its MTs completely stabilised against SI-induced depolymerisation. Therefore these results have to be interpreted carefully. However, these pharmacological studies do have their merits, and at present are the only tools available that allow us to study the interaction between the cytoskeletons.

7.3) Do the punctate F-actin foci represent the point of no return?

The actin cytoskeleton has previously been shown to be heavily involved in the SI response of poppy, with alterations consisting of an initial F-actin depolymerisation phase, followed by the formation of large F-actin foci. **Chapter 5** described the first study of the large F-actin foci. I showed that these F-actin foci are stable structures, resistant to LatB-induced depolymerisation. I also demonstrated that two ABPs, CAP and ADF, increase their association with the F-actin over the course of the SI-response, whilst other ABPs (profilin and fimbrin) do not.

It was proposed by Thomas and Franklin-Tong (2004) that SI in poppy is a biphasic response, with the first step involved in inhibiting pollen tube growth and the second, ‘decision making’ phase involved in preventing re-initiation of pollen tube growth by triggering PCD. It is well established that even very low levels of F-actin depolymerisation can inhibit pollen tube growth (Gibbon et al, 1999; Vidali et al, 2001). One of the first steps in the SI response is the depolymerisation of the F-actin, which shows a 69 % decrease in the F-actin level within the

first 10 min of the SI response (Geitmann et al, 2001; Snowman et al, 2002). Initially, this F-actin depolymerisation would probably inhibit pollen tube growth but further work has also shown that a transient (10 min) depolymerisation of <50 % of the F-actin in pollen tubes, by the drug LatB, is sufficient to induce PCD via a caspase-3-like activity (Thomas et al, 2006). The transient nature of the F-actin depolymerisation was achieved by ‘washing out’ the drug LatB after certain time points. The F-actin levels then rose again, back to levels comparable to that of untreated pollen. The study by Thomas et al (2006) looked at the amount of F-actin present in the pollen tube after the washout, but not at its organisation within the cell. It is possible that the actin repolymerises into F-actin foci and not into the F-actin bundles characteristic of a growing pollen tube. Their study mentioned that the pollen tubes treated with 0.1 μM LatB resumed normal growth, but does not detail whether the pollen tubes treated with 1 μM LatB, the concentration that most closely mimics the F-actin depolymerisation levels observed in SI, also resumed growth. If these pollen tubes did not grow after the washout step it could indicate that the F-actin was not in its proper configuration and thus deserves further attention. If the F-actin does appear as foci in these pollen tubes, it could implicate the F-actin foci in the PCD signalling pathway. Interestingly, *Pyrus pyrifolia* pollen tubes undergoing the SI response (S-RNase-type SI) have also recently been shown to contain F-actin foci (Liu et al, 2007). These F-actin foci have not yet been examined in great detail, so it is not known whether they increase in size during SI, or which ABPs are associated with them. Also, the possible occurrence of PCD of the pollen tube has not been investigated in this SI system. As the F-actin foci are a shared characteristic between the two SI systems it would be interesting to see if PCD was occurring in the pear pollen tubes, which would further support a role of the stable F-actin foci in PCD.

As mentioned in **Chapter 5**, it would be interesting to try and inhibit the formation of the F-actin foci during SI. If this could be achieved, we could investigate whether PCD still proceeds or whether the F-actin foci are necessary for this process. If PCD was inhibited, the F-actin foci could represent the ‘point of no return’ in the SI signalling cascade. The stabilised actin aggregates formed artificially in *S. cerevisiae* by treatment of the cells with jasplakinolide, or using cell lines containing mutations in actin regulatory genes, have been shown to be linked to the triggering of apoptosis in those cells (Gourlay & Ayscough, 2005a;b; 2006). However, the extremely stable actin bodies formed in the same yeast species when it encounters a limited food supply and enters quiescence do not trigger apoptosis and rapidly disappear upon re-feeding (Sagot et al, 2006). This demonstrates the complexity of actin dynamics and signalling, even within cells of the same species.

Furthermore, inducing the formation of the F-actin foci in non-SI-induced pollen tubes could also be informative. One factor that could be involved in their formation is pH. Bosch and Franklin-Tong (2007) demonstrated that SI induces a dramatic drop in cytosolic pH. The exact timing of this pH drop and whether it is a sudden or gradual change is the subject of current work and is presently thought to involve vacuolar degradation (Bosch et al, unpublished data). pH is known to regulate the activity of some ABPs, one of which is ADF, a component of the F-actin foci. Under acidic conditions ADF binds to F-actin (Yonezawa et al, 1985; Hayden et al, 1993; Hawkins et al, 1993) and under conditions of high ADF to actin concentrations, ADF can nucleate actin polymerisation (Andrianantoandro & Pollard, 2006). It would be interesting to see if acidification of the pollen tube cytoplasm resulted in the relocation of ADF from the cytoplasm to the F-actin and whether F-actin foci were formed. It is possible to alter the intracellular pH of pollen tubes by equilibrating them with an external

calibration solution, containing the ionophores nigericin and valinomycin, and setting this at different pHs (Feijo et al, 1999; Michard et al, 2008). If acidifying the pollen tube results in F-actin foci, it could implicate pH alterations in playing a role in their formation. Several mammalian cells have reported cytosolic acidification during apoptosis, which precedes caspase activation in cells undergoing mitochondrial-dependent (intrinsic) apoptosis (reviewed in Matsuyama & Reed, 2000). The caspase-like activities identified in poppy pollen during SI have also been shown to require an acidic pH for optimal activity (Bosch & Franklin-Tong, 2007). Thus, it would also be interesting to see if acidification of the pollen tube cytosol resulted in PCD, thereby implicating pH as a major signalling factor in SI.

7.4) Linking the F-actin foci, ADF and CAP to PCD

In poppy pollen tubes, stabilisation of F-actin with jasplakinolide was able to trigger PCD (Thomas et al, 2006) demonstrating that both depolymerisation and stabilisation of F-actin can cause PCD. It is thought that the stable F-actin foci formed during the later stages of the SI response are playing a role in the PCD signalling pathway because their formation appears to be an active process. Furthermore, stabilised actin aggregates have been shown to play a role in PCD/apoptosis in other cell types, as discussed in **Chapter 1.3.2**. As ADF and CAP co-localise with the punctate actin foci, they too could be playing a role in PCD signalling. Both ADF and CAP have been linked to apoptosis in mammalian cells (Chua et al, 2003; Wang et al, 2008) and CAP has been shown to be a link between stabilised actin and apoptosis in yeast cells (Gourlay & Ayscough, 2006). This suggests that they might also be playing a role in SI-induced PCD.

In mammalian cells it has been shown that dephosphorylated cofilin (a member of the ADF/cofilin group of proteins) translocates from the cytosol into the mitochondria upon induction of apoptosis and this translocation precedes release of cytochrome *c* (Chua et al, 2003). The induction of apoptosis, but not the mitochondrial localisation, is dependent on a functional actin-binding domain of cofilin. Reduction in cofilin levels resulted in inhibition of cytochrome *c* release and prevented apoptosis (Chua et al, 2003). More recently, Wang et al (2008) have demonstrated that CAP1 also translocates to the mitochondria following induction of apoptosis and this translocation was also dependent on a functional actin-binding domain. Similarly, they found that knock-down levels of CAP1 protein resulted in reduced cytochrome *c* release and apoptosis-resistant cells. Over-expression of CAP1 was not able to induce apoptosis on its own, but required the presence of cofilin for apoptosis to occur. Their data suggested that cofilin translocation may be upstream of CAP1 because mitochondrial targeting of cofilin can stimulate CAP1 translocation, but they do not rule out the possibility that the two independently deliver actin to the mitochondria. As both proteins required a functional actin-binding domain to promote apoptosis, it suggests that it is the translocation of actin that is required for cell killing (Chua et al, 2003; Wang et al, 2008). Conversely, neither ADF/cofilin nor CAP has been shown to translocate to the mitochondria in yeast cells. Nevertheless, the actin-binding domain of CAP is required for activation of Ras-cAMP-PKA and the accumulation of ROS that result in apoptosis in cells with stabilised actin aggregates (Gourlay & Ayscough, 2006). Therefore, CAP seems to play a role in apoptosis in both systems, regardless of whether it is associated with mitochondria. It is, therefore, possible that CAP and ADF are playing a role in the SI-induced PCD of poppy pollen.

SI exhibits many of the hallmark features of PCD including cytochrome *c* release from the mitochondria. This was observed within 10 min of SI induction, although substantial amounts were only released after 1 h (Thomas & Franklin-Tong, 2004) which was when both ADF and CAP exhibited nearly 100 % co-localisation with the F-actin foci. As both ADF and CAP have been implicated in disrupting the integrity of the mitochondrial membrane to release cytochrome *c*, it would be interesting to examine whether mitochondria are also localised within the punctate F-actin foci during SI. If so, we may be able to draw some parallels between the roles of these ABPs during SI-induced PCD and mammalian or yeast apoptosis. One approach currently being tested in the laboratory to investigate what is associated with the F-actin foci is immunogold localisation of actin using transmission electron microscopy (TEM). This technique allows us to examine the ultrastructure of the cell to see if any organelles are associated with the punctate F-actin foci. The study by Sagot et al (2006) into the actin bodies formed in quiescent yeast cells used TEM to determine if their actin aggregations were associated with any organelles. They found that the actin bodies were not associated with any membranous structure or particular region of the cytoplasm. TEM has been used previously to look at the alterations that occur to the organelles during the SI response (Geitmann et al, 2004). Their study showed that dramatic morphological alterations occurred in the mitochondria, Golgi and ER within 1 h of SI induction. The mitochondria were often seen fusing with each other in SI-induced pollen, which, if associated with F-actin, could potentially form the large F-actin foci made visible with fluorescently labelled phalloidin. Thus, it remains to be seen whether the large F-actin foci formed during SI are associated with organelles/membranes or whether they are formed freely in the cytoplasm, as is the case for the actin bodies in yeast cells.

7.5) Concluding remarks

The identification of PrpS as the male *S*-determinant (Wheeler et al, 2009) and its localisation at the pollen tube membrane has finally allowed us to establish the first step in how poppy discriminates between ‘self’ and ‘non-self’ pollen. The work in this thesis has also furthered our knowledge of the involvement of the cytoskeleton in the SI response of poppy. We now know that the MT cytoskeleton, although not thought to be important for normal pollen tube growth, is targeted by SI signals very early on in the response and plays a role in the PCD signalling pathway. The punctate F-actin foci have also been shown to have some interesting properties and other ABPs have been identified as potentially playing an important role in SI. In addition, the mass spectrometry analysis of potential F-actin interactors has thrown-up some interesting signalling proteins that deserve further attention in future studies. **Figure 7.1a** shows a model of the SI response of poppy with the results of this thesis incorporated. The timeline of the SI events identified to date is shown in **Figure 7.1b**. Although great progress has been made in understanding the downstream events triggered in an incompatible pollen tube when it lands on a stigma, there is still lots more work ahead of us, some of which is detailed above. The next major challenge will be to integrate all the available data to unravel the full signalling networks that determine whether a pollen grain landing on a stigma is sentenced to death, or is whether it is permitted to germinate, achieve fertilisation and set seed.

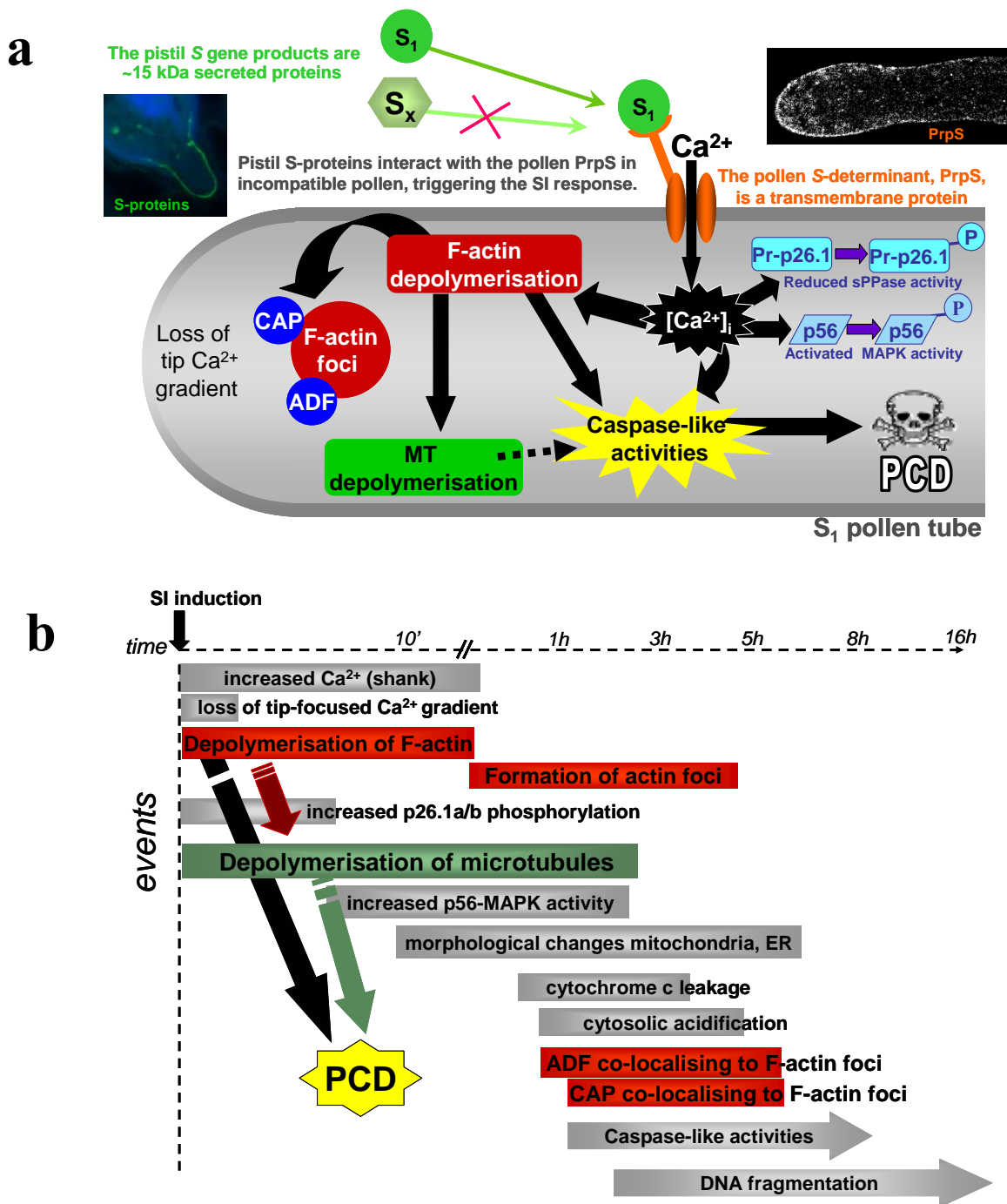


Figure 7.1. The current model of *Papaver rhoeas* SI

a) The pollen *S*-determinant, PrpS, localises to the pollen tube membrane. When it comes into contact with incompatible (self) *S*-proteins a calcium-mediated signalling cascade is triggered in the pollen tube. The tip-focused calcium gradient is lost and there is phosphorylation of several key proteins. The F-actin cytoskeleton is first depolymerised, which causes the MT cytoskeleton to depolymerise, and then forms F-actin foci that increase in size over time. The ABPs, CAP and ADF co-localise with the F-actin foci. Both F-actin and MT depolymerisation are required for caspase-like activities and PCD to occur.

b) A timeline of the SI events characterised to date. The events identified as a result of this thesis are highlighted in red and green. Future work will need to concentrate on integrating these events into a signalling network that governs the rejection of incompatible pollen.

Figure adapted from Bosch & Franklin-Tong (2008).

CHAPTER 8

LIST OF REFERENCES

- Abdrakhamanova A, Wang QY, Khokhlova L, Nick P (2003). Is microtubule disassembly a trigger for cold acclimation? *Plant Cell Physiology*, **44**, 676-686.
- Adams AE, Botstein D, Drubin DG (1991). Requirement of yeast fimbrin for actin organization and morphogenesis *in vivo*. *Nature*, **354**, 404-408.
- Agnew BJ, Minamide LS, Bamburg JR (1995). Reactivation of phosphorylated actin depolymerising factor and identification of the regulatory site. *Journal of Biological Chemistry*, **270**, 17582-17587.
- Ai Y, Singh A, Coleman CE, Ioerger TR, Kheyr-Pour A, Kao T-H (1990). Self-incompatibility in *Petunia inflata*: Isolation and characterization of cDNAs encoding S-allele-associated proteins. *Sexual Plant Reproduction*, **3**, 30-138.
- Aizawa H, Katadae M, Maruya M, Sameshima M, Murakami-Murofushi K, Yahara I. (1999). Hyperosmotic stress-induced reorganization of actin bundles in Dictyostelium cells over-expressing cofilin. *Genes to Cells*, **4**, 311-324.
- Allwood EG, Smertenko AP, Hussey PJ (2001). Phosphorylation of plant actin-depolymerising factor by calmodulin-like domain protein kinase. *FEBS Letters*, **499**, 97-100.
- Allwood EG, Anthony RG, Smertenko AP, Reichelt S, Drobak BK, Doonan JH, Weeds AG, Hussey PJ (2002). Regulation of the pollen-specific actin-depolymerising factor LIADF. *The Plant Cell*, **14**, 2915-2927.
- Amatruda JF, Cannon JF, Tatchell K, Hug C, Cooper JA (1990). Disruption of the Actin Cytoskeleton in Yeast Capping Protein Mutants. *Nature*, **344**, 352-354.
- Amberg DC, Basart E, Botstein D. (1995). Defining Protein Interactions with Yeast Actin *in vivo*. *Nature Structural Biology*, **2**, 28-35.
- Ampe C, Markey F, Lindberg U, and Vandekerckhove J (1988). The primary structure of human platelet profilin: reinvestigation of the calf spleen profilin sequence. *FEBS Letters*, **228**, 17-21.
- Anderhag P, Hepler PK, Lazzaro MD (2000). Microtubules and microfilaments are both responsible for pollen tube elongation in the conifer *Picea abies* (Norway spruce). *Protoplasma*, **214**, 141-157.
- Anderson MA, Cornish EC, Mau S-L, Williams EG, Hoggart R, Atkinson A, Bönig I, Grego B, Simpson R, Roche PJ, Haley JD, Penschow JD, Niall HD, Tregear GW, Coughlan JP, Crawford RJ, Clarke AE (1986). Cloning of cDNA for a stylar glycoprotein associated with expression of self-incompatibility in *Nicotiana glauca*. *Nature*, **321**, 38-44.
- Andrianantoandro E, Pollard T (2006). Mechanism of Actin Filament Turnover by Severing and Nucleation at Different Concentrations of ADF/Cofilin. *Molecular Cell*, **24**, 13-23.
- Asai T, Tena G, Plotnikova J, Willmann MR, Chiu WL, Gomez-Gomez L, Boller T, Ausubel FM, Sheen J (2002). MAP kinase signalling cascade in Arabidopsis innate immunity. *Nature*, **415**, 977-983.
- Åström H, Virtanen I, Raudaskoski M (1991). Cold stability in the pollen tube cytoskeleton. *Protoplasma*, **160**, 99-107.
- Astrom H (1992). Acetylated alpha-tubulin in the pollen tube microtubules. *Cell Biology International Report*, **16**, 871-881.
- Åström H, Sorri O, Raudaskoski M (1995). Role of the microtubules in the movement of the vegetative nucleus and generative cell in tobacco pollen tubes. *Sexual Plant Reproduction*, **8**, 61-69.
- Åström H. (1997) The structure and function of Tobacco pollen tube cytoskeleton. *Academic Dissertation*. University of Helsinki, Finland.

- Ayscough KR (2005). Coupling actin dynamics to the endocytic process in *Saccharomyces cerevisiae*. *Protoplasma*, **226**, 81-88.
- Balcer HI, Goodman AL, Rodal AA, Smith E, Kugler J, Heuser JE, Goode BL (2003). Coordinated regulation of actin filament turnover by a high-molecular-weight Srv2/CAP complex, cofilin, profilin, and Aip1. *Current Biology*, **13**, 2159-2169.
- Bamburg JR, Harris HE, Weeds AG (1980). Partial purification and characterization of an actin depolymerizing factor from brain. *FEBS Letters*, **121**, 178-182.
- Bamburg JR, Bernstein BW (1991). Actin and actin-binding proteins in neurons. In *The Neuronal Cytoskeleton*, ed. RD Burgoyne, pp. 121-60. New York: Wiley-Liss.
- Bamburg JR (1999). Proteins of the ADF/cofilin family: essential regulators of actin dynamics. *Annual Review of Cell Developmental Biology*, **15**, 185-230.
- Barrero RA, Umeda M, Yamamura S, Uchimiya H (2002). *Arabidopsis* CAP regulates the actin cytoskeleton necessary for plant cell elongation and division. *The Plant Cell*, **14**, 149-163.
- Bartolini F, Moseley JB, Schmoranzler J, Cassimeris L, Goode BL, Gundersen GG (2008). The formin mDia2 stabilizes microtubules independently of its actin nucleation activity. *Journal of Cell Biology*, **181**, 523-536.
- Bartolo ME, Carter JV (1991). Microtubules in mesophyll cells of nonacclimated and cold-acclimated spinach: visualization and responses to freezing, low temperature, and dehydration. *Plant Physiology*, **97**, 175-181.
- Bartolo ME, Carter JV (1992). Lithium Decreases Cold-Induced Microtubule Depolymerization in Mesophyll Cells of Spinach. *Plant Physiology*, **99**, 1716-1718.
- Beaumont V (2003). Visualizing membrane trafficking using total internal reflection fluorescence microscopy. *Biochemical Society Transactions*, **31**, 819-823.
- Beers EP. (1997). Programmed cell death during plant growth and development. *Cell Death and Differentiation* **4**: 649-661.
- Bernstein BW, Bamburg JR (1982). Tropomyosin binding to F-actin protects the F-actin from disassembly by brain actin-depolymerizing factor (ADF). *Cell Motility*, **2**, 1-8.
- Bhat RA, Lahaye T, Panstruga R (2006). The visible touch: in planta visualization of protein-protein interactions by fluorophore-based methods. *Plant Methods*, **2**, 12.
- Bibikova TN, Blancaflor EB, Gilroy S (1999). Microtubules regulate tip growth and orientation in root hairs of *Arabidopsis thaliana*. *The Plant Journal*, **17**, 657-665.
- Binet M, Humbert C, Lecourieux D, Vantard M, Pugin A (2001). Disruption of microtubular cytoskeleton induced by cryptogein, an elicitor of hypersensitive response in tobacco cells. *Plant Physiology*, **125**, 564-572.
- Blobe GC, Stribling DS, Fabbro D, Stabel S, Hannun YA (1996). Protein kinase C beta II specifically binds to and is activated by F-actin. *Journal of Biological Chemistry*, **271**, 15823-15830.
- Bonneau L, Ge Y, Drury GE, Gallois P (2008). What happened to plant caspases? *Journal of Experimental Botany*, **59**, 491-499.
- Bosch M, Franklin-Tong VE (2007). Temporal and spatial activation of caspase-like enzymes induced by self-incompatibility in *Papaver* pollen. *PNAS*, **104**, 18327-18332.
- Bosch M, Franklin-Tong VE (2008). Self-incompatibility in *Papaver*: signalling to trigger PCD in incompatible pollen. *Journal of Experimental Botany*, **59**, 481-90.
- Bosch M, Poulter NS, Vatovec S, Franklin-Tong VE (2008). Initiation of programmed cell death in self-incompatibility: Role for cytoskeleton modifications and several caspase-like activities. *Molecular Plant*, **1**, 879-887.

- Bouquin T, Mattsson O, Naested H, Foster R, Mundy J (2003). The *Arabidopsis* lue1 mutant defines a katanin p60 ortholog involved in hormonal control of microtubule orientation during cell growth. *Journal of Cell Science*, **116**, 791–801.
- Bower MS, Matias DD, Fernandes-Carvalho E, Mazzurco M, Gu T, Rothstein S, Goring DR (1996). Two members of the thioredoxin-h family interact with the kinase domain of a *Brassica* S-locus receptor kinase. *Plant Cell*, **8**, 1641–1650.
- Bozhkov PV, Suarez MF, Filonova LH, Daniel G, Zamyatnin Jr AA, Rodriguez-Nieto S, Zhivotovsky B, Smertenko A (2005). Cysteine protease mcII-Pa executes programmed cell death during plant embryogenesis. *PNAS*, **102**, 14463–14468.
- Bradford MM (1976). A rapid and sensitive method for the quantitation of microgram quantities of protein utilising the principle of protein-dye binding. *Analytical Biochemistry*, **72**, 248-254.
- Brandner K, Sambade A, Boutant E, Didier P, Mély Y, Ritzenthaler C, Heinlein M (2008). Tobacco mosaic virus movement protein interacts with green fluorescent protein-tagged microtubule end-binding protein 1. *Plant Physiology*, **147**, 611-623.
- Bredemeijer GMM, Blaas J (1981). S-Specific proteins in styles of self-incompatible *Nicotiana glauca*. *Theories in Applied Genetics*, **59**, 185–190.
- Bretscher A, Weber K (1980). Fimbrin, a new microfilament-associated protein present in microvilli and other cell surface structures. *Journal of Cell Biology*, **86**, 335-340.
- Bretscher A (1981). Fimbrin is a cytoskeletal protein that crosslinks F-actin in vitro. *PNAS*, **78**, 6849-6853.
- Burk DH, Liu B, Zhong R, Morrison WH, Ye ZH (2001). A katanin-like protein regulates normal cell wall biosynthesis and cell elongation. *Plant Cell*, **13**, 807–827.
- Burk DH, Ye ZH (2002) Alteration of oriented deposition of cellulose microfibrils by mutation of a katanin-like microtubule-severing protein. *Plant Cell*, **14**, 2145–2160.
- Buss FC, Temm-Grove C, Henning S, Jochush B (1992). Distribution of profilin in fibroblasts correlates with the presence of highly dynamic actin filaments. *Cell Motility and the Cytoskeleton*, **22**, 51-61.
- Cabrillac D, Cock JM, Dumas C, Gaude T (2001). The S-locus receptor kinase is inhibited by thioredoxins and activated by pollen coat proteins. *Nature*, **410**, 220–23.
- Cahill D, Rookes J, Michalczyk A, McDonald K, Drake A (2002). Microtubule dynamics in compatible and incompatible interactions of soybean hypocotyl cells with *Phytophthora sojae*. *Plant Pathology*, **51**, 629-640.
- Cai G, Moscatelli A, Cresti M (1997). Cytoskeletal organisation and pollen tube growth. *Trends in Plant Science*, **2**, 86-91.
- Cai G, Romagnoli S, Moscatelli A, Ovidi E, Gambellini G, Tiezzi A, Cresti M (2000). Identification and characterization of a novel microtubule-based motor associated with membranous organelles in tobacco pollen tubes. *The Plant Cell*, **12**, 1719-1736.
- Cai G, Del Casino C, Romagnoli S, Cresti M (2005a). Pollen cytoskeleton during germination and tube growth. *Current Science*, **89**, 1853-1860.
- Cai G, Ovidi E, Romagnoli S, Vantard M, Cresti M, Tiezzi A (2005b). Identification and characterisation of plasma membrane proteins that bind to microtubules in pollen tubes and generative cells of tobacco. *Plant Cell Physiology*, **46**, 563-578.
- Cai G, Cresti M (2009). Organelle motility in the pollen tube: a tale of 20 years. *Journal of Experimental Botany*, **60**, 495-508.
- Camacho L, Malho R (2003). Endo/exocytosis in the pollen tube apex is differentially regulated by Ca²⁺ and GTPase, *Journal of Experimental Botany*, **54**, 83–92.

- Cano ML, Lauffenburger DA, Zigmond SH (1991). Kinetic analysis of F-actin depolymerisation in polymorphonuclear leukocyte indicates that chemoattractant stimulation increases actin filament number without altering the filament length distribution. *The Journal of Cell Biology*, **115**, 677-687.
- Cardenas L, Lovy-Wheeler A, Kunkel JG, Hepler PK (2008). Pollen Tube Growth Oscillations and Intracellular Calcium Levels Are Reversibly Modulated by Actin Polymerization. *Plant Physiology*, **146**, 1611-1621.
- Carlier MF, Laurent V, Santolini J, Melki R, Didry D, Xia GX, Hong Y, Chua NH, Pantaloni D (1997). Actin depolymerizing factor (ADF/cofilin) enhances the rate of filament turnover: implication in actin-based motility. *Journal of Cell Biology*, **136**, 1307-22.
- Carlsson L, Nystrom LE, Sundkvist I, Markey F, Lindberg U. 1977. Actin polymerizability is influenced by profilin, a low molecular weight protein in non-muscle cells. *Journal of Molecular Biology*, **115**, 465-483.
- Chan J, Jensen CG, Jensen LC, Bush M, Lloyd CW (1999). The 65-kDa carrot microtubule-associated protein forms regularly arranged filamentous cross-bridges between microtubules. *PNAS*, **96**, 14931-14936.
- Chan J, Calder GM, Doonan JH, Lloyd CW (2003). EB1 reveals mobile microtubule nucleation sites in *Arabidopsis*. *Nature Cell Biology*, **5**, 967-971.
- Chan J, Calder G, Fox S, Lloyd C (2005). Localization of the microtubule end binding protein EB1 reveals alternative pathways of spindle development in *Arabidopsis* suspension cells. *The Plant Cell*, **17**, 1737-1748.
- Chan J, Calder G, Fox S, Lloyd C (2007). Cortical microtubule arrays undergo rotary movements in *Arabidopsis* hypocotyls epidermal cells. *Nature Cell Biology*, **9**, 171-175.
- Chang HY, Smertenko AP, Igarashi H, Dixon DP, Hussey PJ (2005). Dynamic interaction of NtMAP65-1a with microtubules *in vivo*. *Journal of Cell Science*, **118**, 3195-3201.
- Charlesworth D, Vekemans X, Castric V, Glémin S (2005). Plant self-incompatibility systems: a molecular evolutionary perspective. *New Phytologist*, **168**, 61-69.
- Chaudhry F, Guérin C, von Witsch M, Blanchoin L, Staiger CJ (2007). Identification of *Arabidopsis* cyclase-associated protein 1 as the first nucleotide exchange factor for plant actin. *Molecular Biology of the Cell*, **18**, 3002-3014.
- Chen CY, Wong EI, Vidali L, Estavillo A, Hepler PK, Wu H, Cheung AY (2002). The regulation of actin organisation by actin-depolymerising factor in elongating pollen tubes. *The Plant Cell*, **14**, 2175-2190.
- Cheung AY, Chen CY, Glaven RH, de Graaf BH, Vidali L, Hepler PK, Wu HM (2002). Rab2 GTPase regulates vesicle trafficking between the endoplasmic reticulum and the Golgi bodies and is important to pollen tube growth. *The Plant Cell*, **14**, 945-962.
- Cheung AY, Chen CYH, Tao LZ, Andreyeva T, Twell D, Wu HM (2003). Regulation of pollen tube growth by Rac-like GTPases. *Journal of Experimental Botany*, **54**, 73-81.
- Cheung AY, Wang H, Wu HM (1995). A floral transmitting tissue-specific glycoprotein attracts pollen tubes and stimulates their growth. *Cell*, **11**, 383-393.
- Cheung AY, Wu HM. (2004). Overexpression of an *Arabidopsis* formin stimulates supernumerary actin cable formation from pollen tube cell membrane, *The Plant Cell*, **16**, 257-269.
- Cheung, AY; Duan, QH; Costa, SS, de Graaf BHJ, Di Stilio VS, Feijo J, Wu H-M (2008). The Dynamic Pollen Tube Cytoskeleton: Live Cell Studies Using Actin-Binding and Microtubule-Binding Reporter Proteins. *Molecular Plant*, **1**, 686-702.

- Chu B, Kerr GP, Carter JV (1993). Stabilising microtubules with taxol increases microfilament stability during freezing of rye root-tips. *Plant Cell and Environment*, **16**, 883-889.
- Chua BT, Volbracht, C., Tan, K. O., Li, R., Yu, V. C. and Li, P. (2003). Mitochondrial translocation of cofilin is an early step in apoptosis induction. *Nature Cell Biology*, **5**, 1083-1089.
- Clague MJ, Urbé S (2001). The interface of receptor trafficking and signalling. *Journal of Cell Science*, **114**, 3075-3081.
- Clark KR, Okuley JJ, Collins PD, Sims TL (1990). Sequence variability and developmental expression of S-alleles in self-incompatible and pseudo-self-compatible petunia. *The Plant Cell*, **2**, 815-826.
- Coffeen WC, Wolpert TJ (2004). Purification and characterization of serine proteases that exhibit caspase-like activity and are associated with programmed cell death in *Avena sativa*. *The Plant Cell*, **16**, 857-873.
- Collings DA, Asada T, Allen NS, Shibaoka H (1998) Plasma Membrane-Associated Actin in Bright Yellow 2 Tobacco Cells. Evidence for Interaction with Microtubules, *Plant Physiology*, **118**, 917-928.
- Collings DA, Lill AW, Himmelpach R, Wasteneys GO (2006). Hypersensitivity to cytoskeletal antagonists demonstrates microtubule-microfilament cross-talk in the control of root elongation in *Arabidopsis thaliana*. *New Phytologist*, **170**, 275-290.
- Cooperman BS, Baykov AA, Lahti R (1992). Evolutionary conservation of the active site of soluble inorganic pyrophosphatase. *Trends in Biochemical Science*, **17**, 262-266.
- Coué M, Brenner SL, Spector I, Korn ED (1987). Inhibition of actin polymerisation by Latrunculin A. *FEBS letters*, **213**, 316-318.
- Craig KL, Tyers M (1999). The F-box: a new motif for ubiquitin dependent proteolysis in cell cycle regulation and signal transduction. *Progress in Biophysics and Molecular Biology*, **72**, 299-328.
- Cresti M, Lancelle SA, Hepler PK (1987). Structure of the generative cell wall complex after freeze substitution in pollen tubes of *Nicotiana* and *Impatiens*. *Journal of Cell Science*, **88**, 373-378.
- Cyr RJ (1991). Calcium Calmodulin Affects Microtubule Stability in Lysed Protoplasts. *Journal of Cell Science*, **100**, 311-317.
- Davis AJ, Im Y-J, Dubin JS, Tomer KB, Boss WF (2007). *Arabidopsis* phosphatidylinositol phosphate kinase 1 binds F-actin and recruits phosphatidylinositol 4-kinase β 1 to the actin cytoskeleton. *The Journal Of Biological Chemistry* , **282**, 14121-14131.
- de Graaf BH, Cheung AY, Andreyeva T, Levasseur K, Kieliszewski M, Wu HM (2005). Rab11 GTPase-regulated membrane trafficking is crucial for tip-focused pollen tube growth in tobacco. *The Plant Cell*, **17**, 2564-2579.
- de Graaf BHJ, Rudd JJ, Wheeler MJ, Perry RM, Bell EM, Osman K, Franklin FCH, Franklin-Tong VE (2006). Self-incompatibility in *Papaver* targets soluble inorganic pyrophosphatases in pollen. *Nature*, **444**, 490-493.
- Deeks MJ, Hussey PJ, Davies B (2002). Formins: intermediates in signal-transduction cascades that affect cytoskeletal reorganization. *Trends in Plant Science*, **7**, 492-498.
- Deeks MJ, Cvrckova F, Machesky LM, Mikitova V, Ketelaar T, Zarsky V, Davies B, Hussey PJ (2005). *Arabidopsis* group Ie formins localize to specific cell membrane domains, interact with actin-binding proteins and cause defects in cell expansion upon aberrant expression. *New Phytologist*, **168**, 529-540.

- Deeks MJ, Rodrigues C, Dimmock S, Ketelaar T, Maciver SK, Malho R, Hussey PJ (2007). Arabidopsis CAP1 a key regulator of actin organisation and development. *Journal of Cell Science*, **120**, 2609-2618.
- DeLille JM, Sehnke PC, Ferl RJ (2001). The *Arabidopsis* 14-3-3 Family of Signaling Regulators. *Plant Physiology*, **126**, 35-38.
- Desagher S, Osen-Sand A, Nichols A, Eskes R, Montessuit S, Lauper S, Maundrell K, Antonsson B, Martinou JC (1999). Bid-induced conformational change of Bax is responsible for mitochondrial cytochrome c release during apoptosis. *Journal of Cell Biology*, **144**, 891-901.
- Dhonukshe P, Laxalt AM, Goedhart J, Gadella TW, Munnik T (2003). Phospholipase D activation correlates with microtubule reorganization in living plant cells. *Plant Cell*, **15**, 2666-79.
- Dickinson HG (1994). Self-pollination: simply a social disease? *Nature*, **367**, 517-518.
- Didry D, Carlier MF, and Pantaloni D (1998). Synergy between actin depolymerizing factor cofilin and profilin in increasing actin filament turnover. *Journal of Biological Chemistry*, **273**, 25602-25611.
- Dixit R, Cyr R (2004a). The cortical microtubule array: from dynamics to organization. *The Plant Cell*, **16**, 2546-2552.
- Dixit R, Cyr R (2004b). Encounters between dynamic cortical microtubules promote ordering of the cortical array through angle-dependent modifications of microtubule behavior. *The Plant Cell*, **16**, 3274-3284.
- Dixon RD, Arneman DK, Rachlin AS, Sundaresan NR, Costello MJ, Campbell SL, Otey CA (2008). Palladin is an actin cross-linking protein that uses immunoglobulin-like domains to bind filamentous actin. *Journal of Biological Chemistry*, **283**, 6222-6231.
- Dos Remedios CG, Chhabra M, Kekic M, Dedova IV, Tsubakihara M, Berry DA, Nosworthy NJ (2003). Actin Binding Proteins: Regulation of cytoskeleton microfilaments. *Physiology Review*, **83**, 433-473.
- Drenan RM, Nashmi R, Imoukhuede P, Just H, McKinney S, Lester HA (2008). Subcellular trafficking, pentameric assembly, and subunit stoichiometry of neuronal nicotinic acetylcholine receptors containing fluorescently labeled alpha6 and beta3 subunits. *Molecular Pharmacology*, **73**, 27-41.
- Drubin DG, Miller KG, Botstein D (1988). Yeast actin-binding proteins: evidence for a role in morphogenesis. *Journal of Cell Biology*, **107**, 2551-2561.
- Elmore S (2007). Apoptosis: a review of programmed cell death. *Toxicologic Pathology*, **35**, 495-516.
- Entani T, Iwano M, Shiba H, Che FS, Isogai A, Takayama S (2003). Comparative analysis of the self-incompatibility (S-) locus region of *Prunus mume*: identification of a pollen-expressed F-box gene with allelic diversity. *Genes to Cells*, **8**: 203-213.
- Erhardt M, Stoppin-Mellet V, Campagne S, Canaday J, Mutterer J, Fabian T, Sauter M, Muller T, Peter C, Lambert AM, Schmit AC (2002). The plant Spc98p homologue colocalizes with γ -tubulin at microtubule nucleation sites and is required for microtubule nucleation. *Journal of Cell Science*, **115**, 2423-2431.
- Erickson HP, O'Brien ET (1992). Microtubule Dynamic Instability and Gtp Hydrolysis. *Annual Review of Biophysics and Biomolecular Structure*, **21**, 145-166.
- Eskes R, Desagher S, Antonsson B, Martinou, JC (2000). Bid induces the oligomerization and insertion of Bax into the outer mitochondrial membrane. *Molecular Cell Biology*, **20**, 929-935.

- Eun S-O, Shik Youn H, Lee Y (2000). Lead disturbs microtubule organization in the root meristem of *Zea mays*. *Physiologia Plantarum*, **110**, 357-365.
- Evangelista M, Pruyne D, Amberg DC, Boone C, Bretscher A, (2002). Formins direct Arp2/3-independent actin filament assembly to polarize cell growth in yeast. *Nature Cell Biology*, **4**, 32-41.
- Favery B, Chelysheva LA, Lebris M, Jammes F, Marmagne A, De Almeida-Engler J, Lecomte P, Vaury C, Arkowitz RA, Abad P (2004). Arabidopsis formin AtFH6 is a plasma membrane-associated protein upregulated in giant cells induced by parasitic nematodes. *The Plant Cell*, **16**, 2529-2540.
- Fedor-Chaikin M, Deschenes RJ, Broach JR (1990). SRV2, a gene required for RAS activation of adenylate cyclase in yeast. *Cell*, **61**, 329-340.
- Feijó JA, Sainhas J, Hackett GR, Kunkel JG, Hepler PK (1999). Growing pollen tubes possess a constitutive alkaline band in the clear zone and a growth-dependent acidic tip. *Journal of Cell Biology*, **144**, 483-496.
- Ferguson C, Teeri TT, Siika AM, Read SM, Bacic A (1998). Location of cellulose and callose in pollen tubes and grains of *Nicotiana tabacum*. *Planta*, **206**, 452-460.
- Ferl RJ, Manak MS, Reyes MF (2002). The 14-3-3s. *Genome Biology*, **3**, Reviews 3010.1-3010.7.
- Field J, Vojtek A, Ballester R, Bolger G, Colicelli J, Ferguson K, Gerst J, Kataoka T, Michaeli T, Powers S, Riggs M, Rodgers L, Wieland I, Wheland B, Wigler M (1990). Cloning and characterization of CAP, the *S. cerevisiae* gene encoding the 70 kd adenylate cyclase-associated protein. *Cell*, **61**, 319-327.
- Fisher DD, Gilroy S, Cyr RJ (1996). Evidence for opposing effects of calmodulin on cortical microtubules. *Plant Physiology*, **112**, 1079-1087.
- Foissner I, Wasteneys GO (2000). Microtubule disassembly enhances reversible cytochalasin-dependent disruption of actin bundles in characean internodes. *Protoplasma*, **214**, 33-44.
- Foote H, Ride J, Franklin-Tong V, Walker E, Lawrence M, Franklin F (1994). Cloning and expression of a distinctive class of self-incompatibility (S) genes from *Papaver rhoeas*. *PNAS*, **91**, 2265-2269.
- Fowler JE, Quatrano RS. 1997. Plant cell morphogenesis: plasma membrane interactions with the cytoskeleton and cell wall. *Annual Review of Cell and Developmental Biology*, **13**, 697-743.
- Franklin-Tong VE, Ride JP, Read ND, Trewavas AJ, Franklin FCH (1993). The self-incompatibility response in *Papaver rhoeas* is mediated by cytosolic-free calcium. *Plant Journal*, **4**, 163-177.
- Franklin-Tong VE, Ride JP, Franklin FCH (1995). Recombinant stigmatic self-incompatibility (S-) protein elicits a Ca²⁺ transient in pollen of *Papaver rhoeas*. *Plant Journal*, **8**, 299-307.
- Franklin-Tong VE, Hackett G, Hepler P (1997). Ratio-imaging of Ca²⁺ in the self-incompatibility response in pollen tubes of *Papaver rhoeas*. *The Plant Journal*, **12**, 1375-1386.
- Franklin-Tong, VE (1999). Signalling and the modulation of pollen tube growth. *The Plant Cell*, **11**, 727-738.
- Franklin-Tong V, Holdaway-Clark T, Straatman K, Kunkel J, Hepler P (2002). Involvement of extracellular calcium influx in the self incompatibility response of *Papaver rhoeas*. *Plant Journal*, **29**, 333-345.

- Franklin-Tong VE, Gourlay CW. (2008). A role for actin in regulating apoptosis/programmed cell death: evidence spanning yeast, plants and animals. *Biochemical Journal*, **413**, 389-404.
- Freeman NL, Chen Z, Horenstein J, Weber A, Field J (1995). An actin monomer binding activity localises to the carboxyl-terminal half of the *Saccharomyces cerevisiae* cyclase-associated protein. *Journal of Biological Chemistry*, **270**, 5680-5685.
- Freeman NL, Field J (2000). Mammalian homolog of the yeast cyclase associated protein, CAP/Srv2p, regulates actin filament assembly. *Cell Motility and the Cytoskeleton*, **45**, 106–120.
- Fu Y, Wu G, Yang Z (2001). Rop GTPase-dependent dynamics of tip-localized F-actin controls tip growth in pollen tubes. *Journal of Cell Biology*, **152**, 1019–32.
- Fu Y, Gu Y, Zheng Z, Wasteneys G, Yang Z (2005). *Arabidopsis* Interdigitating Cell Growth Requires Two Antagonistic Pathways with Opposing Action on Cell Morphogenesis. *Cell*, **120**, 687-700.
- Fukuda H (2000). Programmed cell death of tracheary elements as a paradigm in plants. *Plant Molecular Biology*, **44**, 245–253.
- Gajate C, Barasoain I, Andreu JM, Mollinedo F (2000). Induction of apoptosis in leukemic cells by the reversible microtubule-disrupting agent 2-methoxy-5-(2',3',4'-trimethoxyphenyl)-2,4,6-cycloheptatrien-1-one: protection by Bcl-2 and Bcl-X_L and cell cycle arrest. *Cancer Research*, **60**, 2651-2659.
- Gardiner JC, Harper JD, Weerakoon ND, Collings DA, Ritchie S, Gilroy S, Cyr RJ, Marc J (2001). A 90-kD phospholipase D from tobacco binds to microtubules and the plasma membrane. *The Plant Cell*, **13**, 2143-2158.
- Gavin AC, Aloy P, Grandi P, Krause R, Boesche M, Marzioch M, Rau C, Jensen LJ, Bastuck S, Dümpelfeld B, Edelmann A, Heurtier MA, Hoffman V, Hoefert C, Klein K, Hudak M, Michon AM, Schelder M, Schirle M, Remor M, Rudi T, Hooper S, Bauer A, Bouwmeester T, Casari G, Drewes G, Neubauer G, Rick JM, Kuster B, Bork P, Russell RB, Superti-Furga G (2006). Proteome survey reveals modularity of the yeast cell machinery. *Nature*, **440**, 631–636.
- Geitmann A, Emons M (2000). The cytoskeleton in plant and fungal cell tip growth. *Journal of Microscopy*, **198**, 218-245.
- Geitmann A, Snowman B, Emons A, Franklin-Tong V (2000). Alterations in the actin cytoskeleton of pollen tubes are induced by the self-incompatibility reaction in *Papaver rhoeas*. *The Plant Cell*, **12**, 1239-1251.
- Geitmann A, Franklin-Tong VE, Emons AC (2004). The self-incompatibility response in *Papaver rhoeas* pollen causes early and striking alterations to organelles. *Cell Death and Differentiation*, **11**, 812-22.
- Genesca M, Sola A, Hotter G (2006). Actin cytoskeleton derangement induces apoptosis in renal ischemia/reperfusion. *Apoptosis*, **11**, 563–571.
- Gerst JE, Ferguson K, Vojtek A, Wigler M, Field J (1991). CAP is a bifunctional component of the *Saccharomyces cerevisiae* adenylyl cyclase complex. *Molecular and Cellular Biology*, **11**, 1248-1257.
- Gibbon BC, Kovar DR, Staiger CJ (1999). Latrunculin B has different effects on pollen germination and tube growth. *The Plant Cell*, **11**, 2349-2363.
- Gieselmann R, Mann, K. (1992). ASP-56, a new actin sequestering protein from pig platelets with homology to CAP, an adenylate cyclase-associated protein from yeast. *FEBS Letters*, **298**, 149-153.

- Gingras AC, Gstaiger M, Raught B and Aebersold R (2007). Analysis of protein complexes using mass spectrometry. *Nature Reviews Molecular Cell Biology*, **8**, 645–654.
- Glenney JR Jr, Kaulfus P, Matsudaira P, Weber K (1981). F-actin binding and bundling properties of fimbrin, a major cytoskeletal protein of microvillus core filaments. *Journal of Biological Chemistry*, **256**, 9283-9288.
- Goldraj A, Kondo K, Lee CB, Hancock CN, Sivaguru M, Vazquez-Santana S, Kim S, Phillips TE, Cruz-Garcia F, McClure B (2006). Compartmentalization of S-RNase and HT-B degradation in self-incompatible *Nicotiana*. *Nature*, **439**, 805-810.
- Goldschmidt-Clermont PJ, Machesky LM, Baldassare JJ, and Pollard TD (1990). The actin-binding protein profilin binds to PIP₂ and inhibits its hydrolysis by phospholipase C. *Science*, **247**, 1575-1578.
- Goldschmidt-Clermont PJ, Machesky LM, Doberstein SK, and Pollard TD (1991). The mechanism of interaction of human platelet profilin with actin. *Journal of Cell Biology*, **113**, 1081-1089.
- Goldschmidt-Clermont PJ, Furman MI, Wachsstock D, Safer D, Nachmias VT, Pollard TD (1992) The control of actin nucleotide exchange by thymosin β_4 and profilin: a potential regulatory mechanism for actin polymerization in cells. *Molecular Biology of the Cell*, **3**, 1015-1024.
- Gómez-Gómez L, Bauer Z, Boller T (2001). Both the extracellular leucine-rich repeat domain and the kinase activity of FSL2 are required for flagellin binding and signaling in *Arabidopsis*. *The Plant Cell*, **13**, 1155-63.
- Goode BL, DG Drubin, Barnes G. (2000). Functional cooperation between the microtubule and actin cytoskeletons. *Current Opinions in Cell Biology*, **12**, 63-71.
- Gossot O, Geitmann A (2007). Pollen tube growth: coping with mechanical obstacles involves the cytoskeleton, *Planta*, **226**, 405-416.
- Gottwald U, Brokamp R, Karakesisoglou I, Scheicher M, Noegel AA (1996). Identification of a cyclase associated protein (CAP) homologue in *Dictyostelium discoideum* and characterisation of its interaction with actin. *Molecular Biology of the Cell*, **7**, 261-272.
- Gourlay CW, Ayscough KR (2005a). A role for actin in aging and apoptosis. *Biochemical Society Transactions*, **33**, 1260-1264.
- Gourlay CW, Ayscough KR (2005b). Identification of an upstream regulatory pathway controlling actin-mediated apoptosis in yeast. *Journal of Cell Science*, **118**, 2119-2132.
- Gourlay CW, Carpp LN, Timpson P, Winder SJ Ayscough KR (2004). A role for the actin cytoskeleton in cell death and aging in yeast. *Journal of Cell Biology*, **164**, 803-809.
- Gourlay CW, Ayscough KR (2006). Actin-induced hyperactivation of the Ras signaling pathway leads to apoptosis in *Saccharomyces cerevisiae*. *Molecular and Cellular Biology*, **26**, 6487–6501.
- Green DR (2000). Apoptotic pathways: paper wraps stone blunts scissors. *Cell*, **102**, 1–4.
- Greenberg JT, Yao N (2004). The role and regulation of programmed cell death in plant-pathogen interactions. *Cell Microbiology*, **6**, 201-211.
- Gross P, Julius C, Schmeltzer E, Hahlbrock K (1993). Translocation of cytoplasm and nucleus to fungal penetration sites is associated with depolymerisation of microtubules and defense gene activation in infected, cultured parsley cells. *EMBO Journal*. **12**, 1735-1744.
- Gu T, Mazzurco M, Sulaman W, Matias DD, Goring DR (1998). Binding of an arm repeat protein to the kinase domain of the S-locus receptor kinase. *PNAS*, **95**, 382–87.
- Gu Y, Vernoud V, Fu Y, Yang Z. (2003). ROP GTPase regulation of pollen tube growth through the dynamics of tip-localized F-actin. *Journal of Experimental Botany*, **54**, 93-101.

- Gungabissoon RA, Jiang CJ, Drobak BK, Maciver SK, Hussey PJ (1998). Interaction of maize actin-depolymerising factor with actin and phosphoinositides and its inhibition of plant phospholipase C. *Plant Journal*, **16**, 689-696.
- Haarer BK, Brown SS (1990). Structure and function of profilin. *Cell Motility and the Cytoskeleton*, **17**, 71-74.
- Hadjosif N (2008). Functional characterisation of PrpS, a pollen S-locus gene that is required for the self-incompatibility reaction in *Papaver rhoeas*. A thesis submitted to the University of Birmingham, UK.
- Hamada T (2007). Microtubule-associated proteins in higher plants. *Journal of Plant Research*, **120**, 79-98.
- Hamada T, Igarashi H, Itoh TJ, Shimmen T, Sonobe S (2004). Characterization of a 200 kDa microtubule-associated protein of tobacco BY-2 cells, a member of the XMAP215/MOR1 family. *Plant Cell Physiology*, **45**, 1233-1242.
- Hancock CN, Kent L, BA McClure (2005) The 120 kDa glycoprotein is required for S-specific pollen rejection in *Nicotiana*. *Plant Journal*, **43**, 716–723.
- Hasezawa S, Ueda K, Kumagai F (2000). Time-sequence observations of microtubule dynamics throughout mitosis in living cell suspensions of stable transgenic Arabidopsis - direct evidence for the origin of cortical microtubules at M/G1 interface. *Plant and Cell Physiology*, **41**, 244-250.
- Hashimoto K, Igarashi H, Mano S, Nishimura M, Shimmen T, Yokota E (2005). Peroxisomal localization of a Myosin XI isoform in *Arabidopsis thaliana*. *Plant and Cell Physiology*, **4**, 782-789.
- Hashimoto K, Igarashi H, Mano S, Takenaka C, Shiina T, Yamaguchi M, Demura T, Nishimura M, Shimmen T, Yokota E (2008). An isoform of *Arabidopsis* myosin XI interacts with small GTPases in its C-terminal tail region. *Journal of Experimental Botany*, **59**, 3523–3531.
- Hatsugai N, Kuroyanagi M, Yamada K, Meshi T, Tsuda S, Kondo M, Nishimura M, Hara-Nishimura I (2004). A plant vacuolar protease, VPE, mediates virus-induced hypersensitive cell death. *Science*, **305**, 855–858.
- Haug JM (2002) Localization of Receptor-Mediated Signal Transduction Pathways: The Inside Story. *Molecular Interventions*, **2**, 292-307.
- Hawkins M, Pope B, Maciver SK, Weeds AG (1993). Human actin depolymerizing factor mediates a pH-sensitive destruction of actin filaments. *Biochemistry*, **32**, 9985-93.
- Hayden SM, Miller PS, Brauweiler A, Bamberg JR (1993) Analysis of the interactions of actin depolymerizing factor with G- and F-actin. *Biochemistry*, **32**, 9994-10004.
- He R, Drury GE, Rotari VI, Gordon A, Willer M, Tabasum F, Woltering EJ, Gallois P (2007). Metacaspase-8 modulates programmed cell death induced by UV and H₂O₂ in *Arabidopsis*. *Journal of Biological Chemistry*, **283**, 774–783.
- Hearn MJ, Franklin FCH, Ride JP (1996) Identification of a membrane glycoprotein in pollen of *Papaver rhoeas* which binds stigmatic self-incompatibility (S-) proteins. *Plant Journal*, **9**, 467-475.
- Hemmingsen SM (1992). What is a chaperonin? *Nature*, **357**, 650.
- Hemmingsen SM, Woolford C, van der Vies SM, Tilly K, Dennis DT, Georgopoulos CP, Hendrix RW, Ellis RJ (1988). Homologous plant and bacterial proteins chaperone oligomeric protein assembly. *Nature*, **333**, 330-334
- Henriquez M, Armisén R, Stutzin A, Quest AF. (2008). Cell death by necrosis, a regulated way to go. *Current Molecular Medicine*, **8**, 187-206.

- Hepler P, Vidali L, Cheung A (2001). Polarized cell growth in higher plants. *Annual. Review of Cell Developmental Biology*, **17**, 159-187.
- Heslop-Harrison J, Heslop-Harrison Y (1990). Dynamic aspects of the apical zonation in the angiosperm pollen tube. *Sexual Plant Reproduction*, **3**, 187-194.
- Heslop-Harrison J, Heslop-Harrison Y, Cresti M, Tiezzi A, Moscatelli A. 1988. Cytoskeletal elements, cell shaping and movement in the angiosperm pollen tube. *Journal of Cell Science*, **91**, 49-60.
- Heslop-Harrison J, Heslop-Harrison Y. (1989). Myosin associated with the surface of organelles, vegetative nuclei and generative cells in angiosperm pollen grains and tubes. *Journal of Cell Science*, **94**, 319-325.
- Higaki T, Goh T, Hayashi T, Kutsuna N, Kadota Y, Hasezawa S, Sano T, Kuchitsu K, (2007). Elicitor-induced cytoskeletal rearrangement relates to vacuolar dynamics and execution of cell death: in vivo imaging of hypersensitive cell death in tobacco BY-2 cells. *Plant and Cell Physiology*, **48**, 1414-1425.
- Hill JE, Hemmingsen SM (2001). *Arabidopsis thaliana* type I and II chaperonins. *Cell Stress Chaperones*, **6**, 190-200.
- Himmelspach R, Wymer CL, Lloyd CW, Nick P (1999) Gravity-induced reorientation of cortical microtubules observed in vivo. *The Plant Journal*, **18**, 449-453
- Hirano A. (1994). Hirano bodies and related neuronal inclusions. *Neuropathology and Applied Neurobiology*, **20**, 3-11.
- Hiscock SJ, McInnis SM (2003) Pollen recognition and rejection during the sporophytic self-incompatibility response: Brassica and beyond. *Trends in Plant Science*, **8**, 606-613.
- Hoerberichts FA, Woltering EJ (2003). Multiple mediators of plant programmed cell death: interplay of conserved cell death mechanisms and plant-specific regulators. *BioEssays*, **25**, 47-57.
- Holdaway-Clarke TL, Feijó JA, Hackett GR, Kunkel JG, Hepler PK (1997). Pollen tube growth and the intracellular cytosolic calcium gradient oscillate in phase while extracellular calcium influx is delayed. *The Plant Cell*, **9**, 1999-2010.
- Huang S, Blanchoin L, Kovar DR, Staiger CJ (2003). *Arabidopsis* capping protein (AtCP) is a heterodimer that regulates assembly at the barbed ends of actin filaments. *Journal of Biological Chemistry*, **278**, 44832-44842.
- Huang S, Blanchoin L, Chaudhry F, Franklin-Tong VE, Staiger CJ (2004). A gelsolin-like protein from *Papaver rhoeas* pollen (PrABP80) stimulates calcium-regulated severing and depolymerization of actin filaments. *The Journal of Biological Chemistry*, **279**, 23364-23375.
- Huang S, Robinson RC, Gao LY, Matsumoto T, Brunet A, Blanchoin L, Staiger CJ (2005). *Arabidopsis* VILLIN1 generates actin filament cables that are resistant to depolymerization. *The Plant Cell*, **17**, 486-501.
- Huang S, Gao L, Blanchoin L, Staiger CJ (2006). Heterodimeric capping protein from *Arabidopsis* is regulated by phosphatidic acid. *Molecular Biology of the Cell*, **17**, 1946-1958.
- Huang Y, Tran PT, Oliferenko S, Balasubramanian MK. (2007). Assembly of Microtubules and Actomyosin Rings in the Absence of Nuclei and Spindle Pole Bodies Revealed by a Novel Genetic Method. *PLoS ONE*, **7**, e618.
- Hubberstey AV, Mottillo EP (2002). Cyclase-associated proteins: CAPacity for linking signal transduction and actin polymerization. *FASEB Journal*, **16**, 487-499.

- Hussey PJ, Hawkins TJ, Igarashi H, Kaloriti D, Smertenko A (2002). The plant cytoskeleton: recent advances in the study of the plant microtubule-associated proteins MAP-65, MAP-190 and the Xenopus MAP215-like protein, MOR1. *Plant Molecular Biology*, **50**, 915-924.
- Hussey PJ, Ketelaar T, Deeks MJ (2006). Control of the actin cytoskeleton in plant cell growth. *Annual Reviews of Plant Biology*, **57**, 109-25.
- Ichetovkin I, Grant W, Condeelis J (2002). Cofilin Produces Newly Polymerized Actin Filaments that Are Preferred for Dendritic Nucleation by the Arp2/3 Complex. *Current Biology*, **12**, 79-84.
- Igarashi H, Orii H, Mori H, Shimmen T, Sonobe S (2000). Isolation of a Novel 190 kDa Protein from Tobacco BY-2 Cells: Possible Involvement in the Interaction between Actin Filaments and Microtubules. *Plant and Cell Physiology*, **41**, 920-931.
- Ioerger TR, Clark AG, Kao T-H (1990). Polymorphism at the self-incompatibility locus in *Solanaceae* predates speciation. *PNAS*, **87**, 9732-9735.
- Ioerger TR, Gohlke J, Xu B, Kao T-H (1991). Primary structural features of the self-incompatibility protein in *Solanaceae*. *Sexual Plant Reproduction*, **4**, 81-87.
- Ishihama Y, Oda Y, Tabata T, Sato T, Nagasu T, Rappsilber J, Mann M (2005). Exponentially modified protein abundance index (emPAI) for estimation of absolute protein amount in proteomics by the number of sequenced peptides per protein, *Molecular & Cellular Proteomics*, **4**, 1265-1272.
- Iwano M, Shiba H, Matoba K, Miwa T, Funato M, Entani T, Nakayama P, Shimosato H, Takaoka A, Isogai A, Takayama S (2007). Actin dynamics in papilla cells of *Brassica rapa* during self- and cross-pollination. *Plant Physiology*, **144**, 72-81.
- Jauh GY, Lord EM (1995). Movement of the tube cell in the lily style in the absence of the pollen grain and the spent pollen tube. *Sexual Plant Reproduction*, **8**, 168-172.
- Jiang C, Sonobe S (1993) Identification and preliminary characterization of a 65 kDa higher-plant microtubule-associated protein. *Journal of Cell Science*, **105**, 891-901.
- Joos U, Vankken J, Kristen U (1994). Microtubules are involved in maintaining the cellular polarity in pollen tubes of *Nicotiana-sylvestris*. *Protoplasma*, **179** (1-2), 5-15.
- Joos U, Vankken J, Kristen U (1995). The anti-microtubule drug carbetamide stops *Nicotiana-sylvestris* pollen-tube growth in the style. *Protoplasma*, **187** (1-4), 182-191.
- Jordan N, Franklin FCH, Franklin-Tong VE (2000). Evidence for DNA fragmentation triggered in the self-incompatibility response in pollen of *Papaver rhoeas*. *Plant Journal*, **23**, 471-479.
- Jordan N, Kakeda K, Conner A, Ride JP, Franklin-Tong VE, Franklin FCH (1999). S-protein mutants indicate a functional role for SBP in the self-incompatibility reaction of *Papaver rhoeas*. *The Plant Journal*, **20**, 119-125.
- Kachroo A, Schopfer CR, Nasrallah ME, Nasrallah JB (2001). Allele-specific receptor-ligand interactions in Brassica self-incompatibility. *Science*, **293**, 1824-1826.
- Kadota A, Wada M (1992). The Circular Arrangement of Cortical Microtubules around the Subapex of Tip-Growing Fern Protonemata Is Sensitive to Cytochalasin B. *Plant and Cell Physiology*, **33**, 99-102.
- Kakeda K, Jordan ND, Conner A, Ride JP, Franklin-Tong VE, Franklin FCH (1998). Identification of Residues in a Hydrophilic Loop of the *Papaver rhoeas* S Protein That Play a Crucial Role in Recognition of Incompatible Pollen. *The Plant Cell*, **10**, 1723-1731.

- Kang E, Purich DL, Southwick FS (1999). Profilin promotes barbed end actin filament assembly without lowering the critical concentration. *Journal of Biological Chemistry*, **274**, 36963-36972.
- Kawamukai, M, Gerst, J, Field J, Riggs M, Rodgers L, Wigler M, Young D. (1992). Genetic and biochemical analysis of the adenylyl cyclase-associated protein, cap, in *Schizosaccharomyces pombe*. *Molecular Biology of the Cell*, **3**, 167-180.
- Kawamura E, Wasteneys GO (2008). MOR1, the *Arabidopsis thaliana* homologue of Xenopus MAP215, promotes rapid growth and shrinkage, and suppresses the pausing of microtubules *in vivo*. *Journal of Cell Science*, **121**, 4114-23.
- Kayalar C, Ord T, Testa MP, Zhong LT, Bredesen DE (1996). Cleavage of actin by interleukin 1 beta-converting enzyme to reverse DNase I inhibition. *PNAS*, **93**, 2234-2238.
- Keith C, Dipaola M, Maxfield FR, Shelanski ML (1983). Microinjection of calcium-calmodulin causes a localised depolymerisation of microtubules. *The Journal of Cell Biology*, **97**, 1918-1924.
- Kerr JFR, Wyllie AH, Currie AR (1972). Apoptosis: a basic biological phenomenon with wide-ranging implications in tissue kinetics. *British Journal of Cancer*, **26**, 239-257.
- Ketelaar T, Faivre-Moskalenko C, Esseling JJ, de Ruijter NC, Grierson CS, Dogterom M, Emons AM (2002). Positioning of nuclei in Arabidopsis root hairs: an actin-regulated process of tip growth. *The Plant Cell*, **14**, 2941-2955.
- Ketelaar T, Allwood EG, Anthony R, Voigt B, Menzel D, Hussey PJ (2004a). The actin-interacting protein AIP1 is essential for actin organization and plant development. *Current Biology*, **14**, 145-149.
- Ketelaar T, Anthony RG, Hussey PJ (2004b). Green fluorescent protein mTalin causes defects in actin organization and cell expansion in *Arabidopsis* and inhibits actin depolymerizing factor's actin depolymerizing activity *in vitro*. *Plant Physiology*, **136**, 3990-3998.
- Kheyr-Pour A, Bintrim SB, Ioerger TR, Remy R, Hammond SA, Kao T-H (1990). Sequence diversity of pistil S-proteins associated with gametophytic self-incompatibility in *Nicotiana glauca*. *Sexual Plant Reproduction*, **3**, 88-97.
- Kim SR, Kim Y, An G (1993). Molecular cloning and characterization of anther-preferential cDNA encoding a putative actin-depolymerizing factor. *Plant Molecular Biology*, **21**, 39-45.
- Klahre U, Friederich E, Kost B, Louvard D, Chua NH (2000). Villin-like actin binding proteins are expressed ubiquitously in *Arabidopsis*. *Plant Physiology*, **122**, 35-47.
- Kobayashi I, Kobayashi Y, Hardham AR (1994). Dynamic reorganization of microtubules and microfilaments in flax cells during the resistance response to flax rust infection. *Planta*, **195**, 237-247.
- Kobayashi Y, Kobayashi I, Funaki Y, Fujimoto S, Takemoto T, Kunoh H (1997a). Dynamic reorganization of microfilaments and microtubules is necessary for the expression of non-host resistance in barley coleoptile cells. *Plant Journal*, **11**, 525-537.
- Kobayashi Y, Yamada M, Kobayashi I, Kunoh H. (1997b). Actin Microfilaments are required for the expression of non-host resistance in higher plants. *Plant and Cell Physiology*, **38**, 725-733.
- Kost B (2008). Spatial control of Rho (Rac-Rop) signaling in tip-growing plant cells. *Trends in Cell Biology*, **18**, 119-27.

- Kost B, Spielhofer P, Chua NH. 1998. A GFP-mouse talin fusion protein labels plant actin filaments in vivo and visualizes the actin cytoskeleton in growing pollen tubes. *Plant Journal*, **16**, 393–401.
- Kovar DR, Drøbak BK, Staiger CJ (2000a). Maize profilin isoforms are functionally distinct. *The Plant Cell*, **12**, 583-598.
- Kovar DR, Staiger CJ, Weaver EA, McCurdy DW (2000b). AtFim1 is an actin filament cross-linking protein from *Arabidopsis thaliana*. *Plant Journal*, **24**, 625-636.
- Kovar DR, Yang P, Sale WS, Drøbak BK, Staiger CJ (2001a). *Chlamydomonas reinhardtii* produces a profilin with unique biochemical properties. *Journal of Cell Science*, **114**, 4293-4305.
- Kovar DR, Gibbon BC, McCurdy DW, Staiger CJ (2001b). Fluorescently-labelled fimbrin decorates a dynamic actin filament network in live plant cells. *Planta*, **213**, 390-395.
- Koyasu S, Nishida E, Kadowaki T, Matsuzaki F, Iida K, Harada F, Kasuga M, Saiki H, Yahara I (1986). Two mammalian heat shock proteins, HSP90 and HSP100, are actin-binding proteins. *PNAS*, **83**, 8054-8058.
- Krichevsky A, Kozlovsky SV, Tian GW, Chen MH, Zaltsman A, Citovsky V (2007). How pollen tubes grow. *Developmental Biology*, **303**, 405-420.
- Krogan NJ, Cagney G, Yu H, Zhong G, Guo X, Ignatchenko A, Li J, Pu S, Datta N, Tikuisis AP, Punna T, Peregrín-Alvarez JM, Shales M, Zhang X, Davey M, Robinson MD, Paccanaro A, Bray JE, Sheung A, Beattie B, Richards DP, Canadien V, Lalev A, Mena F, Wong P, Starostine A, Canete MM, Vlasblom J, Wu S, Orsi C, Collins SR, Chandran S, Haw R, Rilstone JJ, Gandi K, Thompson NJ, Musso G, St Onge P, Ghanny S, Lam MH, Butland G, Altaf-Ul AM, Kanaya S, Shilatifard A, O'Shea E, Weissman JS, Ingles CJ, Hughes TR, Parkinson J, Gerstein M, Wodak SJ, Emili A, Greenblatt JF (2006). Global landscape of protein complexes in the yeast *Saccharomyces cerevisiae*. *Nature*, **440**, 637–643.
- Kropf DL, Bisgrove SR, Hable WE. 1998. Cytoskeletal control of polar growth in plant cells. *Current Opinions in Cell Biology*, **10**, 117–122.
- Kumar S (2007). Caspase function in programmed cell death. *Cell Death and Differentiation*, **14**, 32–43.
- Kuroyanagi M, Yamada K, Hatsugai N, Kondo M, Nishimura M, Hara-Nishimura I (2005). VPE is essential for mycotoxin-induced cell death in *Arabidopsis thaliana*. *Journal of Biological Chemistry*, **280**, 32914–32920.
- Kurup S, Ride J, Jordan N, Fletcher G, Franklin-Tong V, Franklin F (1998). Identification and cloning of related self-incompatibility S-genes in *Papaver rhoeas* and *Papaver nudicaule*. *Sexual Plant Reproduction*, **11**, 192-198.
- Kusaba, M., T. Nishio, Y. Satta, K. Hinata and D. Ockendon, 1997 Striking sequence similarity in inter- and intra-specific comparisons of class I *SLG* alleles from *Brassica oleracea* and *Brassica campestris*: implications for the evolution and recognition mechanism. *PNAS*, **94**, 7673–7678.
- Kusano K, Abe H, Obinata T (1999). Detection of a sequence involved in actin-binding and phosphoinositide-binding in the N-terminal side of cofilin. *Molecular and Cellular Biochemistry*, **190**, 133–141.
- Lai Z, Ma W, Han B, Liang L, Zhang Y, Hong G, Xue Y (2002). An F-box gene linked to the self-incompatibility (S) locus of *Antirrhinum* is expressed specifically in pollen and tapetum. *Plant Molecular Biology*, **50**, 29–42.

- Laitainen E, Nieminen KM, Vihinen H, Raudaskoski M (2002). Movement of generative cell and vegetative nucleus in tobacco pollen tubes is dependent on microtubule cytoskeleton but independent of the synthesis of callose plugs. *Sexual Plant Reproduction*, **15**, 195-204.
- Lam E (2004). Controlled cell death, plant survival and development. *Nature Reviews, Molecular Cell Biology*, **5**, 305-315.
- Lam E, del Pozo O (2000). Caspase-like protease involvement in the control of plant cell death. *Plant Molecular Biology*, **44**, 417-428.
- Lam E, Kato N, Lawton M (2001). Programmed cell death, mitochondria and the plant hypersensitive response. *Nature*, **411**, 848-853.
- Lancelle, SA; Hepler, PK (1991). Association of actin with cortical microtubules revealed by immunogold localization in *Nicotiana* pollen tubes. *Protoplasma*, **165**, 167-172.
- Lane M, Lawrence M (1993). The population genetics of the self-incompatibility polymorphism in *Papaver rhoeas*. *Heredity*, **71**, 596-602.
- Le Clainche C, Carlier MF (2008). Regulation of actin assembly associated with protrusion and adhesion in cell migration. *Physiological Reviews*, **88**, 489-513.
- Lee H-S, Huang S, Kao T-H (1994) S proteins control rejection of incompatible pollen in *Petunia inflata*. *Nature*, **367**, 560-563.
- Lee YR, Liu B (2004) Cytoskeletal motors in *Arabidopsis*. Sixty-one kinesins and seventeen myosins. *Plant Physiology*, **136**, 3877-3883.
- Levee MG, Dabrowska MI, Lelli JL Jr, Hinshaw DB (1996). Actin polymerization and depolymerization during apoptosis in HL-60 cells. *The American Journal of Physiology*, **271**, C1981-C1992.
- Lew DJ (2002) Formin' actin filament bundles. *Nature Cell Biology*, **4**, E29-E30.
- Li S, Samaj J, Franklin-Tong VE (2007). A mitogen-activated protein kinase signals to programmed cell death induced by self-incompatibility in *Papaver* pollen. *Plant Physiology*, **145**, 236-245.
- Li Y-Q, Faleri C, Geitmann A, Zhang H-Q, Cresti M (1995). Immunogold localization of arabinogalactan proteins, unesterified and esterified pectins in pollen grains and pollen tubes of *Nicotiana tabacum* L. *Protoplasma*, **189**, 26-36.
- Liang P, MacRae TH (1997). Molecular chaperones and the cytoskeleton. *Journal of Cell Science*, **110**, 1431-1440.
- Liebe S, Menzel D (1995). Actomyosin-based motility of endoplasmic reticulum and chloroplasts in *Vallisneria mesophyll* cells. *Biology of the Cell*, **85**, 207-222.
- Lieto AM, Cush RC, Thompson NL (2003). Ligand-receptor kinetics measured by total internal reflection with fluorescence correlation spectroscopy. *Biophysical Journal*, **85**, 3294-3302.
- Lila T, Drubin DG (1997). Evidence for physical and functional interactions among two *Saccharomyces cerevisiae* SH3 domain proteins, an adenylyl cyclase-associated protein and the actin cytoskeleton. *Molecular Biology of the Cell*, **8**, 367-385.
- Lind JL, Bönig I, Clarke AE, Anderson MA (1996). A style-specific 120 kDa glycoprotein enters pollen tubes of *Nicotiana glauca* *in vivo*. *Sexual Plant Reproduction*, **9**, 75-86.
- Liu B-Q, Jin L, Zhu L, Li J, Huang S, Yuan M (2009). Phosphorylation of Microtubule-associated Protein SB401 from *Solanum berthaultii* Regulates Its Effect on Microtubules. *Journal of Integrative Plant Biology*, **51**, 235-242.
- Liu X, Yue Y, Li B, Nie Y, Li W, Wu WH, Ma L (2007). A G protein-coupled receptor is a plasma membrane receptor for the plant hormone abscisic acid. *Science*, **315**, 1712-1716.

- Liu ZQ, Xu GH, Zhang SL (2007). *Pyrus pyrifolia* stylar S-RNase induces alterations in the actin cytoskeleton in self-pollen and tubes in vitro. *Protoplasma*, **232**, 61-67.
- Lloyd C, Chan J (2004). Microtubules and the shape of plants to come. *Molecular cell Biology*, **5**, 13-22.
- Lloyd C, Chan J (2008). The parallel lives of microtubules and cellulose microfibrils. *Current Opinion in Plant Biology*, **11**, 641–646.
- Lopez I, Anthony RG, Maciver SK, Jiang CJ, Khan S, Weeds AG, Hussey PJ (1996). Pollen specific expression of maize genes encoding actin depolymerizing factor-like proteins. *PNAS*, **93**, 7415-7420.
- Lovy-Wheeler A, Wilsen KL, Baskin TI, Hepler PK. (2005). Enhanced fixation reveals the apical cortical fringe of actin filaments as a consistent feature of the pollen tube. *Planta*, **221**, 95–104.
- Lovy-Wheeler A, Kunkel JG, Allwood EG, Hussey PJ, Hepler PK. (2006). Oscillatory increases in alkalinity anticipate growth and may regulate actin dynamics in pollen tubes of lily. *The Plant Cell*, **18**, 2182-93.
- Lovy-Wheeler A, Cardenas L, Kunkel JG, Hepler PK (2007). Differential organelle movement on the actin cytoskeleton in lily pollen tubes. *Cell Motility and the Cytoskeleton*, **64**, 217–232.
- Lu G, Sehnke PC, Ferl RJ (1994). Phosphorylation and calcium binding properties of an Arabidopsis GF14 brain protein homolog. *The Plant Cell*, **6**, 501–510.
- Lüthi AU, Martin SJ (2007). The CASBAH: a searchable database of caspase substrates. *Cell Death and Differentiation*, **14**, 641–650.
- Luu D-T, Xike, Q, Morse D, Cappadocia M (2000). S-RNase uptake by compatible pollen tubes in gametophytic self-incompatibility. *Nature* **407**, 649–651.
- Ma Q-H (2007). Small GTP-binding Proteins and their Functions in Plants. *Journal of Plant Growth Regulation*, **26**, 369–388.
- Macejak DG, Luftig RB. (1991). Stabilization of actin filaments at early times after adenovirus infection and in heat-shocked cells. *Virus Research*, **19**, 31-46.
- Machesky LM, Atkinson SJ, Ampe C, Vandekerckhove J, Pollard TD (1994). Purification of a cortical complex containing two unconventional actins from *Acanthamoeba* by affinity chromatography on profilin-agarose. *Journal of Cell Biology*, **127**, 107-115.
- Machesky LM, Gould KL (1999). The ARP2/3 complex: a multifunctional actin organiser. *Current Opinion in Cell Biology*, **11**, 117-121.
- Machesky LM, Insall RH (1998). Scar1 and the related Wiskott-Aldrich syndrome protein WASP, regulate the actin cytoskeleton through the ARP2/3 complex. *Current Biology*, **8**, 1347-1356.
- Maciver SK, Harrington CR (1995). Two actin-binding proteins, actin depolymerizing factor and cofilin, are associated with hirano bodies. *Neuroreport*, **6**, 1985-1988.
- Maekawa S, Sakai H (1987). A novel 60-kDa smooth muscle protein that binds filamin-actin filament complex. *FEBS Letters*, **221**, 68-72.
- Malhó R, Read N, Pais M, Trewavas A. (1994). Role of cytosolic calcium in the reorientation of pollen tube growth. *Plant Journal*, **5**, 331-341.
- Manzano C, Abraham Z, Lopez-Torres G, Del Pozo JC (2008). Identification of ubiquitinated proteins in *Arabidopsis*. *Plant Molecular Biology*, **68**, 145–158.
- Mao G, Chan J, Calder G, Doonan JH, Lloyd CW (2005). Modulated targeting of GFP-AtMAP65-1 to central spindle microtubules during division. *Plant Journal*, **43**, 469–478.

- Marc J, Sharkey DE, Durso NA, Zhang M, Cyr RJ (1996). Isolation of a 90-kD microtubule-associated protein from Tobacco membranes. *The Plant Cell*, **8**, 2127–2138.
- Mascarenhas JP (1993). Molecular mechanisms of pollen tube growth and differentiation. *The Plant Cell*, **5**, 1303–1314.
- Maselli AG, Davis R, Furukawa R, Fechheimer M (2002). Formation of Hirano bodies in *Dictyostelium* and mammalian cells induced by expression of a modified form of an actin-crosslinking protein. *Journal of Cell Science*, **115**, 1939-1949.
- Mathur J, Mathur N, Kernebeck B, Srinivas BP, Hulskamp M (2003). A novel localization pattern for an EB1-like protein links microtubule dynamics to endomembrane organization. *Current Biology*, **13**, 1991-1997.
- Matsudaira PT, Burgess DR (1979). Identification and organization of the components in the isolated microvillus cytoskeleton. *Journal of Cell Biology*, **83**, 667-673.
- Matsuyama S, Reed JC (2000). Mitochondria-dependent apoptosis and cellular pH regulation. *Cell Death and Differentiation*, **7**, 1155-65.
- Matviw H, Yu G, Young, D (1992). Identification of a human cDNA encoding a protein that is structurally and functionally related to the yeast adenylyl cyclase-associated CAP proteins. *Molecular Cell Biology*, **12**, 5033-5040.
- Mazzurco M, Sulaman W, Elina H, Cock JM, Goring DR. (2001). Further analysis of the interactions between the *Brassica* S receptor kinase and three interacting proteins (ARC1, THL1 and THL2) in the yeast two-hybrid system. *Plant Molecular Biology*, **45**, 365–76.
- McClure BA, Haring V, Ebert PR, Anderson MA, Simpson RJ, Sakiyama F, Clarke A (1989). Style self-incompatibility gene products of *Nicotiana glauca* are ribonucleases. *Nature*, **342**, 955–957.
- McClure BA, Mou B, Canevascini S, Bernatzky R (1999). A small asparagine-rich protein required for S-allele-specific pollen rejection in *Nicotiana*. *PNAS*, **96**, 13548-13553.
- McClure BA, Cruz-Garcia F, Beecher BS, Sulaman W (2000) Factors affecting inter- and intra-specific pollen rejection in *Nicotiana*. *Annals of Botany*, **85**, 113–123.
- McClure B (2004). S-RNase and SLF determine S-haplotype-specific pollen recognition and rejection. *The Plant Cell*, **16**, 2840-2847.
- McClure BA, Franklin-Tong VE (2006). Gametophytic self-incompatibility: understanding the cellular mechanisms involved in "self" pollen tube inhibition. *Planta*, **224**, 233-245.
- McCurdy DW, Kim M (1998). Molecular cloning of a novel fimbrin-like cDNA from *Arabidopsis thaliana*. *Plant Molecular Biology*, **36**, 23-31.
- McCurdy DW, Kovar DR, Staiger CJ. (2001). Actin and actin-binding proteins in higher plants. *Protoplasma*, **215**, 89-104.
- McGough A, Pope B, Chiu W, Weeds A (1997). Cofilin changes the twist of F-actin: implications for actin filament dynamics and cellular function. *Journal of Cell Biology*, **138**, 771-781.
- McGough AM, Staiger CJ, Min JK, Simonetti KD (2003). The gelsolin family of actin regulatory proteins: modular structures, versatile functions. *FEBS Letters*, **552**, 75-81.
- McNally FJ, Vale RD (1993). Identification of katanin, an ATPase that severs and disassembles stable microtubules. *Cell*, **75**, 419-29.
- Meagher RB, Williamson RE (1994). The plant cytoskeleton. In: Meyerowitz EM, Sommerville CR, editors. *Arabidopsis. The Plant Cytoskeleton*. Cold Spring Harbor, NY: Cold Spring Harbor Laboratory Press, 1049–1084.
- Miaczynska M, Pelkmans L, Zerial M (2004) Not just a sink: endosomes in control of signal transduction. *Current Opinions in Cell Biology*, **16**, 400–406.

- Michard E, Dias P, Feijó JA (2008). Tobacco pollen tubes as cellular models for ion dynamics: improved spatial and temporal resolution of extracellular flux and free cytosolic concentration of calcium and protons using pHluorin and YC3.1 CaMeleon. *Sexual Plant Reproduction*, **21**, 169-181.
- Michelot A, Guérin C, Huang S, Ingouff M, Richard S, Rodiuc N, Staiger CJ, Blanchoin L (2005). The formin homology 1 domain modulates the actin nucleation and bundling activity of *Arabidopsis* FORMIN1. *The Plant Cell*, **17**, 2296-313.
- Michelot A, Derivery E, Paterski-Boujemaa R, Guerin C, Huang S, Parcy F, Staiger CJ, Blanchoin L (2006). A novel mechanism for the formation of actin-filament bundles by a nonprocessive formin. *Current Biology*, **19**, 1924-1930.
- Michie KA, Löwe J (2006). Dynamic filaments of the bacterial cytoskeleton. *Annual Review of Biochemistry*, **75**, 467-492.
- Milioni D, Hatzopoulos P (1997). Genomic organization of hsp90 gene family in *Arabidopsis*. *Plant Molecular Biology*, **35**, 955-61.
- Miller D, Callahan D, Gross D, Hepler P (1992). Free calcium gradient in growing pollen tubes of *Lilium*. *Journal of Cell Science*, **101**, 7-12.
- Mintzer KA, Field J (1994). Interactions between adenyl cyclase, CAP and RAS from *Saccharomyces cerevisiae*. *Cellular Signalling*, **6**, 681-694.
- Miron T, Wilchek M, Geiger B (1988). Characterization of an inhibitor of actin polymerization in vinculin-rich fraction of turkey gizzard smooth muscle. *European Journal of Biochemistry*, **178**, 543-553.
- Miron T, Vancompernelle K, Vandekerckhove J, Wilchek M, Geiger B. (1991). A 25-kD inhibitor of actin polymerization is a low molecular mass heat shock protein. *Journal of Cell Biology*, **114**, 255-261.
- Mittler, R, Lam, E (1996). Sacrifice in the face of foes: pathogen-induced programmed cell death in plants. *Trends in Microbiology*, **4**, 10-15.
- Mittermann I, Swoboda I, Pierson E, Eller N, Kraft D, Valenta R, Heberle-Bors E (1995). Molecular cloning and characterization of profilin from tobacco (*Nicotiana tabacum*): increased profilin expression during pollen maturation. *Plant Molecular Biology*, **27**, 137-146.
- Mollinedo F, Gajate C (2003). Microtubules, microtubule-interfering agents and apoptosis. *Apoptosis*, **8**, 413-450.
- Moon A, Drubin DG (1995). The ADF/cofilin proteins: stimulus-responsive modulators of actin dynamics. *Molecular Biology of the Cell*, **6**, 1423-1431.
- Moriyama K, Yahara I (2002). Human CAP1 is a key factor in the recycling of cofilin and actin for rapid actin turnover. *Journal of Cell Science*, **115**, 1591-1601.
- Morley SC, Sun GP, Bierer BE (2003). Inhibition of actin polymerization enhances commitment to and execution of apoptosis induced by withdrawal of trophic support. *Journal of Cellular Biochemistry*, **88**, 1066-1076.
- Morton WM, Ascough KR, McLaughlin PJ (2000). Latrunculin alters the actin monomer subunit interface to prevent polymerisation. *Nature Cell Biology*, **2**, 376-378.
- Moscattelli A, Ciampolini F, Rodighiero S, Onelli E, Cresti M, Santo N, Idilli A (2007). Distinct endocytic pathways identified in tobacco pollen tubes using charged nanogold. *Journal of Cell Science*, **120**, 3804-3819.
- Moss DK, Lane JD (2006). Microtubules: forgotten players in the apoptotic execution phase. *Trends in Cell Biology*, **16**, 330-338.
- Mounier N, Arrigo AP (2002). Actin cytoskeleton and small heat shock proteins: how do they interact? *Cell Stress Chaperones*, **7**, 167-176.

- Muller S, Han S, Smith LG (2006). Two kinesins are involved in the spatial control of cytokinesis in *Arabidopsis thaliana*. *Current Biology*, **16**, 888–894.
- Mullins RD, Heuser JA, Pollard TD (1998). The interaction of Arp2/3 complex with actin: nucleation, high affinity pointed end capping, and formation of branching networks of filaments. *PNAS*, **95**, 6181-6186.
- Munday AD, Berndt MC, Mitchell CA (2000). Phosphoinositide 3-kinase forms a complex with platelet membrane glycoprotein Ib-IX-V complex and 14-3-3zeta. *Blood*, **96**, 577-584.
- Murase K, Shiba H, Iwano M, Che F-S, Watanabe M, Isogai A, Takayama S (2004). A membrane-anchored protein kinase involved in *Brassica* self-incompatibility signaling. *Science*, **303**, 1516–19.
- Murfett J, Atherton TL, Mou B, Gasser CS, McClure BA (1994) SRNase expressed in transgenic *Nicotiana* causes S-allele-specific pollen rejection. *Nature*, **367**, 563–566.
- Nakaune S, Yamada K, Kondo M, Kato T, Tabata S, Nishimura M, Hara-Nishimura I. (2005). A vacuolar processing enzyme, {delta}VPE, is involved in seed coat formation at the early stage of seed development. *The Plant Cell*, **17**, 876–887.
- Nakayasu T, Yokota E, Shimmen T (1998). Purification of an actin binding protein composed of 115-kDa polypeptide from pollen tubes of lily. *Biochemical and Biophysical Research Communications*, **294**, 61-65.
- Nam KH, Li J (2002). BRI1/BAK1, a receptor kinase pair mediating brassinosteroid signaling. *Cell*, **110**, 203-212.
- Namba Y, Ito M, Zu Y, Shigesada K, Maruyama K (1992). Human T cell L-plastin bundles actin filaments in a calcium-dependent manner. *Journal of Biochemistry*, **112**, 503-507.
- Nasrallah JB, Kao TH, Chen C-H, Goldberg ML, Nasrallah ME (1987). Amino-acid sequence of glycoproteins encoded by three alleles of the S locus of *Brassica oleracea*. *Nature*, **326**, 617-619.
- Nasrallah JB (2002). Recognition and rejection of self in plant reproduction. *Science*, **296**, 305–308.
- Nebenfuhr A, Gallagher LA, Dunahay TG, Frohlick JA, Mazurkiewicz AM, Meehl JB, Staehelin LA (1999). Stop-and-go movements of plant Golgi stacks are mediated by the actomyosin system. *Plant Physiology*, **121**, 1127-1142.
- Nibau C, Wu HM, Cheung AY (2006). RAC/ROP GTPases: ‘hubs’ for signal integration and diversification in plants. *Trends in Plant Science*, **11**, 309–315.
- Nick P (1999). Signals, motors, morphogenesis - the cytoskeleton in plant development. *Plant Biology*, **1**, 169-179.
- Nishida E, Maekawa S, Sakai H. (1984). Cofilin, a protein in porcine brain that binds to actin filaments and inhibits their interactions with myosin and tropomyosin. *Biochemistry*, **23**, 5307-5313.
- Nishida E (1985). Opposite effects of cofilin and profilin from porcine brain on rate of exchange of actin-bound adenosine 5'-triphosphate. *Biochemistry*, **24**, 1160-1164.
- Nishida E, Koyasu S, Sakai H, Yahara I (1986). Calmodulin-regulated binding of the 90-kDa heat shock protein to actin filaments. *Journal of Biological Chemistry*, **261**, 16033-16036.
- O'Brien M, Kapfer C, Major G, Laurin M, Bertrand C, Kondo K, Kowyama Y, Matton DP (2002) Molecular analysis of the stylar-expressed *Solanum chacoense* asparagine-rich protein family related to the HT modifier of gametophytic self-incompatibility in *Nicotiana*. *Plant Journal*, **32**, 1–12.

- Obermeyer G, Weisenseel M (1991). Calcium channel blocker and calmodulin antagonists affect the gradient of free calcium ions in lily pollen tubes. *European Journal of Cell Biology*, **56**, 319-327.
- Ockendon DJ (2000). The S-allele collection of *Brassica oleracea*. *Acta Horticulturae*, **539**, 25–30.
- Odaka C, Sanders ML, Crews P (2000). Jasplakinolide induces apoptosis in various transformed cell lines by a caspase-3-like protease-dependent pathway. *Clinical and Diagnostic Laboratory Immunology*, **7**, 947–952.
- Okada K, Obinata T, Abe H. (1999). XAIP1: a *Xenopus* Homologue of Yeast Actin Interacting Protein 1(AIP1), which Induces Disassembly of Actin Filaments Cooperatively with ADF/cofilin Family Proteins. *Journal of Cell Science*, **112**, 1553-1565.
- Ono S (2003). Regulation of actin filament dynamics by actin depolymerizing factor/cofilin and actin-interacting protein 1: new blades for twisted filaments. *Biochemistry*, **42**, 13363-13370.
- Palanivelu R, Brass L, Edlund AF, Preuss D (2003). Pollen tube growth and guidance is regulated by POP2, an *Arabidopsis* gene that controls GABA levels. *Cell*, **114**, 47-59.
- Pantaloni D, Carlier MF (1993). How profilin promotes actin filament assembly in the presence of thymosin beta 4. *Cell*, **75**, 1007-14.
- Paredez AR, Somerville CR, Ehrhardt DW (2006) Visualization of cellulose synthase demonstrates functional association with microtubules, *Science*, **312**, 1491–1495.
- Park SJ, Suetsugu S, Sagara H, Takenawa T (2007). HSP90 cross-links branched actin filaments induced by N-WASP and the Arp2/3 complex. *Genes to Cells*, **12**, 611-622.
- Parton RM, Fischer-Parton S, Watahiki MK, Trewavas AJ (2001). Dynamics of the apical vesicle accumulation and the rate of growth are related in individual pollen tubes. *Journal of Cell Science*, **114**, 2685-2695.
- Paul C, Manero F, Gonin S, Kretz-Remy C, Virost S, Arrigo A-P (2002). Hsp27 as a negative regulator of cytochrome c release. *Molecular & Cellular Biology*, **22**, 816–834.
- Perelroizen I, Marchand J-B, Blanchoin L, Didry D, Carlier M-F (1994) Interaction of profilin with G-actin and poly(L-proline). *Biochemistry*, **33**, 8472-8478.
- Perelroizen I, Didry D, Christensen H, Chua NH, Carlier MF (1996). Role of nucleotide exchange and hydrolysis in the function of profilin in actin assembly. *Journal of Biological Chemistry*, **271**, 12302-12309.
- Pierson ES, Derksen J, Traas JA (1986). Organization of microfilaments and microtubules in pollen tubes grown in vitro or in vivo in various angiosperms. *European Journal of Cell Biology*, **41**, 14-18.
- Pierson E, Cresti M (1992). Cytoskeleton and cytoplasmic organisation of pollen and pollen tubes. *International Review of Cytology*, **140**, 73-125.
- Pierson E, Miller D, Callahan D, Van Aken J, Hackett G, Hepler P. (1996). Tip localized calcium entry fluctuates during pollen tube growth. *Developmental Biology*, **174**, 160-173.
- Pinto DM, Boyd RK, Volmer DA (2002). Ultra-high resolution for mass spectrometric analysis of complex and low-abundance mixtures – the emergence of FTICR-MS as an essential analytical tool. *Analytical and Bioanalytical Chemistry*, **373**, 378–389.
- Pollard TD, Cooper JA (1986). Actin and actin-binding proteins. A critical evaluation of mechanisms and functions. *Annual Reviews Biochemistry*, **55**, 987-1035.
- Posey SC, Bierer BE (1999). Actin stabilization by jasplakinolide enhances apoptosis induced by cytokine deprivation. *Journal of Biological Chemistry*, **274**, 4259–4265.

- Poulter NS, Vatovec S, Franklin-Tong VE (2008). Microtubules are a target for self-incompatibility signaling in *Papaver* pollen. *Plant Physiology*, **146**, 1358-1367.
- Preuss ML, Kovar, DR, Lee, Y-RJ, Staiger, CJ, Delmer, DP, Liu, B (2004). A plant-specific kinesin binds to actin microfilaments and interacts with cortical microtubules in cotton fibers. *Plant Physiology*, **136**, 3945-3955.
- Pruyne D, Evangelista M, Yang C, Bi E, Zigmond S, Bretscher A, Boone C (2002). Role of formins in actin assembly: nucleation and barbed-end association. *Science*, **297**, 612-615.
- Puthalakath H, Huang DCS, O'Reilly LA, King SM, Strasser A (1999). The pro-apoptotic activity of the Bcl-2 family member Bim is regulated by interaction with the dynein motor complex. *Molecular Cell*, **3**, 287-296.
- Puthalakath H, Strasser A (2002). Keeping killers on a tight leash: transcriptional and post-translational control of the pro-apoptotic activity of BH3-only proteins. *Cell Death & Differentiation*, **9**, 505-512.
- Qiao H, Wang F, Zhao L, Zhou J, Lai Z, Zhang Y, Robbins TP, Xue Y (2004a). The F-box protein AhSLF-S2 controls the pollen function of S-RNase-based self-incompatibility. *The Plant Cell*, **16**, 2307-2322.
- Qiao H, Wang H, Zhao L, Zhou J, Huang J, Zhang Y, Xue Y (2004b) The F-box protein AhSLF-S2 physically interacts with S-RNases that may be inhibited by the ubiquitin/26S proteasome pathway of protein degradation during compatible pollination in *Antirrhinum*. *The Plant Cell*, **16**, 582-595.
- Qu GQ, Liu X, Zhang YL, Yao D, Ma QM, Yang MY, Zhu WH, Yu S, Luo YB (2009). Evidence for programmed cell death and activation of specific caspase-like enzymes in the tomato fruit heat stress response. *Planta*, Epub ahead of print, DOI 10.1007/s00425-009-0908-4.
- Quintero-Monzon O, Jonasson EM, Bertling E, Talarico L, Chaudhry F, Sihvo M, Lappalainen P, Goode BL (2009). Reconstitution and Dissection of the 600-kDa Srv2/CAP Complex: roles for oligomerization and cofilin-actin binding in driving actin turnover. *Journal of Biological Chemistry*, **284**, 10923-10934.
- Raff, M (1998). Cell suicide for beginners. *Nature*, **396**, 119-122.
- Rao JY, Jin YS, Zheng Q, Cheng J, Tai J, Hemstreet GP 3rd (1999). Alterations of the actin polymerization status as an apoptotic morphological effector in HL-60 cells. *Journal of Cellular Biochemistry*, **75**, 686-97.
- Rathore K, Cork R, Robinson K (1991). A cytoplasmic gradient of calcium is correlated with the growth of lily pollen tubes. *Developmental Biology*, **148**, 612-619.
- Raudaskoski M, Åström H, Pertitila K, Virtanen I, Louhelainen J (1987). Role of the microtubule cytoskeleton in pollen tubes: an immunocytochemical and ultrastructural approach. *Biology of the Cell*, **61**, 177-188.
- Raudaskoski M, Åström H, Laitinen E. (2001) Pollen tube cytoskeleton: structure and function. *Journal of Plant Growth Regulation*, **20**, 113-130.
- Reddy ASN, Day IS (2001) Kinesins in the Arabidopsis genome: a comparative analysis among eukaryotes. *BMC Genomics*, **2**, 2.
- Reichert S, Knight AE, Hodge TP, Baluska F, Samaj J, Volkmann D, Kendrick-Jones J (1999). Characterization of the unconventional myosin VIII in plant cells and its localization at the postcytokinetic cell wall. *Plant Journal*, **19**, 555-567.
- Reisen D, Hanson MR (2007). Association of six YFP-myosin XI-tail fusions with mobile plant cell organelles. *BMC Plant Biology*, **7**, 6.

- Ren H, Xiang Y (2007). The function of actin-binding proteins in pollen tube growth. *Protoplasma*, **230**, 171-182.
- Ressad F, Didry D, Xia G-X, Hong Y, Chua N-H, Pantaloni D, Carlier MF (1998). Kinetic analysis of the interactions of actin-depolymerizing factor (ADF)/cofilin with G- and F-actins. Comparison of plant and human ADFs and effect of phosphorylation. *Journal of Biological Chemistry*, **273**, 20894-20902.
- Richardson DN, Simmons MP, Reddy AS (2006). Comprehensive comparative analysis of kinesins in photosynthetic eukaryotes. *BMC Genomics*, **7**, 18.
- Ride JP, Davies EM, Franklin FCH, Marshall DF (1999). Analysis of *Arabidopsis* genome sequence reveals a large new gene family in plants. *Plant Molecular Biology*, **39**, 927-932.
- Robatzek S, Chinchilla D, Boller T (2006). Ligand-induced endocytosis of the pattern recognition receptor FLS2 in *Arabidopsis*. *Genes and Development*, **20**, 537-542.
- Rodal AA, Tetreault JW, Lappalainen P, Drubin DG, Amberg DC. (1999). Aip1p Interacts with Cofilin to Disassemble Actin Filaments. *Journal of Cell Biology*, **145**, 1251-1264.
- Rolland F, Winderickx, J, Thevelein JM (2002). Glucose-sensing and -signalling mechanisms in yeast. *FEMS Yeast Research*, **2**, 183-201.
- Romagnoli S, Cai G, Cresti M (2003). Kinesin-like proteins and transport of pollen tube organelles. *Cell Biology International*, **27**, 255-256.
- Romagnoli S, Cai G, Faleri C, Yokota E, Shimmen T, Cresti M (2007). Microtubule- and actin filament-dependent motors are distributed on pollen tube mitochondria and contribute differently to their movement. *Plant Cell Physiology*, **48**, 345-361.
- Rost B, Yachdav G, Liu J. (2004). The PredictProtein Server. *Nucleic Acids Research* 32 (Web Server issue): W321-W326.
- Rudd J, Franklin-Tong V (2003). Signals and targets of the self-incompatibility response in pollen of *Papaver rhoeas*. *Journal of Experimental Botany*, **54**, Plant Reproductive Biology Special Issue, 141-148.
- Rudd J, Franklin F, Lord J, Franklin-Tong V (1996). Increased phosphorylation of a 26 kDa pollen protein is induced by the self-incompatibility response in *Papaver rhoeas*. *The Plant Cell*, **8**, 713-724.
- Rudd J, Osman K, Franklin FCH, Franklin-Tong VE (2003). Activation of a putative MAP kinase in pollen is stimulated by the SI response. *FEBS Letters*, **547**, 223-227.
- Sagot I, Klee SK, Pellman D (2002). Yeast formins regulate cell polarity by controlling the assembly of actin cables. *Nature Cell Biology*, **4**, 42-50.
- Sagot I, Pinson B, Salin B, Daignan-Fornier B (2006). Actin bodies in yeast quiescent cells: an immediately available actin reserve? *Molecular Biology of the Cell*, **17**, 4645-4655.
- Saibil H (2000). Molecular chaperones: containers and surfaces for folding, stabilising or unfolding proteins. *Current Opinions in Structural Biology*, **10**, 251-258.
- Šamaj J, Müller J, Beck M, Böhm N, Menzel D (2006). Vesicular trafficking, cytoskeleton and signalling in root hairs and pollen tubes. *Trends in Plant Science*, **11**, 594-600.
- Šamaj J, Read ND, Volkmann D, Menzel D, Baluška F (2005). The endocytic network in plants. *Trends in Cell Biology*, **15**, 425-433.
- Sanabria N, Goring D, Nürnberger T, Dubery I (2008). Self/nonself perception and recognition mechanisms in plants: a comparison of self-incompatibility and innate immunity. *New Phytologist*, **178**, 503-14.
- Sano T, Higaki T, Oda Y, Hayashi T, Hasezawa S (2005). Appearance of actin microfilament 'twin peaks' in mitosis and their function in cell plate formation, as visualized in tobacco BY-2 cells expressing GFP-fimbrin. *Plant Journal*, **44**, 595-605.

- Schafer DA, Jennings PB, Cooper JA (1996). Dynamics of capping protein and actin assembly in vitro: Uncapping barbed ends by polyphosphoinositides. *Journal of Cell Biology*, **135**, 169-179.
- Schaller A (2004). A cut above the rest: the regulatory function of plant proteases. *Planta*, **220**, 183–197.
- Schmit AC (2002). Acentrosomal microtubule nucleation in higher plants. *International Review of Cytology*, **220**, 257–289.
- Schneckenburger H (2005). Total internal reflection fluorescence microscopy: technical innovations and novel applications. *Current Opinions in Biotechnology*, **16**, 13-18.
- Schopfer CR, Nasrallah ME, Nasrallah JB (1999). The male determinant of self-incompatibility in Brassica. *Science*, **286**, 1697-700.
- Shaw SL, Kamyar R, Ehrhardt DW (2003). Sustained microtubule treadmill in *Arabidopsis* cortical arrays. *Science*, **300**, 1715–1718.
- Sheahan MB, Staiger CJ, Rose RJ, McCurdy DW (2004). A green fluorescent protein fusion to actin-binding domain 2 *Arabidopsis* fimbrin highlights new features of a dynamic actin cytoskeleton in live plant cells. *Plant Physiology*, **4**, 3968-3978.
- Shiba H, Takayama S, Iwano M, Shimosato H, Funato M, Nakagawa T, Che FS, Suzuki G, Watanabe M, Hinata K, Isogai A (2001). A pollen coat protein, SP11/SCR, determines the pollen S-specificity in the self-incompatibility of *Brassica* species. *Plant Physiology*, **125**, 2095–2103.
- Shih YL, Rothfield L (2006). The bacterial cytoskeleton. *Microbiology & Molecular Biology Reviews*, **70**, 729-754.
- Shoji T, Suzuki K, Abe T, Kaneko Y, Shi H, Zhu J-K, Rus A, Hasegawa PM, Hashimoto T (2006) Salt Stress Affects Cortical Microtubule Organization and Helical Growth in *Arabidopsis*. *Plant Cell Physiology*, **47**, 1158-1168.
- Sieberer BJ, Timmers AC, Lhuissier FG, Emons AM (2002). Endoplasmic microtubules configure the subapical cytoplasm and are required for fast growth of *Medicago truncatula* root hairs. *Plant Physiology*, **130**, 977-988.
- Sieberer B, Timmers ACJ, Emons AMC. (2005). Nod factors alter the microtubule cytoskeleton in *Medicago truncatula* root hairs to allow root hair reorientation. *Molecular Plant-Microbe Interactions*, **18**, 1195-1204.
- Sijacic P, Wang X, Skirpan AL, Wang Y, Dowd PE, McCubbin AG, Huang S, Kao TH. (2004). Identification of the pollen determinant of S-RNase-mediated self-incompatibility. *Nature*, **429**, 302-305.
- Silva NF, Stone SL, Christie LN, Sulaman W, Nazarian KA, Burnett LA, Arnoldo MA, Rothstein SJ, Goring DR (2001). Expression of the S receptor kinase in self-compatible *Brassica napus* cv. Westar leads to the allele-specific rejection of self-incompatible *Brassica napus* pollen. *Molecular Genetics and Genomics*, **265**, 552–59.
- Sivaguru M, Pike S, Gassmann W, Baskin TI. (2003). Aluminum rapidly depolymerizes cortical microtubules and depolarizes the plasma membrane: Evidence that these responses are mediated by a glutamate receptor. *Plant Cell Physiology*, **44**, 667-675.
- Smertenko AP, Jiang CJ, Simmons NJ, Weeds AG, Davies DR, Hussey PJ (1998). Ser6 in the maize actin-depolymerising factor, ZmADF3, is phosphorylated by a calcium stimulated protein kinase and is essential for the control of functional activity. *The Plant Journal*, **14**, 187-193.
- Smertenko A, Saleh N, Igarashi H, Mori H, Hauser-Hahn I, Jiang CJ, Sonobe S, Lloyd CW, Hussey PJ (2000) A new class of microtubule-associated proteins in plants. *Nature Cell Biology*, **2**, 750–753.

- Smertenko AP, Allwood EG, Khan S, Jiang CJ, Maciver SK, Weeds AG, Hussey PJ (2001). Interaction of pollen-specific actin depolymerising factor with actin. *The Plant Journal*, **25**, 203-212.
- Smertenko AP, Bozhkov PV, Filonova LH, van Arnold S, Hussey PJ (2003). Re-organisation of the cytoskeleton during developmental programmed cell death in *Picea abies* embryos. *The Plant Journal*, **33**, 813-824.
- Smertenko AP, Chang HY, Wagner V, Kaloriti D, Fenyk S, Sonobe S, Lloyd C, Hauser MT, Hussey PJ (2004). The Arabidopsis microtubule-associated protein AtMAP65-1: molecular analysis of its microtubule bundling activity. *The Plant Cell*, **16**, 2035–2047.
- Smertenko AP, Chang HY, Sonobe S, Fenyk SI, Weingartner M, Bogre L, Hussey PJ (2006). Control of the AtMAP65–1 interaction with microtubules through the cell cycle. *Journal of Cell Science*, **119**, 3227–3237.
- Smith L, Oppenheimer D (2005). Spatial control of cell expansion by the plant cytoskeleton. *Annual Reviews of Cell and Developmental Biology*, **21**, 271-295.
- Snowman B, Kovar D, Shevchenko G, Franklin-Tong V, Staiger C (2002). Signal-mediated depolymerisation of actin in pollen during the self-incompatibility response. *The Plant Cell*, **14**, 2613-2626.
- Song Q, Wei T, Lees-Miller S, Alnemri E, Watters D, Lavin MF (1997). Resistance of actin to cleavage during apoptosis. *PNAS*, **94**, 157-162.
- Sorger PK, Dobles M, Tournebize R, Hyman AA (1997). Coupling cell division and cell death to microtubule dynamics. *Current Opinion in Cell Biology*, **9**, 807-814.
- Spector I, Shochet NR, Blasberger D, Kashman Y (1989). Latrunculins-novel marine macrolides that disrupt microfilament organization and affect cell growth: I. Comparison with cytochalasin D. *Cell Motility and the Cytoskeleton*, **13**, 127-44.
- Srivastava J, Barber D (2008). Actin co-sedimentation assay; for the analysis of protein binding to F-actin. *Journal of Visualized Experiments*, **13**, pii: 690. doi: 10.3791/690.
- Staiger CJ, Yuan M, Valenta R, Shaw PJ, Warn RM, Lloyd CW (1994). Microinjected profilin affects cytoplasmic streaming in plant cells by rapidly depolymerizing actin microfilaments. *Current Biology*, **4**, 215-219.
- Staiger CJ (2000). Signaling to the actin cytoskeleton in plants. *Annual Review of Plant Physiology and Plant Molecular Biology*, **51**, 257-288.
- Staiger CJ, Blanchoin L (2006). Actin dynamics: old friends with new stories. *Current Opinions in Plant Biology*, **9**, 554-562.
- Stein JC, Dixit R, Nasrallah ME, Nasrallah JB (1996). SRK, the stigma-specific S locus receptor kinase of *Brassica*, is targeted to the plasmamembrane in transgenic tobacco. *The Plant Cell*, **10**, 429–445.
- Stein JC, Howlett B, Boyes DC, Nasrallah ME, Nasrallah JB (1991). Molecular cloning of a putative receptor kinase gene encoded by the self-incompatibility locus of *Brassica oleracea*. *PNAS*, **88**, 8816–8820.
- Stone SL, Arnoldo M, Goring DR (1999). A breakdown of *Brassica* self- incompatibility in ARC1 antisense transgenic plants. *Science*, **286**, 1729–1731.
- Stone SL, Anderson EM, Mullen RT, Goring DR (2003). ARC1 is an E3 ubiquitin ligase and promotes the ubiquitination of proteins during the rejection of self-incompatible *Brassica* pollen. *The Plant Cell*, **15**, 885–898.
- Stoppin-Mellet V, Gaillard J, Vantard M (2002). Functional evidence for *in vitro* microtubule severing by the plant katanin homologue. *Biochemical Journal*, **365**, 337–342.

- Stoppin-Mellet V, Vantard M, Schmit AC, Lambert, AM (1994). Isolated plant nuclei nucleate microtubule assembly: the nuclear surface in higher plants has centrosome-like activity. *The Plant Cell*, **6**, 1099–1106.
- Straatman K, Dove S, Holdaway-Clark T, Hepler P, Kunkel J, Franklin-Tong V (2001). Calcium signalling in pollen of *Papaver rhoeas* undergoing the self-incompatibility response. *Sexual Plant Reproduction*, **14**, 105-110.
- Suarez MF, Filonova LH, Smertenko A, Savenkov EI, Clapham DH, von Arnold S, Zhivotovsky B, Bozhkov PV (2004). Metacaspase-dependent programmed cell death is essential for plant embryogenesis. *Current Biology*, **14**, R339–R340.
- Suzuki G, Kai N, Hirose T, Fukui K, Nishio T, Takayama S, Isogai A, Watanabe M, Hinataf K (1999). Genomic organization of the S locus: identification and characterization of genes in SLG/SRK region of S9 haplotype of *Brassica campestris* (syn. rapa). *Genetics*, **153**, 391–400.
- Szumanski AL, Nielsen E (2009). The Rab GTPase RabA4d Regulates Pollen Tube Tip Growth in *Arabidopsis thaliana*. *The Plant Cell*, **21**, 526-544.
- Takasaki T, Hatakeyama K, Suzuki G, Watanabe M, Isogai A, Hinata K (2000). The S receptor kinase determines self-incompatibility in Brassica stigma. *Nature*, **403**, 913–916.
- Takayama S, Isogai A (2005). Self-Incompatibility in Plants. *Annual Reviews of Plant Biology*, **56**, 467-489.
- Takayama S, Isogai A, Tsukamoto C, Ueda Y, Hinata K, Okazaki K, Suzuki A (1987). Sequences of S-glycoproteins, products of the Brassica campestris self-incompatibility locus. *Nature*, **326**, 102-105.
- Takayama S, Shiba H, Iwano M, Shimosato H, Che FS, Kai N, Watanabe M, Suzuki G, Hinata K, Isogai A (2000). The pollen determinant of self-incompatibility in *Brassica campestris*. *PNAS*, **97**, 1920–1925.
- Takayama S, Shimosato H, Shiba H, Funato M, Che F-S, Watanabe M, Iwano M, Isogai A (2001). Direct ligand-receptor complex interaction controls Brassica self-incompatibility. *Nature*, **413**, 534-538.
- Takemoto D, Hardham AR (2004). The Cytoskeleton as a Regulator and Target of Biotic Interactions in Plants. *Plant Physiology*, **136**, 3864-3876.
- Tang XJ, Hepler PK, Scordilis SP (1989). Immunochemical and immunocytochemical identification of a myosin heavy chain polypeptide in *Nicotiana* pollen tubes. *Journal of Cell Science*, **92**, 569–574.
- Taylor L, Hepler P (1997). Pollen germination and tube growth. *Annual Reviews Plant Physiology and Plant Molecular Biology*, **48**, 461-491.
- Thevelein JM, de Winde JH (1999). Novel sensing mechanisms and targets for the cAMP-protein kinase A pathway in the yeast *Saccharomyces cerevisiae*. *Molecular Microbiology*, **33**, 904–918.
- Thomas S, Franklin-Tong V (2004). Self-incompatibility triggers programmed cell death in *Papaver rhoeas*. *Nature*, **429**, 305-309.
- Thomas S, Huang S, Li S, Staiger CJ, Franklin-Tong VE (2006). Actin depolymerisation is sufficient to induce programmed cell death in self-incompatible pollen. *The Journal of Cell Biology*, **174**, 221-229.
- Thomas S, Osman, K, de Graaf B, Shevchenko G, Wheeler M, Franklin F, Franklin-Tong V (2003). Investigating mechanisms involved in the self-incompatibility response in *Papaver rhoeas*. *Philosophical transactions of the Royal Society of London*, **358**, 1033-1036.

- Tierney ML, Stowell MH (1998). The functional significance of multimerization in ion channels. *Current Opinions in Structural Biology*, **8**, 186-188.
- Tiezzi A, (1991). The pollen tube cytoskeleton. *Electron Microscopy Reviews*, **4**, 205-219.
- Timmers ACJ, Auriac M-C, Truchet G (1999). Redefined analysis of early symbiotic steps of the Rhizobium-Medicago interaction in relationship with microtubule cytoskeleton rearrangements. *Development*, **126**, 3617-3628.
- Timmers AC, Vallotton P, Heym C, Menzel D (2007). Microtubule dynamics in root hairs of *Medicago truncatula*. *European Journal of Cell Biology*. **86**, 69-83.
- Tirnauer JS, Grego S, Salmon ED, Mitchison, TJ (2002). EB1-microtubule interactions in *Xenopus* egg extracts: Role of EB1 in microtubule stabilization and mechanisms of targeting to microtubules. *Molecular Biology of the Cell*, **13**, 3614-3626.
- Tominaga M, Morita K, Sonobe S, Yokota E, Shimmen T (1997) Microtubules regulate the organization of actin filaments at the cortical region in root hair cells of *Hydrocharis*. *Protoplasma*, **199**, 83-92.
- Tomiya K, Sato K, Doke N (1982). Effect of cytochalasin B and colchicine on hypersensitive death of potato cells infected by incompatible race of *Phytophthora infestans*. *Annals of the Phytopathological Society of Japan*, **48**, 228–230.
- Twell D, Park SK, Hawkins TJ, Schubert D, Schmidt R, Smertenko A, Hussey PJ (2002). MOR1/GEM1 has an essential role in the plant-specific cytokinetic phragmoplast. *Nature Cell Biology*, **4**, 711-714.
- Uren AG, O'Rourke K, Aravind LA, Pisabarro MT, Seshagiri S, Koonin EV, Dixit VM (2000). Identification of paracaspases and metacaspases: two ancient families of caspase-like proteins, one of which plays a key role in MALT lymphoma. *Molecular Cell*, **6**, 961–967.
- Ushijima K, Sassa H, Dandekar AM, Gradziel TM, Tao R, Hirano H (2003). Structural and Transcriptional Analysis of the Self-Incompatibility Locus of Almond: identification of a pollen-expressed F-box gene with haplotype-specific polymorphism. *The Plant Cell*, **15**, 771-781.
- Ushijima K, Yamane H, Watari A, Kakehi E, Ikeda K, Hauck NR, Iezzoni AF, Tao R (2004). The S haplotype-specific F-box protein gene, SFB, is defective in self-compatible haplotypes of *Prunus avium* and *P. mume*. *Plant Journal*, **39**, 573–586.
- Valenta R, Duchêne M, Pettenburger K, Sillaber C, Valent R Bettelheim R Breitenbach M, Rumpold H, Kraft D, Scheiner O (1991). Identification of profilin as a novel pollen allergen: IgE autoreactivity in sensitized individuals. *Science*, **253**, 557-560.
- Valenta R, Ebner C, Valent P, Sillaber C, Deviller R Ferreira F, Tejkl M, Edelman H, Kraft D, Scheiner O (1992) Profilins constitute a novel family of functional plant pan-allergens. *Journal of Experimental Medicine*, **175**, 377-385.
- Van Damme D, Bouget FY, Van Poucke K, Inze D, Geelen D (2004a) Molecular dissection of plant cytokinesis and phragmoplast structure: a survey of GFP-tagged proteins. *Plant Journal*, **40**, 386–398.
- Van Damme D, Van Poucke K, Boutant E, Ritzenthaler C, Inze D, Geelen D (2004b) In vivo dynamics and differential microtubule-binding activities of MAP65 proteins. *Plant Physiology*, **136**, 3956–3967.
- Van Gestel K, Kohler RH, Verbelen JP (2002). Plant mitochondria move on F-actin, but their positioning in the cortical cytoplasm depends on both F-actin and microtubules. *Journal of Experimental Botany*, **369**, 659-667.
- van Hemert, M. J., Steensma, H. Y, van Heusden, G. P (2001). 14-3-3 proteins: key regulators of cell division, signalling and apoptosis. *BioEssays*, **23**, 936-946.

- Vanoosthuyse V, Tichtinsky G, Dumas C, Gaude T, Cock JM (2003). Interaction of calmodulin, a sorting nexin and kinase-associated protein phosphatase with the *Brassica oleracea* S-locus receptor kinase. *Plant Physiology*, **133**, 919–29.
- Vassileva VN, Kouchi H, Ridge RW. (2005). Microtubule dynamics in living root hairs: transient slowing by lipochitin oligosaccharide nodulation signals. *The Plant Cell*, **17**, 1777–1787.
- Vercammen D, Declercq W, Vandenabeele P, Van Breusegem F (2007). Are metacaspases caspases? *Journal of Cell Biology*, **179**, 375–380.
- Vernoud V, Horton AC, Yang Z, Nielsen E (2003). Analysis of the Small GTPase Gene Superfamily of *Arabidopsis*. *Plant Physiology*, **131**, 1191–1208.
- Vidali L, Pérez HE, Valdés López V, Noguez R, Zamudio F, Sánchez F (1995). Purification, characterization, and cDNA cloning of profilin from *Phaseolus vulgaris*. *Plant Physiology*, **108**, 115–23.
- Vidali L, Hepler PK (1997). Characterization and localization of profilin in pollen grains and tubes of *Lilium longiflorum*. *Cell Motility and the Cytoskeleton*, **36**, 323–338.
- Vidali L, McKenna ST, Hepler PK (2001). Actin Polymerisation is essential for pollen tube growth. *Molecular Biology of the Cell*, **12**, 2534–2545.
- Vig M, Beck A, Billingsley JM, Lis A, Parvez S, Peinelt C, Koomoa DL, Soboloff J, Gill DL, Fleig A, Kinet JP, Penner R (2006). CRACM1 multimers form the ion-selective pore of the CRAC channel. *Current Biology*, **16**, 2073–2079.
- Vojtek AB, Cooper JA (1993). Identification and characterization of a cDNA encoding mouse CAP: a homolog of the yeast adenylyl cyclase associated protein. *Journal of Cell Science*, **105**, 777–785.
- Walker E, Ride J, Kurup S, Franklin-Tong V, Lawrence M, Franklin F (1996). Molecular analysis of two functional homologues of the S3 allele of the *Papaver rhoeas* self-incompatibility gene isolated from different populations. *Plant Molecular Biology*, **30**, 983–994.
- Wallar BJ, Alberts AS (2003). The formins: active scaffolds that remodel the cytoskeleton. *Trends in Cell Biology*, **13**, 435–446.
- Wang Q, Kong L, Hao H, Wang X, Lin J, Samaj J, Baluska F (2005). Effects of brefeldin A on pollen germination and tube growth. Antagonistic effects on endocytosis and secretion. *Plant Physiology*, **139**, 1692–1703.
- Wang X (1999). The Role of Phospholipase D in Signaling Cascades. *Plant Physiology*, **120**, 645–651.
- Wang ZY, Seto H, Fujioka S, Yoshida S, Chory J (2001). BRI1 is a critical component of a plasma-membrane receptor for plant steroids. *Nature*, **410**, 380–383.
- Wang X (2002). Phospholipase D in hormonal and stress signaling. *Current Opinions in Plant Biology*, **5**, 408–414.
- Wang YF, Fan LM, Zhang WZ, Zhang W, Wu WH (2004a). Calcium-permeable channels in the plasma membrane of *Arabidopsis* pollen are regulated by actin microfilaments. *Plant Physiology*, **136**, 3892–3904.
- Wang YS, Motes CM, Mohamalawari DR, Blancaflor EB (2004b). Green fluorescent protein fusions to *Arabidopsis* fimbrin 1 for spatiotemporal imaging of F-actin dynamics in root. *Cell Motility & the Cytoskeleton*, **59**, 79–93.
- Wang H-Y, Yu Y, Chen Z-L, Xia G-X (2005). Functional characterization of *Gossypium hirsutum* profilin 1 gene (GhPFN1) in tobacco suspension cells. *Planta*, **222**, 594–603.

- Wang X, Teng Y, Wang Q, Li X, Sheng X, Zheng M, Samaj J, Baluska F, Lin J (2006). Imaging of dynamic secretory vesicles in living pollen tubes of *Picea meyeri* using evanescent wave microscopy. *Plant Physiology*, **141**, 1591-1603.
- Wang X, Zhu L, Liu B, Wang C, Jin L, Zhao Q, Yuan M (2007). Arabidopsis MICROTUBULE-ASSOCIATED PROTEIN18 functions in directional cell growth by destabilizing cortical microtubules. *The Plant Cell*, **19**, 877-889.
- Wang C, Zhou GL, Vedantam S, Li P, Field J (2008). Mitochondrial shuttling of CAP1 promotes actin- and cofilin-dependent apoptosis. *Journal of Cell Science*, **121**, 2913-2920.
- Wasteneys GO (2002). Microtubule organization in the green kingdom: chaos or self-order? *Journal of Cell Science*, **115**, 1345-1354.
- Wasteneys GO. (2004). Progress in understanding the role of microtubules in plant cells. *Current Opinions in Plant Biology*, **7**, 651-660.
- Watanabe N, Lam E (2005). Two *Arabidopsis* metacaspases AtMCP1b and AtMCP2b are arginine/lysine-specific cysteine proteases and activate apoptosis-like cell death in yeast. *Journal of Biological Chemistry*, **280**, 14691-14699.
- Weerasinghe RR, Collings DA, Johannes E, Allen NS (2003). The distributional changes and role of microtubules in Nod factor challenged *Medicago sativa* root hairs. *Planta*, **218**, 276-287.
- Weisenberg RC. (1972). Microtubule formation *in vitro* in solutions containing low calcium concentrations. *Science*, **177**, 1104-1105.
- Wheeler MJ, Franklin-Tong VE, Franklin FCH (2001). The molecular and genetic basis of pollen-pistil interactions. *New Phytologist*, **151**, 565-584.
- Wheeler MJ, de Graaf BHJ, Hadjiosif N, Perry RM, Poulter NS, Osman K, Vatovec S, Harper A, Franklin-Tong VE, Franklin FCH (2009). Identification of the pollen self-incompatibility determinant in *Papaver rhoeas*. *Nature*, in press.
- Whittington AT, Vugrek O, Wei KJ, Hasenbein NG, Sugimoto K, Rashbrooke MC, Wasteneys GO (2001). MOR1 is essential for organizing cortical microtubules in plants. *Nature*, **411**, 610-613.
- Wicker-Planquart C, Stoppin-Mellet V, Blanchoin L, Vantard M (2004). Interactions of tobacco microtubule-associated protein MAP65-1b with microtubules. *Plant Journal*, **39**, 126-134.
- Wightman R, Turner SR (2007). Severing at sites of microtubule crossover contributes to microtubule alignment in cortical arrays. *Plant Journal*, **52**, 742-751.
- Woltering EJ, van der Bent A, Hoerberichts FA (2002). Do Plant Caspases Exist? *Plant Physiology*, **130**, 1764-1769.
- Xing H, Zhang S, Weinheimer C, Kovacs A, Muslin AJ (2000). 14-3-3 proteins block apoptosis and differentially regulate MAPK cascades. *EMBO Journal*, **19**, 349-358.
- Xu J, Scheres B (2005) Cell polarity: ROPing the ends together. *Current Opinions in Plant Biology*, **8**, 613-618.
- Xu T, Qu Z, Yang X, Qin X, Xiong J, Wang Y, Ren D, Liu G (2009). A cotton kinesin GhKCH2 interacts with both microtubules and microfilaments. *Biochemical Journal*, [Epub ahead of print], doi:10.1042/BJ20082020.
- Yamada K, Shimada T, Nishimura M, Hara-Nishimura I (2005). A VPE family supporting various vacuolar functions in plants. *Physiologia Plantarum*, **123**, 369-375.

- Yeung YG, Wang Y, Einstein DB, Lee PSW, Stanley ER (1998). Colony-stimulating Factor-1 stimulates the formation of multimeric cytosolic complexes of signaling proteins and cytoskeletal components in macrophages. *The Journal of Biological Chemistry*, **273**, 17128-17137.
- Yokota E, Takahara K.-I, Shimmen T (1998). Actin-bundling protein isolated from pollen tubes of lily. *Plant Physiology*, **116**, 1421-1429.
- Yokota E, Tominaga M, Mabuchi I, Tsuji Y, Staiger CJ, Oiwa K, Shimmen T (2005). Plant villin, lily P-135-ABP, possesses G-actin binding activity and accelerates the polymerization and depolymerization of actin in a Ca²⁺-sensitive manner. *Plant Cell Physiology*, **46**, 1690-1703.
- Yonezawa N, Nishida E, Sakai H (1985). pH control of actin polymerization by cofilin. *Journal of Biological Chemistry*, **27**, 14410-14412.
- Yonezawa N, Nishida E, Iida K, Yahara I, Sakai H. (1990). Inhibition of the interactions of cofilin, destrin and deoxyribonuclease I with actin by phosphoinositides. *Journal of Biological Chemistry*, **265**, 8382-8386.
- Yonezawa N, Homma Y, Yahara I, Sakai H, Nishida E. (1991). A short sequence responsible for both phosphoinositide binding and actin binding activities of cofilin. *Journal of Biological Chemistry*, **266**, 17218-17221.
- Yu G, Swiston J, Young, D (1994). Comparison of human CAP and CAP2, homologs of the yeast adenylyl cyclase-associated proteins. *Journal of Cell Science*, **107**, 1671-1678.
- Zelicof A, Gatica J, Gerst JE (1993). Molecular cloning and characterization of a rat homolog of CAP, the adenylyl cyclase-associated protein from *Saccharomyces cerevisiae*. *Journal of Biological Chemistry*, **268**, 13448-13453.
- Zerial M, McBride H (2001). Rab proteins as membrane organizers. *Nature Reviews Molecular Cell Biology*, **2**, 107-117.
- Zha J, Harada H, Yang E, Jockel J, Korsmeyer SJ (1996). Serine phosphorylation of death agonist BAD in response to survival factor results in binding to 14-3-3 not BCL-X(L). *Cell*, **87**, 619-628.
- Zhang SQ, Klessig DF. 2001. MAPK cascades in plant defense signaling. *Trends in Plant Science*, **6**, 520-527.
- Zheng Z-L, Yang Z (2000). The Rop GTPase switch turns on polar growth in pollen. *Trends in Plant Science*, **5**, 298-303.
- Zieske LR (2006). A perspective on the use of iTRAQ reagent technology for protein complex and profiling studies. *Journal of Experimental Botany*, **57**, 1501-1508.

APPENDIX I

PUBLISHED PAPERS

Wheeler MJ, de Graaf BHJ, Hadjiosif N, Perry RM, **Poulter NS**, Osman K, Vatovec S, Harper A, Franklin-Tong VE, Franklin FCH (2009). Identification of the pollen self-incompatibility determinant in *Papaver rhoeas*. *Nature*, **459**, 992-995.

My contribution: I carried out the immunolocalisation of PrpS₁ in fixed pollen tubes and contributed to the materials and methods section. I also proof-read the manuscript before submission.

Bosch M, **Poulter NS**, Vatovec S, Franklin-Tong VE (2008). Initiation of programmed cell death in self-incompatibility: Role for cytoskeleton modifications and several caspase-like activities. *Molecular Plant*, **1**, 879-887.

My contribution: I selected the data/images to be presented in the figures. I organised it all into presentable figures and wrote the figure legends. I proof-read the manuscript and corrected any mistakes I came across.

APPENDIX II

FT-ICR-MS DATA

Mascot search results for the F-actin isolation from untreated and 3 h SI samples (**Chapter 6**). These data include the significant protein hits with the identified peptides for each protein.